Universitat
de les Illes Balears

DOCTORAL THESIS

2019

PATTERNS OF PHYTOPLANKTON AND PRIMARY PRODUCTION VARIABILITY IN THE MEDITERRANEAN SEA BASED ON REMOTE SENSING DATA

Paula Maria Salgado Hernanz

Universitat de les Illes Balears

IMEDEA CSIC UIB

DOCTORAL THESIS

2019

Doctoral Programme of Marine Sciences

PATTERNS OF PHYTOPLANKTON AND PRIMARY PRODUCTION VARIABILITY IN THE MEDITERRANEAN SEA BASED ON REMOTE SENSING DATA

Paula Maria Salgado Hernanz

Director: Gotzon Basterretxea Oyarzabal

Tutor: Gabriel Moyà Niell

Doctor by the Universitat de les Illes Balears

A todas las personas y momentos

que forman y añaden gotas

en el mar Mediterráneo.

A mis padres.

Agradecimientos

He de comenzar por agradecer formalmente esta tesis a la financiación concedida por parte del Ministerio de Economía y Competitividad (MINECO) de España a través del contrato a la Formación de Personal Investigador del que fui merecedora (ayuda con referencia BES-2013-067305) dentro del marco del proyecto GRADIENTS (CTM2012-39476) en el año 2014. Agradecer al Centro Superior de Investigaciones Científicas (CSIC), en concreto al Instituto Mediterráneos de Estudios Avanzados (IMEDEA), y a la Universitat de les Illes Balears (UIB), por haber sido mis centros de acogida para la realización de la Tesis Doctoral en Ecología Marina. Me parece necesario mencionar que, en última instancia, la financiación de mi contrato durante 4 años ha sido posible gracias a los impuestos de los ciudadanos españoles. Gracias por contribuir en la financiación de mi Doctorado en Ecología Marina, del mismo modo que se costean muchos estudios necesarios en el avance científico. Espero que nunca deje de apostarse por la Ciencia española.

Llegados a este punto siento que puedo definir mi tesis como un largo camino definido por una función sinusoidal, con los consecuentes altibajos que ésta conlleva, alternando momentos de cumbres y momentos de desorientación que parecían interminables. Han sido años con un eterno sentimiento de que todo va demasiado lento, de pensar que MATLAB y Google eran mis "mejores aliados". pero también mis "peores enemigos". Pues bien, resulta que es verdad que poco a poco se van consiguiendo figuras y versiones "definitivas" (eso sí, he de reconocer que yo empecé a poner fechas a las versiones, pues aprendí que en esta profesión la palabra "definitiva" o "final", es mejor no usarla...). Estoy contenta y aliviada de que haya llegado este momento final de tesis, pero sobre todo me siento muy agradecida y orgullosa de haber conseguido contribuir, aunque sea en una parte pequeñita, a la mejora del conocimiento del medio marino en el mar Mediterráneo. Antes de nada, agradecer a todas las personas que en algún momento han tenido un instante para darme ánimo, pues este camino hubiera sido imposible sin el apoyo de todas las personas que han estado a mi lado de uno u otro modo estos años, y por eso pretendo con esta sección hacerles un poco de justicia.

Me gustaría mencionar a mi director de tesis, el Dr. Gotzon Basterretxea Oyarzabal, por confiar en mí en el principio y haberme dado la oportunidad de desarrollar este proyecto sin conocerme. Quiero agradecerte que, a pesar de nuestras diferencias y esas correcciones en rojo que me han hecho suspirar al abrir el mail, han sido fundamentales en la mejora y progreso del trabajo. Agradecerte el empujón que hemos dado, especialmente en los últimos meses, para que hoy yo pueda escribir estas palabras.

Reconocer también la financiación por parte del MINECO al concederme dos estancias de investigación en el Plymouth Marine Laboratory (PML) de Inglaterra en el 2016 y en la University of Santa Cruz, California (UCSC) en el 2017. Mandar mi gratitud a todas las personas que contribuyeron que estas estancias fuesen posibles (Marie-Fanny Racault, Raphael Kudela, Clarissa Anderson, ...). Sin duda, estas estancias contribuyeron a un gran enriquecimiento profesional y personal que me permitió ver la investigación desde perspectivas distintas.

Eso sí, si hay dos personas que realmente merecen ser citadas en esta sección son mis padres: Loli y Agustín. Además, son ya muchos años en los que constantemente habéis contribuido, tanto anímica como económicamente, a mi formación personal y profesional y, creo que es momento de dejarlo por escrito. Gracias a los dos por haber confiado siempre en mí, por intentar que yo también creyera en mí misma, por vuestro incondicional cariño y por estar siempre al teléfono cuando os necesito. Mamá, gracias por aguantar tanto mis quejas y estar siempre presente. Y como no, ¡gracias por la cantidad de *tuppers* preparados que tantas horas de cocinado me han salvado! Papá, gracias por haber siempre transmitido lo orgulloso que te sentías de mí ante cualquier cosa que hiciera sin importar el resultado de las mismas. Ah, ¡gracias por la cantidad de viajes que te has metido al aeropuerto para contribuir en que las idas y venidas Madrid-Mallorca fuesen un poquito más fácil! He normalizado este hecho, pero en realidad, es merecedor de todo reconocimiento.

No puedo olvidar a otras dos personas muy importantes: mi tía Núria y mi hermana Noelia. Nurita, gracias por ser una mezcla entre mi segunda mamá y mi segunda hermana. Gracias por haberme consentido tantos caprichos en estos años y por saber que siempre puedo contar contigo. Noelia, gracias por ser la hermana pequeña que ha enseñado a la hermana mayor como ser fuerte, ir a por todas y quererse a sí misma. Tu fortaleza y entereza es un ejemplo a seguir. Además de ellas dos, gracias a toda mi 'Familia Hernanz' y 'Familia Salgado', pues tener unos tíos y primos unidos siempre ayuda. Sabéis que me he perdido pocos momentos importantes con vosotros en los últimos años, pero espero que en el futuro pueda tener incluso algo más de tiempo para compartirlo con vosotros. Gracias sobre todo a los vídeos mandados por los más pequeñajos de la casa, que siempre conseguían arrancarme una sonrisa cuando estaba pegada al ordenador.

La realización de esta tesis me ha permitido vivir en Mallorca, una isla que me sorprendió desde el primer mes de vivir en ella no sólo por lo maravillosas que son sus costas, montañas y pueblos, sino también por la calidad de las personas que he encontrado en ella. El IMEDEA es un centro de mucho movimiento de personal y, a pesar de que son pocos los compañeros actuales que ya estaban cuando empecé mi andadura en el centro aquel lejano lunes 3 de marzo de 2014, es un centro idóneo para trabajar al que tengo que agradecer su acogida. Gracias al centro y a todas las personas de formación, investigación, dirección, administración, informática (Juanjo y Miguel, siempre resolutivos cuando se os necesita), limpieza (Cati, Ramona, Inés, ... parlanchinas pero eficaces) y conserjería (¡menos mal que vienen a buscarme al despacho antes de echar el cierre para no dejarme encerrada dentro!). Gracias a todos lo que a largo de estos años me han ayudado de una u otra manera. Siempre tendré buenos recuerdos del IMEDEA y de Esporles, mi pueblo de acogida.

Gracias a todos los "Imedeicos" y compañeros de doctorado con los que he tenido el placer de compartir buenos recuerdos tanto dentro como fuera del IMEDEA. No sé qué hubiera sido de la tesis sin todas las "actividades transversales" que he realizado con vosotros. Me da morriña recordar al estimado grupo de "xupitys" (Josep, Albert, Marina, Noe, Ana Payo, Jaume) por haberse convertido en mis primeras amistades en la isla. Pero también a muchos más que poco a poco se han sumado en el camino y que han hecho que mi estancia en IMEDEA sea un saco de buenos recuerdos: Gema, Romain, Andrea, Eva, Adrián, Juanma, Dani Chaparro, Carlos, Inés Mazarrasa, Johna, Franchesca, Laura, Guillem, Alex, Miguel, Vero, Carlota, Xisca, Julia, Guillermo, Melo, Lucia, Susana, Javi, Edu, Ángel, Conchi, Sara, Almu, Chema, Aarne, Fran, Cristina, Andreu, Silvia, Gema, Carlos... Gracias por haber convertido el Ágora en un lugar en el que siempre se disfruta de compañía privilegiada durante la hora de la comida. Tampoco

puedo olvidar a todos los compañeros de SOCIB (Marc, Manu, Inma, Emma, Jaime, Eugenio, ...) por unirse a nuestras batallas fuera del trabajo. Especial mención quería hacer a los que en algún momento han sido compañeros de despacho (Josep, Eva Aguiar, Inés Castejón, Jorge, Merit, Laura, Dani Conti, Julia... gracias por compartir risas y por aguantar mis momentos de sargento pidiendo silencio y "¡cerrar la puerta con cuidado y bajad la música de los auriculares por favor!". Gracias por haber también compartido lloros que se quedan en el despacho C018). Quiero reconocer a Romain y a Josep la gran ayuda que me prestaron en esos primeros años de tesis con el adorado Matlab. ¡Romain, creo que hubiera desesperado (sí, aún más) sin tu entusiasmo con Matlab! Y también muchas gracias a todos los que habéis estado súper pendientes de mí en las últimas semanas (Miguel, Jorge, Andrea, Alex, Estercilla, ..., ¡gracias por cuidarme!).

Estos años de tesis también me han permitido disfrutar un poquito más del mar Mediterráneo con alguna que otra campaña que me ha permitido conocer su interior un poco más. Gracias a los compañeros de grupo con los que he tenido ocasión de trabajar alguna vez y con los que tantos buenos recuerdos guardo: Itzi, Ana Massanet, David, Cayetana, Joan, Marly, Lucia, Aurore, Toni, Xavi, ... Gracias por cualquier ayuda prestada durante este tiempo y por los ánimos y apoyos recibidos.

No puedo olvidar a todos mis "olivitos" Fuenlabreños (Raquel, Carmen, David, Mari, Aroa, Molina, Cris, Juani, Fran, Javi...) por haber confiado siempre en mí y tenerme como una científica friki a la que valoran el trabajo que hace. Especial mención he de otorgarle a mi incondicional amiga Raquel. Gracias por literalmente todo lo que me has aguantado y empujoncitos de ánimo que has dado cuando he necesitado. Gracias por todas tus "sube ánimo-visitas" a Mallorca y por formar parte de mi vida durante tantos años.

Quiero agradecer también una parte de esta tesis a "las ambientólogas" (Ester, Elena, Bea, Mitxu, Ana, Lucía, Sonia y Noe) porque con vosotras empecé a soñar en poner nuestro granito de arena para que en el futuro todos podamos seguir disfrutando del mar, tierra y aire que nos rodea. Importante también fueron en mi vida mis dos años de estudio en el Mater de Teledetección de Valencia, donde se incrementó mi pasión por las herramientas que la teledetección aporta en el estudio de observación terrestre. Gracias a Vicente, pues influiste mucho en la estima que hoy en día le tengo a la Ciencia y a la Teledetección. Gracias por haber compartido conmigo una parte importante de este camino.

En los últimos años, y sobre todo en los últimos meses, he participado en una carrera de fondo que parecía no acabar. Pues bien, después de haber reflexionado mucho sobre el tema, y a pesar de que la realización de una tesis doctoral requiera de la participación, ayuda y apoyo de mucha gente, he decido finalizar por agradecer esta tesis a la realmente única persona sin la cual este proyecto no se hubiese podido realizar: "a mí". Durante estos casi cinco años de andaduras, muchas han sido las circunstancias personales y contextos que me han puesto trabas en el camino, pero siempre ha estado presente un factor común: mi constancia. Por muy obvio y elemental que resulte, siento que es necesario terminar estos párrafos agradeciendo esta tesis a mi incondicional empeño y aguante. ¡Gracias Paula por tu infinita perseverancia!

List of acronyms and abbreviations

BMU	Best-Matching Unit
CbPM	Carbon-based Production Model
CDOM	Colored Dissolved Organic Matter
Chl	Chlorophyll-a pigment (mg m^{-3})
CMAP	Center Merged Analysis of Precipitation
CMEMS	Copernicus Marine Environmental Monitoring Service
CZCS	Coastal Zone Color Scanner
DOC	Dissolved Organic Carbon
DMS	Dimethyl sulfide
ECMWF	European Centre for Medium-Range Weather Forecasts
ENSO	*El Niño* Southern Oscillation index
ENVISAT	ENVIonmental SATellite
EOS	Earth Observation System
$E_S(\lambda)$	Spectral surface irradiance (μW cm^{-2} nm^{-1})
ESA	European Space Agency
FRS	Full Resolution Swath
gC	Grams of Carbon
GPP	Gross Primary Production (gC m^{-2} $time^{-1}$)
GtC	Gigatons of Carbon
IOCCG	International Ocean-Color Coordinating Group
IOP	Inherent Optical Properties
JPSS	Joint Polar Satellite System
K_d490	Diffuse attenuation coefficient of downward irradiance at 490 nm
LAC	Local Area Coverage
$L_w(\lambda)$	Spectral water-leaving radiance (μW cm^{-2} nm^{-1} sr^{-1})
MERIS	Medium Resolution Imaging Spectrometer
MLAC	Merged Local Area Coverage
MODIS	Moderate Resolution Imaging Spectroradiometer
MOI	Mediterranean Oscillation Index
NAO	North Atlantic Oscillation
NASA	National Aeronautics and Space Administration
NASDA	Japanese Space Agency
nLw	Normalized water-leaving radiance
NPP	Net Primary Production (gC m^{-2} $time^{-1}$)
NWMS	North Western Mediterranean Sea
OBPG	Ocean Biology Processing Group
OC-CCI	Ocean Color-Climate Change Initiative
OCTS	Ocean Color Temperature Scanner
OCy-vx	Ocean Chlorophyll algorithms (y = no of spectral bands: 2, 3, 4; v = version no)

OLCI	Ocean and Land Color Instrument
P - I	Photosynthesis - Irradiance
PAR	Photosynthetically Available Radiation
PFT	Phytoplankton Functional Type
PgC	Pentagrams of Carbon
POC	Particulate Organic Carbon
PP	Primary Production (gC m^{-2} d^{-1})
$R_{rs}(\lambda)$	Remote sensing reflectance (Lw(λ) / ES(λ);sr^{-1})
SeaWiFS	Sea-viewing Wide Field-of-view Sensor
SST	Sea Surface Temperature (°C)
VGPM	Vertically Generalized Production Model
VIIRS	Visible and Infrared Imager/Radiometer Suite
Zeu	Depth of the bottom of the euphotic layer

Table of contents

SUMMARY

This PhD thesis aims to assess the spatial and temporal patterns of phytoplankton variability and primary production in the surface waters of the Mediterranean Sea. The research is organized in three studies and it is mainly based on the use of satellite ocean color data acquired during the period 1998-2015. Complementary datasets (e.g. sea surface temperature, climatic indices, meteorological data, and atmospheric dust) are also used to address the different specific studies included in this work.

A first study is aimed to analyze the contribution of the seasonal and non-seasonal components of phytoplankton variability at basin scale. Then, seasonality is analyzed from a phenological perspective i.e. by parameterizing the seasonal cycles (*bloom*) using a pixel-by-pixel threshold-based algorithm. We observe that seasonality dominates variability representing up to 80% of total chlorophyll (Chl) variance in oceanic areas, whereas in shelf-sea regions high frequency variations may be dominant representing up to 49% of total Chl variance. Seasonal variations are typically characterized by a phytoplankton growing period occurring in spring and spanning on average 170 days in the western basin and 150 days in the eastern basin. Also, in the western basin, a positive trend in Chl biomass and an increase in the amplitude and duration of the phytoplankton growing period is observed. On the contrary, changes in Chl concentration in the eastern (and more oligotrophic) basin are generally low, but it is observed that the Chl peak has declined and the growing period duration has also decreased. The trends in phytoplankton Chl and phenology, estimated in this study during the 1998-2014 period, do not reveal significant overall decline/increase in Chl concentration or earlier/delayed timings of the seasonal peak on average over the entire Mediterranean Sea. However, large regional variations are detected, suggesting that the response of phytoplankton to environmental and climate forcing may be complex and regionally driven.

The second study addresses the regional patterns of interannual variability in satellite-derived Chl. A neural network classification, based on the Self-Organizing Maps (SOM) analysis in the time domain, is used to reveal regions of similar temporal variability of Chl in the Mediterranean Sea. Characteristic temporal patterns extracted by the SOM analysis show different scales of variation

that can be related to already identified oceanographic features and biogeochemical variability in the Mediterranean Sea. Clear differences are observed between regions located in the western basin and Adriatic Sea, where rivers, winter mixing and winds are known to drive variations in primary production at regional scale and regions located in the eastern basin, represented by a large and rather homogeneous region. The study suggests that North Atlantic Oscillation (NAO) has more influence in the Chl variations occurring in regions located in the western basin whereas *El Niño* Southern Oscillation index (ENSO) exhibits higher impact on the central Mediterranean and eastern basin during its positive phase. Both NAO and ENSO show non-stationary coherence with Mediterranean Chl. The analysis also reveals a sharp regime shift occurring in 2004–2007, when NAO changed from positive to negative values. This shift particularly affected the winter phytoplankton biomass and it is indicative of climate driven ecosystem-level changes in the Mediterranean Sea. Our results stablish a regional connection between interannual phytoplankton variability exhibited in different regions of the Mediterranean Sea and climate variations.

The third study focusses on satellite derived primary production rates in the coastal waters of the Mediterranean Sea. We observe that 20% of the overall PP in the basin comes from shelf regions (i.e. <200m depth) and from that, most of it (~80%) is regenerated production. Almost 50% of this production occurs in the coastal waters of the eastern basin, whereas the western and Adriatic shelf contribute with 28 and 24% respectively. High regional scale variability is observed ranging from more than 350 gC m^{-2} yr^{-1} in the most productive areas, generally associated with major river discharges, to highly unproductive provinces (<50 PgC m^{-2} yr^{-1}) in the south eastern Mediterranean. The long-term PP variability was dominated by interannual variations that were inversely correlated in with sea-surface temperature and more loosely with NAO and Mediterranean Oscillation Index (MOI) climatic indices. Regionally, most coastal areas presented either non-significant or weakly declining PP trends whereas positive PP trends were observed in the Adriatic region. To complete the study, a classification has been made in 18 alongshore coastal regions with mean PP magnitudes varying fivefold. Two groups of coastal waters were identified; regions showing low cross-shore variability, mainly located in narrow width shelf areas, and regions showing strong cross-shore gradients, observed in wider regions with river discharges.

Approximately 50% of the global primary production takes place in the ocean and, consequently, marine phytoplankton play a fundamental role in global carbon fluxes. Studying the spatial and temporal variability of phytoplankton, as well as estimating factors that determine this variability, is essential to understand the dynamics, productivity and biogeochemical cycles of the ocean, and to anticipate the effects of climate change on the marine environment. It is expected that this PhD thesis can contribute to a better understanding of these changes in the Mediterranean Sea.

RESUMEN

La presente tesis doctoral tiene como objetivo evaluar los patrones espaciales y temporales de la variabilidad del fitoplancton marino y la producción primaria en las aguas superficiales del mar Mediterráneo. La investigación se organiza en tres estudios y se basa principalmente en el uso de datos de satélite del color del océano adquiridos durante el período 1998-2015. Asimismo, datos complementarios (por ejemplo, temperatura superficial del mar, índices climáticos, datos meteorológicos o concentración de polvo atmosférico) son utilizados para abordar cuestiones específicas.

El primer estudio tiene como objetivo analizar la contribución de las componentes estacionales y no estacionales de la variabilidad del fitoplancton en la cuenca del mar Mediterráneo. La componente estacional se aborda mediante la caracterización de la fenología del fitoplancton; es decir, mediante la parametrización de los ciclos estacionales su periodo de floración (*bloom*). Para ello, se ha utilizado un algoritmo basado en detección de umbrales de crecimiento de la biomasa de fitoplancton que ha sido ejecutado píxel a píxel. Los resultados demuestran que la variabilidad debida a la componente estacional puede suponer hasta el 80% de la varianza total de clorofila (Chl) en áreas oceánicas, mientras que en las regiones de plataforma continental la variabilidad de alta frecuencia puede dominar y representar hasta un 49% de dicha variabilidad total de Chl. Las variaciones estacionales típicamente se caracterizan por un período de crecimiento del fitoplancton que se produce en primavera y abarca en promedio 170 días en la cuenca oeste u occidental y 150 días en la cuenca este u oriental. Además, en la cuenca occidental se observa una tendencia positiva en la biomasa de Chl y un aumento en la amplitud y duración del período de floración del fitoplancton. Por otro lado, en la cuenca oriental (y más oligotrófica) las tendencias en la concentración de Chl son generalmente despreciables, pero el valor máximo de Chl alcanzado durante el *bloom* y la duración del periodo de crecimiento si muestran una disminución. A nivel de toda la cuenca del mar Mediterráneo, las tendencias en el fitoplancton y en la fenología, estimadas en este estudio durante el período 1998-2014, no revelan en promedio ni una disminución/aumento general significativo en la concentración de Chl ni un avance/retraso del valor máximo de biomasa estacional. Sin embargo, sí se detectan grandes variaciones

regionales, sugiriendo que la respuesta del fitoplancton a las variables ambientales y climáticas pueda ser compleja y local.

El segundo estudio aborda los patrones regionales de variabilidad interanual en series temporales de Chl derivadas de datos de satélites. Se utiliza una clasificación de redes neuronales de aprendizaje no supervisado basada en el análisis de Mapas de Autoorganización (SOM, de las siglas en inglés *Self-Organizing Maps*) ejecutados en el dominio temporal, con el objetivo de discernir regiones donde la variabilidad temporal de la Chl sea similar en el mar Mediterráneo. Los patrones temporales característicos extraídos a través del análisis SOM muestran diferentes escalas de variación que pueden relacionarse con las características oceanográficas y con la variabilidad biogeoquímica presente en el mar Mediterráneo. Se observan claras diferencias entre las regiones ubicadas en la cuenca occidental y el mar Adriático, donde se sabe que los ríos, la mezcla de invierno y los vientos impulsan variaciones en la producción primaria a escala regional; y también en las regiones ubicadas en la cuenca oriental, representadas por una gran región bastante homogénea. El estudio sugiere que el índice climático *North Atlantic Oscillation* (NAO) tiene una influencia mayor en las variaciones de Chl ubicadas en la cuenca occidental, mientras que el índice *El Niño Southern Oscillation* (ENSO) muestra un mayor impacto en la cuenca central del Mediterráneo, principalmente apreciable durante su fase positiva. Tanto NAO como ENSO muestran coherencia no estacionaria con la variabilidad de la Chl en el Mediterráneo. El análisis también revela un cambio brusco producido durante los años 2004-2007, cuando el índice NAO cambió de valores positivos a negativos. Este cambio afectó particularmente a la biomasa de fitoplancton en invierno y es un claro indicador del impacto climático sobre el ecosistema del mar Mediterráneo. Nuestros resultados establecen una conexión regional entre la variabilidad interanual del fitoplancton en diferentes regiones del mar Mediterráneo y las variaciones climáticas globales.

El tercer estudio se centra en las tasas de producción primaria en las aguas costeras del mar Mediterráneo estimadas mediante datos de satélites. El estudio revela que aproximadamente el 20% del total de la producción primaria de la cuenca Mediterránea proviene de áreas situadas en la plataforma continental (<200 m de profundidad) y que, además, la mayor parte (~80%) constituye producción regenerada. Casi el 50% de esta producción ocurre en las aguas costeras de la cuenca oriental, mientras que las plataformas occidental y Adriática contribuyen con el 28 y el 24% respectivamente. Se observa una gran variabilidad a escala regional que varía desde zonas muy productivas que superan 350 gC m^{-2} al año, típicamente situadas en las áreas más productivas asociadas con descargas de ríos importantes, a zonas altamente improductivas (<50 PgC m^{-2} al año) situadas principalmente en el sureste Mediterráneo. La variabilidad de la producción primaria a largo plazo está dominada por variaciones interanuales que se correlacionan inversamente con datos de temperatura superficial del mar y, del mismo modo, aunque en menor grado, con los índices climáticos NAO y *Mediterranean Oscillation Index* (MOI). A escala regional, la mayoría de las áreas costeras presentan tendencias de producción primarias no significativas o con un débil declive. No obstante, se observan tendencias de producción primaria altamente positivas en el mar Adriático. Para finalizar el estudio, se ha hecho una clasificación en 18 regiones costeras con valores medios de producción primaria que pueden quintuplicarse entre regiones. Además, el análisis permite la identificación de dos grupos de aguas costeras: por un lado, regiones que muestran una baja variabilidad a lo largo de la costa, ubicadas principalmente en áreas donde la plataforma continental es estrecha; y por otro lado

regiones que muestran fuertes gradientes a lo largo de la costa, situadas en regiones donde la plataforma continental es típicamente más ancha y/o existen descargas de ríos.

Aproximadamente el 50% de la producción primaria mundial tiene lugar en el océano y, en consecuencia, el fitoplancton marino desempeña un papel fundamental en los flujos globales de carbono. Estudiar la variabilidad espacial y temporal del fitoplancton, así como estimar los factores que determinan esta variabilidad, es esencial para comprender la dinámica, la productividad y los ciclos biogeoquímicos del océano, y para anticipar los efectos del cambio climático en el ecosistema marino. Se espera que esta tesis doctoral pueda contribuir a una mejor comprensión de estos cambios en el mar Mediterráneo.

RESUM

La present tesi doctoral té com a objectiu avaluar els patrons espacials i temporals de la variabilitat del fitoplàncton marí i la producció primària a les aigües superficials de la mar Mediterrània. La investigació s'organitza en tres estudis i es basa principalment en l'ús de dades de satèl·lit del color de l'oceà adquirides durant el període 1998-2015. Així mateix, dades complementàries (per exemple, temperatura superficial de la mar, índexs climàtics, dades meteorològiques o concentració de pols atmosfèrica) són utilitzats per abordar qüestions específiques.

El primer estudi té com a objectiu analitzar la contribució dels components estacionals i no estacionals de la variabilitat del fitoplàncton en el conjunt de la mar Mediterrània. El component estacional s'aborda mitjançant la caracterització de la fenologia del fitoplàncton; és a dir, a costa de la parametrització dels cicles estacionals del seu període de floració (*bloom*). Per aconseguir-ho, s'ha utilitzat un algoritme fonamentat en la detecció de frontera que ha estat executat píxel a píxel. Els resultats assenyalen que la variabilitat deguda al component estacional pot suposar fins al 80% de la variància total de clorofil·la (Chl) en zones oceàniques, mentre que a les regions de plataforma continental la variabilitat d'alta freqüència pot dominar i representar fins a un 49% d'aquesta variabilitat total de Chl. Les variacions estacionals típicament es caracteritzen per un període de creixement del fitoplàncton que es produeix a la primavera i presenta de mitjana 170 dies a la conca oest o occidental i 150 dies a la conca est o oriental. A més, en la conca occidental s'observa una tendència positiva en la biomassa de Chl i un augment en l'amplitud i duració del període de floració del fitoplàncton. D'altra banda, en la conca oriental (i més oligotròfica) els canvis en la concentració de Chl són generalment menyspreables, però si que el valor màxim de Chl assolit durant el *bloom* s'ha reduït, alhora que la duració del període de creixement també ha disminuït. En referència a tota la conca de la mar Mediterrània, les tendències en el fitoplàncton i en la fenologia, estimades en aquest estudi durant el període 1998-2014, no mostren de mitjana cap disminució/augment general significatiu en la concentració de Chl ni tampoc un avanç/retard del màxim estacional. No obstant això, si que es detecten grans variacions regionals, suggerint que la resposta del fitoplàncton als forçaments ambientals i climàtics pugui ser complexa i local.

El segon estudi aborda els patrons regionals de variabilitat interanual en sèries temporals de Chl derivades de dades de satèl·lits. S'utilitza una classificació de xarxes neuronals d'aprenentatge no supervisat basada en l'anàlisi de Mapes d' Autoorganització (SOM, de les sigles en anglès *Self-Organizing Maps*) executats en el domini temporal, amb l'objectiu de discernir regions on la variabilitat temporal de la Chl sigui similar a la mar Mediterrània. Els patrons temporals característics extrets mitjançant l'anàlisi SOM mostren diferents escales de variació que poden relacionar-se amb les característiques oceanogràfiques i amb la variabilitat biogeoquímica present en la mar Mediterrània. S'observen clares diferències entre les regions situades a la conca occidental i el mar Adriàtic, on se sap que els rius, la barreja d'aigües que passa al mar a l'hivern, i els vents impulsen variacions en la producció primària a escala regional; i també en les regions situades a la conca oriental, representades per una gran regió bastant homogènia. L'estudi suggereix que l'índex climàtic *North Atlantic Oscillation Index* (NAO) té una influència més gran en les variacions de Chl ubicades a la conca occidental, mentre que l'índex *El Niño Southern Oscillation* (ENSO) mostra un major impacte en la conca central de la Mediterrània principalment apreciable durant la seva fase positiva. Tant NAO com ENSO mostren coherència no estacionària amb la variabilitat de la Chl a la Mar Mediterrània. L'anàlisi també revela un canvi sobtat produït durant els anys 2004-2007, quan l'índex NAO va canviar de valors positius a negatius. Aquest canvi va afectar particularment la biomassa de fitoplàncton a l'hivern i és indicatiu clar de canvis en el nivell de l'ecosistema impulsats pel clima en la mar Mediterrània. Els nostres resultats estableixen una connexió regional entre la variabilitat interanual del fitoplàncton en diferents regions de la Mediterrània i les variacions climàtiques globals.

El tercer estudi se centra en les taxes de producció primària a les aigües costaneres de la mar Mediterrània estimades mitjançant dades de satèl·lits. L'estudi revela que aproximadament el 20% del total de la producció primària de la conca mediterrània prové d'àrees situades a la plataforma continental (<200 m de profunditat) i que, a més, la major part (~80%) constitueix producció regenerada. Gairebé el 50% d'aquesta producció es produeix en les aigües costaneres de la conca oriental, mentre que les plataformes occidental i Adriàtica contribueixen amb el 28 i el 24% respectivament. S'observa una gran variabilitat a escala regional que varia des de zones molt productives que superen 350 gC m^{-2} a l'any, típicament situades a les àrees més productives generalment associades amb descàrregues de rius importants, fins a províncies altament improductives (<50 PgC m^{-2} al any) situades principalment al sud-est mediterrani. La variabilitat de la producció primària a llarg termini és dominada per variacions interanuals que es correlacionen inversament amb dades de temperatura superficial del mar i, de la mateixa manera encara que en menor mesura, amb els índexs climàtics NAO i *Mediterranean Oscillation Index* (MOI). En l'àmbit regional, la majoria de les àrees costaneres presenten tendències de producció primàries no significatives o amb un lleuger declivi, encara que, si bé s'observen tendències de producció primària altament positives al mar Adriàtic. S'han classificat les aigües costaneres en 18 regions amb valors mitjans de producció primària que poden variar fins a cinc vegades d'unes regions a altres. L'anàlisi permet la identificació de dos grups d'aigües costaneres: d'una banda, regions que mostren una baixa variabilitat al llarg de la costa, situades principalment en àrees on la plataforma continental és estreta; i d'altra banda regions que mostren forts gradients al llarg de la costa, situades en regions on la plataforma continental és típicament més ampla i/o hi ha descàrregues de rius.

Aproximadament el 50% de la producció primària mundial té lloc a l'oceà i, en conseqüència, el fitoplàncton marí té un paper fonamental en els fluxos globals de carboni. Estudiar la variabilitat espacial i temporal del fitoplàncton, així com estimar els factors que determinen aquesta variabilitat, és essencial per comprendre la dinàmica, la productivitat i els cicles biogeoquímics de l'oceà, i per anticipar els efectes del canvi climàtic en l'ecosistema marí. S'espera que aquesta tesi doctoral pugui contribuir a una millor comprensió d'aquests canvis a la Mediterrània.

I. GENERAL INTRODUCTION

1. Marine phytoplankton and its productivity

1.1. Phytoplankton in the ocean

Phytoplankton are free-floating unicellular microscopic algae that live near the ocean's surface where enough light reaches to support photosynthesis. They use sunlight energy and nutrients to convert inorganic to organic carbon, releasing oxygen to the environment in the photosynthesis process. Phytoplankton constitutes the base of the marine pelagic food web and, therefore, are key to life in the oceans (Field et al., 1998). Phytoplankton encompasses a wide range of organisms extremely diverse in shape and size. According to Sournia et al. (1991), there are more than 4,000 species of marine phytoplankton, including diatoms, dinoflagellates, green algae, coccolithophores and cyanobacteria, amongst the most common groups. Being the source of organic carbon in the ocean, phytoplankton is embedded in complex interactions with other components of the marine ecosystem and with the physical environment (Fig. I-1) and, thereby, is structurally and compositionally molded by these interactions. This control may be exerted by higher level organisms such as grazers ('top-down') or it can be regulated by nutrients and light availability ('bottom-up') (Cushing, 1975; Sarmiento et al., 1990). In these interactions bacteria play a fundamental role remineralizing the released Organic Carbon (Particulate and Dissolved; POC and DOC) into nutrients and providing with complex compounds that many phytoplankton species are unable to synthesize, such as some vitamins, and making them available by phytoplankton (Azam, 1998; Suthers and Rissik, 2009).

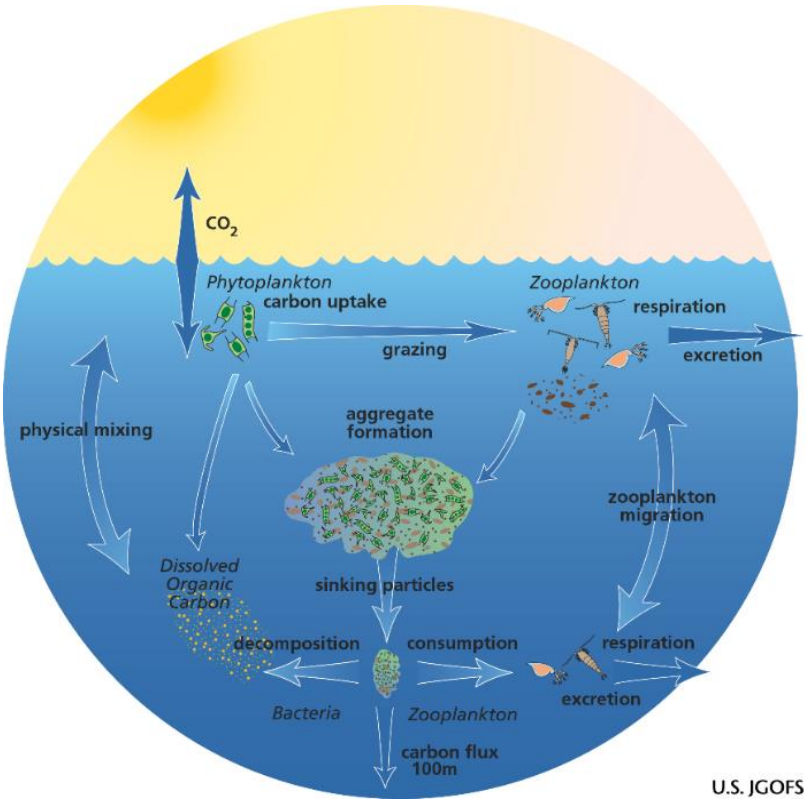

Fig I-1. Major constituents and processes composing the ocean's biological carbon pump or transfer of carbon from the atmosphere (inorganic CO_2) to the deep ocean (organic C). From Steinberg and Landry, (2017) and the U.S Joint Global Ocean Flux Study (U.S. JGOFS).

The spatial variability of phytoplankton in the sea is controlled by multiple endogenous (internal) and exogenous (external) mechanisms. The endogenous factors are related to the physiology of the organism and its life cycles, including carbon fixation, respiration and mortality rates. Phytoplankton growth mainly depends on the availability of carbon dioxide, sunlight, and nutrients. The changing light conditions and the concentrations of nutrients such as nitrate, phosphate, silicate and iron in the water determine the productivity of the water. The exogenous factors depend on the influence of the physical environment and on the interaction with other organisms (Margalef, 1974). Since it is mostly passively transported by ocean motions, marine currents, turbulence and diffusive transport regulate its distribution (Mann and Lazier, 1991; Steele, 1978). Likewise, viral infections, parasitism, competition for resources with other organisms and grazing pressure, also determine its distribution and variability patterns in the ocean (e.g. Calbet and Landry, 2004; Cushing, 1975; Park et al., 2004).

Ocean variability occurs at spatial scales spanning from microns to thousands of kilometers, and at time scales extending from seconds to tens of years. Different processes influence the distribution of phytoplankton attending to the scale considered. From these, remotely-sensed data, objective of this thesis, mostly resolves processes at special scales above few kilometers and temporal scales larger than days (Dickey et al., 2006; Fig. I-2). Limitations in the lower range of these scales are consequence of the sensor resolution and satellite coverage. As the spatial, temporal and radiometric sensor resolution increase, it is expected that remote sensing will serve to resolve processes at higher scales and greater accuracy.

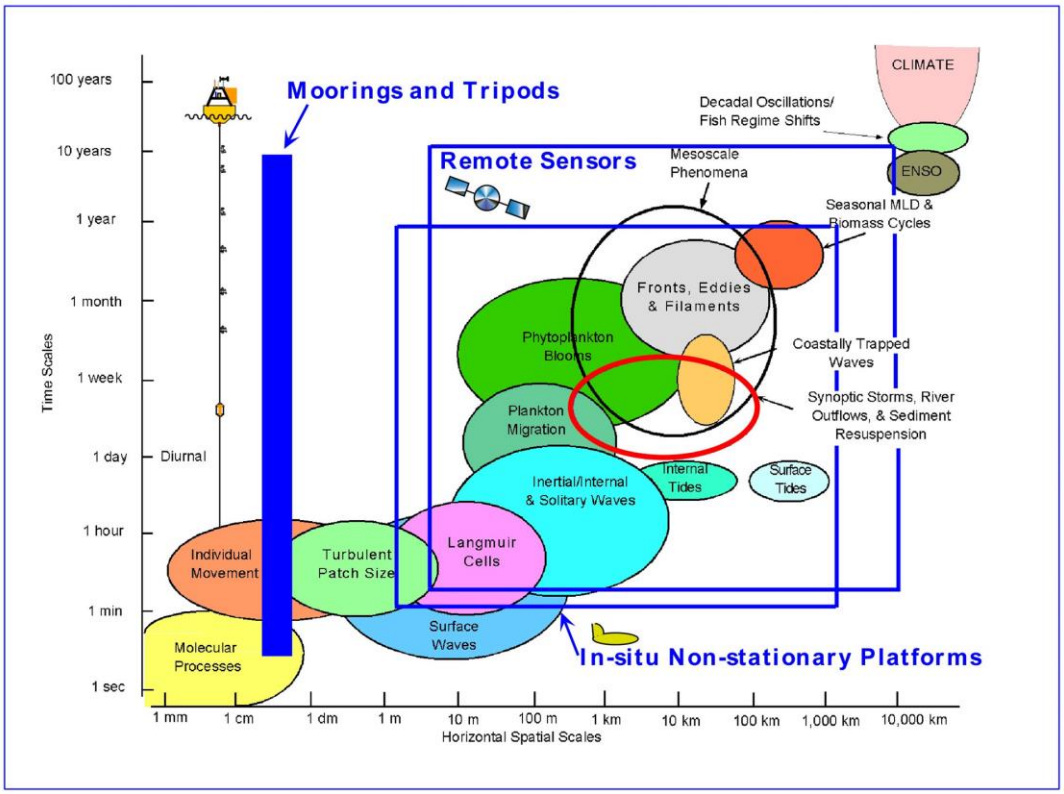

Fig. I-2. Time-horizontal space scale diagram illustrating some physical and biological processes overlain with sampling domains of various platforms (moorings, satellites, autonomous underwater vehicles, etc.) (Dickey et al., 2006).

1.2. Primary production in the ocean

Pelagic Primary Production (PP) refers to the production of organic matter by marine phytoplankton. It is the rate of carbon fixation by photosynthesis (Falkowski and Raven, 2007). As the description of the light-dependent photosynthesis reaction: $CO_2 + 2H_2O$ ---> $(CH_2O) + H_2O + O_2$, the process releases carbohydrates (CH_2O) and oxygen (O_2). Up to 50% of the carbon fixation in the planet (~5 GtC yr^{-1}) is indebted to marine phytoplankton photosynthesis, which plays a fundamental role in global carbon fluxes (Falkowski et al., 1998; Field et al., 1998). Indeed, microalgae organisms are key mediators of the biological pump that exports carbon to the deep ocean through sinking of the fixed organic matter (Antoine et al., 1996; Sathyendranath and Platt, 2007). The biological carbon pump is the part of the global carbon cycle that transfers heat-trapping carbon dioxide (CO_2) from the atmosphere and the upper ocean to the deep sea, where the carbon remains sequestered on time scales of months to millennia (Siegel et al., 2016). Thereby, phytoplankton maintains atmospheric CO_2 at significantly lower levels than would be the case if it did not exist, having a critical role in global carbon fluxes and regulating the earth's climate (Basu and Mackey, 2018; Hays et al., 2005).

The amount of carbon fixed during photosynthesis is called Gross Primary Production (GPP), whereas the amount of carbon fixed in excess of internal metabolic costs (e.g. autotrophic respiration by phytoplankton) is referred to as Net Primary Production (NPP). NPP is associated with the phytoplankton growth or phytoplankton biomass accumulation and is the value estimated by ocean color PP algorithms (Fig. I-3) (Cullen, 2001; Behrenfeld et al., 2006).

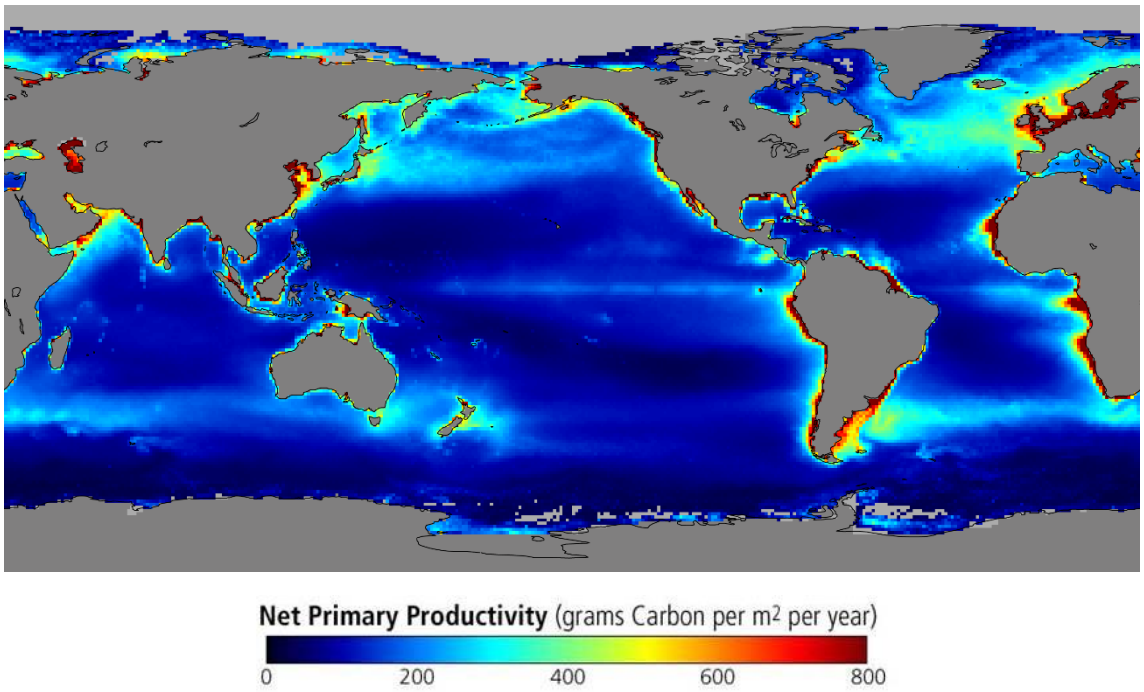

Fig. II-3. Annual NPP distribution in the global ocean from the SeaWiFS sensor (1997-2002). Light gray areas indicate missing data. Credit: NASA GSFC Earth Observatory.

There are other concepts associated with PP such as new, regenerated and export production, which need to be characterized in order to describe food web dynamics and biochemical cycling (Dugdale and Goering, 1967). New production is the fraction of NPP that is supported by the introduction of new nutrients into the euphotic zone whereas regenerated production is sustained by bacterial oxidation of organic matter. Lastly, some portion of this production is exported; i.e. fixed carbon sinks out the euphotic zone as POC from the surface layers by physical processes (Fig. I-1) (Eppley and Peterson, 1979). This ratio of export net production is referred to as the *ef-ratio* and it varies from 0 to 1, being higher in coastal and high productivity regions (Laws et al., 2011).

Variations in PP are influenced by two main factors: light intensity and nutrient availability. However, PP rates can also be controlled by other secondary drivers such as temperature, phytoplankton cell sizes and species composition (Boyd et al., 2014; Sathyendranath and Platt, 2001). Nutrient supply is supported by either its recycling through bacteria, reintroduction from deeper waters by mixing or from external sources (i.e. rivers or atmospheric deposition). The optimal macronutrient pattern of C:N:P molar ratio for phytoplankton growing is 106:16:1 (Redfield, 1934), which means that for every 106 atoms of carbon (C) phytoplankton transfer into organic matter, there is a need 16 of atoms of nitrogen (N) and 1 atom of phosphorous (P). Under these ratios, biological PP could be constrained. C is never a limiting nutrient in the environment, therefore oceans and seas are known for being N-limited (N:P < 16) or P-limited (N:P > 16) (Falkowski, 1997; Howarth, 1988; Tyrrell, 1999). Generally, N is the most common element limiting phytoplankton growth in most marine ecosystems (Vitousek and Howarth, 1991). Silica (Si) is another nutrient needed for diatoms to construct their siliceous skeleton (Brümmer, 2003). Also, the role of Iron (Fe) as limiting micronutrient in some oceanic areas was proposed by Martin and Fitzwater (1988). If Fe is introduced in the Redfield ratio, the C:N:P:Fe molar ratio for

phytoplankton growing will become 106:16:1:0.0075 (Bristow et al., 2017). Fe is an enzymatically essential trace metals for photosynthesis that might be limited in zones beyond shelves, because it mostly enters the marine environment through windblown dust (Jumars, 1993; Ward et al., 2013).

PP is also sensitive to irradiance (i.e., light intensity) and this relationship is shaped by the P-I curve (Photosynthesis versus Irradiance) reflecting the positive correlation between light intensity and photosynthesis rate. Light is limiting until it exceeds a compensation intensity level where respiration and photosynthesis is balanced (Jassby and Platt, 1976; Platt and Jassby, 1976). On the contrary, an excess of light under for example low physical mixing circumstances in the water may cause photoinhibition due to the degradation of the cellular machinery (Platt et al., 1980).

Since photosynthesis is a light-requiring process, it occurs in the upper ocean. The so-called the euphotic zone is commonly defined as the region that extends from the surface to the photic depth at which Photosynthetically Active Radiation (PAR: 400-700 nm) is reduced to 1% of its surface value (Kirk, 2011). This limit may occur at depths exceeding 100 m in oligotrophic waters to even less than 10 m in eutrophic waters (Sathyendranath and Platt, 2001). It is noteworthy that phytoplankton cells themselves are a major factor responsible for modifying the optical properties of sea water, and hence the rate of penetration of solar radiation into the ocean (Cullen, 2001; Sathyendranath and Platt, 2001).

Generally, highly productive systems are associated with dominance of larger phytoplankton such as diatoms and their contribution to the biological pump is high because fewer trophic steps are taken to produce sinking particles. Conversely, in oligotrophic systems where picoplankton are the dominant primary producers, there may be 4–5 trophic transfers before reaching a trophic level capable of producing sinking particles (Carlson et al., 2001a). This system is considered 'regenerative', and reflects complex trophic networks dominated by microbial communities (Azam et al., 1983; Fenchel, 2008) .

2. Observing marine phytoplankton from remote sensing

2.1. Ocean color remote sensing data

Ocean color sensors have provided an unprecedented view of the abundance and distribution of marine water constituents in the upper ocean, in particular of algal blooming markers such as the concentration of chlorophyll-like pigments that are proxies for phytoplankton biomass (Cullen, 1982). The development of the so-called 'ocean color' advanced techniques, coupled to the buildup of large-scale, long-term data collections, can be used systematically for characterizing and monitoring the status and trends of marine ecosystems (Barale et al., 2008; Blondeau-Patissier et al., 2014).

Ocean color remote sensing techniques allow repetitive global-coverage data over a variety of scales and resolutions that are unable to be achieved with *in situ* observations registered by oceanographic buoys or during ship-based surveys. Remote sensing of ocean color, has been applied, among other, to the analysis of phytoplankton biomass variability (Yoder et al., 1993),

detection of seasonal timings of phytoplankton blooms (Racault et al., 2012), estimates of PP (Behrenfeld and Falkowski, 1997), quantifying carbon budgeting (Field et al., 1998), influence of phytoplankton in marine fisheries (Platt et al., 2003), river plume detection and estuary influences (Cloern et al., 2014; Hopkins et al., 2013), or perceiving coastal upwelling episodes (Kudela et al., 2008; Shi and Wang, 2007). Despite its benefits and applications, optical properties derived from ocean color imagery are limited to vertically-integrated values from roughly the first spectral optical depth in the water column, and thereby do not provide information on the vertical structure (Smith and Baker, 1978). Moreover, spatial and temporal coverages of optical remotely sensed data are limited by a fixed schedule and by problems such as sun-glint, clouds, atmospheric aerosol, sensor saturation over ice, sand or snow, and high solar zenith angle (Racault et al., 2014b).

Phytoplankton biomass has been continuously monitored from ocean color sensors since the 1980s. Yet, the most widely used empirical approach for estimating chlorophyll (Chl) from satellites can involve an error by a factor of 5 or more. Such variability is due to differences in absorption, scattering and backscattering properties of the water sample (i.e., its Inherent Optical Properties, IOPs) that depend on the related concentrations of phytoplankton, Colored Dissolved Organic Matter (CDOM) and minerals (Dierssen, 2010). Empirical traditional bio-optical algorithms have built-in assumptions of oligotrophic regions with low phytoplankton biomass, whereas more productive regions contain larger bloom-forming phytoplankton (Dierssen, 2010). Detailed information on ocean color algorithms is provided in the methodological section (Section II).

2.2. Phytoplankton composition and size-structure from remote sensing data

Traditionally, remote sensing has been able to resolve successfully large and mesoscale phytoplankton distribution patterns. However, one of the present challenges of ocean color research is to obtain information on other descriptors of marine plankton such as its composition or its cell size. Phytoplankton Functional Types (PFT) are conceptual groupings of phytoplankton species, which have an ecological functionality in common either in terms of the food web or biogeochemical cycles (export of organic carbon to the deep ocean vs. local recycling). Examples include nitrogen fixers (cyanobacteria, e.g. *Trichodesmium*), calcifiers (coccolithophores), dimethyl sulphide (DMS) producers (e.g., Phaeocystis, coccolithophores, dinoflagellates) and silicifiers (e.g., diatoms) (IOCCG, 2014).

The importance of PFT rely on their different functionality in the marine ecosystem. For instance, the presence of phytoplankton with calcite skeletons diminishes the surface ocean carbonate concentration, reduces sea water alkalinity with an acidification of the surface seawater and increases the release of CO_2 to the atmosphere (Rost and Riebesell, 2004). Siliceous phytoplankton is responsible of about 40% of the total marine PP. Both calciferous and siliceous shells cause phytoplankton to sink faster, contributing to the carbon export to deep sea (Sarthou et al., 2005). Nitrogen-phytoplankton fixers are important in the new production so they are able to dissolve nitrogen gas (N_2) into available nitrogen such as ammonium (NH_4+) and dissolved or particulate organic nitrogen (Capone et al., 2008). DMS-producers generates this volatile organic compound that can escape into the atmosphere producing atmospheric sulphate aerosols that

act as a nucleus for cloud condensation that can back-scatter the radiation from the sun and therefore cause a negative feedback on temperature by cooling the earth (Keller et al., 1989).

First attempts to detect distinct phytoplankton groups from space were limited by bloom conditions; e.g. Brown and Yoder (1994) for coccolithophores, Morel (1997) for the cyanobacteria *Synechococcus*, Subramaniam et al. (1999) for the cyanobacteria *Trichodesmium* and Sathyendranath et al. (2004) for diatoms. Identifying several PFT from satellite born data requires distinguishing changes in the shape of the spectral signal of each type (e.g., changes in phytoplankton composition can lead to changes in the reflectance spectra) (Nair et al., 2008). Under this idea, Alvain et al. (2005) developed a method, named PHYSAT, which enables the identification of four different phytoplankton groups thanks to the natural variability of the optical properties of phytoplankton species. The method uses the anomalies of the normalized water-leaving radiance (*nLw*) measured by ocean color sensors at different wavelengths in the visible spectrum. Later, it associates this variability in the spectral signal to the different optical properties of the phytoplankton species. This variability is used in the PHYSAT classification to detect four dominant phytoplankton groups: *Prochloroccocus*, *Synechococcus*-like cyanobacteria, haptophytes (recently named nanoeukaryotes; Alvain et al., 2008) and diatoms.

Another way to study the phytoplankton community from space is by estimating Phytoplankton Size Class (PSC). Most studies of this type are based on the classification of Sieburth et al. (1978) that splits phytoplankton size groups into picoplankton (0.2 - 2 µm), nanoplankton (2 - 20 µm) and microplankton (20 - 200 µm). These size classes occupy different physical and chemical niches based on their nutrient-uptake ability, light-harvesting efficiency, and sinking rate through the euphotic zone (Nair et al., 2008). For example, microplankton cells are likely to sink faster out of the surface layer, and therefore are more likely to transport organic carbon to the deep, than smaller cells. It is accepted that phytoplankton size impact on export carbon flux in the global ocean (Mouw et al., 2016). Likewise, there is a general tendency for the phytoplankton community to change from small-cell dominated phytoplankton populations such as *Prochlorococcus* and *Synechococcus* in oligotrophic waters to large-cells dominated microphytoplankton cells such as diatoms in eutrophic waters like upwelling, high-latitudes and coastal regions. This is due to their high surface-area-to-volume ratio, that allows to absorb nutrients with high efficiency under nutrient-limited conditions (Chisholm, 1992; Guidi et al., 2009; Uitz et al., 2006). Furthermore, picoplankton dominant populations are tightly coupled with the microbial loop so most organic carbon is recycled by the bacteria with low export efficiency of carbon to deep ocean layers (Henson et al., 2012; Pomeroy, 1974).

Different methods are used to distinguish different PSCs from satellite data. For instance, the spectral characteristics of the absorption spectrum can be used to infer different PSC (IOCCG, 2014). Generally, when phytoplankton abundance increases, larger size-classes appear, so the absorption flatters with the increase in cell size of phytoplankton (Ciotti et al., 2002; Li, 2002). Other methods separate the phytoplankton into different size classes using High-Performance Liquid Chromatography (HPLC) to determine pigment markers (Uitz et al., 2006; Vidussi et al., 2001). Recently, Brewin et al. (2010) developed a method that calculates the fractional contribution of three phytoplankton size classes (micro-, nano- and picoplankton) to the overall Chl-a concentration using a multiple regression analysis between *in situ* and satellite data. A regional version of the model is applied in Section II - Chapter 2 of the present work. The analysis

of phytoplankton composition is still a major challenge, although relevant progress is expected as sensors with higher spectral, spatial, and radiometric resolutions become operative.

2.3. Primary production estimation from remote sensing data

Remote sensing is considered as the only presently approach able to quantify PP at global and basin scales (Falkowski et al., 1998; Lee et al., 2015). Estimates of NPP are a useful tool to quantify global carbon cycles. Despite the huge amount of data, discrete PP measurements only provide information for reduced areas at the ocean surface. As a consequence, these discrete measurements need mathematical models that quantitatively relate PP to Chl and scale up them to satellite-based estimates (Falkowski and Woodhead, 1992).

Over the past two decades, there has therefore been a concerted effort to estimate PP from satellite ocean color using models based on the following input parameters: (1) Phytoplankton biomass expressed as Chl-a, carbon concentration, or phytoplankton absorption; (2) photo-physiology or photosynthetic rates, and (3) the light field (Lobanova et al., 2018). Early models estimated PP as a simple function of sea surface remote sensing Chl acknowledging that the vertical distribution of Chl and photosynthesis is not uniform (Eppley et al., 1985; Smith et al., 1982; Smith and Baker, 1978). In a further step, the surface irradiance concept was included in the models with the concept of the constant water-column averaged quantum yield of photosynthesis for carbon fixation (Φ) to obtain a deep-integrated production value (Platt, 1986).

Platt and Sathyendranath (1988) proposed that daily irradiance and attenuation coefficients could be combined with the characteristics of pigment-biomass profiles and photosynthetic response. Under the simplified assumption of vertical homogeneity, only the photosynthetic parameters were required as auxiliary data (Platt and Sathyendranath, 1993). Photosynthetic parameters were extracted from the P-I curves in which P was normalized to Chl-a concentration which was taken as a surrogate for biomass B, (P^B). The two parameters required to describe the P-I relationship were α^B, the initial slope of the relationship, and P^B_m, the light-saturated production plateau. These parameters were derived from experiments made under light-controlled conditions in a light-gradient incubation box. This method was compared and ratified by PP measurements in other regional studies (e.g. Falkowski, 1981; Morel, 1978). In a further step ahead, more complex bio-optical models were used to estimate production over the depth-integrated water column accounting for the spectrally dependent attenuation of PAR (from 400 to 700 nm) in the euphotic zone and the vertical and spatial Chl cross-section for photosynthesis (Morel, 1991; Morel and Berthon, 1989; Platt et al., 1991).

The different satellite-derived PP models differ with respect to their computational complexity (i.e. depth and wavelength integrated versus resolved). They can be divided into three modeling approaches: (1) depth-integrated and wavelength-integrated models (e.g. Behrenfeld et al., 2005; Behrenfeld and Falkowski, 1997; Carr, 2002; Eppley et al., 1985), (2) depth-resolved and wavelength-integrated models (e.g. Armstrong, 2006; Marra et al., 2003) and at a more complex level, (3) depth-resolved and wavelength-resolved models (e.g. Antoine and Morel, 1996; Smyth et al., 2005; Westberry et al., 2008). In general, PP from satellite-derived estimations underestimate the observed variance of PP, mainly at low PP values (<0.2 gC $m^{-2}d^{-1}$) but still they

are an key resource for biogeochemical and ecological studies at global and regional scales (Friedrichs et al., 2009).

Behrenfeld and Falkowski (1997) pointed out that the big challenge of PP estimations was to control the optimal assimilation efficiency of the productivity profile; i.e., modelling the temperature-dependent P^B_{opt} parameter. They developed a Vertically Generalized Production Model (VGPM) which was a light-dependent, depth-integrated model for carbon fixation that accounts for the influence of the euphotic zone, the Chl in the integrated photosynthetic depth and the temperature. The VGMP is called 'vertically generalized' because is based on the use of a large data base of open ocean vertical PP profiles (^{14}C determinations) that were normalized to get an average PP profile shape to be used at global scale. As a different strategy to modeling PP but under the same depth- and wavelength-integrated approach, Behrenfeld et al. (2005) modelled productivity by using remote sensing retrievals of particulate backscattering coefficients to estimate phytoplankton carbon concentration instead of the traditional Chl biomass. The method is referred to as the Carbon-based Production Model (CbPM) and it relates productivity to the product of carbon biomass and phytoplankton growth rate, rather than the product of Chl biomass and photosynthetic efficiency (quantum yield) which is dependent on light acclimation, nutrient stress and physiological variability implied by taxonomy.

As an example of the depth-resolved and wavelength-integrated approach, Armstrong (2006) determined PP through an optimality-based model of nitrogen allocation and photoacclimation determined as a function of light and temperature assuming that Chl was constant over the euphotic zone and equal to the one at the surface. Alternatively, Marra et al. (2003) based their PP estimations on Chl-specific phytoplankton absorption, parameterized empirically as a function of Sea Surface Temperature (SST), and considering that absorption by photosynthetic pigments differ from the total absorption of the water components, being the second one used to estimate light attenuation in the water column.

The more complex algorithms concern depth- and wavelength-resolved models. An example of these models is the algorithm developed by Antoine and Morel (1996), an improved 'satellite' version of the light-photosynthesis model by Morel (1991). This model derives the spectrally-resolved instantaneous PP (λ, z, t), at depth (z) of the water column, time of the day (t), and for absorption of irradiance at wavelength (λ). Another sophisticated model is the carbon-based algorithm of Westberry et al. (2008). This model is an expansion of the CbPM that includes information on the subsurface light field and the nitracline depth to parameterize photoacclimation and nutrient stress throughout the water column.

In the present thesis we use the algorithm developed by Antoine and Morel (1996). The method has been successfully applied before for estimating PP in the Mediterranean basin (Antoine et al., 1995; Morel and André, 1991) and at global scale (Antoine et al., 1996; Antoine and Morel, 1996). More details of the wavelength- and depth-integrated PP method used in the present thesis are given in Section III – Chapter 3.

3. The Mediterranean Sea

3.1. General characteristics of the study area

The Mediterranean Sea is a marginal and semi-enclosed sea composed of two main basins: the western and the eastern one (also called occidental and oriental basins), separated by the Sicily strait. To the north, the Adriatic basin is separated from the eastern sink by the Strait of Otranto. It is connected to the Atlantic Sea through the Strait of Gibraltar, to the Black Sea through the Turkish strait system (Dardanelles Strait, Sea of Marmara, Bosphorus Strait) and to the Red Sea through the artificial narrow Suez Canal (Durrieu De Madron et al., 2010). It comprises an area of 2.5 million km^2 with a width of 3,860 km in longitude and 1,600 km in latitude, and it has a perimeter of 26,000 km of coast. The average depth is 1,500m and the maximum depth and a maximum depth of 5,150 m is reached in the Ionian Sea (Millot and Taupier-Letage, 2005) (see Mediterranean bathymetry in Fig. I-4).

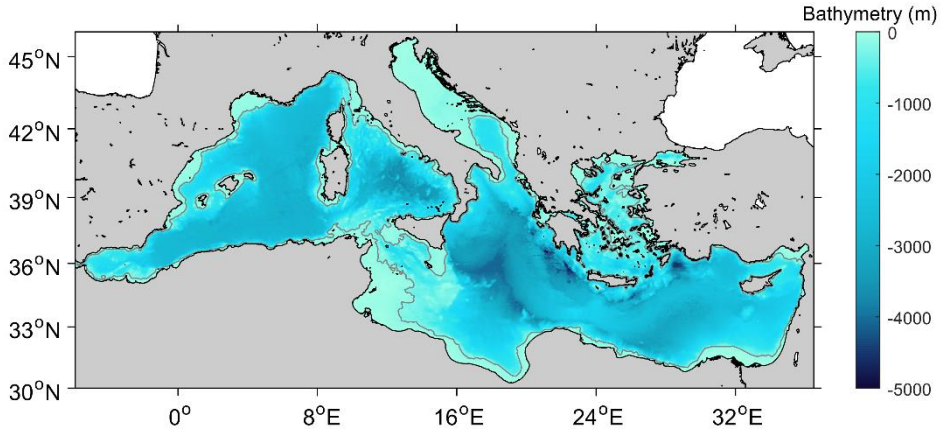

Fig. I-4 Mediterranean Sea bathymetry. Gray contour line delimits coastal waters (200 m isobath). Bathymetric data were obtained from ETOPO 1 (Amante and Eakins, 2009).

The Mediterranean Sea has been considered as a 'small-scale ocean' or 'laboratory basin' since it presents a wide range of physical processes occurring on global scales (Lacombe et al., 1981; Robinson and Golnaraghi, 1993). It has a three-layer thermohaline circulation with a surface (from 0 to ~150 m depth), intermediate (~150 - 400m), and deep layer-system (>400m); and presents some sub-basin gyres defined by the geometry and topography of the basin, similar to those occurring in the world ocean (Bethoux et al., 1990). The Atlantic water enters the Gibraltar Strait in the upper part of the water column (surface layer) and during its path towards the east, it progressively mixes with the saltier resident Mediterranean waters. The Atlantic flow is characterized by intense mesoscale activity and it creates an accumulation of quasi-permanent cyclonic gyres and eddies such as those observed in the Algerian, Ionian and Levantine basins (Hamad et al., 2005; Millot, 1999). In the latter basin, continental winds and increasing evaporation rates force part of the Atlantic water to sink down to the intermediate layer forming the Levantine Intermediate Water, that flows back to the Atlantic through the Strait of Gibraltar after having crossed westward the entire basin (Fig. I-5; Nittis and Lascaratos, 1999).

The Mediterranean basin presents three regions where dense water formation processes occur and where surface waters are transformed into intermediate waters; the Gulf of Lion-Ligurian Sea

in the northwester Mediterranean, the southern Adriatic Sea and the Rhodes gyre in the Crete region (Bergamasco and Malanotte-Rizzoli, 2010; Macias et al., 2018). Fig. I-5 upper shows the main circulation paths, eddies and dense water formation structures. The water circulation in the Mediterranean Sea, although relatively complex, is the result of three fundamental driving mechanisms: the deficit of water in the basin (evaporation exceeds precipitation and river runoff), the Coriolis effect due to Earth rotation (air and water masses rotate clockwise in the northern hemisphere- cyclonic movement in the same direction as the Earth's rotation) and the mesoscale variability (generally induced by the topographic structure and instability of along-slope currents or by the atmospheric wind forces; Fig. I-5 down) (Millot and Taupier-Letage, 2005).

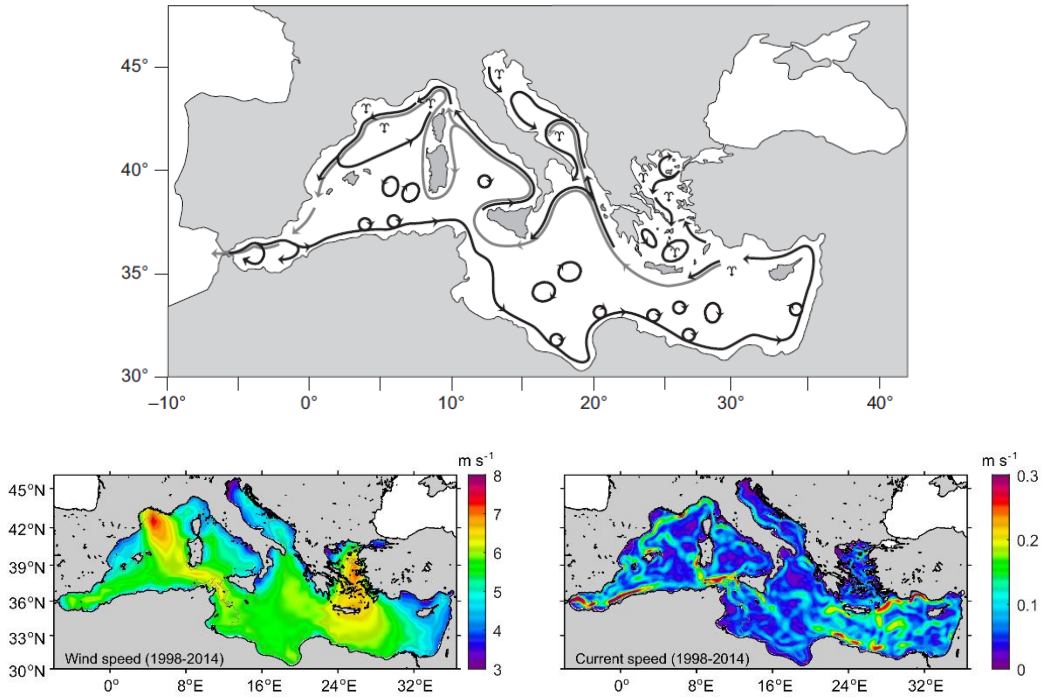

Fig. I- 5. Upper: Main circulation features of the Mediterranean Sea (surface circulation is in black, intermediate circulation is in grey, symbol ϒ indicates site of dense water formation). Upper figure taken from Durrieu De Madron et al. (2010). Down figure: mean distribution of wind speed and current speed mean values during the period 1998-2014. Data was obtained from the European Center for Medium-Range Weather Forecast (ECMWF), available at: http://apps.ecmwf.int/datasets/data/interim-full-daily/levtype=sfc/.

From a climatological perspective, the Mediterranean Sea is characterised by hot, humid and dry summers with mild and rainy winters. SST range from minima of ~12°C in winter to maxima of ~25°C in summer (Lionello et al., 2006). Mean SST values decrease from the north towards the south whereas mean salinity values increase from the western towards the eastern basin (Fig. I-6). The climatic indices that mostly affect the Mediterranean region are the North Atlantic Oscillation index (NAO), El Niño Southern Oscillation index (ENSO) and the Mediterranean Oscillation index (MOI). Both NAO and ENSO are atmospheric modes of variability with stronger impacts on global climate during the North Hemisphere winter, but they trigger a cascade effects that also affects conditions in the European and Mediterranean region (Brönnimann, 2007; Hurrell and Van Loon, 1997; Jacobeit et al., 2001; Mariotti et al., 2002b; Marshall et al., 2001; Pozo-Vazquez et al., 2001).

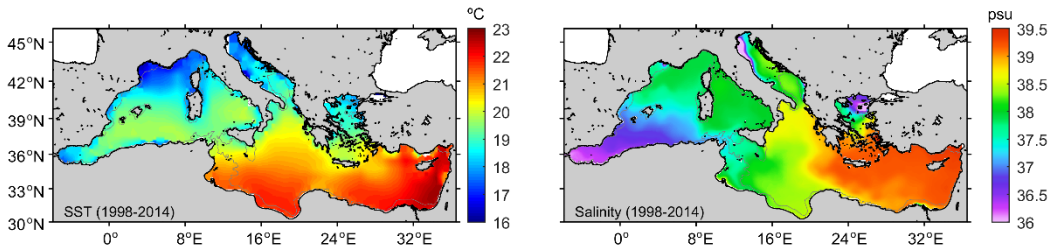

Fig I-6: Mean distribution of surface Sea Surface Temperature (SST) and Salinity during the period 1998-2014. Grey contour line delimits coastal waters (200m isobath). Monthly data was obtained from the Mediterranean physics reanalysis carried out by CMEMS, available at http://marine.copernicus.eu/

From a biogeochemical approach, the Mediterranean Sea presents a west-to-east gradient of increasing oligotrophy with an average Chl value of 0.3 and 0.05 mg m m^{-3} in the western and eastern basin (Santoreli et al., 2008). It is considered one of the most oligotrophic seas of the world and some authors contemplate the ultra-oligotrophic character of the eastern basin, where its average phytoplankton productivity is 60 - 80 gC m^{-2} yr^{-1}, which is half that measured in other oligotrophic areas of the world's ocean (Krom et al., 2010). This difference has been attributed to the combination of the anti-estuarine circulation with nutrient-richer waters in the western side, and the biological pump (Crise et al., 1999). The eastern basin is the largest body of water in the world in which the PP is P-limited rather than N-limited (Bethoux, 1989; Krom et al., 2003, 1991). N:P ratios considerably higher than 16:1 have been commonly viewed as indicators of P limitation in the sea (Morán et al., 2001). Although the typical winter phytoplankton bloom is usually due to a lack of phosphate, there is a well-marked north-south gradient for nitrates (Fig. I-7; Lazzari et al., 2016).

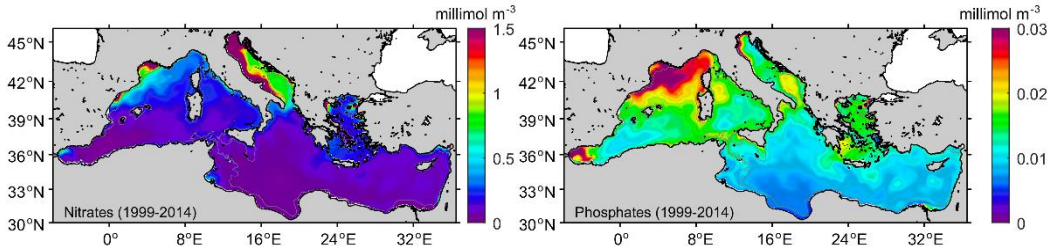

Fig I-7: Mean distribution of surface nitrate (NO_3) and phosphate (PO_4) during the period 1998-2014 at 1.472 m depth. Grey contour line delimits coastal waters (200m isobath). Monthly data was obtained from the Mediterranean Biochemistry reanalysis carried out by CMEMS available at http://marine.copernicus.eu/

Notwithstanding the oligotrophic character of the global basin, there are also enriched regions where PP increase substantially. The most productive regions of the Mediterranean Sea are the coastal regions and the north-western Mediterranean Sea (NWMS), with blooming regimes where Chl peak can be >1 mg m^{-3} (D'Ortenzio and Ribera d'Alcalà, 2009). In the NWMS, Marty et al. (2002) reported that nitrate and phosphate concentrations may reach, respectively, 2 - 3 µmol kg^{-1}, 0.15 - 0.2 µmol kg^{-1} in surface layers during winter mixing conditions.

Nutrients in the Mediterranean Sea come from atmospheric deposition or from external inputs of water. In both cases, their temporal dynamics response to the sum of natural and anthropogenic inputs (Ludwig et al., 2009; Moon et al., 2016). External sources of water are the

inflow of the Atlantic water jet in the surface layer through the Strait of Gibraltar (14,5 km wide and 320 m deep), water inflow from the Black and Marmara Seas into the north Aegean Sea, precipitations across the Mediterranean catchment basin and also, freshwater rivers inputs discharges along the coast. River discharge variability is mainly driven by precipitation events and large-scale climate modes. The annual mean river discharge into the Mediterranean basin is about 8,000 m^3 s^{-1} with dominant contributions from the European side. Major freshwater river inputs into the Mediterranean Sea occurs in the north Adriatic Sea (total annual discharge contribution of 2,700 m^3 s^{-1}, 57% coming from the Po River), in the Gulf of Lions (freshwater flux average of 1800 m^3 s^{-1}, 95% coming from the Rhone River), the Aegean Sea (adding about 500 m^3 s^{-1}, mainly due to the Danube discharge into the Black Sea), and also in the Nile Estuary region (Nile River supporting with a flux of 1400 m^3 s^{-1}). Seasonal river cycles in the north western side, placed in the Adriatic, Gulf of Lions and Aegean Sea, have two maximum river discharge capacity in fall-winter and spring due to intense precipitations and snowmelt processes, and a dry season in mid-summer. Contrary, in the eastern side, represented by the Nile River in the North African coast, the maximum discharge rate occurs between spring and autumn where intense precipitations fall during the summer months. Nonetheless the external sources of water into the Mediterranean basin, evaporation exceeds precipitation budget all year round (Ludwig et al., 2009; Struglia et al., 2004).

The Mediterranean Sea has a continental shelf (<200 m bathymetry, see Fig. I-4 for limits) that corresponds to a 21% of the surface area of the entire basin, 3-times higher than the percentage for the global ocean (7% of the total surface; Gattuso et al. (1998). The existance of an intense urbanization, industrial and agriculture activities along the 46,000 km coastline entiles a potential massive input of localized terrestrial organic matter, nutrient through run-off and groundwater discharges (Rodellas et al., 2015). External inputs of nutrients play a significant role in sustaining marine productivity in oligotrophic seas such as the Mediterranean Sea.

Physical processes, such as advection or mixing mainly control the fluxes of matter from the coastal enriched areas to the depleted interior of the basin. Currents on the shelves are driven mainly by wind forcing, freshwater inflows and by the influence of slope current circulation (Fig. I-5). The thermohaline circulation flow basically follows the basins' boundaries and, consequently, it is possible for the large-scale currents eventually intrude on the shallower coastal regions provoking an exchange of matter between the shelf and the slope waters (Durrieu De Madron et al., 2010).

3.2. Phytoplankton composition in the Mediterranean Sea from remote sensing

The different phytoplankton species and/or functional groups contribute in a different proportion way to carbon fixation rates in the ocean (more information in sub-head 2.2). This has encouraged the development of algorithms for discriminating distinct groups of phytoplankton (species or size classes) from ocean color remote sensing in the Mediterranean Sea (Ciotti and Bricaud, 2006; Di Cicco et al., 2017; Navarro et al., 2014; Sammartino et al., 2015; Uitz et al., 2012). The discrimination of the main PFT in the Mediterranean Sea, was addressed by Navarro et al. (2014). They adapted version the PHYSAT method to estimate the dominant group. They observed the dominance of picoplankton during spring-summer months, but higher nanoplankton abundance

during the autumn-winter period. More recently, Di Cicco et al. (2017) complemented the results of the PHYSAT-Med, including the estimation of the dominant PSC using a similar approach than Uitz et al. (2012). They used a class specific bio-optical model based on empirical relations between the Chl and the signal from different pigments as marker for the main algal groups. This specific procedure for the Mediterranean Sea is applied in Section II - Chapter 2 of the present study. PSC spatial distribution studies have shown that that micro- and nano-phytoplankton such as diatoms and haptophytes generally dominate in the western basin and coastal areas whereas in the eastern ultra-oligotrophic waters pico-phytoplankton size classes such as Prokaryotes predominate over the other groups. Some other studies report a similar spatial pattern (Ignatiades et al., 2009; Siokou-Frangou et al., 2010).

4. Objectives

This PhD thesis aims to study the spatial and temporal variability of phytoplankton and primary production in the surface waters of the Mediterranean Sea. The study is based on the use of remote sensing data and seeks to provide a global perspective. Although there are previous studies of phytoplankton in the Mediterranean Sea, they are mostly focused on climatological issues and/or regional aspects. This thesis aims to fulfill specific aspects that have not been addressed until now, such as phenological trends, climate induced regional variability or coastal primary production. The following specific objectives are addressed:

1. To characterize the seasonal and non-seasonal components of phytoplankton variability in the Mediterranean Sea, as well as the long-term trends phytoplankton biomass and phenology.

2. To investigate the regional differences in the response of phytoplankton biomass to climate induced variability.

3. To analyze primary production in the coastal Mediterranean Sea, its contribution to basin scale production and the regional differences in carbon fixation rates.

These issues are addressed using 17 years (1998 – 2015) of ocean-color remote sensing datasets as well as other complementary information such as remote sensing SST, nutrients reanalysis (i.e. nitrates and phosphates), mixed layer deep, meteorological data (e.g. precipitation, climatic indices) or atmospheric dust concentration.

5. Structure of the thesis

The present thesis is structured in five main Sections (I to V). The first section includes an introduction to the subject and identifies the objectives of the research. The second section deals with the common methodological aspects of the thesis, remote sensing concepts and main methodologies applied. The third section is devoted to the results. It is constituted by three chapters that analyze the main goals of the thesis. These chapters are structured as a collection of research articles, each one addressing specific scientific issues.

Chapter 1: This chapter characterizes the seasonal and non-seasonal patterns of variability and long-term trends of phytoplankton Chl and phenology in the open and coastal Mediterranean Sea using ocean-color data. It infers the possible natural and anthropogenic forcings that may determine this variability. Published in: Salgado-Hernanz, P.M., Racault, M.-F., Font-Muñoz, J.S., Basterretxea, G. *Trends in phytoplankton phenology in the Mediterranean Sea based on ocean-color remote sensing*. Remote Sensing of the Environment (ISSN 0034-4257), volume 221, February 2019, pages 50-64. doi: 10.1016/j.rse.2018.10.036.

Chapter 2: This chapter characterizes the open and coastal Mediterranean Sea into nine biogeographical regions attending to their Chl variability. This regionalization is based on Self-Organizing Maps (SOM) analysis in the time domain using ocean-color data. Furthermore, the influence of two teleconnection climate indices in each of the SOM-defined regions is analyzed. Published in: Basterretxea, G., Font-Muñoz, J.S., Salgado-Hernanz, P.M., Arrieta, J., Hernández-Carrasco, I., 2018. *Patterns of chlorophyll interannual variability in Mediterranean biogeographical regions*. Remote Sensing of the Environment (ISSN 0034-4257), volume 215, 15 September 2018, pages 7-17. doi:10.1016/j.rse.2018.05.027.

Chapter 3: This chapter aims to characterize phytoplankton primary production in Mediterranean coastal waters based on satellite-borne data for the period 2002-2016. It assesses the contribution of coastal waters to basin scale budgets, their interannual variability and long-term trends. Also, the contribution the different coastal regions to total coastal PP in the Mediterranean Sea is assessed. To be submitted: Salgado-Hernanz, P.M., Regaudie de Gioux, A., Antoine, D., Basterretxea, G. *Primary production in coastal waters of the Mediterranean Sea: variability, trends and contribution to basin scale budgets*.

Section IV includes a general discussion of the results achieved in this thesis and section V summarizes the conclusions.

II. GENERAL METHODOLOGY

1. Introduction to remote sensing concepts

Remote sensing is the observation and adquisition of information about an object or phenomenon without coming into direct physical contact with it from sensors aboard aircrafts or satellites platforms (Schowengerdt, 2007). The 'remote sensing' term was used for the first time in 1950 by Evelyn Pruitt in the U.S. Office of Naval Research. It was develped in the second half of the 20th century and it is now used in numerous fields including military and intelligence purposes, telecomunications or earth sciences disciplines (Barale and Gade, 2008). Remote sensing data is a useful alternative to *in situ* measurements as it provides high spatial coverage and temporal frequency. The technique is based on the use of electromagnetic radiation to obtain the desidered information. The main components of the electromagnetic spectrum are gamma-rays, x-rays, ultra-violet, visible light, infra-red, microwaves and radio-waves (Fig. II-1). Sensors specifically devoted to obtain ocean color measurements use spectral bands ranging wavelength from the visible to the near-infrared domain (380-750 nm and 750-1,400 nm respectively) (Bakker et al., 2009).

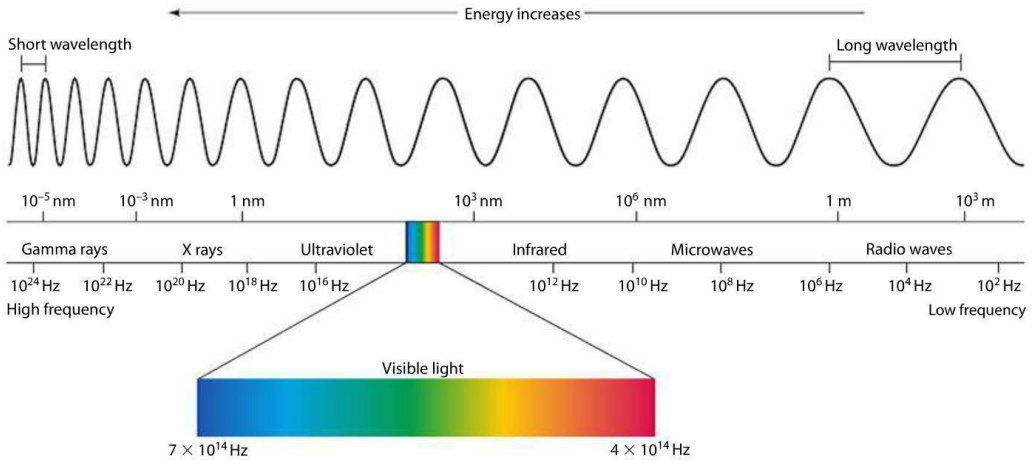

Fig II-1. The electromagnetic spectrum from the highest energy (short wavelength) to the lowest energy (long wavelength). Credit: https://www.cyberphysics.co.uk/

There are two types of sensors on board satellite platforms: passive (e.g. radiometric spectral sensors) and active sensors (e.g. radar, lidar, etc.). Passive sensors measure the energy naturally reflected or emitted by the earth surface. Active sensors provide their own source of electromagnetic radiation emitted toward the object to be studied that is later reflected back to the sensor. All data used in this thesis come from passive sensors placed in a sun-synchronous orbit, i.e., a polar orbit where the satellite always crosses the Equator at the same local solar time with an altitude from 700 to 950 km depending on the spacecraft (Bakker et al., 2009).

Sensors placed onboard satellites measure upwelling radiances that strictly include contributions by three components, the atmosphere, the water surface, and the water column (Fig. II-2). The atmospheric contribution (L_a) comes from solar radiance that is scattered by atmospheric gases and aerosols into the sensor. Hence, this signal has to be atmospherically-corrected before data exploitation. The water surface reflects the downwelling solar radiance towards the (L_r). The third component, the water-leaving radiance (L_w), comes from light that is transmitted through the surface into the ocean (L_t), where is absorbed and scattered by components in the water into an upward direction (L_u), and eventually leaves the sea surface in the sensor direction (L_w). The sensor collecting the signal measures the total radiance $L_u = L_a + L_r + L_w$ (Mobley et al., 2011). The reflected signal provides its color and is called normalized water leaving radiance (*nLw*). It is defined as the ratio between the emittance of the surface and the irradiance. *nLw*, which is called in the marine environment 'ocean-color', is determined by any substance present in the water. Therefore, phytoplankton biomass, CDOM or other sediments contribute to this signal. The quantity and distribution of the nLw is directly related to the type of surface. The spectral signature as a function of the wavelength is characteristic of the natural variability of a given material type.

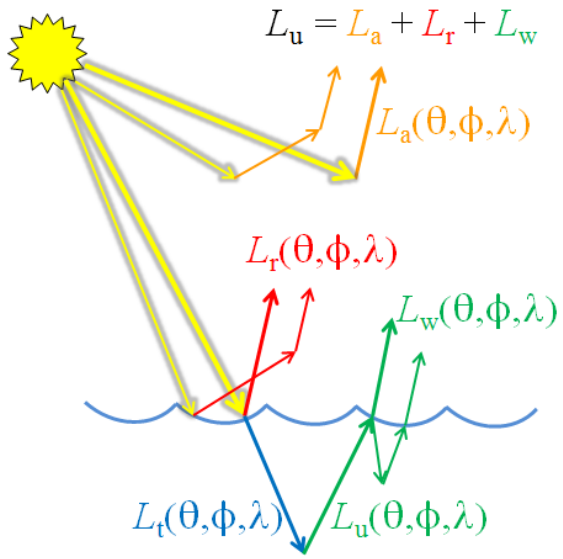

Fig. II-2. Contributions to the total upwelling radiance above the sea surface (L_u) . Yellow arrows are the sun's unscattered radiation; orange arrows are atmospheric path radiance (L_a); red is surface-reflected radiance (L_r) ; green is water-leaving radiance (L_w); blue is light transmitted through the surface into the ocean (L_t). Thick arrows represent single-scattering contributions; thin arrows illustrate multiple scattering contributions. From Mobley et al. (2011) and http://www.oceanopticsbook.info/.

Remote sensing data is provided in different degrees of processing. The concept of different processed remote sensing levels was first defined by the National Aeronautics and Space Administration (NASA) in 1986 as part of its Earth Observation System (EOS) and it has been mantained since then (Table II-1). The remote sensing parameter from which this thesis is based is Chl. Chapter 1 and 2 in Section IV uses a highly processed L3 data whereas Chapter 3 in Section IV uses L2 data. Futher specifications of the algorithm used in each level is given at each corresponding chapter in Section III, but they all rely on the same blue to green ration of the *nLw* that quantifies the amount of light reflecting from the ocean surface (O'Reilly et al., 1998a).

Table II-1: Level of remote sensing data process and description.

Level	Description
L0	Reconstructed unprocessed instrument data at full resolutions
L1a	Reconstructed unprocessed instrument data at full resolution, time referenced, and annotated with ancillary information, including radiometric and geometric calibration coefficients and georeferencing parameters (i.e., platform ephemeris) computed and appended but not applied to the Level 0 data.
L1b	Level 1a data that have been processed to sensor units (e.g, radar backscatter cross section, brightness temperature, etc.). Not all instruments have Level 1b data
L2	Geophysical variables at the same resolution and location as Level 1 source data. E.g.: Chlorophyll (Chl-a), sea surface temperature (SST), sea level height (SSH), etc.
L3	Geophysical variables mapped on uniform spacetime grid scales, usually with some completeness and consistency (e.g. missing points interpolated, complete regions mosaicked together from multiple orbits, etc.).
L4	Model output or results from reanalyses of lower level data (i. e., variables that were not measured by the instruments but instead are derived from these measurements). E.g: salinity (S), mixed layer depth (MLD), Nitrate (NO_3), Phosphate (PO_4), primary production (PP), current velocity, wind).

2. Ocean color

2.1. Optical principles

Sensors that measure color of the ocean refer to the visible part of the electromagnetic spectrum (Fig. II-1). Variations in the absorption and scattering of light (water-leaving radiances or remote sensing reflectance) are controlled by the amount and type of the constituents of ocean water that absorb and scatter light in the visible domain. They include phytoplankton, CDOM, or also called yellow substances, and suspended sediments such as detritus or inorganic matter (Morel and Prieur, 1977). They are the principal substances in sea water that contribute to variations in its IOPs, so they are the principal causes of changes in ocean color. Pure water absorbs more strongly long wavelength light (red, orange and yellow) than short wavelength light (blue), so blue light is what gets returned. But then, Chl pigments in phytoplankton absorb more blue and red light than green, so as the concentration of phytoplankton pigments increases, energy reflected from the sea surface ocean changes progressively from blue to green (Yentsch, 1960).

Morel and Prieur (1977) introduced an optical water classification into Case-I and Case-II waters, being Case-I waters those where the variability due to phytoplankton dominates the IOPs of the signal whereas in Case-II waters there is a higher contribution to IOPs from substances other than phytoplankton such as CDOM from terrestrial runoff or benthic inputs, mineral particles or microbubbles. In an ideal sample of Case-I waters, reflectance values would present low minimums in the 440 - 443 nm (blue) and around 665 - 700 nm (red), corresponding to the two maximum peak absorption of Chl pigments. On contrary, the minimum absorption and the maximum reflectance is around 500 - 555 nm (green light), explaining why Chl appears green in the visible spectrum.

However, some spectral limitations exists in Case-II waters, typically placed in turbid waters with bottom resuspension such as near-coastal waters or estuarine regions due to the complexity of separating the various contributions to the spectrum of visible light emerging from the sea surface (Sathyendranath et al., 2017). Morel and Prieur (1977) emphasized that these ideal cases are not encountered in nature but they suggested the use of high or low values of the ratio of pigment concentration to scattering coefficient as a basis for discriminating between the two types of water (Mobley et al., 2004).

2.2. Ocean color sensors

Several ocean color sensors have been developed to monitor the ocean waters since the early 70s, (Fig. II-3). The pioneer sensor developed specifically to study ocean-color properties was the Coastal Zone Color Scanner (CZCS), aboard the Nimbus 7 satellite. It was launched in 1978 and remained operational until 1986 (Evans and Gordon, 1994). A decade later, the Ocean Color and Temperature Scanner (OCTS) was launched by the Japanese Space Agency (NASDA) in November 1996 and it collected data during seven months. The next major advance in ocean color remonte sensing was the Sea-viewing Wide Field-of-view Sensor (SeaWiFS) onboard the Orview-2/SeaStar spacecraft, developed by Orbital Sciences Corporation and processed by NASA. It was operative from 1997 until the end of 2010 (Hooker et al., 1992; Mcclain et al., 2004). In 2002, under the EOS program by NASA, the MODerate resolution Imaging Spectroradiometer (MODIS) aboard Terra and Aqua satellites were launched. They have been acquiring data to present, although well past their design lifespan. The MEdium Resolution Imaging Spectrometer (MERIS) onboard the ENVIronmental SATellite (ENVISAT), launched by the European Space Agency (ESA) was operational from 2002 to 2012.

Recently, a new generation of ocean color sensors with improved capabilities has been developed, including the NASA Visible and Infrared Imager/Radiometer Suite (VIIRS), flown on the Joint Polar Satellite System (JPSS) series of spacecraft since 2011, and in the JPSS-1 satellite (also known as NOAA-20) in orbit since November 2017. Also, the ESA Ocean and Land Color Instrument (OLCI) aboard both Sentinel-3A and Sentinel-3B was launched in February 2016 and April 2018, respectively. VIIRS is consider the successor to MODIS for Earth science data product generation whereas OLCI instrument is the continuity of MERIS.

Resolution is an important concept to address. Ocean color sensors have increased their temporal (days-hours), spatial (m-km), spectral (number of bands) and radiometric (generally 8, 10 or 16

bits/pixel) resolution. As concerns their spectral resolution, CZCS had 6 spectral bands. Sensors used in the current thesis have the multispectral resolution of SeaWiFS, MERIS and MODIS with 8, 15 and 36 bands respectively. Fig. II-4 shows the spectral band positions in the visible domain for each of these sensors. Out of the scope of this thesis, OLCI is the newest sensor that it will be used in future applications. It acquires data with 31 spectral bands allowing the scientists to analyze the ocean with unprecedented quality.

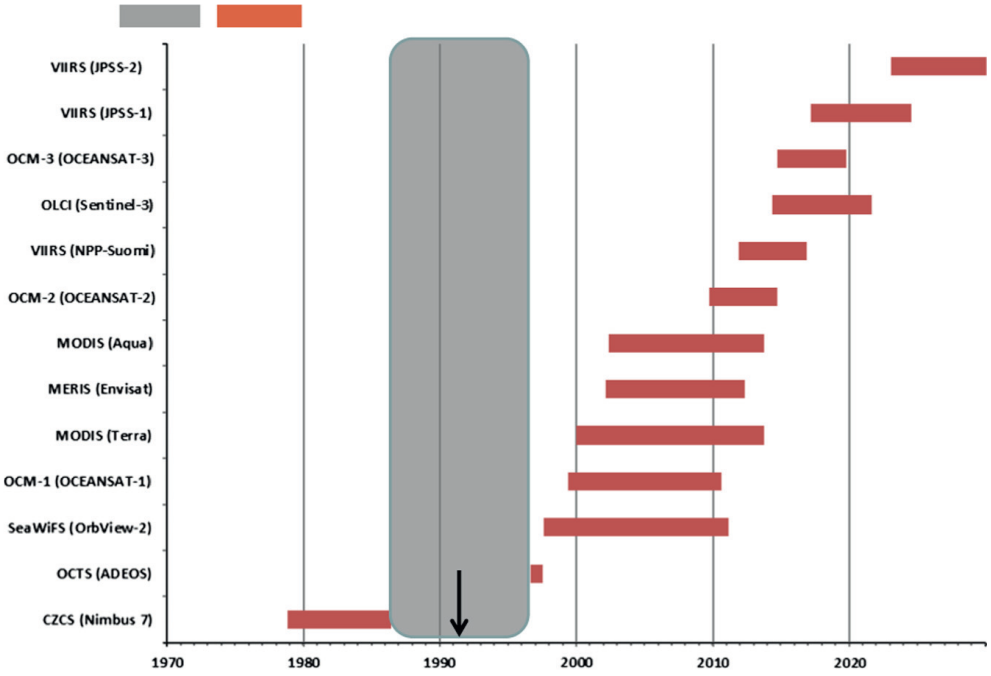

Fig. II-3. Timeline 1970–2030 illustrating past, current, and future global ocean-color sensor missions with the satellite platform indicated between brackets. Figure taken from Blondeau-Patissier et al. (2014).

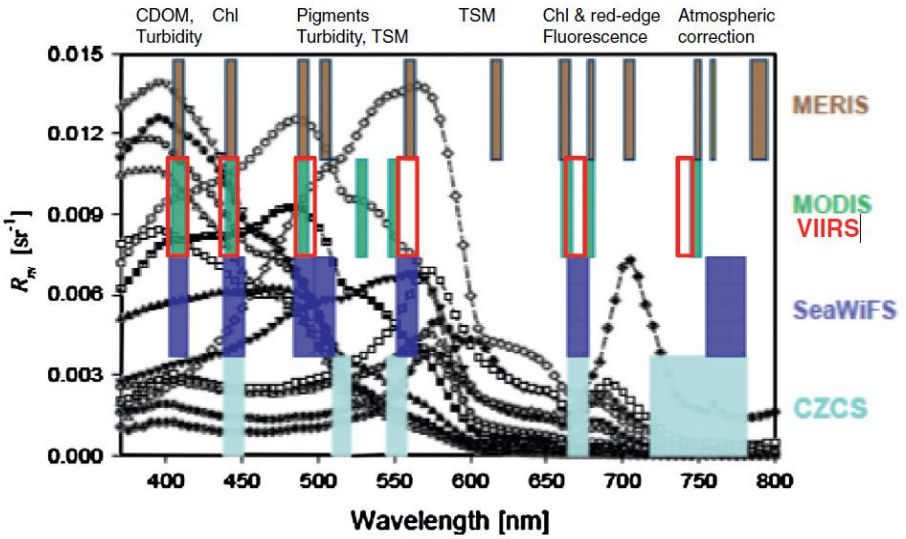

Fig. II-4. Comparison of the spectral band positions for five ocean color sensors of the first (CZCS), second (SeaWiFS), third (MERIS, MODIS) and fourth (VIIRS) generations. The potential applications for each spectral region are indicated at the top. Figure taken from Blondeau-Patissier et al. (2014). The authors used 14 remote sensing reflectance spectra from various waters around the world to do the graph.

2.3. Ocean color algorithms

A variety of bio-optical algorithms have been developed to estimate Chl concentration from the normalized water-leaving radiance above the surface (*nLw*, in W m^{-2} sr^{-1}), or the similar quantity, ocean remote sensing reflectance ($R_{rs}(\lambda)$, in sr^{-1}) at several specific wavelengths (λ). Most of the algorithms are empirical as they relate R_{rs} directly to a bio-optical property based on observations of both quantities. Indeed, a bio-optical model is derived by fitting a mean relationship from a large dataset of coincident *nLw* and Chl-a *in situ* measurements acquired in various waters (Sathyendranath et al., 2017). Spectral bands located in the blue, green, yellow, red or near-infrared portion of the reflectance spectrum can be used in many ways to detect algal blooms (Blondeau-Patissier et al., 2014; Sathyendranath et al., 2017). There are other methods beyond the empirical algorithms that allow ocean color to be expressed as a function of IOP of seawater, such as the absorption and the backscattering coefficient (Brewin et al., 2015; Sathyendranath et al., 2017).

The empirical ocean color algorithms are polynomial functions based on the *Maximum-Band-Ratio* concept that maximizes the sensor signal; that is, it maintains the highest possible satellite sensor signal:noise ratio over a 3-orders-of-magnitude range in Chl concentration (O'Reilly et al., 1998a). These algorithms use the spectral irradiance reflectance (R, dimensionless), which is a $R_{rs}(\lambda)$ ratio at different wavebands within the visible spectrum. The dissimilarity between the algorithms variants is based on different $R_{rs}(\lambda)$ at two, three or four wavelengths between 440 and 670 nm depending on the sensor (Werdell and Bailey, 2005). Main algorithms are: the Ocean-Chlorophyll 2-band (OC2) and its updated Ocean-Chlorophyll 4-band (OC4) version for SeaWiFS (O'Reilly et al., 2000, 1998a), the Ocean-Chlorophyll 3-band (OC3) variant algorithm for MODIS, the Ocean Color Index (OCI) for MERIS proposed by Hu et al. (2012) for clean waters with Chl ≤ 0.25 mg m^{-3} (which employs the difference between R_{rs} in the green band (R_{555}) and a reference formed linearly between R_{rs} in the blue (R_{443}) and red bands (R_{670}), and the semi-analytical MERIS Chlorophyll algorithm (OC4Me) which is the latest version of the MERIS pigment index algorithm also used in the OLCI sensor (Morel et al., 2007). The OC4Me, is a semi-analytical algorithm, so it considers the spectral inherent optical properties, namely the absorption coefficient a(λ) and the backscattering coefficient b(λ), into a simplified solution of the radiative transfer equation. In the case of the Mediterranean Sea, several regional algorithms have been developed, such as DORMA-SeaWiFS (D'Ortenzio et al., 2002), BRIC-SeaWiFS (Bricaud et al., 2002), MedOC4-SeaWiFS (Volpe et al., 2007), MedOC3-MODIS and MedOC4ME-MERIS (Santoreli et al., 2008).

As an attempt of merging the different sensor-specific data records of $R_{rs}(\lambda)$ to produce a coherent record of ocean color data, the Climate Change Initiative (CCI) program was created in 2010. The CCI exploits the full potential of long-term, global, Earth Observations archives that organizations such as NASA or ESA had established over the past 30 years. The ESA Ocean Color-CCI (OC-CCI) is committed to merge ocean-color data using SeaWiFS, MODIS, MERIS sensors and, in the newest versions, VIIRS and OLCI sensors. It provides global scale, high-quality, bias-corrected and error-characterized data record of ocean color. Merging CZCS data has not been possible due to the absence of overlapping periods with the rest of the sensors, so no inter-sensor bias was possible (Sathyendranath and Krasemann, 2014). Recently, some research studies are using the OC-CCI and its associated products, such as the Copernicus Marine Environment

Monitoring Service (CMEMS) funded by the European Union with a catalogue for global and regional oceanographic products (e.g. Mediterranean Sea, Black Sea, Artic Sea or Baltic Sea).

3. Main methods used in the present thesis

3.1. Phenology algorithm

Phenological metrics of timings of initiation, peak and termination, and duration of a phytoplankton growing period, also called 'bloom', can be calculated based on relative changes in the concentration of pigment biomass (Fig. II-5; Platt and Sathyendranath, 2008). In the present thesis, the methodology used to characterize the bloom is based on a pixel-by-pixel threshold approach and a calculation of the derivate of the cumulative sum of Chl anomalies to estimate then phenological indices. This algorithm is able to estimate two Chl peaks per annual cycle at each pixel: one in the warming phase and another one in the cooling phase. This methodology is based on that of Racault et al. (2017) with some variations for the Chl levels observed in the Mediterranean Sea. In particular, the threshold criterion has been modified from the original algorithm. The Chl long-term median plus 20% was selected as the best performing criteria. Further details are given in the methodology head of Section III – Chapter 1.

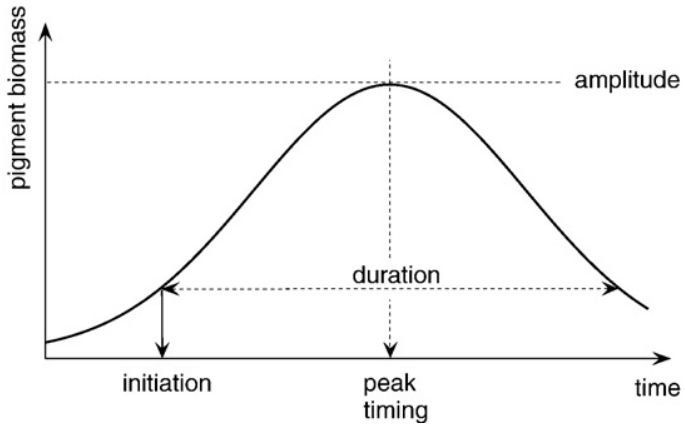

Fig. II-5. Characterization of the properties of a phytoplankton growing period at a given pixel from a Chl time serie (Platt and Sathyendranath, 2008)

3.2. Self-Organizing Map (SOM) algorithm

Self-Organizing Maps (SOM) analysis in the time domain, is as a classification technique used to distinguish regions of similar temporal variability of Chl in the Mediterranean Sea. It is a statistical tool used to unveil underlying patterns or structures in data (Kohonen, 1982). SOM is probably the most popular artificial neural network algorithm that uses unsupervised machine learning algorithms for the training process, in particular by the relationship between neighboring neurons (Kohonen, 1997). One of its main uses is for imaging clustering purposes where a variable is partitioned into *k* different groups and is created in accordance with a code vector density after a learning iterative training method based on similarity and dissimilarity between separable feature space data groups to be classified. Patterns with similar characteristics are obtained

(Kohonen, 2001). This application of the SOM analysis is generally used as an alternative to the *k*-means clustering with the advantage that is topology preserving; i.e., similar clusters are usually grouped together. This one is the SOM application used in this thesis.

SOM is based on a non-linear neural network, where each resulting neuron represents a pattern. When working with satellite images, two different analyses can be performed. The output can be a temporal pattern, if the time domain of the data is analyzed (the input vectors of the SOM are the time series at each pixel) or it can be a spatial distribution map, if the spatial domain of the data is analyzed (the SOM input vectors are spatial maps for at a specific time). These analyses are also referred to 'Kohonen Neural Networks', 'Topological Neural Networks' or 'Topology preserving feature maps' (Kohonen, 2001).

In this thesis, we have analyzed the time series of Chl (Section III-Chapter 2) or PP (Section III-Chapter 3) estimations in the time domain since the purpose is to identify regions with similar temporal variability of the studied parameter. The input vectors of the SOM algorithm are time series in each pixel and the output vectors after the SOM training are temporal patterns (called neurons) of Chl or PP that are common to a set of pixels of specific geographical regions. In this case, SOM technique places the neurons topologically ordered based on the Euclidean metric. Then, based on these neurons, a map of the Mediterranean is constructed by grouping pixels with the same pattern. This property has been used to classify the Mediterranean in regions that have a similar behavior/pattern (neuron) in terms of plankton dynamics. SOM computations in the current thesis were performed using the MATLAB toolbox of SOM v.2.0 (Vesanto et al., 2000a, 2000b) provided by the Helsinki University of Technology (http://www.cis.hut.fi/somtoolbox/). Additional details are given in the methodology head of Section III – Chapter 2 and 3. However, further details about the general SOM algorithm can be found in Kohonen (1997) and Vesanto et al. (2000).

3.3. Primary production algorithm

In Section III-Chapter 3, PP is estimated from satellite-derived Chl, SST and PAR values using the the wavelength-, depth-, time-resolved version of the light-photosynthesis model initially proposed by Morel (1991) and later improved in (Antoine et al., 1996; Antoine and Morel, 1996). It is a bio-optical model that improves productivity estimates by integrating instantaneous PP values over the water column accounting for the variability in phytoplankton optical absorption cross sections and the quantum yield of photosynthesis for carbon fixation. The model uses an empirical equation that relationships three basic variables: the PAR (400 - 700 nm) at the surface, the column-integrated Chl content and the cross section for photosynthesis per unit of Chl. This methodology is deeply explained step by step in Section III-Chapter 3.

III. RESULTS

Chapter 1. Trends in phytoplankton phenology in the Mediterranean Sea based on ocean-color remote sensing.

This chapter is based on the publication:

Salgado-Hernanz, P.M., Racault, M.-F., Font-Muñoz, J.S., Basterretxea, G. *Trends in phytoplankton phenology in the Mediterranean Sea based on ocean-color remote sensing*. Remote Sensing of the Environment (ISSN 0034-4257), volume 221, February 2019, pages 50-64. doi: 10.1016/j.rse.2018.10.036.

ABSTRACT

Seventeen years (1998–2014) of satellite-derived chlorophyll concentration (Chl) are used to analyse the seasonal and non-seasonal patterns of Chl variability and the long-term trends in phytoplankton phenology in the Mediterranean Sea. With marked regional variations, we observe that seasonality dominates variability representing up to 80% of total Chl variance in oceanic areas, whereas in shelf-sea regions high frequency variations may be dominant representing up to 49% of total Chl variance. Seasonal variations are typically characterized by a phytoplankton growing period occurring in spring and spanning on average 170 days in the western basin and 150 days in the eastern basin. The variations in peak Chl concentrations are higher in the western basin (0.88 ± 1.01 mg m^{-3}) compared to the eastern basin (0.35 ± 1.36 mg m^{-3}). Differences in the seasonal cycle of Chl are also observed between open ocean and coastal waters where more than one phytoplankton growing period are frequent (> 0.8 probability). During the study period, on average in the western Mediterranean basin (based on significant trends observed over ~95% of the basin), we show a positive trend in Chl of +0.015 ± 0.016 mg m^{-3} $decade^{-1}$, and an increase in the amplitude and duration of the phytoplankton growing period by +0.27 ± 0.29 mg m^{-3} $decade^{-1}$ and +11 ± 7 days $decade^{-1}$ respectively. Changes in Chl concentration in the eastern (and more

oligotrophic) basin are generally low, with a trend of -0.004 ± 0.024 mg m^{-3} $decade^{-1}$ on average (based on observed significant trends over ~70% of the basin). In this basin, the Chl peak has declined by -0.03 ± 0.08 mg m^{-3} $decade^{-1}$ and the growing period duration has decreased by -12 ± 7 days $decade^{-1}$. The trends in phytoplankton Chl and phenology, estimated in this study over the period 1998 - 2014, do not reveal significant overall decline/increase in Chl concentration or earlier/delayed timings of the seasonal peak on average over the entire Mediterranean Sea basin. However, we observed large regional variations, suggesting that the response of phytoplankton to environmental and climate forcing may be complex and regionally driven.

1. INTRODUCTION

Phytoplankton chlorophyll (Chl) and productivity exhibit variations in timing and magnitude in different regions of the oceans due to several processes affecting their growth and demise, such as incident solar irradiance, water column stratification, nutrient supply and grazing pressure, which may vary with latitude, as well as regional and local oceanographic conditions (Cushing, 1975). Temporal and spatial variations of phytoplankton Chl and production affect carbon fluxes and other elemental cycles in the oceans (Falkowski et al., 1998; Laufkötter et al., 2016) and can lead to upper trophic mismatch altering the function of marine ecosystems with important consequences for fisheries (Edwards and Richardson, 2004). Indeed, for many commercially-important fish species, their spawning season is closely tied with the phytoplankton seasonal cycle (Chambers and Trippel, 1997; Cushing, 1975; Kassi et al., 2018; Lo-Yat et al., 2011; Platt et al., 2003).

Seasonal dynamics of phytoplankton pigment concentrations in the oceans are indicative of variations in bio-physical processes such as primary production, grazing and/or structural changes driving phytoplankton diversity in response to environmental change in the ocean surface layer (Shevyrnogov and Vysotskaya, 2006). The seasonal bloom is one of the dominant features in the growth patterns of phytoplankton in the pelagic environments, particularly in temperate and cold oceans, and it responds primarily to changes in light and nutrient availability (Legendre, 1990; Sverdrup, 1953). Interannual and long-term variations in plankton phenology may be used as indicators to assess how changes in the marine environment propagate from primary producers to higher trophic levels. At high latitudes, the trophic transfer relies on a single seasonal peak of phytoplankton, providing the main energy source for zooplankton and fish production (Platt et al., 2009; Racault et al., 2012). However, in temperate areas, a less intense secondary peak may occur in fall (Bosc et al., 2004; Mayot et al., 2017a; Morel and André, 1991; Racault et al., 2017b; Siokou-Frangou et al., 2010; Zingone et al., 1995).

The phase of the seasonal phytoplankton bloom can be characterised by a suite of phenological metrics: timings of initiation, termination, maximum, and duration of the phytoplankton growing period; and also amplitude of the phytoplankton Chl concentration (Platt and Sathyendranath, 2008; Racault et al., 2012). These metrics are valid for shelf areas where phytoplankton seasonal cycles are readily apparent in both satellite and in-situ time series (Corredor-Acosta et al., 2015; Fendereski et al., 2014; Friedland et al., 2015; Ji et al., 2010; Jordi et al., 2009; Platt et al., 2009; Zhai et al., 2011). However, in these areas, local effects caused by the interaction of ocean processes with the seafloor and terrestrial sources can also play a fundamental role. Short spatial

and temporal variability may account for a large fraction of total phytoplankton variance (Cloern and Jassby, 2008). Furthermore, the seasonal cycle may be masked by variability on longer timescales (Kahru and Mitchell, 2001). Non-seasonal variability in pigment concentrations have been associated with different physical drivers, such as synoptic fields of wind stress and sea level heights (Strub et al., 1990), frontal dynamics (Sokolov and Rintoul, 2007), or climatological variations (Lin et al., 2014; Thomas et al., 2012). In addition, in coastal shelf areas, factors regulating phytoplankton variability may be significantly different from the processes dominating in the open ocean. Signal variability in coastal areas can be driven by the effects of river plumes (Walker and Rabalais, 2006) or by topographically induced variability occurring in the vicinity of islands, headlands and straits (Arístegui et al., 1997; Gomez et al., 2017).

The Mediterranean is a marginal sea divided in two main sub-basins separated by the Sicily channel. It has been considered for many years as a 'small-scale ocean' presenting a wide range of physical processes including deep water formation and thermohaline circulation (Lacombe et al., 1981; Robinson and Golnaraghi, 1993; Volpe et al., 2012). External sources of water are the inflow of the Atlantic water jet in the surface layer through the Strait of Gibraltar, the Black and Marmara Seas through Bosporus Strait and freshwater rivers inputs mainly in the northern western side (The MerMex Group., 2011). Biogeochemically, the Mediterranean Sea presents an apparent west-east gradient of increasing oligotrophy. A deficiency of phosphorous relative to nitrogen increases eastwards (Béthoux et al., 1998). The dynamics of oceanic phytoplankton in the western basin are characterized by a winter phytoplankton growing period similar to that of temperate seas whereas in summer, low Chl concentration generally prevails (i.e. Marty et al. 2002). Phytoplankton dynamics in the eastern basin resemble that in subtropical waters, with low Chl variations throughout the year. D'Ortenzio and Ribera d'Alcalà (2009) and Lavigne et al. (2015) refer to this region as a 'no-bloom' region because changes in Chl values are limited. Due to the low nutrient availability, phytoplankton assemblages in the Mediterranean Sea are generally dominated by small picoplankton (<2 μM) for most of the year although the contribution of larger nanoplankton and microplankton cells have been shown to increase during winter and in coastal areas (Ignatiades et al., 2009; Vidussi et al., 2001).

Several studies have addressed the seasonal and interannual variability of phytoplankton at regional and basin-wide scales. For instance, Mélin et al. (2011) analysed the phenology in the Adriatic Sea using monthly ocean-color composites and signal decomposition applying a simplified X-11 algorithm for the period 1997 - 2004. Using empirical orthogonal functions analyses, Volpe et al. (2012) investigated the seasonal response of phytoplankton in practically the entire Mediterranean Sea during the period 1998-2006. Some studies have also examined the biogeography and changes in magnitude in Chl concentration in relation to changing environmental conditions during different time periods (Colella et al., 2016; D'Ortenzio and Ribera d'Alcalà, 2009; Mayot et al., 2016) but, with some exceptions (e.g. Lavigne et al., 2013), less is known about the long-trends of phytoplankton Chl and phenology. Barale et al. (2008) reported symptoms of an increased nutrient-limitation, resulting from reduced vertical mixing due to a more stable stratification of the basin, in line with the general warming trend of the Mediterranean. While warming of Mediterranean Sea surface appears to be a consistent pattern (e.g. Belkin, 2009; Rixen et al., 2005; Skliris et al., 2012), some uncertainties remain on long-term phytoplankton response that it is the result of complex processes, including variations in nutrient sources and availability, as well as changes in food web interactions.

The present work aims to characterize patterns of variability and trends of phytoplankton Chl and phenology in the Mediterranean Sea. Our study uses a regionally-tuned Chl product for the Mediterranean Sea based on the OC-CCI dataset, which is the longest, continuous, climate quality-controlled, 17-year time series (1998 - 2014) of fine space-time resolution remotely sensed ocean-color data. First, we assess the contribution of seasonality to overall variability and the long-term tendencies of deseasonalized Chl concentration. Then, using a threshold-based phenology approach, we identify and characterize spatial patterns in phytoplankton phenology over the entire Mediterranean Sea basin. Finally, we calculate the trends in the estimated phytoplankton phenological metrics for the period of study. The observed changes in phytoplankton Chl and phenology are key to understand functional and structural aspects of marine communities.

2. DATA AND METHODS

2.1. Ocean-color remotely sensed data

The present study is based on sea surface Chl concentration (mg m^{-3}) Level-4 (L4) reprocessed product, obtained from the EU Copernicus Marine Environment Monitoring Service (CMEMS) at 8-day and 1-km resolution, from the website http://marine.copernicus.eu/ (OCEANCOLOR_MED_CHL_L4_ REP_OBSERVATIONS_009_078). The analysed series covers the period from January 1998 to December 2014 for the Mediterranean Sea (30-to 46°N and 6°W to 37°E, Fig. 1). This ocean-color data record is a regionally-tuned reprocessing of the climate-quality, error-characterised, and bias-corrected merged product of multi satellite observations (SeaWiFS, MODIS-Aqua and MERIS sensors) initially developed by the European Space Agency Ocean-Color Climate Change Initiative Program (ESA OC-CCI) (Sathyendranath et al., 2017; Sathyendranath and Krasemann, 2014). The Chl product available from CMEMS has been tailored to the Mediterranean region by using the regional algorithm MedOC4 (Mediterranean Ocean-Color 4 bands, Volpe et al., 2007) for Case-I waters and the AD4 algorithm (ADriatic 4 band, Berthon and Zibordi, 2004; D'Alimonte and Zibordi, 2003) for Case-II waters. In this product, the merging of Case-I and Case-II information was performed following D'Alimonte et al. (2003). In practice, the CMEMS processor ingests the OC-CCI remote sensing reflectance, which is the result of a merging procedure that accounts for the inter-sensor bias among different sensors and then applies the specific regional algorithm. The OC-CCI processing removes inter-sensor bias by band-shifting (Mélin and Sclep, 2015) and bias-correcting the MODIS and MERIS bands and values to the SeaWiFS reference ones and finally, by merging the individual sensors datasets with a weighted averaging (Mélin, 2016; Mélin et al., 2017). The overall correlation between measured and estimated Chl, reprocessing time series REP, L4 product in Mediterranean Sea yield a correlation coefficient of $r^2 = 0.764$ (Pitarch et al., 2016), and the specific correlation for Case-II waters is $r^2 = 0.56$ (D'ALimonte and Zibordi, 2003).

In order to reduce missing data, Chl values were first re-gridded to a 4 km regular grid by averaging all available data points within each new, larger pixel. Then, remaining gaps were filled by applying linear interpolation scheme in the sequential steps: longitude, latitude, and time (Racault et al., 2014b). Specifically, the gaps were filled with the average value of the surrounding grid points along the indicated axis. The averaging window had a width of three points and the

surrounding points were weighted equally. Along the indicated axis, if one of the points bordering the gap was invalid, it was omitted from the calculation. If the two surrounding points were invalid, then the gap was not filled. Finally, the data were smoothed by applying moving average filter of previous and next time step. The study area with its bathymetry and main sea surface circulations patters is shown in Fig. 1.

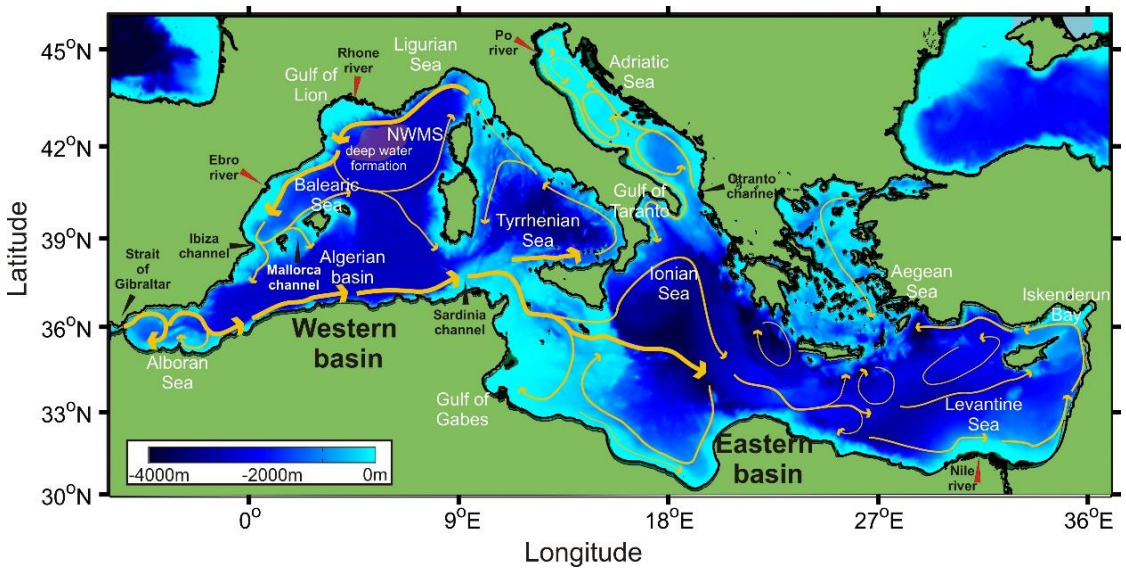

Fig. 1. Mediterranean Sea geography with main surface circulation patterns. Bathymetric data were obtained from ETOPO1 (Amante and Eakins, 2009). Red arrows indicate de position of major river mouths. Circulation patterns are redrawn based on (Millot and Taupier-Letage, 2005; Pinardi et al., 2004; Robinson et al., 2001; Siokou-Frangou et al., 2010).

2.2. Relative contribution of seasonal and non-seasonal variations in chlorophyll

Census X-13 seasonal adjustment methodology, an improved version of X-11, is used to remove the seasonal signal from the Chl time series and to investigate the temporal variation patterns (methodology applied following the X-13 seasonal adjustment equations from the U.S. Census Bureau, 2017). Briefly, the X-13 technique is based on an iterative bandpass-filtering method that relies on the application of successive filters. Each component is estimated with an iterative procedure consisting of an alternate computation of the trend component from the seasonally adjusted series, and of the seasonal component from the series corrected for the trend. A principal feature of the X-13 decomposition is that the seasonal term is defined locally in time allowing year-to-year variations, and therefore has a variable amplitude accounting for interannual variations in seasonality. The procedure assumes that an original time series X(t), here a 8-day Chl composites, can be decomposed into three components: as $X(t) = S(t)+I(t)+T(t)$ where *S, I* and *T*, represent, respectively, a seasonal signal, and an irregular (or high frequency residual), and a low frequency (> 1year) or interannual component (Shiskin, 1978).

Trends in Chl time series were calculated by the Sen-slope estimator to the *T*(t) component (see details in section 2.4). The relative contribution of each of the three components (*S,I,T*) of Chl is calculated as in Vantrepotte and Mélin (2009). The total variance σ_x^2 of the original time series can be written as $\sigma_x^2 = \sigma^2_S + \sigma^2_I + \sigma^2_T + 2\mathrm{cov}(S, I, T)$ where σ^2_S, σ^2_I and σ^2_T represent the variance associated with the *S, I* and *T* components respectively, and cov(*S, I, T*) represents the covariance

terms between these components. The covariance term 2cov(*S, I, T*) accounts only for few percentage of the total variance (typically, 5% in absolute value). Therefore, the relative contribution p_z^2 of each component to the total variance (with z = *S, T* or *I*) is approximated as $\rho_z^2 = 100\ \sigma_z^2\ (\sigma^2_S + \sigma^2_I + \sigma^2_T)$ (expressed in %). Time series with more than 12% of missing values were excluded from the analysis.

2.3. Estimation of phenological indices

We applied the algorithm of Racault et al. (2017) to calculate a series of phenological indices: timings of initiation (b_i), peak (b_t), termination (b_e), duration (b_d) and peak amplitude (b_a) of up to two phytoplankton Chl peaks during each year. The phenology algorithm uses Sea Surface Temperature (SST) seasonality to define two time intervals (i.e., a SST warming phase and a SST cooling phase) during which up to two phenological growing periods can be estimated. In the Mediterranean Sea, the main phytoplankton growing period is associated with the minimum winter SST. In winter, cool, dense surface waters deep and causes a vertical mixing convection process in the water column that brings nutrients to the surface photosynthetic layers (Marty et al., 2002). In spring and summer, there is a setting of stratification in the water column due to the increase in SST. A second growing period may be observed in fall when water-column becomes less stratified, generally associated with storms or wind events. The fall growing is generally shorter than the spring one, and Chl concentration remain lower (Morel and André, 1991). Similar approaches to the one we use in the present work have been successfully applied at global scale (including tropical and subtropical regions (e.g. Kostadinov et al., 2017; Racault et al., 2017), as well as at regional scale in tropical regions such as the Red Sea (e.g., Gittings et al., 2018; Racault et al., 2015).

In the present study, the method to estimate the phenological indices is based on a long-term Chl median plus 20% pixel-by-pixel threshold criterion and calculation of the derivative of the cumulative sum of Chl anomalies. The selection of this threshold depends on the magnitude of the seasonal Chl peak with respect to baseline variations. For example, Siegel et al. (2002) find little differences between using values ranging from 5 to 30% in the North Atlantic spring bloom. In our case, the threshold of 5% yields to the detection of multiple small Chl peaks and, therefore, we chose the median plus 20% threshold to avoid the detection of these small peaks, especially in coastal regions. The timing of initiation b_i was obtained based on the first time step when the cumulative sum of Chl changes signs (i.e., from positive to negative), and the timing of termination b_e is calculated as the previous time step before falling below the threshold criterion. To identify b_i and b_e, the Chl concentration needs to fulfil the latter conditions during at least two consecutive time steps. The duration b_d is the time elapsed between b_i and b_e. The timing and amplitude of the Chl peak, b_t and b_a respectively, and correspond to the time and amplitude at which the Chl value reaches the highest signal. Lastly, the method of detection of the timing of events is centred around b_t, hence b_i and b_e times can span the calendar year. In any particular year, if two phytoplankton growing periods are estimated, the main growing period is defined as the one with highest Chl peak whereas the second growing period is defined as the one with lower Chl concentration. Further details about the method implementation are provided in Racault et al. (2015) for Chl climatology and Racault et al. (2017) for interannual Chl time series. A schematic representation of the phenology method is shown in Fig. 2.

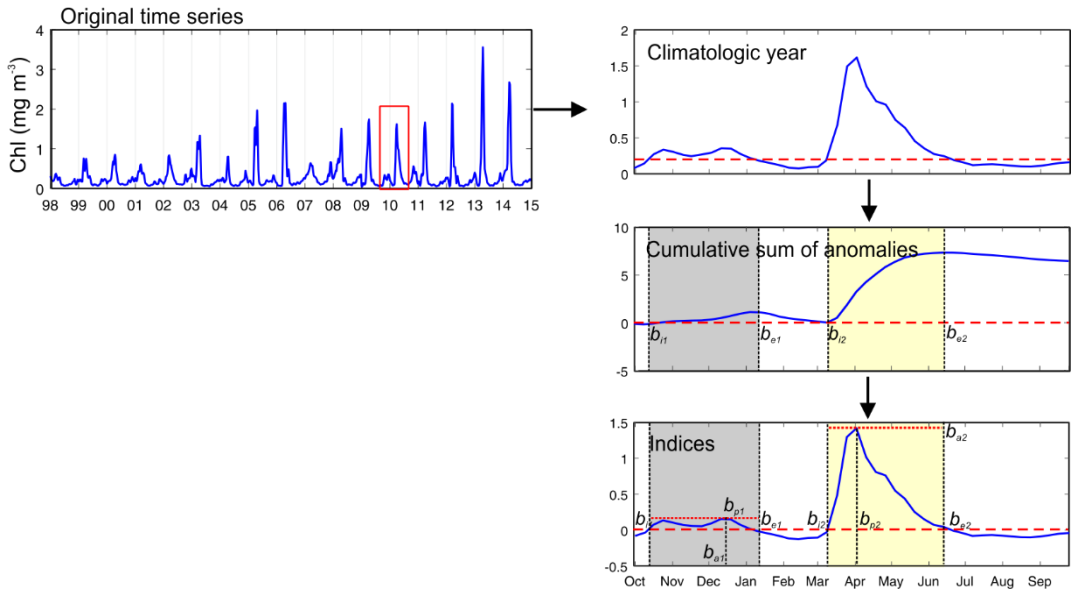

Fig. 2. Schematic diagram of the phenology method used to detect up to two phytoplankton growing period from a Chl time series. The example provided correspond to the location [5.43°W and 42.47°N] in the North Western Mediterranean Sea (NWMS).

In addition to computing phenology maps, the seasonal climatology of ten selected regions was estimated from the average of 300 detrended time series representing a surface area of 4600 km^2. We selected these regions based on previous studies looking at spatio-temporal features of phytoplankton variability in the Mediterranean Sea which showed that these areas exhibit distinct seasonal patterns (Colella et al., 2016; D'Ortenzio and Ribera d'Alcalà, 2009; Lavigne et al., 2017; Macias et al., 2017; Mélin et al., 2017).

2.4. Trend calculation

Trends on the 8-day *T* component (de-seasonalized Chl time series obtained from X-13 decomposition) and on the yearly phenological indices time series were calculated pixel-by-pixel. The existence of linear trends and their significance was evaluated with the Sen slope estimator, which calculates the slope and the constant of the linear models as the median of those derived by linear interpolations of any pair of available data (Gilbert, 1987; Sen, 1968). A Mann-Kendall statistics test is applied to each pixel to identify the statistically significant trend values at a 95% confidence level (Salmi et al., 2002). The use of this non-parametrical test is suitable for non-normally distributed data and has been previously used in the trend examination of remote-sensing Chl time series (Colella et al., 2016; Coppini et al., 2013; Erasmi et al., 2014; Kahru et al., 2011; Vantrepotte and Mélin, 2011). As missing data could mask the trend results, only de-seasonalized Chl time series with at least 90% of the pixels were used and linear interpolation was performed on the rest of the data. A minimum of nine years (~50% of the total number of years 1998-2014) with bloom indices was set as a requirement to perform the regression (i.e., if phenological indices were available for less than nine years then the trend was not calculated). Trends in phenological indices are given in days per decade, which have been calculated by

multiplying the phenology timing index estimates by eight based on the 8-day resolution of the ocean-color composites.

Trends in Chl concentration estimated from ocean-color products that includes observations from single sensor, and from multiple sensors (i.e., merged products) have shown to give comparable results, and that changes in sampling rate have limited influence on the estimation of long-term trend in Chl (Mélin et al., 2017). For the calculation of phytoplankton phenological metrics, the influence of the sampling rate (i.e., number of observations) has been estimated to introduce a bias <2% and RMSE <10% when the observation coverage is between 80 - 100% (Racault et al., 2014b). In the Mediterranean Sea, the individual sensor (SeaWiFS, MODIS, MERIS) can provide coverage within this range and allow us to estimate phenological metrics and trends with low uncertainty.

Considering the length of the ocean-color record 1998-2014, we would like to note that our analysis is representative of the variations during the last two decades. Longer datasets (i.e. >30 years) may be necessary to identify climate change driven trends (Henson et al., 2018). Phenological metrics are sensitive to gaps in the time series, which can result in error and bias in the estimates (Racault et al., 2014b). However, compared with other regions, the Mediterranean Sea tends to benefit from low cloudiness (Sanchez-Lorenzo et al., 2017). In addition, we also note that phenological changes may not be effectively detected when noise levels are larger than the signal amplitude (Verbesselt et al., 2010). Uncertainty in the estimation of phenological metrics can be improved by the use of preprocessing techniques such as gap-filling and smoothing (Ferreira et al., 2014; Racault et al., 2014b). We use 8-day composites of the OC-CCI dataset, which result in quasi-continuous time series (no gap) in the Mediterranean Sea. While averaging over 8 days reduces the resolution at which events in the phytoplankton growing period can be estimated, it does not significantly affect the spatial pattern of the estimated trends, as shown by Henson et al. (2018).

3. RESULTS

3.1. Seasonal and non-seasonal components of chlorophyll variability

The *S, I* and *T* components of Chl variability derived by the X-13 methodology are displayed in Fig. 3. Seasonality prevails in most of the oceanic areas, representing up to 80% of the total variance (Fig. 3a). Interestingly, most of the northern Mediterranean (i.e. above latitude 39°N) presents higher high frequency (irregular) variability. Low frequency variations are particularly intense in the Ibiza and Mallorca channels, in the northern Aegean Sea and Otranto channel (Fig. 3c). Generally, Chl variations in coastal areas present a more complex scenario compared to oceanic regions. This is especially evident in the Northern Adriatic and along the Po River plume path, and also in the northern Alboran Sea, where the contribution of high frequency to total variance is >60%. Regions with a cyclonic circulation and a blooming dynamic also present strong part of irregular variability (NWMS, South Adriatic and Rhodes gyre; Fig. 3b).

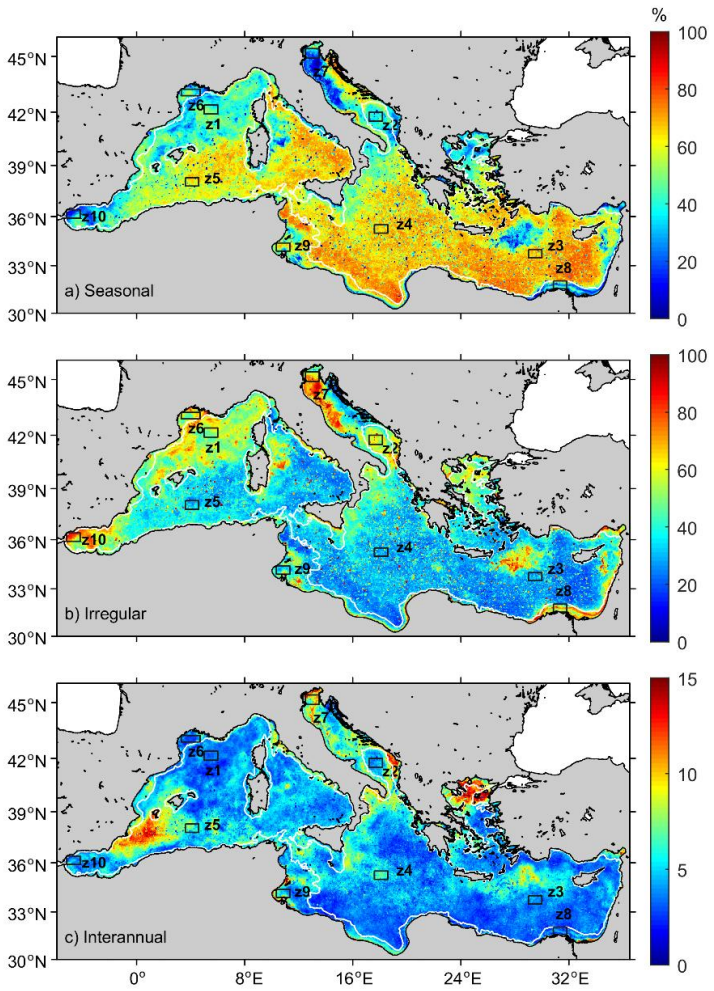

Fig. 3: Distribution of the a), Seasonal, b) Irregular and c) Interannual variance components, as derived from the X-13 procedure. Variance maps are relative contribution to each component to the total variance of Chl. Note that a different percentage scale is used in the interannual component. White contour line delimits coastal waters (200 m isobath). Black squares at each figure delimits the ten areas over which temporal decomposition is shown in Fig. 4 (zones, z, 1 to 10).

Fig. 4 and Table 1 shows the seasonal, irregular and interannual Chl variations at the ten selected oceanic and coastal areas. The oceanic areas include the North western Mediterranean Sea (NWMS), the South Adriatic pit, the Levantine Sea, the Ionian Sea and the South Western Mediterranean Sea (SWMS) in the Algerian basin; whereas the coastal areas are represented by a subset of pixels of the Gulf of Lion, the North Adriatic coast, the Nile estuary, the Gulf of Gabes and the northern Alboran Sea. Variability in oligotrophic oceanic areas such as the Levantine and Ionian Seas (Chl <0.06 mg m^{-3}) and in the more productive SWMS (0.15 ± 0.02 mg m^{-3}) is dominated by seasonality (ρ_s^2 >73% of the variance, see Table 1). Conversely, high-frequency variations constitute an important part of total variance in the NWMS and the South Adriatic oceanic areas. Among the coastal areas, the Gulf of Gabes is the one that most resembles the oceanic areas, except for its higher Chl values (0.83 ± 0.54 mg m^{-3}), this region is dominated by the seasonal component (ρ_s^2 = 71% of the variance). Other coastal areas such as the Gulf of Lion and Nile Estuary present a lower seasonality, but still, it dominates total Chl variance (ρ_s^2 = 58 and 57% respectively). Contrastingly, the contribution of irregular variations in the North Adriatic (ρ_I^2 = 61%) and Alboran (ρ_I^2 = 64%) largely exceeds seasonality. Interannual variations represent a

small proportion of the observed variability (ρ_T^2 generally between 3 and 7%, and exceptionally 12% in the Northern Adriatic Sea) even though the contribution of this component is higher in coastal areas.

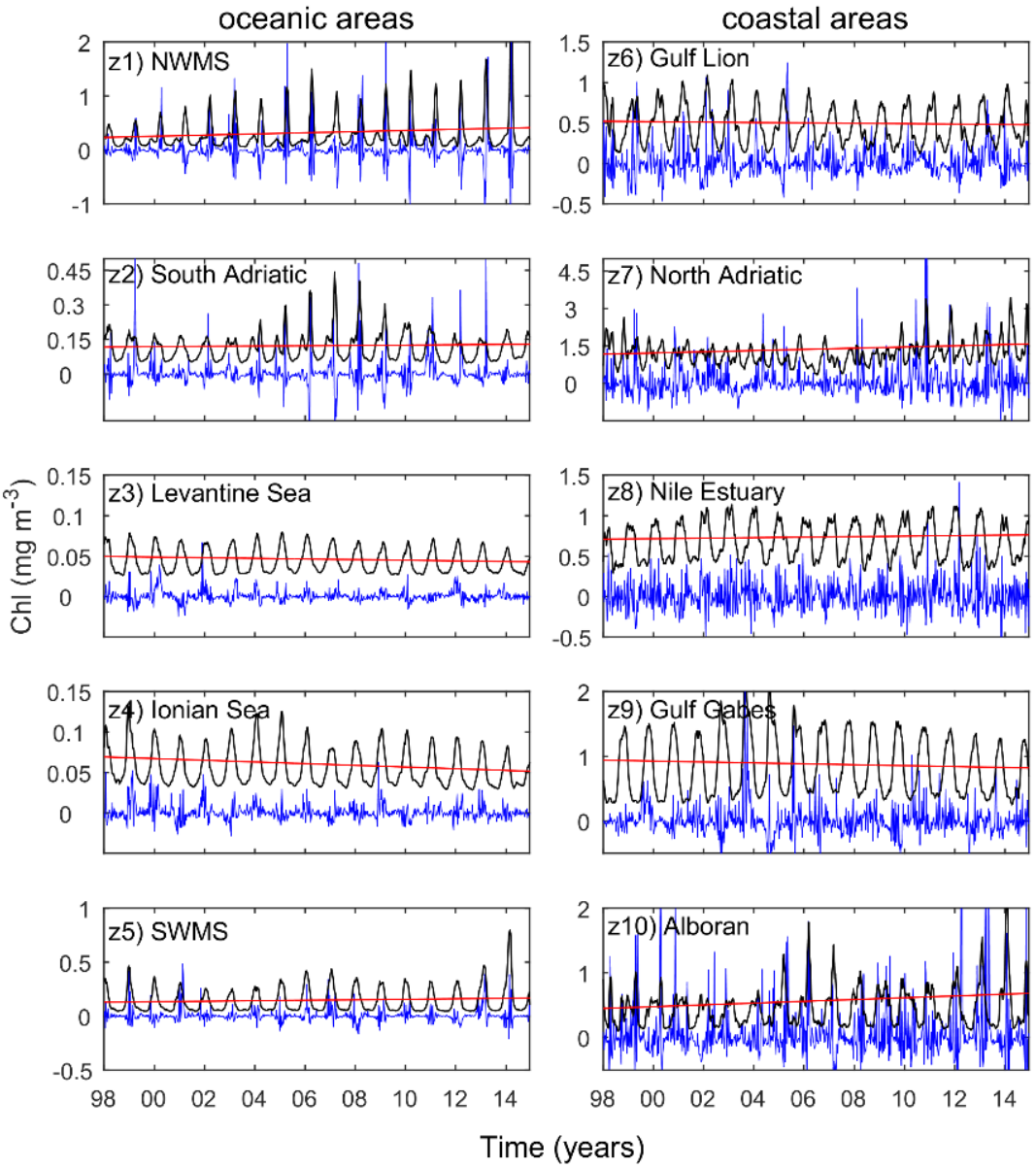

Fig. 4. Mean seasonal (black), irregular or high frequency (blue) and interannual trend (red) components, of Chl variability over the ten selected oceanic and coastal areas. The location of each zone z1 to z10 is displayed in Fig. 2. Note that different scales are used in some subplots.

Table 1. Mean Chl; variances contribution explained by the seasonal (ρ_S^2), irregular (ρ_I^2), and interannual (ρ_T^2) components; slope of the interannual Chl variability (*T* component) and its associated r^2 value, as derived from the X-13 procedure of the ten selected oceanic and coastal areas.

		Chl mean (mg m^{-3})	ρ_S^2 (%)	ρ_I^2 (%)	ρ_T^2 (%)	Chl slope (mg m^{-3} $decade^{-1}$)	r^2
Oceanic areas	z1: NWMS	0.40 ± 0.45	53	43	3	0.107 ± 0.004	0.409
	z2: South Adriatic Sea	0.12 ± 0.09	47	49	4	0.007 ± 0.001	0.021
	z3: Levantine Sea	0.04 ± 0.02	78	18	4	-0.004 ± 0.000	0.242
	z4: Ionian Sea	0.06 ± 0.03	78	14	7	-0.010 ± 0.000	0.485
	z5: SWMS	0.15 ± 0.02	73	21	6	0.022 ± 0.002	0.166
Coastal areas	z6: Gulf Lion	0.48 ± 0.31	58	39	4	-0.024 ± 0.004	0.022
	z7: North Adriatic	1.29 ± 0.95	27	61	12	0.241 ± 0.022	0.185
	z8: Nile Estuary	0.68 ± 0.31	57	39	5	0.031 ± 0.000	0.050
	z9: Gulf Gabes	0.83 ± 0.54	71	22	7	-0.071 ± 0.009	0.068
	z10: Alboran	0.53 ± 0.15	31	64	5	0.138 ± 0.007	0.334

Fig. 5 shows the global distribution of the long-term Chl trend (*T*). Most regions in the western Mediterranean and Adriatic Sea present a positive trend. The average value in the western basin is +0.015 ± 0.016 mg m^{-3} $decade^{-1}$ and it intensifies in the NWMS region to +0.107 ± 0.004 mg m^{-3} $decade^{-1}$ and in the northern Alboran Sea (+0.138 ± 0.007 mg m^{-3} $decade^{-1}$, Table 1). Large positive trends are found in the Adriatic Sea where the mean increase is +0.047 ± 0.085 mg m^{-3} $decade^{-1}$, and maximum values are found along the north-western shore (+0.241 ± 0.022mg m^{-3} $decade^{-1}$, Table 1). In the eastern Mediterranean Sea, either Chl does not show a relevant trend or it presents a slight decrease of -0.004 ± 0.024 mg m^{-3} $decade^{-1}$. This decreasing trend is stronger in the Gulf of Gabes region (-0.071 ± 0.009 mg m^{-3} $decade^{-1}$, Table 1). However, some regions corresponding to 30% of the basin, like the eastern Aegean Sea, Iskenderun Bay and the Nile delta present consistent positive slopes with a mean value of +0.031 ± 0.172 mg m^{-3} $decade^{-1}$.

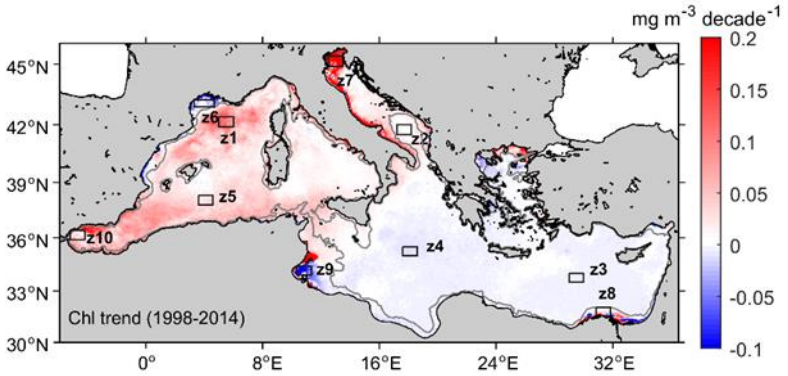

Fig. 5. Chl trends in the Mediterranean Sea for the 1998–2014. Scale units represent the changes in mg m^{-3} $decade^{-1}$. Only 95% significant Theil-Sen trends ($p < 0.05$) are shown. Black squares at each figure delimits the ten areas over which trend estimation is shown in Fig. 4 and Table 1 (zones, z1 to z10). Grey contour line delimits coastal waters (200 m isobath).

3.2. Basin-wide phytoplankton phenology

The spatial distribution of mean phytoplankton phenological indices in the Mediterranean Sea for the period 1998-2014 is presented in Fig. 6 (see Suppl. Fig. 1 for Standard Deviation and Coefficient of Variation values). The seasonal cycle in oceanic areas (>200 m) is typically characterized by a single growing period initiating early, around the 8-day period -8 (i.e., corresponding to the beginning of November) and terminating between the 8-day periods +13 and +20 (corresponding to the end March and mid-May respectively). Largest spatial differences in b_i and b_e are observed in the NWMS where the main growing period is delayed by approximately 60 days with respect to other surrounding areas (the growing period starts in mid-January and ends in late May; Fig. 6a-b). Chl peaks from late January to April, with clear regional differences (Fig. 6c). The growing period duration is shorter in the eastern basin (b_d ~ 150 days) compared to the western basin (b_d ~170 days) (Fig. 6d). In the same way, b_a is lower in the eastern basin, with Chl values expanding from 0.1 to 0.5 mg m^{-3} (mean b_a ~ 0.35 ± 1.36 mg m^{-3}) compared to the western basin, where mean values range from 0.5 to 2.5 mg m^{-3} (mean b_a ~ 0.88 ± 1.01mg m^{-3}; Fig. 6e). A spatial variation is seen in the NWMS where the main seasonal peak is more intense but shorter (b_a values of up to 3 mg m^{-3} and b_d spanning ~ 120 – 150 days) compared to the rest of the western oceanic region (Fig. 6d-e).

Shelf regions (< 200m) present similar phenological patterns to the oceanic areas, but with some particularities. For example, in the Gulf of Gabes, the Adriatic coast of Italy, and in the eastern Mediterranean coast expanding form Egypt to Lebanon, the timings of b_t and b_e shifted earlier by about 40 days compared to the oceanic areas i.e. b_t December – January and b_e in February – March (Fig. 6b-c). These coastal regions also present shorter growing periods compared to the open ocean areas (b_d ~ 100 days, Fig. 6d) and higher peak amplitude (b_a ~ 5-7 mg m^{-3}, Fig. 6e). Coastal waters are the areas where the probability of occurrence of an autumn growing period is higher (>0.7 probability of occurrence). Nevertheless, a second peak is not limited to neritic regions. Some oceanic areas such as the NWMS, the Strait of Gibraltar and the northern Aegean Sea also present secondary growing periods (Fig. 6f).

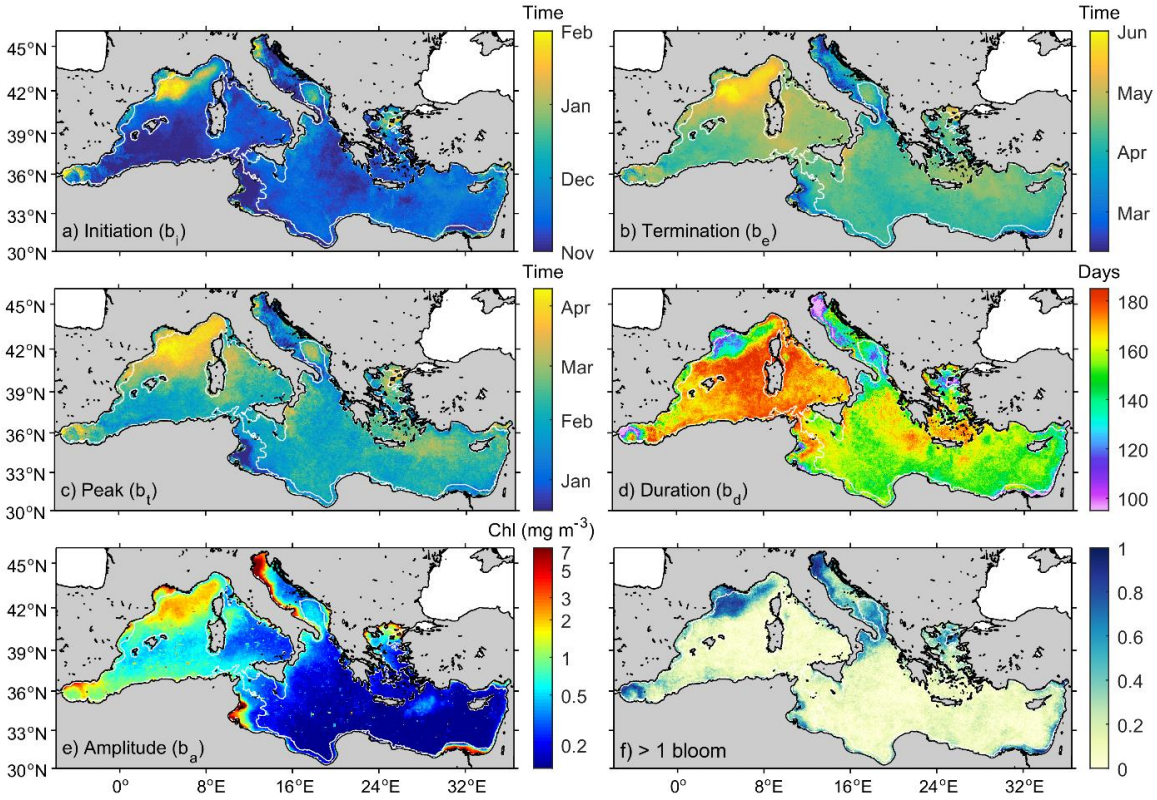

Fig. 6. Mean (1998 – 2014) phenological indices of the main growing period. Panels a to c indicate timing of initiation (b_i), termination (b_e) and peak (b_t) respectively (with the corresponding month); panel d the duration (b_d) of the growing period (in days); panel e the maximum Chl amplitude (b_a) during the growing period (in mg Chl m^{-3}); and panel f the probability of the occurrence of a second growing period (from 0 to 1). White contour line separates coastal from offshore waters (200 m isobath).

Fig. 7 shows the mean Chl value during the period 1998-2014 over the Mediterranean Sea (Fig. 7a) and the 8-day seasonal climatological cycle of five oceanic (Fig. 7 z1-z5) and five coastal (Fig. 7 z6-z10) areas during that period. Coastal areas show higher b_a and background Chl values compared with oceanic areas. Coastal climatological cycles also present higher standard deviation (see dashed lines). Marked seasonal climatological differences are observed between the oceanic regions. For example, the NWMS (Fig. 7 z1) presents a well-defined seasonal peak in April (1.3 ± 0.2 mg m^{-3}) whereas a weaker (~0.1 mg m^{-3}) and earlier growing period occurring in February in the Levantine, Ionian Sea and SWMS (Fig. 7 z3-z5). The South Adriatic Sea (Fig. 7 z2) present two intense phytoplankton growing periods, one in April (0.30 ± 0.03 mg m^{-3}) and the second one in November (0.16 ± 0.01 mg m^{-3}).

With the exception of the Gulf of Lion and Alboran Sea, coastal regions present a large interannual variability (standard deviation of 0.7, 1 and 0.7 mg m^{-3} for North Adriatic, Nile estuary and Gulf of Gabes respectively). The North Adriatic Sea (Fig. 7 z7) is markedly different to other coastal areas, exhibiting two phytoplankton growing periods (May and November) with similar characteristics in duration and intensity (~2 mg m^{-3}). The Nile estuary (Fig. 7 z8) has its Chl peak around February (1.11 ± 1.25 mg m^{-3}) and is the coastal area with the highest standard deviation. Finally, the Gulf of Gabes (Fig. 7 z9) presents one single peak (1.6 ± 1.4 mg m^{-3}) with the particularity to occur earlier compared to the rest of the coastal areas, starting in June, peaking in September and terminating in February. Finally, even though the Alboran Sea (Fig. 7 z10) present relatively large

variations in the seasonal cycle, the interannual variations are low, as reported in the low Standard Deviation.

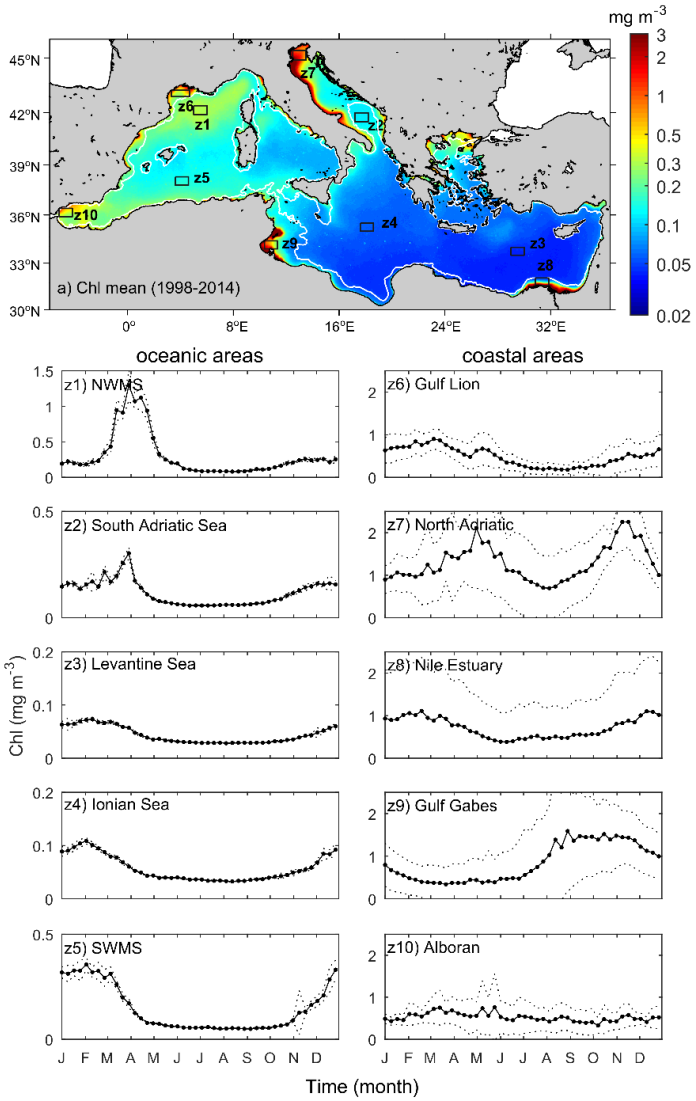

Fig. 7. a) Mean Chl in the Mediterranean Sea. Black squares delimit the ten areas from which seasonal climatology was derived. White contour lines separate shelf waters from offshore areas (200 m isobath). Panels z1 to z10: Mean climatology of 8-day Chl time series for a composite year, relative to 1998-2014, of oceanic (z1-z5) and coastal areas (z6-z10). Note that different scales are used in some subplots.

3.3. Trends in phytoplankton phenology

Trends in phytoplankton phenology metrics are displayed in Fig. 8. A positive trend in b_i is observed in most of the Mediterranean Sea (~70% of the pixels) indicating a mean delay of +9 ± 5 days decade^{-1}. In shelf regions and some areas such as the Alboran Sea or the Rhodes gyre the main growing period starts earlier (mean -6 ± 5 days decade^{-1}; Fig. 8a). b_e is delayed mainly in the south-western Mediterranean Sea by +9 ± 7 days decade^{-1}on average, whereas an early b_e is observed in the eastern basin (mean -6 ± 5 days decade^{-1}; Fig. 8b). As shown in Fig. 8c, b_t is generally earlier with a mean value of +12 ± 8 days decade^{-1} in the 71% of the Mediterranean basin. In the eastern and north-western Mediterranean Sea b_d has decreased by -12 ± 7 days decade^{-1}on average, and increased mainly in the Algerian basin (+11 ± 7 days decade^{-1}; Fig. 8d).

The trend in b_a, displayed in Fig. 8e, shows an overall increase in 86% of the western basin of +0.27 ± 0.29 mg m^{-3} $decade^{-1}$, reaching +1 mg m^{-3} $decade^{-1}$ in the NWMS and Alboran Sea. The exception to this positive pattern is observed in coastal areas such as the Gulf of Lion and less intensely south of the Balearic Islands (mean decrease in b_a of -0.15 ± 0.24 mg m^{-3} $decade^{-1}$). In contrast, the eastern basin presents a decreasing b_a of -0.03 ± 0.08 mg m^{-3} $decade^{-1}$ in 66% of the basin. However, some positive trends are observed in coastal areas, particularly in the Nile Estuary and the north Aegean Sea (mean increase of +0.08 ± 0.23 m^{-3} $decade^{-1}$).

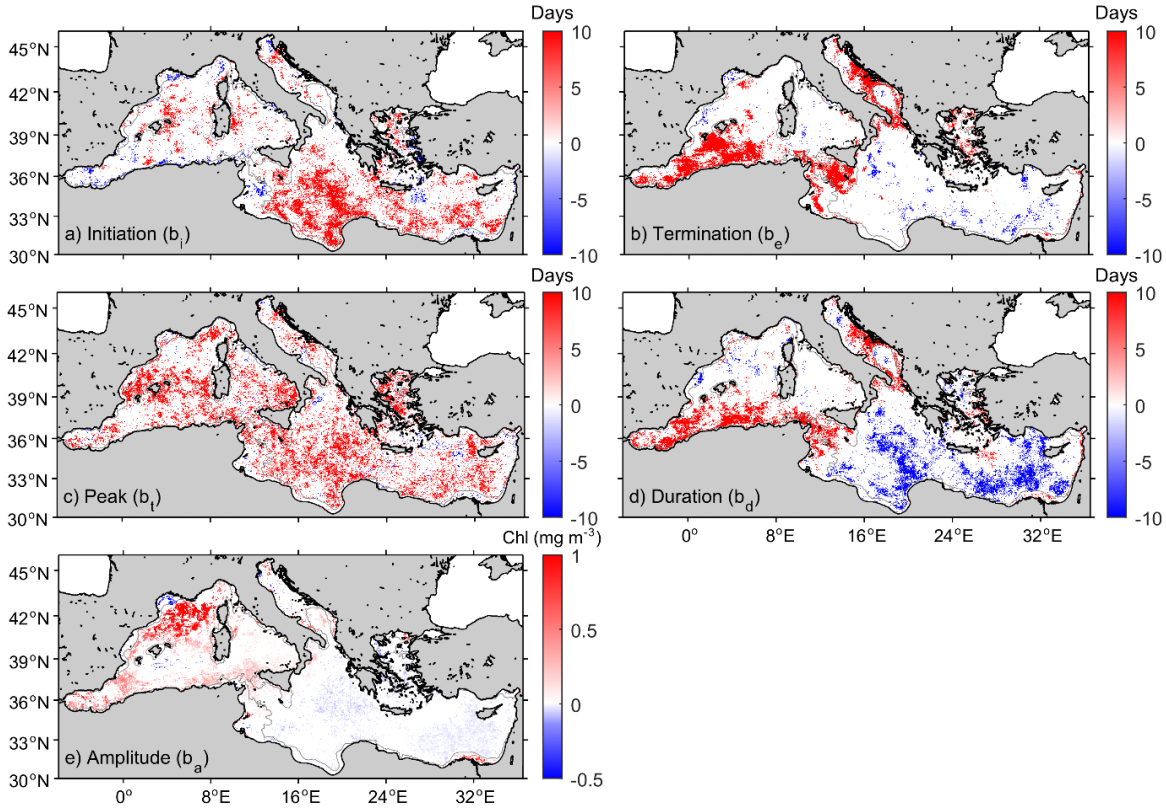

Fig. 8. Sen Slope trends in phenological indices over the Mediterranean Sea for the period 1998-2014. a) timing of initiation, b) timing of termination, c) timing of Chl peak, d) duration and e) peak Chl amplitude trends of the main phytoplankton growing period. Only significant values (95% confidence level) are shown. Color bars a-c represent the number of days/decade that each index advance (negative) or delay (positive) in timing. Color bar in d indicates the number of days/decade by which the growing period duration has decreased (negative) or increased (positive). Color bar in e indicates the variation in mg m^{-3} $decade^{-1}$ of the seasonal Chl peak. Grey contour line delimits coastal waters (200 m isobath).

4. DISCUSSION

4.1. Patterns of seasonal and non-seasonal phytoplankton chlorophyll variation

In the present analysis, seasonality is shown as the main contributing component to Chl variability in the Mediterranean Sea, representing from 50 to 80% of total variance. Lower values are observed in oceanic compared with coastal areas where high frequency episodes may be locally important (Fig. 3a). Our estimations are consistent with the values reported by Vantrepotte and Mélin (2009) who estimated that the contribution of seasonality in the global ocean was 64% of the total variance, and obtained values >80% in the Mediterranean Sea. The latter value is consistent with our estimations for low Chl oceanic regions such as Levantine and Ionian Sea

(Table 1). However, it is less representative of the northern regions of the Mediterranean Sea (i.e. NWMS and North Adriatic). The coastal areas present a higher proportion of high frequency episodes (irregular variability) as shown in Fig. 3b. Seasonal Chl peaks in these areas are highly irregular and characterized by a series short-lived (1 to 3 weeks) enhanced Chl episodes during the productive season. Moreover, these events are not restricted to the main growing season (i.e. winter) but, instead, are also observed during other periods. This suggests that Chl is driven by other forcing mechanisms such as intense winds, river outflows and exchanges with adjacent Seas (i.e in Alboran and Northern Aegean Seas). Indeed, high frequency variability is enhanced in the Northern Mediterranean where winds are more intense during winter (Zecchetto and De Biasio, 2007).

Low frequency variations only represent a small fraction of variance (i.e. <15%) and interestingly, they are intensified in key bottleneck areas. The channels of Ibiza, Mallorca, Otranto, Sardinia-Sicily and northern Aegean with its connection with the Marmara Sea, present higher variability. According to Astraldi et al. (1999), the channels and straits of the Mediterranean Sea are crucial for intercepting the major cells of the Mediterranean Sea circulation and often present complex circulation patterns (Fig. 3c). In the case of the Balearic channels, it is a transitional area where strong and highly variable meridional exchanges take place between the north and the south of the western Mediterranean (Lopez-Jurado et al., 1996). Jordi et al. (2009) observed deviations in the non-seasonal Chl patterns in the region influenced by the Balearic current and southeast of Mallorca and Ibiza. Also, Pinot et al. (1995) reported that winter intermediate waters formed further north, accumulate to the north of the channels in late spring obstructing the circulation through the Ibiza Channel. This process is determinant for the regulation of the interannual meridional water exchange in the sub-basin and has consequences in the distribution on the functioning of the marine ecosystem (Balbín et al., 2014; Pinot and Ganachaud, 1999). In the case of the northern Aegean Sea, previous studies have reported that variations in water input from the Black Sea can have the same influence, or even higher, compared with variations that may be observed in relation to water discharge from any Mediterranean rivers (Zervakis et al., 2004). Exchanges through the Marmara Sea have also been reported to present a clear interannual component having the similar influence compared with water discharge from large rivers discharges (Macias et al., 2018; Maderich et al., 2015). For instance, an increase in nutrient availability is associated with an increase in Chl amplitude or peak.

Low frequency shifts in phytoplankton abundance and composition in the Mediterranean Sea have been attributed to long-term alterations in the nutrient stoichiometry (Mercado et al., 2005). It has been observed that changes in the availability of reduced N and the N:P-ratios in inorganic and organic forms could be important factors in the control of bloom succession and ecosystem organization (Pujo-Pay et al., 2006). These nutrient variations can be motivated by climate driven variations. For example, decadal changes in winter cooling or evaporation can vary the intensity of vertical motions controlling the exchange of properties between the surface and deeper layers can influence the uplift of mineralized nutrients in the photic layers enhancing biological production (Polovina et al., 1995). García-Comas et al. (2011) observed decadal periodicity in secondary production forced by winter hydrographic conditions in the NWMS. Gregg and Conkright, (2002) observed, for the global ocean, decadal changes in ocean Chl likely to be associated with climate oscillations. Furthermore, temperature driven variations in top-down controls of phytoplankton have been regarded as an important climate-related factor in

the NWMS (Molinero et al., 2005). Indeed, large scale teleconnection patterns such as the North Atlantic Oscillation (NAO) are found to be the most important modes of atmospheric variability related to Chl concentration and distribution in the Mediterranean Sea (Basterretxea et al., 2018; Katara et al., 2008). However, our analysis shows more spatially localized differences in the long-term trends (Fig. 3c), which appear to be closely related with hydrographic variations, such as changes in eddy kinetic energy or intensified exchange through channels and straits. Large interannual variations in eddy kinetic energy at regional scale have been observed in the Mediterranean Sea (Pujol and Larnicol, 2005). Sannino et al. (2009) have discussed the importance of decadal variations of the Atlantic water inflow through the Gibraltar Strait in determining decadal variations in the western Mediterranean circulation patterns, water column stratification and convection events; and Civitarese et al. (2010) have emphasized the relevance of decadal scale variations through the Otranto channel on de biogeochemistry of the Adriatic Sea.

In the present analysis, the basin scale differences in phytoplankton Chl concentration are marked and appear to be enhanced associated with the positive trend in the western basin and in the Adriatic Sea (Fig. 5). Increasing Chl concentration in the western basin was also observed by Vantrepotte and Mélin, (2009) and further confirmed in more recent studies (Colella et al., 2016; Coppini et al., 2013). Nevertheless, sub-basin and regional differences appear to stand out from this general tendency. For example, changes are intensified along the NWMS, in the Alboran Sea and along the path of the Algerian Current in the SWMS region. Increased phytoplankton Chl concentration in the NWMS (+0.107 ± 0.004 mg m^{-3} $decade^{-1}$, Table 1) has been investigated by Marty et al. (2002) who report an increase in small-sized phytoplankton in response to the lengthening of the summer stratification. A marked positive trend is also observed in the northern Adriatic (+0.241 ± 0.022 mg m^{-3} $decade^{-1}$, Table 1). This trend differs from previous studies, which reported Chl decrease in the Adriatic associated with a decline in productivity due to a reduction in precipitations and a decrease in nutrient supply from river run-off (Colella et al., 2016; Mélin et al., 2011; Mozetič et al., 2009). Discrepancies with these studies may be explained by the inclusion in the present analysis of an additional six years (i.e. 2009-2014) displaying an important enhancement in phytoplankton Chl concentration. The main driver of this recent increase is uncertain, but it could be related to an increase in the Po River flow including higher phosphates and dissolved nitrogen concentrations (Giani et al., 2012). Long-term variations are typical from large river systems which are affected by climatic factors (e.g. Donner and Scavia, 2007; Goolsby and Battaglin, 2001) and the linear trends used for open waters may not capture well the overall trend.

In summary, Fig. 5 reveals that trends in Chl concentration of opposite sign are observed between the western and eastern basin. It is plausible that, these differences could be attributed to the different forcing mechanisms that regulate phytoplankton productivity in both basins. The western basin is more responsive to short-term processes such as wind pulses, deep winter convection and river discharges. Conversely, as suggested by Siokou-Frangou et al. (2010), the functioning of the eastern basin resembles that of subtropical regions. This region is expected to be particularly affected by long-term changes in evaporation and precipitation that can influence vertical mixing and, subsequently, modify nutrient availability (Ozer et al., 2017; Schroeder et al., 2017).

4.2. Patterns of phytoplankton phenological variation

The underlying mechanisms driving the variability of phenological indicators (Fig. 6) at each region can be complex (Thackeray et al., 2016). In the open ocean, the development of an upper mixed layer following the summer solar heating, and the convective processes caused by winter cooling and strong winds are the main driving forces of the seasonal signal in phytoplankton Chl concentration (Lavigne et al., 2013; Siokou-Frangou et al., 2010; Tanhua et al., 2013). However, variations in open waters, the phenology appear to be more closely related to regional scale than to basin scale processes. In particular, three regions have been shown to present distinct phytoplankton phenological characteristics: the NWMS, the Alboran Sea and the Adriatic Sea. The NWMS is a well-studied area displaying an intense seasonal peak (> 1 mg Chl m^{-3}, Fig. 7 z1) that is generated by the nutrients provided by deep water convection processes driven by cold and dry winds causing loss of surface water buoyancy and mixing with large depths (Macias et al., 2018; Mayot et al., 2016; Severin et al., 2014). In the case of the Alboran Sea, productivity is regulated by the input of Atlantic waters through the Strait of Gibraltar. Mixing in the Gibraltar sill, the development of strong geostrophic cross-frontal circulation and upwelling of the Atlantic jet near the Spanish coast increase the fertility of these waters (Estrada, 1996; Oguz et al., 2014; Solé et al., 2016). The influence of Atlantic waters may extend beyond the Alboran Sea by indirectly enrichening the waters of the Algerian current through the generation of instabilities, as suggested by Mayot et al., (2016). Finally, the phenology of the Adriatic Sea is driven by interactions between the outflows of major river discharges and wind induced convection processes (e.g. Gačić et al., 2002; Mauri et al., 2007). These three areas present high Chl amplitude but short duration in the spring growing period. Also, the probability of occurrence of a secondary growing period during water column de-stratification in autumn is higher than in other open ocean areas (Fig. 6 d-f).

There are some differences in phenological metrics between the south-west and the eastern basin. In the specific case of the SWMS in the Algerian basin (Fig. 7 z5) seasonal patterns are similar to those in the eastern Mediterranean, as previously observed by D'Ortenzio and Ribera d'Alcalà (2009). Indeed, even the contribution of seasonality to total Chl variability is relatively similar (73% contribution, Table 1). However, the main difference is that the SWMS is a more productive area fueled by a shallower nitracline, and weaker mixing efficiency in the eastern basin, as reported by Lavigne et al. (2015). Furthermore, the phytoplankton growing period last about ~30 days more in the SWMS compared with the oligotrophic areas of the eastern basin (Fig. 6 c&d). In the ocean eastern oligotrophic areas such as the Ionian (Fig. 7 z4), and Levantine Sea (Fig. 7 z3), the increase in winter Chl concentration is very low (~0.1 mg m^{-3}). Barbieux et al. (2018) reported that in these areas, phytoplankton Chl is essentially constant throughout the year. However, field evidence reveals that the eastern Mediterranean is not a stationary system but, instead, it presents significant seasonality with primary production and phytoplankton Chl generally increasing in response to winter phosphate and/or nitrate increase, particularly in coastal areas (Azov, 1986; Balkis, 2009; Ignatiades et al., 2002).

Coastal areas are shown to display different phenological pattern compared to the open ocean regions. Fueled by land sources and/or by coastal upwelling (Estrada, 1996), the amplitude of the main growing period b_a in coastal areas exceeds that in oceanic waters (Fig. 6 and Fig. 7a). Secondary growing periods are also frequent in these areas such as the Northern Adriatic, the

Gulf of Lion, the Nile delta, the northern Aegean Sea and the Gulf of Gabes (Fig. 6f). The first four areas are Regions Of Fresh water Influence (ROFI) regulated by the discharge cycles of the Po, Rhone, Nile and other smaller flows such as the Thracian rivers (Nestos and Aliakmon rivers). However, while the Po and Rhone rivers often display discharge peaks in fall and spring related to precipitation and snow melt periods (Mariotti et al., 2002a; Montanari, 2012; Sempéré et al., 2000), this is not the case of Thracian and Nile rivers (Milliman and Farnsworth, 2011). Regarding the upwelling influence, it will be particularly important in coastal areas where wind fields pulses are predominant. These areas are characterized by local decrease in SST accompanied by a deep-water mixing, which brings nutrient-rich deep waters into the coastal euphotic layer associated with an increase in phytoplankton Chl. These mainly occurs in the Gulf of Lion, west coast of Greece in the Aegean Sea and in the Algerian Coast (Bakun and Agostini, 2001). In the shallow Gulf of Gabes, frequent tidal movements can cause vertical mixing and increase productivity levels (Sammari et al., 2006). In coastal regions displaying autumnal growing periods (see Fig. 6f) other factors providing new nutrients, such as surface run-off from terrestrial inputs or sediment resuspension, can be regarded as main drivers of phytoplankton variability as observed by Arin et al. (2013).

4.3. Trends in phytoplankton chlorophyll concentration and phenology

Phytoplankton growing periods are influenced by global, regional and local driving-factors and they are likely to be altered by climate change. The Chl and phenological trends presented here for the Mediterranean Sea may lead to significant variations in the functioning of the marine ecosystem as result of the alteration of food web structures. The observed trends in phytoplankton Chl concentration and phenology present notable variations at basin and regional scale. Perhaps the most striking observation regarding the trends in phenology is the delay in the timings of initiation b_i and peak b_t (Fig. 8a and Fig. 8c respectively). These trends do not follow global general trends described for a warming ocean, i.e. earlier b_i and b_t and b_a decline (Hays et al., 2005; Poloczanska et al., 2013). In fact, our analysis reveals a delay in the b_i and b_t, mainly in oceanic waters. Consistently with our results, a delay in the timing of the phytoplankton growing period in the Mediterranean Sea is coherent with predicted changes in phytoplankton phenology in mid-latitudes reported by Henson et al. (2018) using an ecosystem model-based analysis. A second major pattern observed in the phenological trends is the earlier growing period termination b_e (Fig. 8b) and a reduction of duration b_d in the eastern basin (Fig. 8d). These phenological changes are coupled with a weakening in the winter growing period amplitude b_a (Fig. 8e), which can further reduce the limited productivity of these ultraoligotrophic waters and increase the period in which picoplankton dominates the algal community. These structural changes will have major consequences on the transfer efficiency to higher trophic levels. In the Mediterranean Sea, most fish species are late spring – early summer spawners, indicating that their spawning seasonality is coupled to plankton dynamics: fisheries stocks spread their larvae when food availability arises just after the phytoplankton bloom (Álvarez et al., 2012; Tsikliras et al., 2010). The hypothesis is that if the timing of the onset of the phytoplankton growing period advances, fisheries spawning seasonality may also initiate earlier or may become out of phase (mismatch, such as shown in Koeller et al., 2009). Furthermore if the phytoplankton growing period becomes shorter in the eastern basin, the fish assemblage could be less abundant or diverse, causing possible changes in the ecosystem structure and functioning. While an earlier

termination b_e of the growing period in the eastern basin may be explained by the limited phytoplankton growth (low Chl concentration) caused by scarce nutrient availability in this region, delays in the initiation b_i of the main growing period are more difficult to explain on the basis of mixing and subsequent stratification and, more complex processes may be need to examined. Trophic interactions may play an important role modulating the seasonal patterns of Chl concentration in some oceanic regions (Gomez et al., 2017). The delays observed in the timing of initiation b_i (Fig. 7a) might be explained by the grazing pressure exerted by winter zooplankton, as reported in other systems (Smetacek and Cloern, 2008). The relative importance of bottom-up and top-down controls at each biogeographical area may explain the different responses observed in the phytoplankton phenological indices. In fact, changes in timing and intensity are not uniform over the globe owing to oceanographically distinct regions and latitudinal drivers (Friedland et al., 2018).

The trends in Chl peak b_a observed in the eastern basin are consistent with studies reporting ocean regions, which are becoming more oligotrophic (e.g. Gregg and Rousseaux, 2014). However, globally, this trend has been recently questioned in the light of new and revised data showing no significant trend in global annual median Chl (Gregg et al., 2017). The trend in b_a in the western basin is positive. This particularly apparent in the NWMS an in the northern Adriatic (Fig. 8e). The dynamics of phytoplankton in these NWMS is mainly driven by the deep convective formation of Western Mediterranean Water and influenced by the North Atlantic Oscillation NAO (Macias et al., 2017; Mayot et al., 2017a). Based on ecosystem model analysis, Macias et al. 2018 predicted that in the near future (~2030) the spring bloom may occur later in the year and last longer. In the Adriatic Sea, convection is an important mechanism controlling the spring phytoplankton growing period (Gačić et al., 2002); however, the spatial distribution of the positive trend seems to follow the area of influence of Po River. Both winter mixing and river flow in the Mediterranean are closely related to the NAO (Brandimarte et al., 2011; Rixen et al., 2005; Struglia et al., 2004). Patterns of decadal variability driven by NAO could be influencing the trends in the amplitude of the Chl peak b_a in these regions (e.g. Basterretxea et al., 2018).

Phytoplankton functional group or species-specific responses to changing environmental conditions are likely to differ from total phytoplankton Chl responses, offering insights into mechanisms of trophic interactions, which are not possible with measurements and analyses of bulk Chl alone (Agirbas et al., 2015; Cabré et al., 2016; Ji et al., 2010; Racault et al., 2014a). The changes in Chl concentration and species composition have complex implications in the dynamics and diversity of higher trophic levels that the scientific community is only in the beginning to anticipate. Likewise, mismatch between production cycles and spawning season influences the recruitment success of some fish and crustaceans species (Asch, 2015; IOCCG, 2009; Koeller et al., 2009; Platt et al., 2003). Phenological changes can propagate to the rest of the food web and alter the functioning of the marine ecosystem with important consequences for commercially important species (Druon et al., 2015; Kassi et al., 2018).

5. CONCLUSIONS

We have analyzed the regional patterns of seasonal and non-seasonal variations in the Mediterranean Sea using ocean-color remote-sensing data. Our results show that seasonal

variations are dominant in oceanic areas whereas that non-seasonal variations play an important role in some specific areas of the Mediterranean Sea. In particular, irregular variations may be found in areas of intense wind forcing and/or well strong stablished current flows, and large interannual variations are mainly found in straits and water-exchange zones.

The timings of initiation, peak and termination of the main phytoplankton growing period show differences at regional scale, and between open ocean and shelf waters. The duration of the spring growing period in the western basin (~170 days) is longer than in the more oligotrophic eastern basin (~150 days). The duration generally shortens towards the coast where Chl is enhanced and where the probability of occurrence of a second growing period is higher (i.e. in fall).

Using the longest, continuous, bias-corrected ocean-color record, reaching nearly two decades of observations (17 years), we observed significant trends in the phenological indices. The duration of phytoplankton growing period has generally increased (+10 ± 7 days decade^{-1} on average during the period of study 1998 - 2014) in the western Mediterranean basin whereas an average decrease of -12 ± 7 days decade^{-1} is observed in the eastern basin. Exceptions to these trends are found in some coastal areas where more complex processes may control phytoplankton phenology. The observed variations in the phytoplankton phenological metrics will be relevant to investigate further and may help us advance understanding of the regulation of the energy flow in the Mediterranean Sea trophic chain.

6. ACKNOWLEDGEMENTS

This article is a result of the Ministry of Economy and Competitiveness (MINECO) of Spain Project Fine-scale structure of cross-shore GRADIENTS along the Mediterranean coast (CTM2012-39476). P.M. Salgado-Hernanz, was supported by a Ph.D. Doctoral research fellowship FPI (*Formación Personal Investigación*) fellowship BES-2013-067305 from MINECO. J.S. Font-Muñoz was supported by a Ph.D. Fellowship from *Conselleria the Educació - Govern de les Illes Balears* and the *European Social Fund* (ESF). M-F. Racault was supported by a grant from the Simons Foundation (549947, SS), the European Space Agency (ESA) Living Planet Fellowship program grant number 4000112798/15/I/SBo and the National Centre for Earth Observation (NCEO) of the Natural Environment Research Council (NERC) of the UK. This work is a contribution to the European Space Agency Ocean Color Climate Change Initiative (ESA OC-CCI). The authors acknowledge the Copernicus Marine Environment Monitoring Service (CMEMS) for providing Chl products tailored to the Mediterranean Sea version OCEANCOLOR_MED_CHL_L4_ REP_OBSERVATIONS_009_078, available online at http://marine.copernicus.eu/; and G. Volpe for helpful discussion about the CMEMS Chl product.

7. SUPLEMENTARY FIGURES

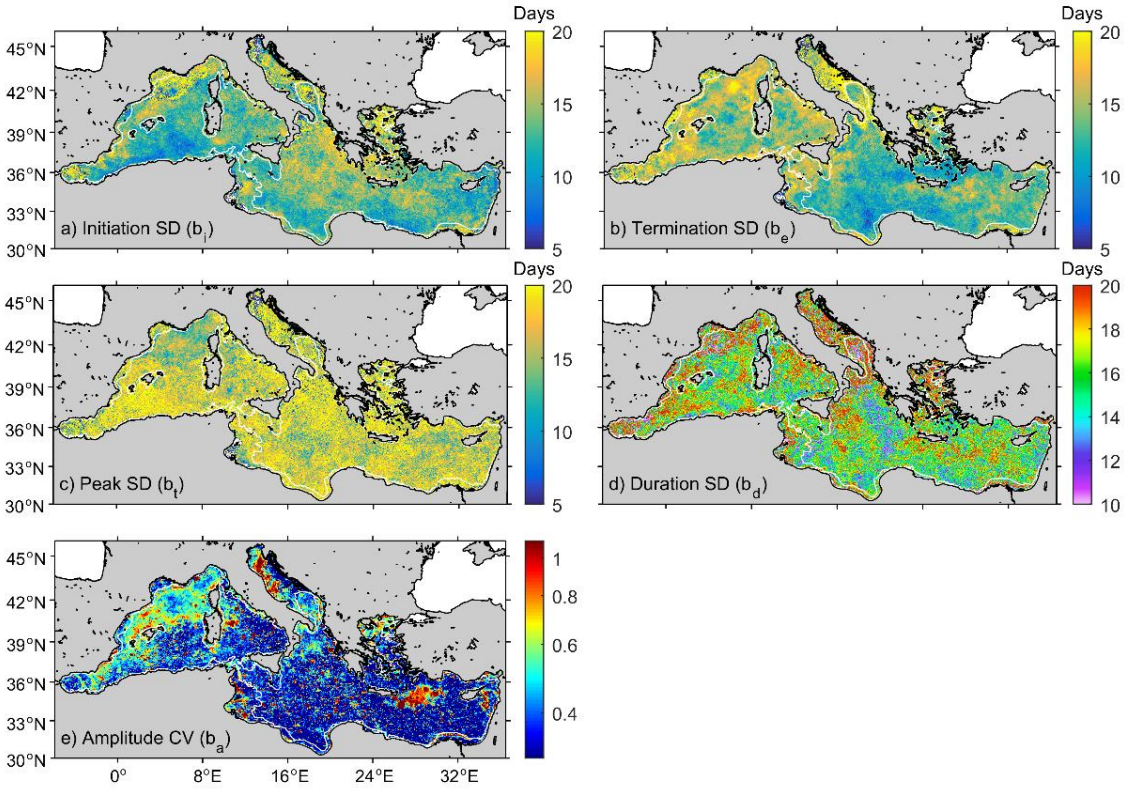

Supp. Fig S1: Standard Deviation (SD) and Coefficient of Variation (CV) for the phenological indices of the main growing period (1998 - 2014). White contour line separates coastal from offshore waters (200 m isobath).

Chapter 2. Patterns of chlorophyll interannual variability in Mediterranean biogeographical regions.

This chapter is based on the publication:

Basterretxea, G., Font-Muñoz, J.S., Salgado-Hernanz, P.M., Arrieta, J., Hernández-Carrasco, I., 2018. *Patterns of chlorophyll interannual variability in Mediterranean biogeographical regions*. Remote Sensing of the Environment (ISSN 0034-4257), volume 215, 15 September 2018, pages 7-17. doi:10.1016/j.rse.2018.05.027.

ABSTRACT

The Mediterranean Sea exhibits a strong basin and regional scale phytoplankton variability correlated to its semi-enclosed nature, complex orography and the variety of physical and chemical processes that regulate its productivity. Herein, using 17 years of ocean-color composites, we investigate differences in the regional patterns of interannual variability in satellite-derived chlorophyll (Chl), a proxy for phytoplankton biomass. A neural network classification, based on the Self-Organizing Maps (SOM) analysis in the time domain, is used to reveal regions of similar temporal variability of Chl in the Mediterranean Sea. Characteristic temporal patterns extracted by the SOM analysis show different scales of variation that can be related to already identified oceanographic features and biogeochemical variability in the Mediterranean Sea. Clear differences are noticed between regions located in the western basin and Adriatic Sea, where rivers, winter mixing and winds are known to drive variations in primary production at regional scale and regions located in the eastern basin, represented by a large and rather homogeneous region. Using the SOM-defined characteristic temporal patterns of Chl, we analyzed the regional influence of the North Atlantic Oscillation (NAO) and El Niño Southern Oscillation (ENSO) in the long-term (>1 year) Chl variability. Our results indicate that NAO has

more influence in the Chl variations occurring in regions located in the western basin whereas ENSO exhibits higher impact on the central Mediterranean and eastern basin during its positive phase. Both NAO and ENSO show non-stationary coherence with Mediterranean Chl. The analysis also reveals a sharp regime shift occurring in 2004 - 2007, when NAO changed from positive to negative values. This shift particularly affected the winter phytoplankton biomass and it is indicative of climate driven ecosystem-level changes in the Mediterranean Sea. Our results stablish a regional connection between interannual phytoplankton variability exhibited in different regions of the Mediterranean Sea and climate variations.

1. INTRODUCTION

A major challenge in the spatial analysis of oceanic systems is to classify and identify regions with common patterns since, unlike terrestrial ecosystems the sea is an intrinsically dynamical system often with diffuse boundaries and shallow gradients (Hinchey et al., 2008). Furthermore, numerous biological and environmental factors are non-linearly involved in the two-way environment-organism relations in the sea (e.g. Kavanaugh et al., 2016). Despite these difficulties, the classification of marine areas into clear cut geographical units, displaying similar biogeochemical characteristics and/or dynamical behavior, has become essential in the understanding of the plankton community responses to present and future climate scenarios. These represent fundamental abstractions of the geographical organization of life in response to past or current physical and biological forces (Kreft and Jetz, 2010). Biogeographical regions not only facilitate the understanding of the functioning of marine ecosystems but they are also useful when trying to define indicators of the environmental state as well as when undertaking the management of resource and conservation decisions (Spalding et al., 2007). An example of this is the Marine Strategy Framework Directive (Directive 2008/56/EC; MSFD, 2008) that, in order to achieve its ecosystem conservation goals, establishes marine regions and sub-regions based on geographical and environmental criteria.

Biogeographical regionalization can be based on geographic or on ecologically relevant attributes of the abiotic (i.e., temperature, salinity, eddy kinetic energy, hydrodynamics, etc.) or the biotic environment (i.e., biomass, taxonomy, size structure, etc.) from measured records or from data obtained using various modeling approaches. Satellite ocean-color data provides synoptic and long-term time coverage, which is ideal when attempting this classification. Several approaches have been traditionally used to identify coherent areas of the sea using ocean color and other complementary information (see Ayata et al., 2018). Multivariate clustering methods, such as *k*-means analysis, Principal Component Analysis (PCA) or Empirical Orthogonal Functions (EOFs), have proven to be efficient at obtaining coherent patterns of variation that can be explained on the basis of the main oceanographic characteristics (D'Ortenzio and Ribera d'Alcalà, 2009; Foukal and Thomas, 2014; Yoder and Kennelly, 2003). However, these methods are not capable of capturing the non-linear and turbulent character of the ocean dynamics. In addition, these approaches have drawbacks when managing datasets with missing values as they need some particular functional relationship or assumptions about the data such as distribution normality or preservation of the variance.

The Self-Organizing Maps (SOMs) developed in the last decades is a useful bioregionalization method since robustly clusters and identifies patterns in large datasets (Kohonen, 1982; Vesanto et al., 2000a). The SOM is a neural network algorithm based on unsupervised learning that works as a nonlinear alternative to the above mentioned linear grouping methods. While the SOM may show performance limitations in some cases (Liu et al., 2006; Solidoro et al., 2007) an advantage of the algorithm is that it preserves topology, and the obtained patterns are topologically ordered. Similar patterns are arranged to be neighboring units on the neural network, while dissimilar patterns are located far away from each other. In the case of biological regionalization, this topological ordination permits the establishment of similarity relationships in the dynamical behavior of each region defined by the SOM classification. This method has been successfully used in diverse climate, atmospheric and oceanographic applications (e.g. Lachkar and Gruber, 2012; Leloup et al., 2007; Richardson et al., 2003; Uvo, 2003). In the case of satellite ocean-color data, SOM classification has been used for a variety of applications including the synthesis of spatial patterns of chlorophyll (Chl) variation, the optimization of image processing, the classification of spectral signals for subsequent inference of phytoplankton groups, or for linking of sea-surface with vertical profiles of Chl (Ainsworth, 1999; Ben Mustapha et al., 2014; Charantonis et al., 2015; Farikou et al., 2015; Richardson et al., 2003; Yacoub et al., 2001). SOM classification can be applied to both space and time domains and provides a powerful tool for diagnosing ocean processes, as demonstrated by Liu et al. (2016).

Owing to its semi-enclosed nature in between two continents and to its intricate orography, the Mediterranean Sea exhibits regions of highly contrasting physical and chemical processes affecting their biological properties (e.g. Dubois et al., 2016; Reygondeau et al., 2017; Rossi et al., 2014). This seascape emerges from the three predominant and interacting spatial scales of the marine flow-basin scale, sub-basin scale, and mesoscale (Robinson et al., 2001), and from the differences in the geochemical inputs at these scales that determine phytoplankton productivity. The large scale factors, like the influx of nutrients by the Atlantic jet or the water-column stratification processes, result into a west-east oligotrophic gradient (e.g. Christaki et al., 2001; Dolan, 2000). This gradient is modulated by regional differences in terrestrial and atmospheric loads, dynamical features emerging from exchanges across straits and channels, as well as from mesoscale activity, frontal dynamics and local meteorology. Regional variations in the physical and chemical forcings generate a complex mosaic of biogeochemical environments, particularly in areas with river outflow and/or intricate topography. For example, enhanced Chl values along the northern coastal areas of the Mediterranean Sea have been associated with the impact of runoff from continental margins, vertical mixing due to the prevailing winds, or cooling and density mixing processes as well as persistent mesoscale dynamical features (Barale and Zin, 2000). Furthermore, the influence of the runoff can extend far from the deltas of major rivers such as the Rhone, Po or Nile, sustaining high phytoplankton production on the Mediterranean shelves that contrasts with the general oligotrophy prevailing in open waters (e.g. Antoine et al., 1995; Forget and André, 2007).

Even though the dynamics and pattern of seasonal phytoplankton variability in the Mediterranean Sea are well founded (e.g. Volpe et al., 2012), less is known about the longer timescale variability. At this scale, climate regulatory factors can be more important than direct anthropogenic influence in driving primary production and phytoplankton composition shifts (e.g. Dandonneau et al., 2004; Martinez et al., 2012; Rousseaux and Gregg, 2014). Several studies show

that large-scale atmospheric circulation patterns described by climatic indices have an influence over ecological processes in the Mediterranean region (see Lionello et al., (2006). Being located at the southern limit of the North Atlantic storm tracks, the Mediterranean region is particularly sensitive to interannual shifts in the trajectories of mid-latitude cyclones that can lead to remarkable anomalies of precipitation and, to a lesser extent, of temperature (Trigo et al., 2006). The consequences of these climate scale changes in the dynamics of the marine ecosystem are different to those guiding seasonal ecological change and the response of phytoplankton to this type of variability may be spatially variable and depending on the main factors limiting production at each location. Indeed, the ecology-climate interaction is not always straightforward (Stenseth et al., 2003) and climate induced interannual variations and ecosystem shifts may depend on multi-scale processes with interactive variability giving rise to considerable uncertainties in the prediction of the responses of the marine ecosystems.

Previous studies have reported the influence of large-scale modes of atmospheric variability on Chl distributions and variability in the Mediterranean Sea (e.g. Katara et al., 2008). In the present study, we focus on the influence of climatic forcing on the long-term (>1 year) regional variability of Chl in the Mediterranean Sea. Using satellite-derived Chl datasets, we first classify the Mediterranean Sea into regions of different characteristic temporal variability revealed by the SOM analysis in the time domain. By this method, we are able to define coherent biogeographical regions that will form the basis of our interannual variability analysis. We then used cross-wavelets analysis of the characteristic temporal Chl patterns of each SOM-defined region to identify the coherent correlations with two of the most relevant large-scale climate indices influencing the Mediterranean Sea, the North Atlantic Oscillation (NAO) and El Niño–Southern Oscillation (ENSO).

2. MATERIALS AND METHODS

2.1. Remotely sensed ocean-color and Climate indices data

Our analysis is based on the sea surface Chl concentration (mg m^{-3}) data product developed by the European Space Agency Ocean-Color Climate Change Initiative Program (ESA OC-CCI) (Sathyendranath et al., 2017; Sathyendranath and Krasemann, 2014). This Chl data has been tailored to the Mediterranean region by reprocessing the ocean color CCI product with the specific regional algorithm MedOC4 (Mediterranean Ocean-Color 4 bands, (Volpe et al., 2007). The resulting Level-4 product is distributed by the EU Copernicus Marine Environment Monitoring Service (CMEMS) and it can be downloaded from http://marine.copernicus.eu. This ocean-color data product is the result of merging MODIS-Aqua, SeaWiFS and MERIS sensors and it measures the average Chl content over the first optical depth. The analyzed Chl time series covers the period 1998 - 2014 for the Mediterranean Sea (30-to 46°N and 6°W to 37°E) and gridded 8-day temporal resolution and 1-km spatial resolution was downloaded. In order to reduce missing data, Chl values were first re-gridded to a 4 km regular grid and then the remaining gaps were filled in by applying spatial and temporal linear interpolation scheme (i.e., spanning three adjacent values).

NAO and Eastern Pacific and Central Pacific el Niño-3.4 (hereafter ENSO) indices were obtained from the National Oceanic and Atmospheric Administration (NOAA) Earth System Research

Laboratory website (https://www.esrl.noaa.gov/psd/data/climateindices/list/). 8-day averages were obtained from daily climate index data in order to use the same temporal resolution than the Chl time series. Other environmental variables such as precipitation and Sea Surface Temperature (SST) were obtained from available datasets in order to infer possible mechanisms driving Chl-climate relationships. Monthly precipitation data were obtained from gridded means provided by the Climate Prediction Center Merged Analysis of Precipitation (CMAP; https://www.esrl.noaa.gov/psd/data/gridded/data.cmap.html). Monthly SST were downloaded from the European Center for Medium-Range Weather Forecast (ECMWF; http://apps.ecmwf.int/datasets/data/interim-full-daily/levtype=sfc/). Monthly means of surface dust mass concentrations over the Mediterranean Sea were obtained from the Modern Era Retrospective analysis for Research and Application version 2 (MERRA-2) dataset from the NASA's Goddard Space Flight Center (Bosilovich et al., 2016; https://gmao.gsfc.nasa.gov/reanalysis/MERRA/). Data on MLD and nutrients was downloaded from CMEMS (http://marine.copernicus.eu/). MLD data was obtained from a reanalysis based on the version 3.1 of NEMO (Nucleus for European Models of the Ocean) ocean model (Madec, 2008). The nutrient data correspond to a reanalysis of Mediterranean Sea biogeochemistry based on OGSTM-BFM biogeochemical model and data assimilation of surface Chl concentration (Teruzzi et al., 2016).

2.2. Bioregionalization using SOM classification

Self-organizing maps, SOM, is a powerful visualization technique based on an unsupervised learning neural network which is especially suited to extract patterns in large datasets (Kohonen, 1997, 1982). SOM is a nonlinear mapping implementation method that reduces the high dimensional feature space of the input data to a lower dimensional (usually two dimensional) networks of units called neurons. In this way, SOM is able to compress the information contained in a large amount of data into a single set of maps. Since it preserves topology, similar neurons are mapped close together on the network facilitating the visualization of patterns.

The learning process algorithm consists of a presentation of the input Chl data to a preselected neuronal network which is modified during an iterative process. Each neuron (or unit) is represented by a weight vector with the number of components equal to the dimension of the input sample data. In each iteration the neuron whose weight vector is closest (more similar) to the presented sample input data vector, called Best-Matching Unit (BMU), is updated together with its topological neighbors towards the input sample. At the end of the training process the probability density function of the input data is approximated by the SOM and each unit is associated with a reference pattern, with a number of components equal to the number of variables in the dataset, so this process can be interpreted as a local summary or generalization of similar observations.

For typical satellite imagery the SOM can be applied to both space and time domains. For this work and since we are interested in the temporal variability, we have addressed the analysis in the time domain of the Chl datasets. In this case, the input row vector has been built using the Chl time series at each pixel, so each neuron corresponds to a characteristic Chl temporal pattern, composed of a specific time series of different values of Chl over the period of study. Since each of the step iterations has an associated time and location for the sample, we can obtain the

location of a particular temporal pattern computing the BMU for each pixel providing a map of regions with different phytoplankton variability.

When using SOM some parameters that control the initialization, training processes and final output have to be finely tuned. For instance, the optimal size of map (number of neurons) depends on the number of samples and on the complexity of the patterns to be analyzed. We choose the map size as [3 x 3], with 9 neurons. Using different sizes, for instance [4 x 4] the temporal patterns are more detailed and more regions of Chl variability emerge. However, these new patterns only split the boundaries of regions without providing sufficient insight into regions with different biochemical or physical behavior. Conversely, when using a [2 x 2] neural map, patterns are simplified in a few rough patterns without discriminating regions with different biogeochemical processes. We use hexagonal map lattice in order to have equidistant neighbors and which do not introduce anisotropy artifact. Concerning the initialization, we opted for a linear mode, batch training algorithm, and 'ep' type neighborhood function since this parameter configuration produces the lower quantitative and topological error and computational cost (Liu et al., 2006). These SOM computations have been performed using the MATLAB toolbox of SOM v.2.0 (Vesanto et al., 2000a, 2000b) provided by the Helsinki University of Technology (http://www.cis.hut.fi/somtoolbox/).

2.3. Influence of climate indices in the Mediterranean Sea

We base our long-term study on the use of selected mid-latitude climate indices (NAO and ENSO) with known influence on the Mediterranean region (e.g. Brönnimann, 2007; Jacobeit et al., 2001; Ropelewski and Halpert, 1997) and characteristic Chl variations for each SOM-defined Mediterranean biogeographical region. Other indices such as the Arctic Oscillation (AO), the East Atlantic/Western Russian pattern (EAWR) or the Mediterranean Oscillation Index (MOI) have been used to describe different aspects of climate variability in the Mediterranean Sea but we restricted our analysis of NAO and ENSO because they are widely used indices for which there are well known mechanistic explanations. Both of these large-scale indices of variability in the climate system coexist at different temporal and spatial scales reflecting the various atmospheric features influencing the Mediterranean region (Rodó et al., 1997).

NAO is the dominant mode of climate variability in Europe. It is defined as the normalized average sea level pressure difference between Ponta Delgada (Azores Lisbon) in Portugal and Stykkisholmur in Iceland. It characterizes the pressure difference between the middle of the North Atlantic Ocean and Iceland which affects winter conditions in the North Hemisphere (Hurrell and Van Loon, 1997; Marshall et al., 2001). For example, large pressure difference (positive NAO) results in a relatively dry winter in the Mediterranean but a warmer and wetter winter in northern Europe, and vice and versa. According to Trigo et al., (2004), the NAO is significantly correlated with Mediterranean winter precipitation, especially in the western basin. Because of the increased precipitation, river outflow varies considerably, with most Mediterranean river flows being anti-correlated with the NAO. Related runoff winter anomalies are about 10 - 20% of the winter means (Struglia et al., 2004). The NAO also impacts on other atmospheric variables such as air temperature and wind intensity (e.g. Hurrell et al., 2001).

ENSO index concerns with variations in temperature in the tropical Pacific or combines different variables in a multivariate index (MEI index). We selected NINO3.4 index, which is considered one of the most ENSO-representative indices (Barnston et al., 1997). The influence on the Mediterranean Sea is believed to be indirect in the sense that changes in the underlying circulation must have strong impact elsewhere between the ENSO area and Europe (Brönnimann, 2007). With some differences, the signal in European climate is most consistent in late winter and resembles the negative mode of NAO. In particular, it is demonstrated that ENSO impacts most significantly on European wintertime rainfalls during positive (warm) phases of the Pacific Decadal Oscillation (Zanchettin et al., 2008). It also influences wind and precipitation in North Africa, the eastern Mediterranean and the Middle East (Shaman and Tziperman, 2007). Mariotti et al. (2002) also found that western Mediterranean-averaged rainfall is significantly correlated with ENSO variability during autumn, with the sign being opposite to that found in spring.

2.4. Coherence between long-term chlorophyll variability and climate indices

To examine the long-term (>1year) Chl variability and their relationship with climate variations, we first identify the dominant low frequencies of Chl variation using wavelet analysis. We use Wavelet Transform Coherence (WTC) analysis (Grinsted et al., 2004) to statistically identify the time (when and the duration) where low-frequency Chl variations and climate indices (NAO and ENSO) are correlated. Coherence is defined as a measure of the intensity of the covariance of the two series in time-frequency space (Torrence and Webster, 1999). WTC computations identify possible relationships between two variables by searching frequency bands and time intervals during which they covary (Gurley et al., 2003; Gurley and Kareem, 1999). WTC is based on the Continuous Wavelet Transform (CWT) defined as the convolution of the time series with a scaled and translated mother wavelet function. Wavelet transform is an extension of the concept of the Fourier transform. While a Fourier transform only provides the global power spectral density of the characteristic frequencies (it cannot provide changes in frequency structure over time), a wavelet transform allows to know the power of the characteristic frequencies and when. This is due to the fact that the kernel in the Fourier transform can only extract frequency information of the signal, while the kernel of the wavelet is able to extract both frequency and time. In particular, we use the Morlet kernel wavelet with a number of wavelet cycles $\omega_0 = 6$ since it provides the best tradeoff between temporal and frequency precision (Grinsted et al., 2004). Therefore, CWT expands a time series into time-frequency domain thus allowing the analysis of how the frequency content of a time series changes over time.

Lets $W_n^X(\mathrm{s})$ and $W_n^Y(\mathrm{s})$ be the wavelet transforms of X and Y signals, respectively, where X is the i^{th} SOM temporal pattern of Chl after removing the seasonal signal subtracting its mean climatology and Y is the time series of the climatic index (NAO or ENSO), n is time index and s is the time scale in inverse proportion to frequency (Torrence and Compo, 1998). The Cross-wavelet Transform $(W_n^{XY}(\mathrm{s}))$ is defined as

$$\mathrm{Y} * (\mathrm{s})$$

$$W_n^{XY}(\mathrm{s}) = W_n^X(\mathrm{s})\, W_n\,, \quad (1)$$

where (*) indicates complex conjugate. The Cross Wavelet Power spectra are given by $|W^{XY}(\mathrm{s})|^2$. The XWT finds regions in time frequency space where the time series shows high common power spectra. The wavelet squared coherency $(R_n^2(\mathrm{s}))$, is defined as the absolute value squared of the smoothed cross-wavelet spectrum, normalized by the smoothed wavelet power spectra,

$$R_n^2(\mathrm{s}) = \frac{\left|\langle \mathrm{s}^{-1} W_n^{XY}(\mathrm{s})\rangle\right|^2}{\langle \mathrm{s}^{-1}|W_n^X(\mathrm{s})|^2\rangle \langle s^{-1}|W_n^Y(\mathrm{s})|^2\rangle} \quad (2),$$

where the brackets $\langle\ \rangle$ indicate smoothing in both time and scale. The factor s^{-1} is used to convert to an energy density. $\mathrm{R}_\mathrm{n}^2(\mathrm{s})$ ranges between 0 and 1 and can be thought of as the local correlation between two CWTs searching regions in time frequency space where the two time series co-vary over time (but does not necessarily showing high power).

The wavelet-coherency phase (ϕ_n) difference is given by

$$\phi_n = tan^{-1}\left(\frac{I\{\mathrm{s}^{-1} W_n^{XY}(s)\}}{R\{\mathrm{s}^{-1} W_n^{XY}(s)\}}\right) \quad (3),$$

where the smoothed real (R) and imaginary (I) parts should have already been calculated in (2), both $R_n^2(s)$ and ϕ_n are functions of the time index n and the scale s. In this study, we used the MATLAB-based package downloaded from http://grinsted.github.io/wavelet-coherence/ (Grinsted et al., 2004). This software package uses a Morlet wavelet as a default mother wavelet function, since it provides a good balance between time and frequency localization. The statistical significance level of $R_n^2(\mathrm{s})$ was calculated using a Monte Carlo simulation by 300 surrogate data set pairs.

3. RESULTS AND DISCUSSION

3.1. Bioregionalization using SOM classification

Fig. 1 shows the 9 characteristic Chl temporal patterns extracted from the 3x3 SOM analysis (panel a) and the corresponding biogeographical regions depicted from the classification of the time series of each pixel considering its BMU (panel b). In addition, a mean climatology and its standard deviation for each time pattern are displayed as inset in Fig. 1a. The topological ordering of the temporal patterns in the neural network performed by SOM highlights the differences/similarities between regions. Patterns with large variability (large standard deviation) and high mean values are located around the bottom-left corner of the neural network and those with low variability and low mean value around the top-right corner. A common feature observed in all the characteristic temporal patterns is the seasonal variability of Chl over the study area, which follows the canonical Mediterranean annual cycle with a late winter-spring bloom and a mid-summer minimum. Variation in mean Chl among these regions reflects the well-known west-east phytoplankton biomass large-scale gradient produced by the progressive nutrient depletion of the Atlantic waters in their progress to the eastern basin (D'Ortenzio and Ribera d'Alcalà, 2009; Lazzari et al., 2012). Increased concentrations in Chl are found in regions of major river discharge, wide continental shelf areas, and regions where particular ocean dynamics enhances phytoplankton productivity (i.e. Alboran Sea and NW Mediterranean).

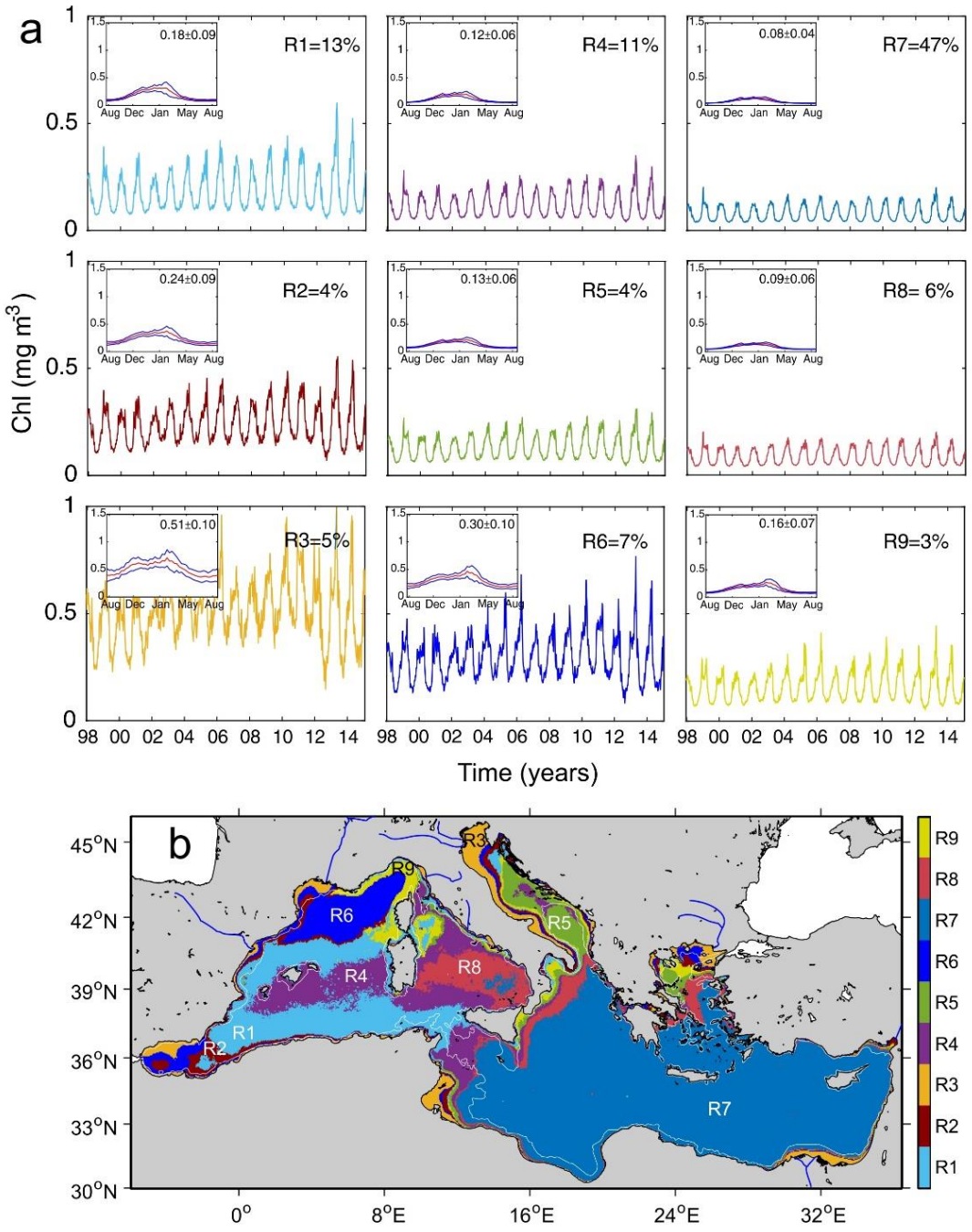

Fig. 1 a) Characteristic temporal patterns of Chl obtained from 3x3 Self-Organizing Map (SOM) computation of Mediterranean Chl fields, and their corresponding climatology (inset). Units for the climatology y-axis are also mg m^{-3}. b) Regions of different temporal Chl variability depicted from the classification of the time series of each pixel according to its BMU. The white line in the map indicates the 200 m isobath. Blue lines indicate the location of major rivers.

A prominent feature in the obtained bioregionalization is the difference in the spatial extension of the regions between the eastern basin, almost entirely included in R7, and the western basin which shows higher spatial complexity and regional compartmentalization. R7 embraces a vast oceanic area (median depth = 1962m) displaying very low mean Chl values and reduced seasonal variations (0.08 ± 0.04 mg m^{-3}). Other oceanic regions such as R5 and R8 show a similar characteristic pattern (see similarity matrix in Suppl. Fig. S1) albeit with slightly higher Chl values.

Jointly, these three regions comprise 57% of the Mediterranean Sea. These regions broadly correspond to areas where nitracline and mixed layer depth (MLD) are generally decoupled (Pasqueron De Fommervault et al., 2015; see the computed climatology of MLD and nutrients corresponding to each SOM regions shown in Suppl. Fig. S2). Other regions (R6 and R2) exhibit a decoupling of months when nutrients are supplied and consumed suggesting that other mechanisms drive the supply of nutrients into the euphotic layer, i.e. the cyclonic circulation in the northwestern Mediterranean (R6) during winter acting as previous conditions favoring phytoplankton blooms in spring (Lavigne et al., 2013). Indeed, the nitrate increase in surface layers during winter mixing at R7 and R8 is modest (<0.5 mmol m^{-3}; Suppl. Fig. S2).

In the opposite side of the neural network arrangement, R3 includes the pixels representing the most productive areas in the Mediterranean Sea. These areas correspond to shallow (median depth = 28m) Regions Of Freshwater Influence (ROFIs) in the northern Adriatic, the Nile and Ebro deltas, as well as in the Rhone river mouth, and to the productive areas in the Northern Alboran and Gabes Seas. Primary production in this region is not only controlled by winter mixing but also by the hydrological flow of the aforementioned rivers that maintains enhanced nutrient concentrations throughout the year (suppl. Fig. S2). As shown in Fig. 1b, SOM provides good definition of areas displaying strong Chl gradients. This is of particular interest in complex regions such as the Adriatic, the Aegean or the Alboran Sea, and shelf areas, where cross-shore gradients may be intense. For example, the narrow regions around the Ebro and Nile river deltas are well-defined in our SOM classification showing clear cross-shore and alongshore zonation (see major river discharge areas in Fig. 1b) and are not as clearly resolved in other clusterization schemes (see examples in Ayata et al. (2018).

The Rhone plume which enriches a large region extending along the coast of the Gulf of Lions (Forget and Ouillon, 1998) is adequately captured in our biological regionalization. Similarly, the area affected by the Po River discharge extends at least one hundred kilometers southward from the delta along the coast and approximately twenty kilometers offshore with maximum Chl concentrations following closely the river waters (Marini et al., 2010). According to Struglia et al. (2004), the Adriatic is the sub-basin with the greatest freshwater input (about 2500 m^3 s^{-1} on annual basis), which is mostly due to the Po River and the confluence of other alpine rivers. Discharge into this basin has an unusual seasonal cycle with a minimum in summer and two maxima in May and November (Montanari, 2012). The consequent variations in terrestrial loadings may induce variations in phytoplankton phenology with respect to open ocean waters (i.e. occurrence of several blooms).

SOM classification reveals strong cross-shore gradients from R3 to open ocean patterns (i.e. R1 or R7) that are structured by regions R6, R2 and R9. Besides the Adriatic, this transition is also observed in the Ebro river area, the Gulf of Gabes or even in small bays like the Gulf of Naples. R3 is also present along the upwelling region of the northern Alboran Sea. In this coast, the offshore transition is spatially structured by the presence of the incoming Atlantic jet from Gibraltar Strait, and by the two Alboran gyres. In particular, it is worth observing how the SOM bioregionalization reveals the two Alboran gyres including their productive region (R3) in the periphery of the gyres, and the boundary jet and a less productive region (R2) in their core (e.g. Macías et al. (2007).

A third major pattern, accounting for 7% of total area, is that occurring in the more productive waters of the North Western Mediterranean Sea (NWMS), bounding the Alboran gyres and,

marginally, in the northern Aegean Sea (R6). This region located to the north of the Balearic Islands, is represented by the larger R6 cluster that matches well with the area of Western Mediterranean Deep Water formation (WMDM), as described by Somot et al. (2018). The climatology for this region shows a seasonal Chl peak in late March, following deep mixing processes occurring in this area (Suppl. Fig. S2, D'Ortenzio et al., 2005; Houpert et al., 2015). This pattern suggests that deep winter mixing may dominate nitrate supply at the surface layer in the NW Mediterranean. However, recent studies found that nitrate supply in this region is also controlled by the depth and gradient of the nitracline at the end of winter, with the particular cyclonic circulation during winter as a precondition driving the nitracline depth (Lavigne et al., 2013; Pasqueron De Fommervault et al., 2015). Nonetheless, it should be pointed out that in our case this SOM typology incorporates information from other Mediterranean areas. This also influences the climatology pattern of R6 which shows lower Chl mean values than those reported for the NW Mediterranean (i.e. >1.0 mg m^{-3}, D'Ortenzio et al., (2014).

The results of the above-described classification reveal the suitability of SOM for a consistent regionalization of the Mediterranean in accordance with the main Chl temporal patterns and geographical limits described for this Sea. As compared to classifications obtained using k-means, SOM is able to introduce non-linear correlations through the neighborhood function, extracting more details in the definition of areas, particularly where non-linearities may be important (i.e. complex dynamical features like eddies, fronts and jet interactions, river plumes and strong continental slope or coastal transition zones). On the other hand, while studies based on other variables and classification methods report regional differences in the eastern Mediterranean patterns (Berline et al., 2014; Rossi et al., 2014) the SOM classification of satellite Chl does not find significant differences in this region.

To test the relevance of the size of SOM in the regionalization of this large area, we performed a 4x4 SOM classification (Suppl. Fig. S3). The results of using 16 neurons, while increasing the detail of gradient areas, does not substantially vary the general features observed in the regionalization. In fact, the main difference between both classifications (3x3 and 4x4) is that a zonal transition region between the Aegean and the eastern basin emerges to the north of Crete. In addition, a number of small regions (<3% of total surface) that for many applications are meaningless is also generated. The detail required for the definition of the bioregions is often variable since, apart from responding to ecological differences, it often obeys to resource planning and management necessities. For example, differences between some regions describing oceanic areas are low, and regionalization could be further reduced to 6 regions by merging similar neurons (i.e. R1 with R4; R5, R7 and R8; see Suppl. Fig. S1).

The observed variations in Chl convey structural and compositional changes in phytoplankton assemblages that can be inferred by different algorithms (Brewin et al., 2011; Nair et al., 2008; Uitz et al., 2006). Although our regionalization is based on Chl variation patterns, a correspondence can be established between these temporal patterns and phytoplankton structure characteristics. We have estimated the regional size structure of phytoplankton assemblages at each mean Chl following Di Cicco et al. (2017); see Table 1. The resultant variations in the dominant groups can be associated with underlying physical and biogeochemical forcings prevailing at each region. For instance, picoplankton is typically dominant in open waters where growth is strongly limited by nutrient limitation (R4, R7 and R8). Conversely, nanoplankton

is predominant in R3, were terrestrial nutrients are supplied, and in the R6 where strong winter convection injects nutrients into the mixing layer. These two regions exhibit increased percentages of cryptophytes and diatoms (>5% and >14%; Suppl. Table S1). Differences in size and composition are enhanced during the winter-spring bloom, when Chl differences between regions are highest i.e., microplankton exceeds 20% in R3 and R6. This is in agreement with the observations obtained by Sammartino et al. (2015) who reported higher microphytoplankton dominance in regions with different and atypical dynamical features, i.e., the NW Mediterranean Sea and the Alboran Sea, as well as several coastal areas, such as the North Adriatic Sea during the spring bloom season. In coastal and riverine areas, such as R3, microphytoplankton dominates in all seasons as the result of the nutrient supply from the terrestrial inputs.

Table 1. Seasonal and annual contribution (%) of the different size classes (pico- nano- and microplankton) contributing to the phytoplankton community at each region, as estimated from the empirical equations of Di Cicco et al. (2017).

	Picoplankton					Nanoplankton					Microplankton				
	Spring	Summer	Fall	Winter	Annual	Spring	Summer	Fall	Winter	Annual	Spring	Summer	Fall	Winter	Annual
R1	38±4	47±1	43±4	34±1	40±6	44±2	38±1	41±3	47±0	43±4	18±2	15±0	16±1	20±1	17±2
R2	34±3	41±1	38±2	32±1	36±4	46±2	42±0	44±1	47±0	45±2	19±1	16±0	18±1	20±0	19±2
R3	27±1	31±0	29±1	27±0	29±2	48±0	47±0	48±0	48±0	48±0	24±1	21±0	23±1	25±0	23±2
R4	43±5	54±1	50±4	38±1	46±7	41±4	32±1	36±3	44±1	38±5	16±1	13±0	14±1	18±0	16±2
R5	41±4	51±1	47±4	38±1	44±6	42±3	34±1	38±3	44±1	40±4	17±1	14±0	15±1	18±0	16±2
R6	32±2	38+1	35±2	31±0	34±3	47±1	45±1	46±1	48±0	46±1	21±1	18±0	19±1	21±0	20±2
R7	50±6	61±1	56±5	43±1	52±8	36±4	27±1	31±4	41±1	34±6	15±1	12±0	13±1	16±0	14±2
R8	47±5	59±1	54±5	42±1	51±7	38±4	29±1	32±4	41±1	35±6	15±1	12±0	13±1	16±0	14±2
R9	38±4	48±1	44±3	37±1	42±5	44±2	37±1	40±2	45±0	41±4	18±1	15±0	16±1	18±0	17±2

3.2. Long-term chlorophyll variability and teleconnections

The dominant time scales of Chl variability over each SOM-defined region are revealed by wavelets analysis. As shown in Fig. 2, the seasonal (1-yr) periodic mode is by far the most intense signal in the nine regions (see also wavelets power spectrum in Suppl. Fig. 4). A semi-annual period is also relevant in some of the regions, particularly in those corresponding to large open sea areas (R1, R4 and R7). One or two secondary peaks occur at longer periods (>1 year), particularly in the 2 to 4-year band. The wavelet power in these lower frequencies is much weaker than the annual period but shows significant local peaks. Peak periods in this band are centered in 2.3 and 3.5 years, albeit a sole peak centered in 2.6 years occurs in R3, R6 and R9. Once the climatological seasonal cycle is subtracted from the Chl time series a considerable variability still remains over a wide range of time scales.

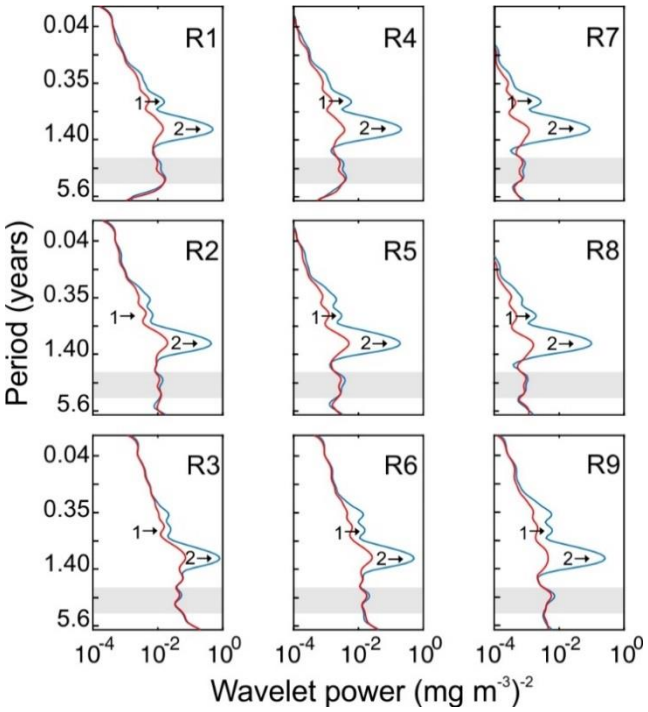

Fig 2. Global wavelet power spectra (mg $m^{3})^{2}$ of the characteristic Chl time-patterns as extracted by SOM analysis (see Fig. 1). The blue line corresponds to the complete time series and the red line to the deseasonalized residual. 1 and 2 mark the semi-seasonal and seasonal periods respectively. The gray band indicates the 2 to 4-year band.

Variations in NAO and ENSO indices are displayed in Fig. 3. During the study period, low frequency variations in NAO were slightly positive until 2005, and declined thereafter to recover back to positive in 2013 (Fig. 3a). ENSO was mostly negative throughout, except between 2001 and 2006 (Fig. 3b).

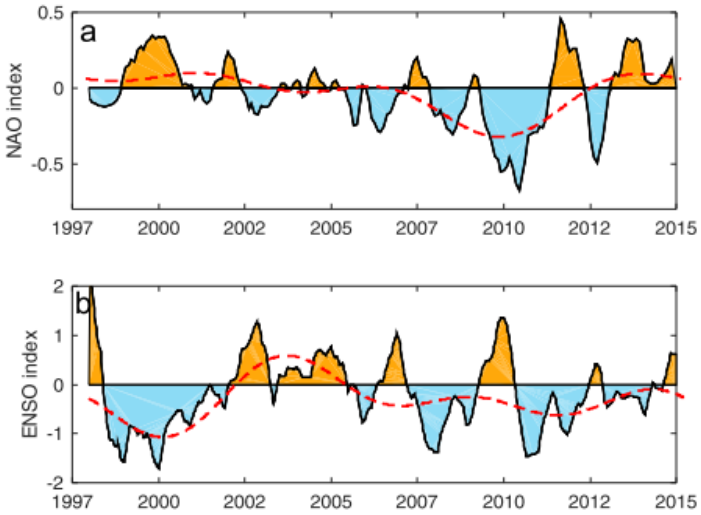

Fig. 3. The NOAA Climate Prediction Center monthly time series of North Atlantic Oscillation (NAO) and El Niño 3.4 (ENSO) anomalies. The dashed line shows the low frequency variation (>2 years).

WTC between the NAO and the deseasonalized characteristic Chl variations of each region are shown in Fig. 4. Black contour lines in the wavelet spectra enclose energy peaks significant at 95%

confidence level. High correlation of these two signals is observed at periods of 1.2 years and in a band extending from ~2 to 4 years and peaking at 3.4 years. As indicated by the arrows in the figure, a phase difference of 180° is observed in the first period whereas slightly longer phases are identified in the second one in these coherency period bands. The fact that both signals are in anti-phase indicates an increase in Chl when the NAO is negative (e.g. more rain or wind over the Mediterranean) and vice versa.

Regionally, the highest coherence for the 1.2 year period occurs in the western Mediterranean (R1, R2, R3, R4, R5 and R6). Conversely, the central (R8) and eastern Mediterranean basin (R7) exhibit a weak influence at this band. The 3.2 year centered band is more widely distributed, although in R3, R6 and R9, mainly representing the most productive waters in the north Mediterranean; this band is displaced towards higher frequencies (i.e. 4 - 5 years). The two coherence bands are non-stationary (present discontinuities over time). A shift is found after 2005, being the 1.2 period relevant until this date, and the 3.4-year period, thereafter. This suggests a variation in the pathways through which climate factors are influencing Mediterranean productivity. Our analysis reveals that this regime shift has an important effect on winter phytoplankton productivity.

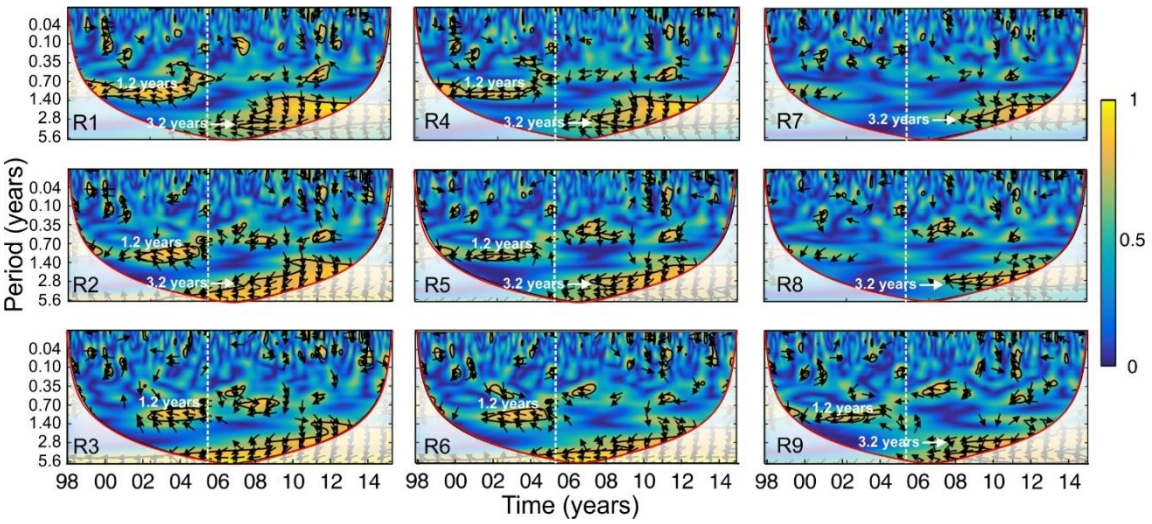

Fig. 4. Wavelet coherence and phase difference between the SOM temporal patterns of Chl variability shown in Fig. 1a and NAO. The relative phase relationship is shown as arrows (with in-phase pointing right, anti-phase pointing left). The black contour lines enclose peaks of >95% significance level using the red noise model. The red line curve depicts the cone of influence beyond which the edge effects become important. The dashed line marks the summer 2005. Values in x-axis are years starting in 1998. Colorbar shows power spectral density.

Due to its control over weather conditions, NAO affects mixing and thus the flow of nutrients to the photic zone. In consequence, the effect of NAO on marine phytoplankton is more noticeable during winter when vertical nutrient exchange is not dampened by seasonal stratification. It also affects river discharges across the Mediterranean catchment primarily in winter (Struglia et al., 2004). Fig. 6 shows the mean winter (December, January and February) Chl anomalies before and after 2005, when NAO varies from positive to negative. Most regions show positive winter Chl anomalies after 2005, and particularly enhanced values between 2008 and 2010, when NAO was

persistently negative (see Fig. 4). This period was coincident with years of positive precipitation anomalies and, except in R1, R7 and R8, cooler sea surface temperatures (Fig. 6). Indeed, Chl anomalies show low but significant correlation with rainfall anomalies (r^2 = 0.42, p<0.01). As in the case of NAO-Chl coherence, the weakest correlation is that of R7 (r^2 = 0.18, p=0.1). Blake et al. (2011) suggest that the relationship between NAO and rainfall in the eastern Mediterranean is non-linear and reflects complex links between the large-scale atmosphere and the Mediterranean circulation. Krichak et al. (2014) also found low influence of precipitation and wind in the eastern basin, associated with NAO events. In any case, the shift occurring in 2005 cannot be solely attributed to increased inputs from the atmosphere or rivers. It seems part of a more global environmental variation which includes changes in the Mediterranean water masses and variations in the fluxes through Gibraltar driven by the influence of NAO (i.e. through sea level changes). In fact, as shown in Fig. 5, open ocean waters such as R1 show greater winter Chl anomalies than ROFI regions (i.e. R3). Moreover, McGinty et al. (2016) also observed a shift in the NAO-Chl relationships in the North Atlantic after 2005, suggesting that the effects of this climate scale variation exceed the Mediterranean Sea. Regime shifts in the Atlantic and Mediterranean Sea associated with NAO phases have been studied in the past and are known to expand throughout all marine trophic levels (Alheit and Bakun, 2010; Conversi et al., 2010). Schroeder et al. (2016, 2010) observed an abrupt change in the convective formation of Western Mediterranean Water affecting the intermediate and deep water masses during this year. This convective water-mass formation, occurring in R6, is strongly correlated to the NAO (Rixen et al., 2005).

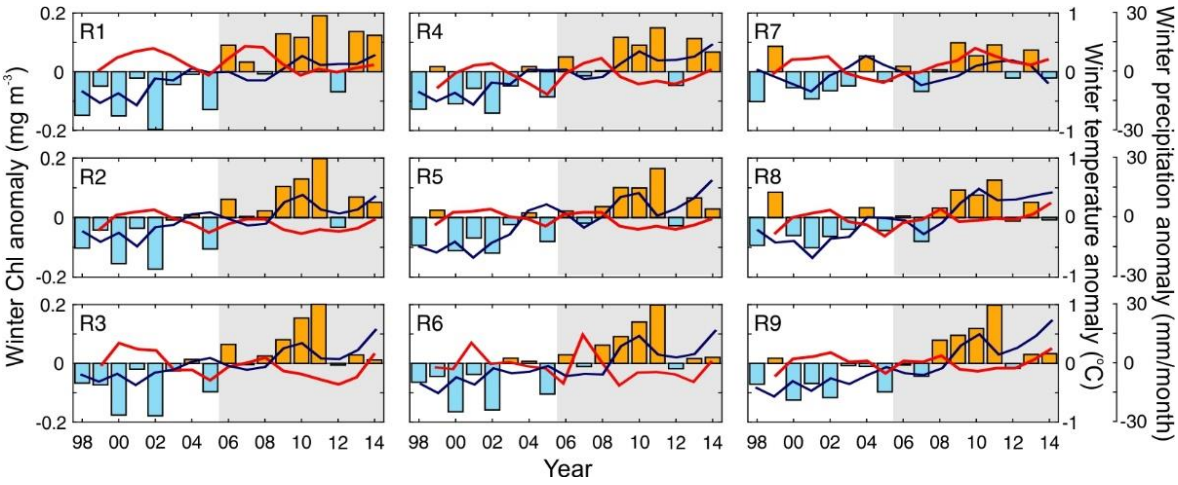

Fig 5. Variations in winter Chl anomalies (bars) and low–pass filtered winter precipitation (blue lines, right axis) and sea surface temperature (red line, right axis) anomalies at each Mediterranean region. Chl values are depicted from the characteristic time series obtained using SOM analysis. *x*-labels indicate years starting in 1998. Years after 2005 are plotted over a gray background.

The influence of ENSO in the different biogeochemical regions is weaker and the overall coherence is less significant than in the case of the NAO though a good correlation is observed at time scales of 2- year period in R7 and R8 (Fig. 6). This correlation is higher when ENSO is mostly positive (from 2001 to 2007). A plausible explanation is that it is the result of the influence of nutrient rich Saharan dust deposition over these regions. Gallisai et al. (2014) reported good correlation between Chl in these central and eastern Mediterranean oligotrophic areas and

Saharan dust deposition. ENSO is also known to exert a control on North African dust export during summer through its influence on the North African dipole intensity (DeFlorio et al., 2016).

Table 2. Annual mean ± SD of surface dust concentration over the 9 SOM-defined regions and correlation coefficient (*r*) with ENSO variations.

Region	Concentration ($\mu g\ m^{-3}$)	*r*
R1	21 ± 10	0.27
R2	25 ± 9	0.29
R3	33 ± 14	0.45
R4	22 ± 10	0.21
R5	22 ± 11	0.37
R6	17 ± 7	0.30
R7	40 ± 24	0.58
R8	23 ± 11	0.33
R9	16 ± 7	0.29

Satellite depicted surface mass concentrations of dust exhibit clear differences in mean dust concentration among regions and increases of up to 74% in R7 during positive ENSO phases (Suppl. Fig. S5). Indeed, concentrations in R7 (40 ± 24 μg m^{-3}) almost double those observed in other regions and correlate well with ENSO ($r = 0.58$, $p<0.01$; Table 2). However, the correlation between atmospheric dust concentration and Chl is not significant ($p>0.01$). This is attributed to the generally low Chl concentrations in this region and to the rapid transfer through the food web, as observed by Tsagaraki et al. (2017). While Chl response to Saharan dust storms may be occasionally important (Gallisai, 2016), in many cases, changes in the eastern Mediterranean are close to the detection limit of either field or remote sensing measurements (Herut et al., 2005). In addition, the role of dust fertilization in the eastern Mediterranean Sea is controversial and some studies indicate that it does not play a significant role in the sustainment of the phytoplankton dynamics in the Mediterranean Sea (Volpe et al., 2009). Therefore, unraveling the control of ENSO on Chl necessitates a better understanding of the effects of atmospheric dust on the long term responses of phytoplankton assemblages in the Mediterranean Sea.

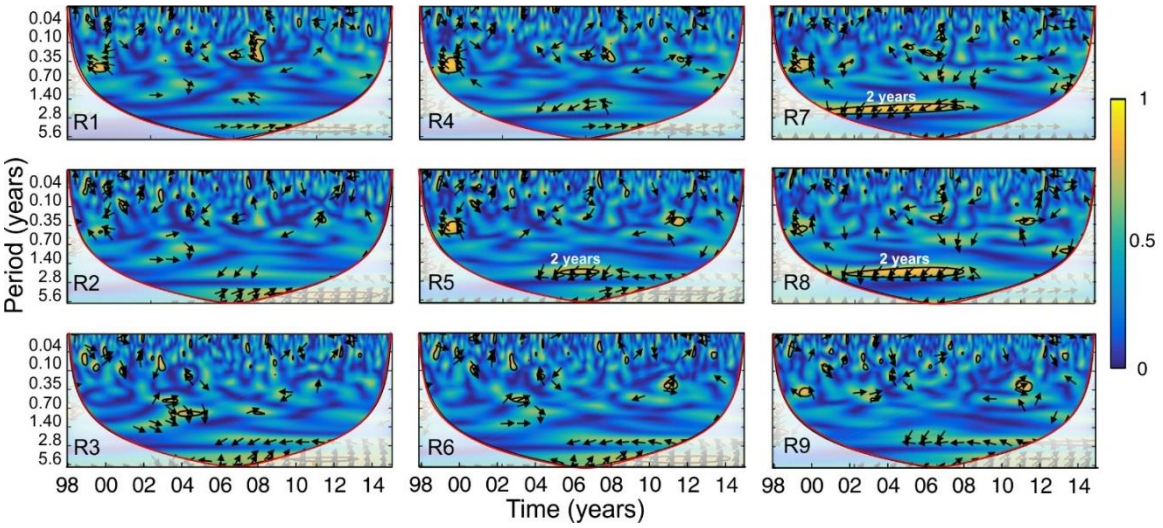

Fig. 6. Wavelet coherence and phase difference between the SOM temporal patterns of Chl variability shown in Fig. 1b and ENSO. The relative phase relationship is shown as arrows (with in-phase pointing right, anti-phase pointing left). The thick black line is the 95% significance level using the red noise model, and the red line curve depicts the cone of influence beyond which the edge effects become important. Colorbar shows power spectral density.

4. CONCLUSIONS

Various bioregions in the Mediterranean Sea have been identified based on the satellite depicted temporal variability of Chl using SOM classification, and the associated size classes of phytoplankton have been estimated. Firstly, we identified the characteristic time series of Chl that facilitates the classification of the Mediterranean waters into nine meaningful regions which are consistent with recognized oceanographic and biogeochemical characteristics of the Mediterranean Sea. Secondly, we used these characteristic series for the long-term analyses of Chl variability and its coherence with NAO and ENSO.

Although a comparison between various clustering algorithms was not the focus of this paper, our observations suggest that in some aspects SOM provides more detailed results than previous Chl-based bioregionalizations of the Mediterranean Sea (i.e. Ayata et al., 2018; D'Ortenzio and Ribera d'Alcalà, 2009). SOM tends to preserve data topology (i.e. preserves neighboring regions) and, therefore, it is particularly suited for pattern recognition (Liu and Weisberg, 2005) allowing adequate classification of areas with high spatial complexity and strong gradients. Furthermore, reclassifications can be achieved from the topological ordination of the classified areas and the relative distance among neurons. This allows further analysis based on similarities between regions and thus some of the areas representing transition zones could indeed be merged with larger areas for certain conservation and management applications.

The interannual Chl variability at each SOM-defined region has been investigated in relation to the NAO and ENSO. Both NAO and ENSO exhibit non-stationary coherence with Mediterranean Chl. NAO effect on phytoplankton variability, mainly in the western biogeographical region, but the temporal scale at which affects Chl might produce different phytoplankton responses. In fact, we observed a shift in the coherence between NAO and Chl occurring in 2005 that is paralleled by an increase in winter Chl after this year (up to 0.4 mg m^{-3} increase from low Chl years, see Fig.

6). Enhanced Chl in winters are broadly related with increased precipitation and lower sea surface temperatures, but the causative effect of the higher productivity during these negative NAO years should be further studied in relation to more global environmental factors, including variations in the thermocline, in the mixing and the exchanges through Gibraltar. In fact, the Alboran Sea and southwestern Mediterranean are the regions exhibiting higher winter Chl anomalies.

The long-term Chl variability central and eastern basins exhibit a lower response to NAO and better coherence with ENSO. In the absence of other atmospheric mechanisms, such as precipitation or wind forcing as an explanation for this atmosphere-ocean coupling we suggest that variations in atmospheric dust deposition could account for this link between ENSO and Chl. We show that satellite depicted surface dust mass concentrations in R7 (40 ± 24 µg m^{-3}) almost doubles the values observed in other regions and correlate well with ENSO ($r=0.58$, $p<0.01$). However, direct relationships between dust concentration and Chl are difficult to determine most likely because Chl variations in the eastern Mediterranean are low and close to the detection limit of field and of remote sensing measurements.

5. ACKNOWLEDGEMENTS

We are grateful to EU Copernicus Marine Environment Monitoring Service (CMEMS) for the freely available ocean-color remotely-sensed data. NAO and el Niño-3.4 climate indices were obtained from the National Oceanic and Atmospheric Administration (NOAA). This article is a result of the MINECO grants GRADIENTS (CTM2012-39476) and SIFOMED (CTM2017-83774-P). P.M. Salgado-Hernanz was supported by a FPI fellowship BES-2013-067305 from the Ministry of Economy and Competitiveness (MINECO) of Spain. J.S. Font-Muñoz was supported by a Ph.D. Fellowship from Conselleria d'Educació (Govern de les Illes Balears) and Fondo Social Europeo (FSE). I. Hernandez-Carrasco acknowledges the Juan de la Cierva contract funded by the Spanish Government.

6. SUPPLEMENTARY INFORMATION

Suppl. Table S1. Depth (median [q1 q3]) and phytoplankton functional types (PFTs) for each SOM-defined region. PFTs are expressed as a fraction of total community (%) and were estimated following Di Cicco et al. (2017).

	Depth (m)	Diatoms	Dinophytes	Cryptophytes	Haptophytes	Prochlorophytes	Prokariotes
R1	2136 [385 2752]	12±2	6±1	4±1	39±0	8±3	32±6
R2	164 [67 1149]	13±2	6±1	4±1	39±0	10±2	28±5
R3	28 [14 58]	18±2	5±1	7±1	40±0	13±0	17±3
R4	1061 [262 2318]	10±1	5±1	3±1	39±1	6±2	37±6
R5	245 [117 850]	11±1	5±1	3±1	39±0	6±2	36±5
R6	1660 [108 2556]	14±2	6±1	5±1	39±0	11±2	25±4
R7	1962 [735 2812]	9±1	5±1	2±1	38±1	4±2	42±5
R8	1662 [499 2777]	9±1	5±1	3±1	38±1	4±2	41±5
R9	710 [150 1359]	11±1	5±1	4±1	39±1	7±3	33±5

Suppl. Fig. S1. Similarity colored according to the distance matrix of the nine neurons shown in Fig. 1. Similar neurons are coded with blue values in the colorbar and indicate relative distance between neurons.

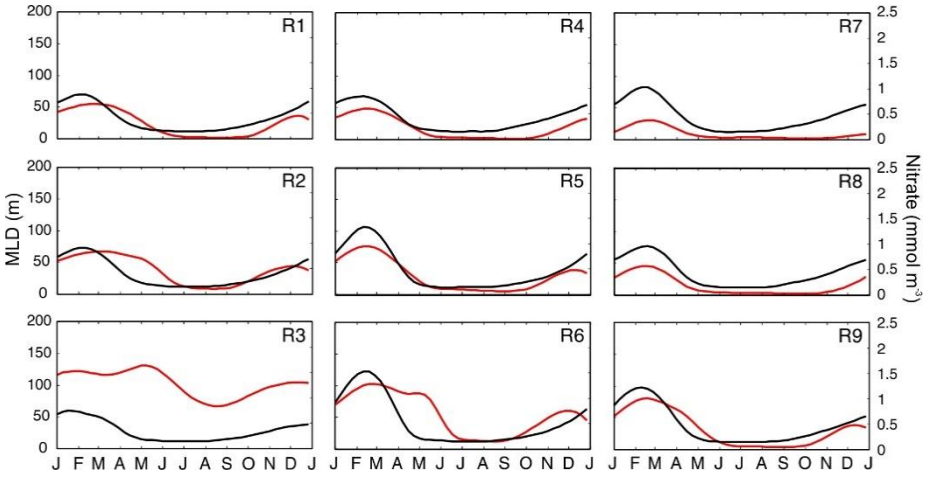

Suppl. Fig. S2. Climatology of mixed layer depth (black) and nitrate concentration at 50 m depth (red) corresponding to each biogeographical region depicted from SOM analysis. Data obtained from CMEMS reanalysis (http://marine.copernicus.eu/).

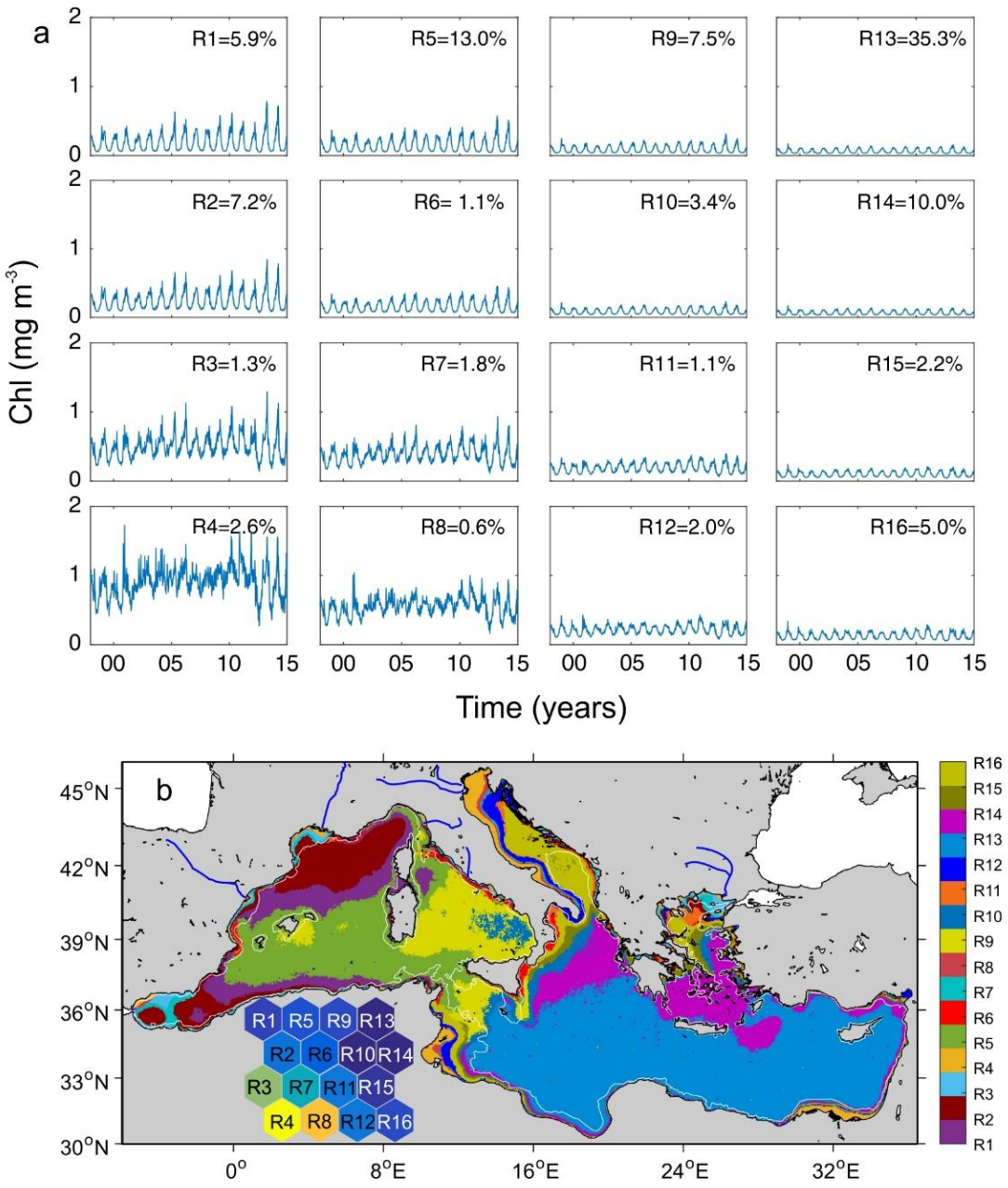

Suppl. Fig. S3. a) Characteristic temporal patterns of Chl obtained from 4x4 Self-Organizing Map (SOM) computation of Mediterranean Chl fields. X-axis is time in years starting in 1998. b) Regional map depicted from the classification of the time series of each pixel according to its BMU. The white line in the map indicates the 200 m isobath. Blue lines indicate the location of major rivers. The similarity of the 16 neurons colored according to the distance matrix are shown in the map inset.

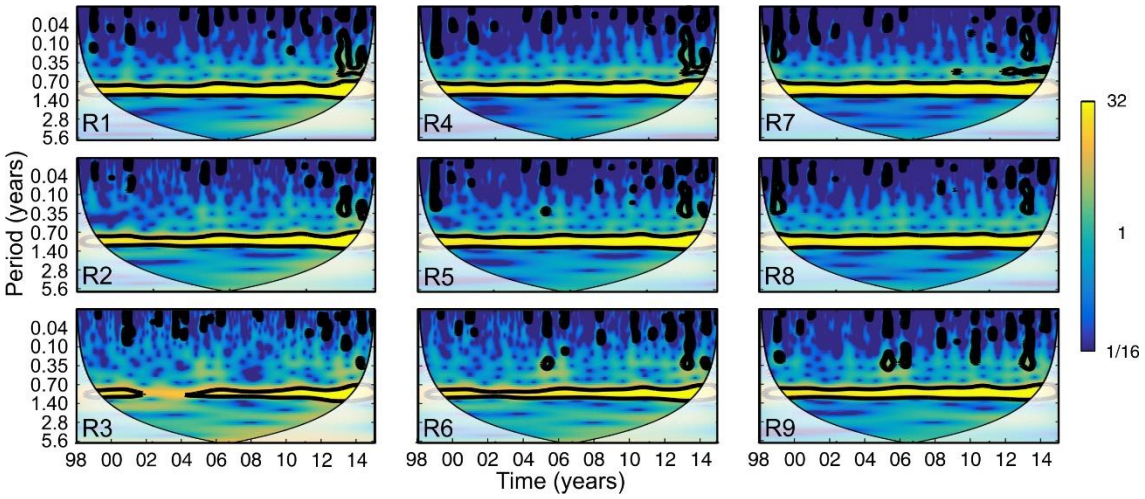

Suppl. Fig. S4. Wavelet power spectrum of the SOM-derived characteristic temporal patterns of Chl variability shown in Fig. 1a. The black contour lines enclose peaks of >95% significance level using the red noise model. Colorbar shows power spectral density.

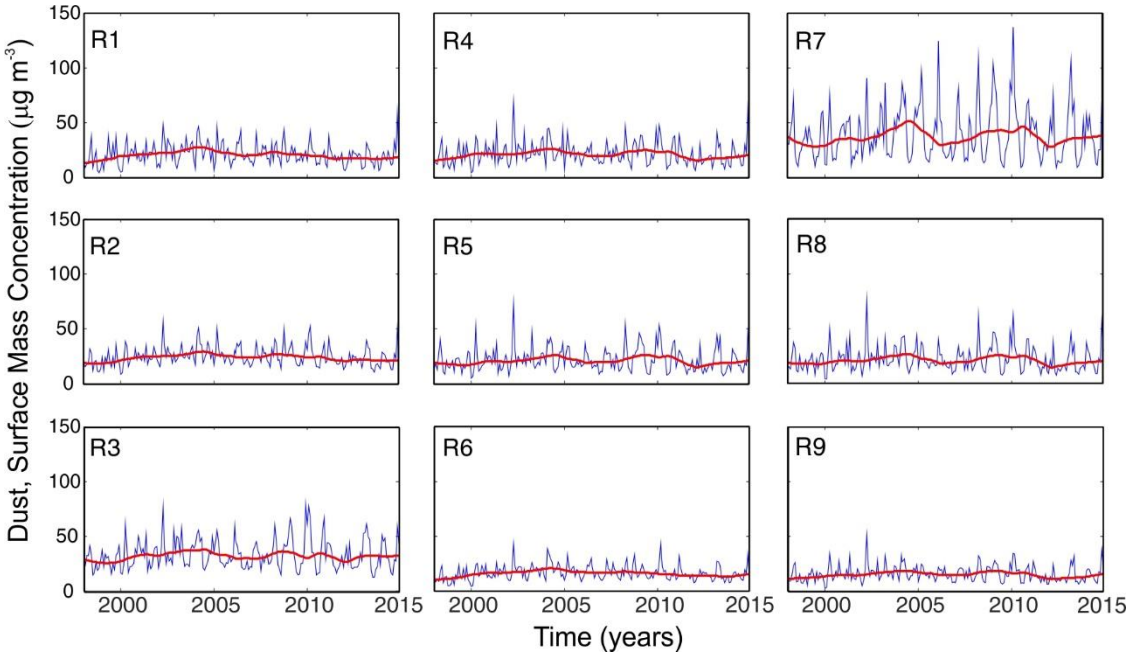

Suppl. Fig. S5. Variations in dust concentration in the nine SOM-defined regions. Blue, weekly data. Red, low frequency (> 1 year) variations.

Chapter 3. Primary production in coastal waters of the Mediterranean Sea: variability, trends and contribution to basin scale budgets.

This chapter is to be submitted.

Salgado-Hernanz, P.M., Regaudie de Gioux, A., Antoine, D., Basterretxea, G. *Primary production in coastal waters of the Mediterranean Sea: variability, trends and contribution to basin scale budgets*.

ABSTRACT

We estimate primary production (PP) rates in the coastal (<200 m depth) Mediterranean Sea from satellite-borne data, their contribution to basin scale carbon fixation, their variability, and long-term trends during the period 2002 - 2016. Global production estimates on the coast yield 0.075 GtC yr^{-1}, which approximately represent 20% of total carbon fixation of the Mediterranean Sea. Almost 50% of this coastal production occurs in the eastern basin, whereas the western and Adriatic shelves contribute with 28 and 24% respectively. Regional coastal production is strongly variable, from high productive areas generally associated with major river discharges (>350 gC m^{-2} yr^{-1}) to unproductive provinces (<50 gC m^{-2} yr^{-1}) in the south eastern Mediterranean. During the 15 analysed years (2002 - 2016), the long-term PP variability is dominated by interannual variations that are inversely correlated with Sea Surface Temperature (SST) ($r = -0.5$, $p<0.001$) and more loosely with the climatic indices North Atlantic Oscillation (NAO) and Mediterranean Oscillation Index (MOI) ($r = -0.29$ and -0.40 respectively, $p<0.001$). Regionally, most coastal areas present either non-significant or weakly declining PP trends (-0.05 to -0.1 gC m^{-2} $decade^{-1}$) whereas they exceeds +0.1 gC m^{-2} $decade^{-1}$ in the Adriatic region. Using the temporal variations

observed at each pixel and Self-Organizing Maps (SOM) we classify the coastal waters into 18 alongshore regions with mean PP magnitudes varying five-fold. The SOM analysis reveals two groups of coastal waters: regions showing low cross-shore variability, mainly located in narrow width shelf areas, and regions showing strong cross-shore gradients, observed in wider regions with river discharges. Our study provides insight on the contribution of coastal waters to basin scale carbon balances in the Mediterranean Sea while highlighting the importance of the different temporal and spatial scales of variability.

1. INTRODUCTION

Coastal ocean waters (i.e. <200 m depth) are an important link between land and the open ocean. They act as a buffer for terrestrial and human influences before such impacts reach the open ocean (Gattuso et al., 1998; Liu and Chao, 2000). Despite their relatively reduced extension (~7 % of ocean surface area; Gattuso et al. (1998), they behold some of the most productive habitats on the planet. Therefore, they have a disproportionate importance in many basin-scale biogeochemical and ecological processes, including carbon and nitrogen cycling, and in the maintenance of marine diversity (Cebrian, 2002; Coll et al., 2010; Dunne et al., 2007). Besides, continental shelves generate a biological production supporting over 90% of global fish catches (Pauly et al., 2002; Pauly and Christensen, 1995).

Coastal sea waters support high rates of primary production (PP), contributing to 14 - 30 % of the global ocean productivity (Gattuso et al., 1998). These high rates of organic productivity occur in the coastal oceans due to the rapid turnover of the large inputs of nutrients and organic carbon from land. PP drives a significant carbon sink in the ocean (Falkowski et al., 2000; Field et al., 1998; Muller-Karger et al., 2005), and is a key regulator of ecological processes such as elemental cycling, trophic structure variabilities and climate change (Bauer et al., 2013; Chavez et al., 2011; Pauly and Christensen, 1995). In coastal waters, physical and biological processes enhance the carbon transport out of the continental margins into the deep layers of the oceans, thus connecting terrestrial with deep oceanic systems (e.g. Cai, 2011; Carlson et al., 2001; Cole et al., 2007). The productivity of coastal sea areas is also of strategic socio-economic importance for many countries considering that PP constrains the amount of fish and invertebrates available to expanding fisheries, a primary resource for many coastal human communities (Chassot et al., 2010). The estimation and understanding of PP evolution and trends in the coastal seas is therefore essential to improve our knowledge of the oceanic carbon cycle.

Scaling up local measurements to estimate the contribution of coastal regions to global carbon fluxes has been hindered by the high spatial and temporal heterogeneity of these waters. Global models of oceanic systems produce carbon fixation estimates with a high degree of uncertainty in coastal regions (Muller-Karger et al., 2005). Coastal waters are complex because of the tight connection between terrestrial and oceanic systems. Terrestrial uploads of nutrients and organic matter originating from groundwater inputs, flashfloods and/or river runoff as well as exchanges with seafloor importantly control the productivity of these waters (Woodson and Litvin, 2015). The amplitude of seasonal variation of surface chlorophyll (Chl) and surface temperature is often higher on coastal waters compared to the open ocean (Cloern and Jassby, 2008). Furthermore, coastal topography and its interaction with winds, waves and currents generates a high variety of

physicochemical niches for phytoplankton growth. Likewise, benthic-pelagic coupling allows the remineralization of nutrients present in shelf sediments during most intense storms. These episodic variations may constitute an important contribution to the overall productivity of shelf waters. Because of the high spatio-temporal heterogeneity in the main coastal subsystems and the concomitant lack of data, most estimated carbon fluxes in these subsystems have relatively high uncertainties (Bauer et al., 2013). In addition, direct human activities and climate change lead to a long-term variation in terrestrial fluxes and coastal biogeochemistry that can potentially have important consequences for the global carbon cycle (Gregg et al., 2003; Muller-Karger et al., 2005).

In the Mediterranean Sea, coastal and shelf areas represent about 21% of the global basin (259,000 km^2) contributing in a higher percentage to the total basin surface than in other global ocean (Pinardi et al., 2004). Although the Mediterranean Sea is amongst the most oligotrophic areas of the world oceans, few seas display such a variety of environmental conditions. This variability is owed to the variety of regional climate and oceanographic conditions in the Mediterranean basin as well as to the multiple land-derived fluxes that locally fertilize the coastal waters (e.g. Goffart et al., 2002). Human activities on river discharges and nutrient inputs affect continental shelf productivity in this sea sustaining locally enhanced pelagic and benthic biomass. Indeed, the influence of some river flows has been notably reduced by damming affecting water chemistry and sediment loads and, thereby, the productivity of coastal waters at local and regional scales (Ludwig et al., 2009; Tovar-Sanchez et al., 2016). Moreover, intensive agricultural practices and urbanization have brought unprecedented use and contamination of coastal groundwater (Basterretxea et al., 2010; Tovar-Sánchez et al., 2014). For example, the use of fertilizers have resulted in higher nutrient flowing into the Adriatic and lagoons of the Nile, which has led to eutrophication (Turley, 1999). However, the impact of this anthropogenic nutrient enrichment may vary between regions, and modelling projections suggest spatial variations in PP as results of climate change.

Accurate quantification and assessment of the heterogeneity of coastal PP is fundamental for the understanding and the characterization of global carbon cycling in this region. Changes in PP have important effects on fish stocks that are socially relevant because of the economical dependency of many Mediterranean coastal communities on marine food products. Several studies have assessed PP at the scale of the entire Mediterranean Sea from remote sensing data (Bosc et al., 2004; Lazzari et al., 2012). However, the contribution of coastal waters to basin scale budgets is still largely unknown. Most coastal studies have a focus on specific regions and/or times (e.g. Estrada, 1996; Marty, 2002; Moutin and Raimbault, 2002; Rahav et al., 2013). Moreover, in despite that observed rates of climate change in the Mediterranean basin exceed global trends (Cramer et al., 2018), and despite that expectations of future warming in the Mediterranean region is expected to exceed global rates by 25% (Lionello and Scarascia, 2018), long term responses of PP in coast areas to climate forcing remain uncertain because of the scarcity of adequate field datasets (e.g. Gasol et al., 2016).

In this study, we present major characteristics of PP in Mediterranean coastal waters based on high spatial and temporal resolution satellite-borne information for the period 2002 - 2016. First, we provide global estimations of PP in coastal waters and we assess their contribution to basin scale budgets, their interannual variability and long-term trends. Then, we regionalize the coastal

waters based on their temporal patterns of PP using Self-Organizing Maps (SOM) and we analyse the contribution of each region to total coastal PP.

2. METHODOLOGY

2.1. Remote sensing data

Ocean color products from the Moderate Resolution Imaging Spectroradiometer (MODIS) aboard the Terra and Aqua satellites, the Medium Resolution Imaging Spectrometer (MERIS) on board the ENVISAT satellite, and the Sea-Viewing Wide Field-of-View Sensor (SeaWiFS) aboard SeaStar were downloaded from the National Aeronautics and Space Administration (NASA) ocean color archive website (http://oceancolor.gsfc.nasa.gov/). These data products are processed and distributed by the NASA Ocean Biology Processing Group (OBPG) at the Goddard Space Flight Center (GSFC). All available MODIS Local Area Coverage (LAC), MERIS Full Resolution Swath (FRS) and SeaWiFS Local Area Coverage (MLAC) Level-2 ocean color satellite orbits available within the Mediterranean Sea (30° to 46°N and 6°W to 37°E; Fig. 1), from January 2002 to December 2016, were downloaded for the following variables: Chlorophyll-a (Chl, mg m^{-3}), and sea surface temperature (SST, °C). Daily (24-hour averaged) photosynthetically active radiation (PAR, in E m^{-2} day^{-1}) was obtained as a Level 3 product at 9 km, the best available resolution.

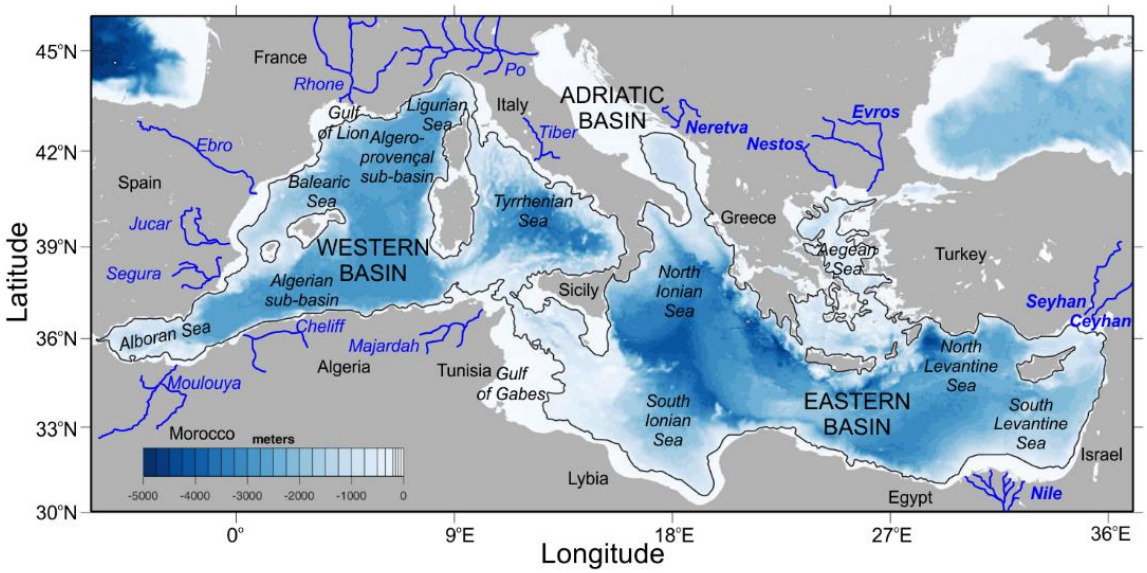

Fig. 1. Mediterranean Sea geography with its main sub-basins. Main sea regions, surrounding countries and rivers are indicated. Bathymetric data were obtained from ETOPO1 (Amante and Eakins, 2009).

We use Chl as values derived from the maximum-band-ratio NASA OC4v4 algorithm for SeaWiFS and MERIS, and the OC3 variant algorithm from MODIS (O'Reilly et al., 2000, 1998b). At global scale, the OC4v4 algorithm yields a median difference of 33% with *in situ* data, which is comparable to measurement uncertainties in the field (Behrenfeld et al., 2006). However, OC4v4 is known to overestimate low Chl concentrations in the Mediterranean Sea (i.e. when Chl < 0.15 mg m^{-3}; Bricaud et al., 2002). These low values represent 31% of our database and mainly correspond to summer conditions and outer shelf zones. In addition, Chl may be overestimated in regions such as the Gulf of Gabes and off the Nile delta were high dissolved organic matter and suspended particles can exert an adverse effect on Chl estimations (Katlane et al., 2011; Lavender

et al., 2009). Despite these limitations, we decided to use the NASA algorithm in order to obtain comparable results to previous PP estimations in the Mediterranean Sea that use this algorithm (e.g. Bosc et al., 2004; Bricaud et al., 2002). In the case of SST data, only night-time orbits were selected to avoid problems with skin temperature during daylight. Orbits with quality flag 2 in SST were included after checking their validity and accuracy in order to have a more complete dataset.

All satellite-derived variables were remapped onto a regular 1-km spatial grid over the study area, by averaging all available pixel within each grid cell. For each parameter, outliers were removed whenever they exceeded about 3-times the mean ± SD of the time series. For the purpose of this study, coastal areas are defined as the waters lying between 5 and 200 m depth. Only values at depths exceeding 5 m depth were considered in order to avoid any Chl bias due to the bottom reflectance.

2.2. Primary production estimations

We estimated PP from satellite-derived Chl, SST and PAR values using the time-, depth-, and wavelength-resolved light-photosynthesis model of Morel (1991). This model was previously used for estimating PP in the Mediterranean sea (Antoine et al., 1995) and at global scale (Antoine et al., 1996; Antoine and Morel, 1996). This model was shown to perform well when compared to *in situ* measurements (Campbell et al., 2002; Friedrichs et al., 2009) or when compared to other similar algorithms designed for use with satellite observations (Carr et al., 2006; Saba et al., 2011).

This model derives the instantaneous PP at depth z of the water column, time t of the day, and for absorption of irradiance at wavelength λ, P(λ z, t), via:

$$\mathrm{P}(\lambda,\mathrm{z},\mathrm{t}) = \mathrm{E}(\lambda,\mathrm{z},\mathrm{t})\ \mathrm{Chl}(\mathrm{z},\mathrm{t})\ \ \mathrm{a}^{*}(\lambda,\mathrm{z},\mathrm{t})\ \phi(\lambda,\mathrm{z},\mathrm{t}) \quad (\mathrm{gC\ m^{-3}\ s^{-1}}) \qquad (1)$$

where quantities at depth z and time t are: E(λ), the spectral scalar irradiance, Chl, the chlorophyll concentration, a*(λ) the spectral chlorophyll-specific absorption coefficient of phytoplankton, and Φ, the quantum yield of photosynthesis for carbon fixation (its possible spectral changes are ignored).

The triple integration of (1) w.r.t. wavelength, depth and time gives the daily column-integrated primary production, PP:

$$\mathrm{PP} = \int^{\mathrm{D}} \int_{0}^{\mathrm{Z_p}} \int_{400}^{700} \mathrm{P}(\lambda,\mathrm{z},\mathrm{t})\ d\lambda\, d\mathrm{z}\, d\mathrm{t} \quad (\mathrm{gC\ m^{-2}}) \qquad (2)$$

where D is the day length, Z_p the depth of the productive layer, and the spectral integration is performed over the visible range (400 to 700 nm). Zp is the depth where the integrated Photosynthetically Available Radiation (PAR) falls to 0.1% of its value just below the sea surface (so approximately 1.5 times the euphotic depth). The spectral integration was performed at a 5nm resolution, the depth integration with intervals equal to one fiftieth of Z_p (but stopped at the bottom depth when that depth was lower than Z_p), and the time integration with intervals equal to one thirtieth of the day length (so about 20 to 30min depending on season).

The spectral irradiance at a given depth, E(λ, z), is calculated as (starting from just below the sea surface):

$$E(\lambda, z) = E(\lambda, z - dz)\exp(-K_d(\lambda, z)z) \qquad (3)$$

where the diffuse attenuation for downward irradiance, $K_d(\lambda, z)$, is computed from Morel and Maritorena (2001):

$$K_d(\lambda, z) = K_w(\lambda, z) + X(\lambda)\,Chl(z)^{e^{\lambda}}\ (m^{-1}) \qquad (4)$$

Details about how values are assigned to the parameters a*, Φ, and $X(\lambda)$ and their dependence on temperature, and other features of this model, are to be found in Morel (1991) and Morel et al. (1996).

The model was operated both for clear sky conditions and the actual PAR values given by the MODIS product, in which case a reduction of the clear-sky irradiance is uniformly applied across the entire day, as being the ratio between the actual satellite PAR value to the clear-sky PAR value. The Chl was assumed to be uniformly distributed with depth, and equal to the satellite-derived value. This simplification was considered more appropriate for the generally shallow and well-mixed waters of coastal areas than the use of global parameterisation of the shape of the vertical profile as a function of the surface Chl value (e.g. Morel and Berthon, 1989; Uitz et al., 2006), whose validity outside of open ocean waters is not established.

From PP estimates, new (PP_{new}) and regenerated (PP_{reg}) production was calculated using the *ef*-ratio of export to total production (Laws et al 2000). Assuming a steady state, this export production must equal the new production fuelled by new nutrients brought to the surface layers. The *ef*-ratio as a function of satellite-derived temperature and production can be obtained from the empirical relationship obtained by Laws et al. (2011):

$$ef\ \text{ratio} = \frac{(0.5857 - 0.0165\,T)\,PP_{mean}}{(51.7 + PP_{mean})} \qquad (5)$$

where T is temperature in degrees Celsius (°C), PPmean is the daily mean PP in mgC m^{-2} d^{-1}. *ef*-ratios and export production values calculated using (5) reflect the fact that the equation is derived from estimates of new production based on nitrate uptake and are considered to be an upper bound on new production (Laws et al., 2011; Yool et al., 2007). In order to estimate the sinking Particulate Organic Carbon (POC) flux settling to the deep Mediterranean seafloor we have used the exponential decay empirical model developed in Pace et al. (1987) and previously and globally used by Muller-Karger et al. (2005). This model employs the annual PP mean, in gC m^{-2} d^{-1} and the bathymetry, in m:

$$\text{POC flux} = 3.523\,PP_{mean}\,\text{bathymetry} \qquad (6)$$

Besides mapping PP, we report global (ΣPP) and basin scale integrated (ΣPP_{basin}) estimations in GtC yr^{-1}. We divided the Mediterranean into three main basins, western, eastern and Adriatic basin. While some authors include this latter basin in the eastern basin (e.g. Bosc et al., 2004), we separated the Adriatic shelf from the eastern Mediterranean shelf considering its peculiarities - bathymetry, influence of rivers, eutrophic character- that differentiate it from the rest of the Mediterranean Sea (Cushman-Roisin et al., 2001). Characteristically, most of the Adriatic has a shallow (<200m) bathymetry and it collects some 30% of the freshwater flowing into the Mediterranean acting as a dilution basin of the nutrients discharged by the Po and other Adriatic rivers.

2.3. Coastal regionalization

We used a two-step classification procedure to define coastal regions along the Mediterranean based on their temporal patterns of PP. First, a classification in 9 regions (R1 to R9) was made using a classification technique based on an unsupervised learning neural network (self-organizing maps or SOM; Kohonen, 2001, 1982). Then, 18 alongshore marine ecoregions were obtained considering the most relevant cross-shore limits of the SOM-derived regions (Z1 to Z18).

SOM is an unsupervised neural network model method that reduces the high dimensional feature space of the input data to a lower dimensional networks of units called neurons. SOM is especially suited to extract patterns in large datasets and has been previously used in studies encompassing satellite data (Basterretxea et al., 2018; Ben Mustapha et al., 2014; Charantonis et al., 2015; Farikou et al., 2015). Unlike other classification methods, like *k*-means, SOM tends to preserve data topology (i.e. preserves neighboring regions) and, therefore, it is particularly suited for pattern recognition (Liu and Weisberg, 2005) allowing adequate classification of areas with high spatial complexity and strong gradients. Similar neurons are mapped close together on the network facilitating the visualization of patterns and a topological ordination of the classified areas and the relative distance among neurons is obtained as results of the analysis.

For typical satellite imagery, SOM can be applied to both space and time domains. Here, we have addressed the analysis in the time domain of the datasets, which allows regionalising the studied area on the basis of similitudes in the time variation of PP. We chose a map size of [3 x 3], with 9 neurons (for further details, see Basterretxea et al., (2018a). We used a hexagonal map lattice in order to have equidistant neighbours and to avoid introducing anisotropy artefacts. For the algorithm initialization, we opted for linear mode, batch training algorithm, and 'ep' type neighbourhood function since this parameter configuration produces the lower quantitative and topological error and computational cost (Liu et al., 2006). These SOM computations were performed using the MATLAB toolbox of SOM v.2.0 (Vesanto et al., 2000a, 2000b) provided by the Helsinki University of Technology (http://www.cis.hut.fi/somtoolbox/).

2.4. Climate data

To estimate possible drivers of long-term variability in PP we searched for correlations with two climate indices, the North Atlantic Oscillation index (NAO) and the Mediterranean Oscillation Index (MOI). The corresponding data were downloaded from the Climate Research Unit at the University of East Anglia (https://crudata.uea.ac.uk/cru/data/). Climate indices are defined either as anomalies of a climatic variable, using the difference between two geographical points, or as principal components (Hurrell, 1995; López-Bustins et al., 2008). NAO is the central mode of climate variability of the Northern Hemisphere atmosphere. It characterizes the pressure difference between the middle of the North Atlantic Ocean and Iceland, which affects winter conditions in the North Hemisphere (Hurrell and Van Loon, 1997; Marshall et al., 2001). Positive NAO results in a relatively dry winter in the Mediterranean but a warmer and wetter winter in northern Europe, and vice versa. Because of its effects on precipitation, Mediterranean river inflows are generally anti-correlated with the NAO. MOI is the most widely used teleconnection index for the Mediterranean basin. There are different versions depending on the points of reference (Criado-Aldeanueva and Soto-Navarro, 2013). We used the version obtained as the normalized pressure difference between Gibraltar and Israel (Palutikof, 2003). It reflects

differences in temperature, precipitation, circulation, evaporation and other parameters between the eastern and western basin. Positive MOI phases are associated with increased atmospheric pressures over the Mediterranean Sea that promote a shift of the wind trajectories toward lower latitudes leading to milder winters (Criado-Aldeanueva and Soto-Navarro, 2013). Under these conditions, reduced precipitation is observed in the southeastern Mediterranean region (Törnros, 2013). With some regional differences, NAO and MOI express relatively similar climate patterns over the Mediterranean Sea since they are highly positively correlated in winter, and weakly but still significantly correlated in summer (Efthymiadis et al., 2011; Martínez-Asensio et al., 2014).

2.5. Statistical analyses

Linear trends in the PP series were calculated using Theil-Sen slope adjustment (Sen, 1968) of the residuals of the deseasonalized series. Only pixels where the trend is statistically significant at the 95% level were considered. Correlation analyses used to statistically investigate relationships between datasets were tested using the Pearson Product Moment correlation. Differences between means were tested using Kolmogorov-Smirnov test (Frank and Maseey, 1951).

3. RESULTS

3.1. Coastal primary production

Annual integrated coastal primary production (ΣPP_{Coast}) in the Mediterranean Sea is estimated here at 0.075 ± 0.002 GtC yr^{-1}, which represents some 20% of total carbon fixation in the Mediterranean Sea (Table 1). Mean annual PP (PP_{Amean}) per surface area is 16% higher than in the open ocean (158 ± 126 and 136 ± 40 gC m^{-2} yr^{-1} respectively; see Table 1). Approximately, 80% of this ΣPP_{Coast} is sustained by recycling processes and, the rest, is new production exported to the seafloor or to nearby areas.

Marked differences in PP are observed between the more productive western coasts and shelf waters in the eastern basin (PP_{Amean} = 167 ± 106 gC m^{-2} yr^{-1} and 139 ± 120 gC m^{-2} yr^{-1}, $p<0.001$). However, the Adriatic shelf is by far the most productive basin of the Mediterranean Sea (PP_{Amean} = 198 ± 148 gC m^{-2} yr^{-1}, Table 1). Annual carbon fixation is 76% higher in the eastern (ΣPP_{east} = 0.037 ± 0.002 GtC yr^{-1}) than in the western shelf (ΣPP_{west} = 0.021 ± 0.001 GtC yr^{-1}) which is due to greater eastern surface area (about twice the western surface area; Table 1). PP_{Amean} varies between 90 and 300 gC m^{-2} yr^{-1} in the western shelf, and between 50 and 220 gC m^{-2} yr^{-1} in the eastern basin where lowest values (<75 gC m^{-2} yr^{-1}) are found along the Gulf of Sirte. Contrastingly, PP_{Amean} exceeds 120 gC m^{-2} yr^{-1} in the Adriatic basin reaching values above 400 gC m^{-2} yr^{-1} in the north western coast (Fig. 2a). The most productive coastal regions (>180 gC m^{-2} yr^{-1}) are mainly located in the European coast and are related with the outflow regions of major rivers. This is best revealed by the coefficient of variation of PP (CV_{PP}) that it is enhanced in the mouth of the Ebro, Rhone, Tiber, Po, Neretva or Nestos/Evros (Fig. 1 and Fig. 2b). Along the western African coast, PP_{Amean} is not particularly low (>180 gC m^{-2} yr^{-1}); however, being the shelf very narrow, its contribution to ΣPP_{Coast} is marginal.

Table 1. Surface area, annual mean surface Chl (Chl_{mean}), annual averaged PP (PP_{Amean}) and annual integrated PP (ΣPP) for the Mediterranean Sea, open ocean waters, and coastal waters during the period 2002–2016.

	Surface area (10^3 km^2)	(%)	Chl_{mean} (mg m^{-3})	PP_{Amean} (gC m^{-2} yr^{-1})	ΣPP (GtC yr^{-1})	(%)
Mediterranean Sea	2,504		0.19 ± 0.78*	141 ± 32**	0.383 ± 0.118***	
Open ocean waters	1,975		0.11 ± 0.18*	136 ± 40**	0.308 ± 0.118	
Coastal waters	529	100	0.49 ± 0.65	158 ± 126	0.075 ± 0.002	100
Western shelf	141	27	0.44 ± 0.95	167 ± 106	0.021 ± 0.001	28
Eastern shelf	287	54	0.45 ± 0.64	139 ± 120	0.037 ± 0.002	48
Adriatic shelf	101	19	0.65 ± 0.98	198 ± 148	0.018 ± 0.001	24

* Annual mean surface Chl values (Chl_{mean}) obtained by averaging the 8-days and 4-km resolution of surface satellite Chl values obtained from CMEMS time series (2002–2014).
** PP_{mean} estimated by averaging published satellite data shown in Table 2.
*** ΣPP estimated from published data for open ocean waters and values from the present study.

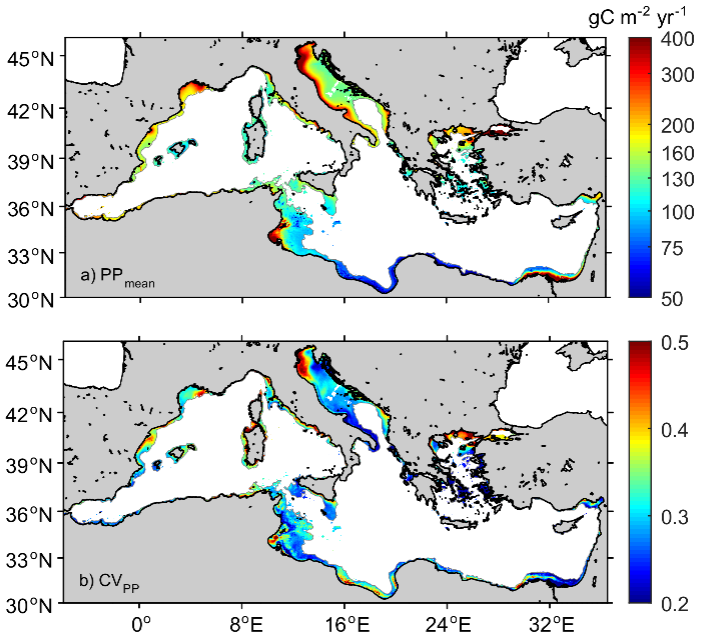

Fig. 2. a) Distribution of annual mean PP ($PP_{Amean,}$) and b) PP coefficient of variation (CV_{PP}).

Table 2. Published values of annual mean PP (PP_{Amean}) and annual integrated PP (ΣPP) estimations for the different Mediterranean basins.

Region	Period (years)	PP_{Amean} (gC m^{-2} yr^{-1})	ΣPP (GtC yr^{-1})	Method	Reference
Global estimation	-	80 - 90		*In situ* (^{14}C data)	*(Sournia, 1973)*
	1981	94 ± 60 - 117.5 ± 75*		Satellite (CZCS)	*(Morel and André, 1991)*
	1979 - 1983	125 - 156*	0.308-0.385*	Satellite (CZCS)	*(Antoine et al., 1995)*
	1997 - 1998	190		Satellite (SeaWiFS)	*(Bricaud et al., 2002)*
	1998 - 2001	79.1 - 88.4		Satellite (SeaWiFS)	*(Colella et al., 2003)*
	1998 - 2001	130 - 140		Satellite (SeaWiFS)	*(Bosc et al., 2004)*
	1998 - 2007		0.5	Satellite (SeaWiFS)	*(Uitz et al., 2010)*
	1998 - 2013	116		Satellite (5 sensors)	*(O'Reilly and Sherman, 2016)*
Western basin	1980 - 1985	120		*In situ* (Oxygen)	*(Bethoux, 1989)*
	1981	157,7		Satellite (CZCS)	*(Morel and André, 1991)*
	1979 - 1983	157 - 197*		Satellite (CZCS)	*(Antoine et al., 1995)*
	1996	140 - 150		*In situ* (^{14}C data)	*(Conan et al., 1998)*
	1997 - 1998	198		Satellite (SeaWiFS)	*(Bricaud et al., 2002)*
	1991 - 1999	83 - 235		*In situ* (^{14}C data)	*(Marty et al., 2002)*
	1996	145		*In situ* (^{14}C data)	*(Moutin and Raimbault, 2002)*
	1998 - 2001	93.8 - 98.8		Satellite (SeaWiFS)	*(Colella et al., 2003)*
	1998 - 2001	163 ± 7		Satellite (SeaWiFS)	*(Bosc et al., 2004)*
Eastern basin (including Adriatic)	1980 - 1985	137 - 150 **		*In situ* (Phosphorous)	*(Béthoux et al., 1998)*
	1981	109.4		Satellite (CZCS)	*(Morel and André, 1991)*
	1979 - 1983	110 - 137*		Satellite (CZCS)	*(Antoine et al., 1995)*
	1997 - 1998	183		Satellite (SeaWiFS)	*(Bricaud et al., 2002)*
	1996	99		*In situ* (^{14}C data)	*(Moutin and Raimbault, 2002)*
	1998 - 2001	69.1 - 81.5		Satellite (SeaWiFS)	*(Colella et al., 2003)*
	1998 - 2001	121 ± 5		Satellite (SeaWiFS)	*(Bosc et al., 2004)*
Adriatic basin	1978 - 1983	241 - 301*	0.0235	Satellite (CZCS)	*(Antoine et al., 1995)*
	1998 - 2001	92.4 - 104.4		Satellite (SeaWiFS)	*(Colella et al., 2003)*

* The estimates from Antoine et al.(1995) and Morel and André (1991) have been corrected by a factor of 1.25 as recommended by Morel et al. (1996).
** Obtained from Colella et al. (2003), who estimated it using *f* ratios (the ratio between new and total PP) obtained from Boldrin et al. (2002).

ef-ratios are generally low, varying between 0.1 and 0.3 (Fig. 3a). Highest PP_{new} values are highly constrained to shallow coastal areas and riverine discharge areas (Fig. 3b). These values are in the range of early estimations by Dugdale and Wilkerson (1998). In the rest of the coastal regions, PP_{new} is quite homogeneous varying between 10 and 60 gC m^{-2} yr^{-1}. PP_{reg}, that may exceed 200 gC m^{-2} yr^{-1}, represents on average 77 ± 3% of total production (Fig. 3c). The annual POC flux, ranging from ~5 up to ~100 gC m^{-2} yr^{-1} reveals that high flux values (>50 gC m^{-2} yr^{-1}) correspond to the riverine continental margins, coinciding with the areas where the contribution of PP_{new} is higher (Suppl. Fig. S3). The relationship obtain for the satellite derived PP_{new} and POC correlate for the Mediterranean coastal waters is of r = 95%. In the Mediterranean Sea shelves, the mean value of PP deposited as carbon on the seabed is 56 gC m^{-2} yr^{-1}, corresponding to 28% of the total mean PP.

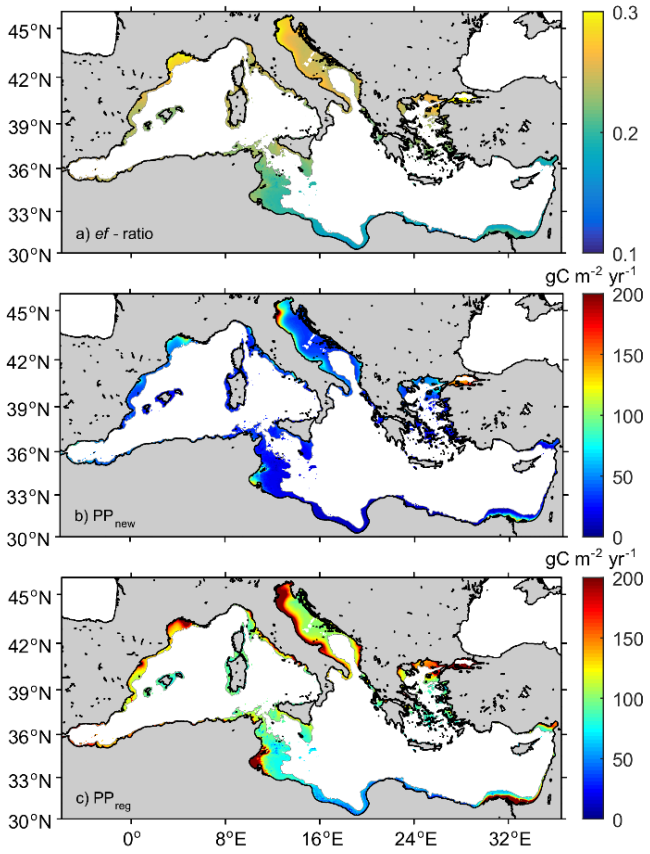

Fig. 3: a) Averaged *ef* – ratio, b) annual new PP (PP_{new}) and c) annual regenerated PP (PP_{reg}) for the Mediterranean coastal during the period 2002-2016.

Spring is the most productive season in coastal waters of the Mediterranean Sea (Fig. 4). Average seasonal PP values from spring to winter are 54 ± 36, 44 ± 36, 34 ± 7 and 33 ± 26 gC m^{-2} $season^{-1}$, respectively. The maximum mean daily production (PP_{Amean}) occurs around mid-March in both western and eastern basins (PP_{Amean} = 0.70 ± 0.23 and 0.49 ± 0.30 gC m^{-2} d^{-1} respectively). Although mean global values indicate that summer is highly productive, summer PP values are biased by high rates remaining early in the season in northern coastal regions such as the Adriatic Sea, the Gulf of Lions and, less so, the northern Aegean. In particular, PP in the Adriatic peaks late in the year, between May and June (PP_{Amean} = 0.82 ± 0.51 gC m^{-2} d^{-1}). Seasonal coefficient of variations are shown in Supp. Fig1.

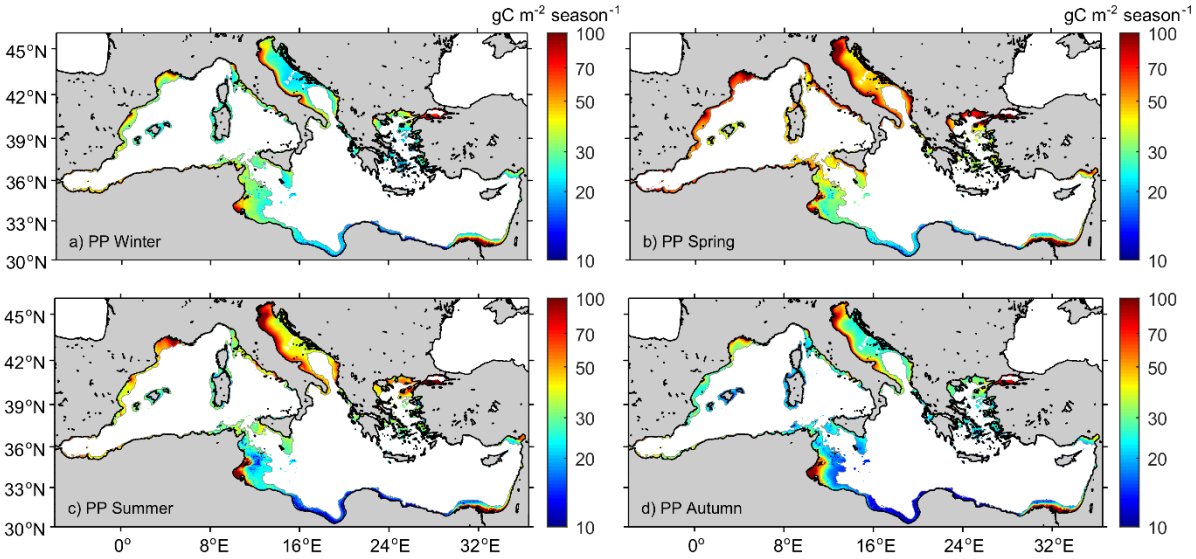

Fig. 4. Mean seasonal PP over the 2002–2016 period for coastal Mediterranean areas (< 200 m isobath). Quarterly composites: winter (Dec-Jan-Feb), spring (Mar-Apr-May), summer (Jun-Jul-Aug) and autumn (Sep-Oct-Nov).

3.2. Long-term variability and trends

As shown in Fig. 5, long-term variability is dominated by short scale variations (i.e. subdecadal). ΣPP_{Coast} exhibits moderate interannual variability (up to 12%) whereas basin scale interannual variations range between 19% in the eastern and western basins to 22% in the Adriatic basin. Positive anomalies extended between 2004 and 2010 (mean 0.076 ± 0.001 GtC yr^{-1}; Fig. 5a). Year 2012 was particularly anomalous in all three basins. This anomaly was apparent between 2012 and 2014 in the eastern basin (Fig. 5c). The difference between the estimated maximum and minimum annual $\Sigma PP_{Coastal}$ is 0.01GtC yr^{-1}.

Long-term trends in PP at the 95% level are only significant in the eastern and Adriatic Sea ($p<0.05$; Fig. 5). However, while a slight negative tendency is observed in the eastern basin (-12.5 TC $decade^{-1}$), the Adriatic Sea displays a positive trend (+10.5 TC $decade^{-1}$). As revealed by Fig. 6, several regionally coherent patches of significant trend in PP are observed along the coast. Most of these regions presented declining PP trends. Typical trend magnitudes observed along the Spanish Mediterranean coast and the North African coastal from the Gulf of Gabes range from -0.05 to -0.1 gC m^{-2} $decade^{-1}$. Contrastingly, coherently with basin scale trends, significant positive PP trend is observed in the Adriatic Sea exceeding +0.1 gC m^{-2} $decade^{-1}$.

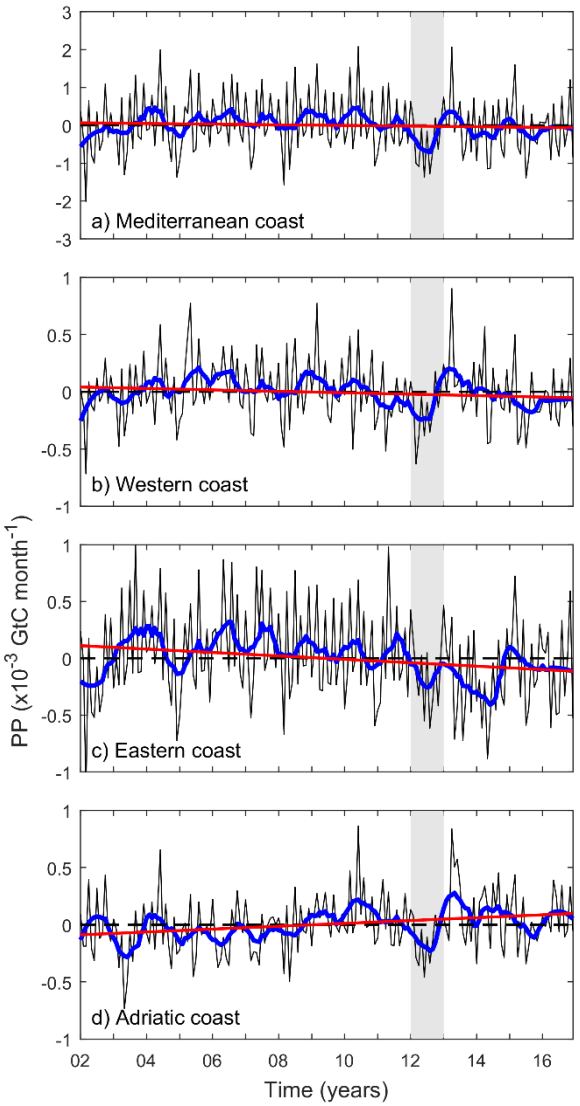

Fig. 5. Monthly integrated PP anomalies, where black solid lines indicate the original data and blue solid lines show its low frequency, over the 2002-2016 period for the Mediterranean coastal areas (< 200 m isobath). Each panel shows the entire and the different sub-basin: a) Mediterranean coast, b) western coast, c) eastern coast and d) the Adriatic coast. The grey band indicates year 2012.

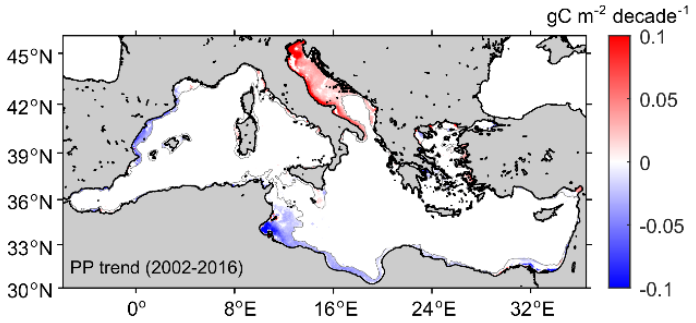

Fig. 6. Theil-Sen trend in primary production over the Mediterranean coastal Sea estimated from daily values for the 2002–2016 period. Only significant trends (p<0.05) are shown.

An inverse correspondence between long-term ΣPP and SST variations (r = -0.54, p<0.001; Fig. 7a) is found at global scale. This correlation was similar in the western and the eastern basin (r = -0.51, p<0.001), but it was not significant in the Adriatic basin. In addition, we observed evidence of inverse relationship between PP variability and the phase of the climatic indices NAO and MOI (Fig. 7b-c). A positive phase of the indexes resulted in a decrease in ΣPP and the opposite pattern (r = -0.29, p<0.001 and r = -0.40, p<0.001 respectively). We also observed different connection between the index variability and the different regions depending on the season. In autumn, NAO had more influence in the PP variations in the western basin (r = 0.37, p = 0.02) whereas in summer, it presented higher influence in PP variations in the eastern basin (r = 0.22, p = 0.08). MOI variations correlated best with PP variations in spring (r = 0.39, p = 0.01), when productivity is high. No significant correlation was found during the winter season for any index.

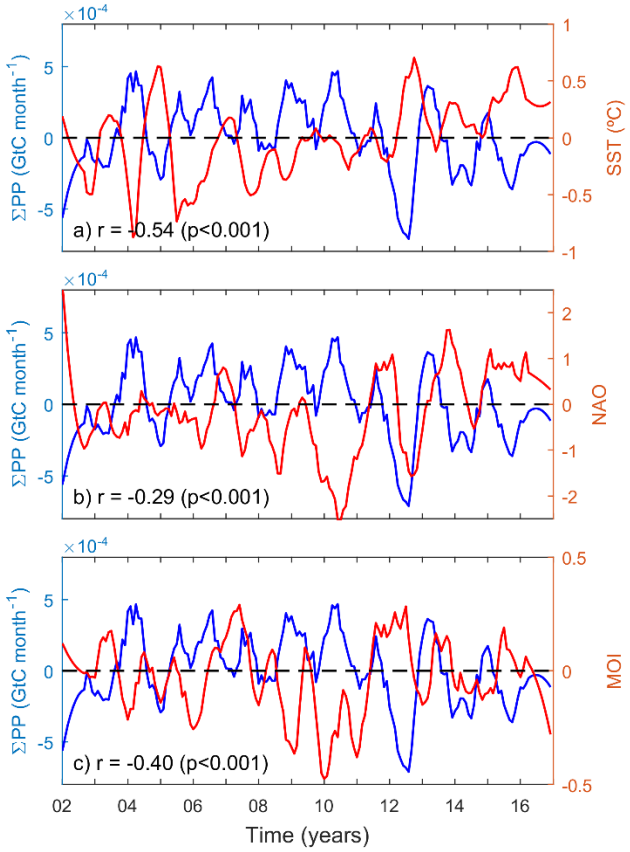

Fig. 7: Monthly ΣPP_{tot} for the coastal Mediterranean and a) SST anomalies, b) NAO and c) MOI

3.3. Coastal regionalization

The nine characteristic temporal PP patterns, their corresponding spatial distribution obtained from SOM analysis and the 18 zones in which the coastal region was classified are shown in Fig. 8. Generally, wider shelfs present higher spatial complexity manifested as a larger number of SOM patterns present in these zones. More than 65% of the shelf waters correspond to R1, R2 and R4 regions. While R1 and R2 corresponds to the less productive areas influenced by oceanic conditions (PP_{Amean} = 73 ± 39 and 115 ± 50 gC m^{-2} yr^{-1}, respectively; Table 3), R4 presents slightly higher productivity than R1 and R2 (PP_{Amean} = 151 ± 63 gC m^{-2} yr^{-1}; Table 3) and a wider daily range

of variation (0.17 - 0.74 gC m^{-2} d^{-1}; Fig. 8) mainly corresponding to the Adriatic Sea open waters and slope regions in the western Mediterranean (22.1% of the coastal surface).

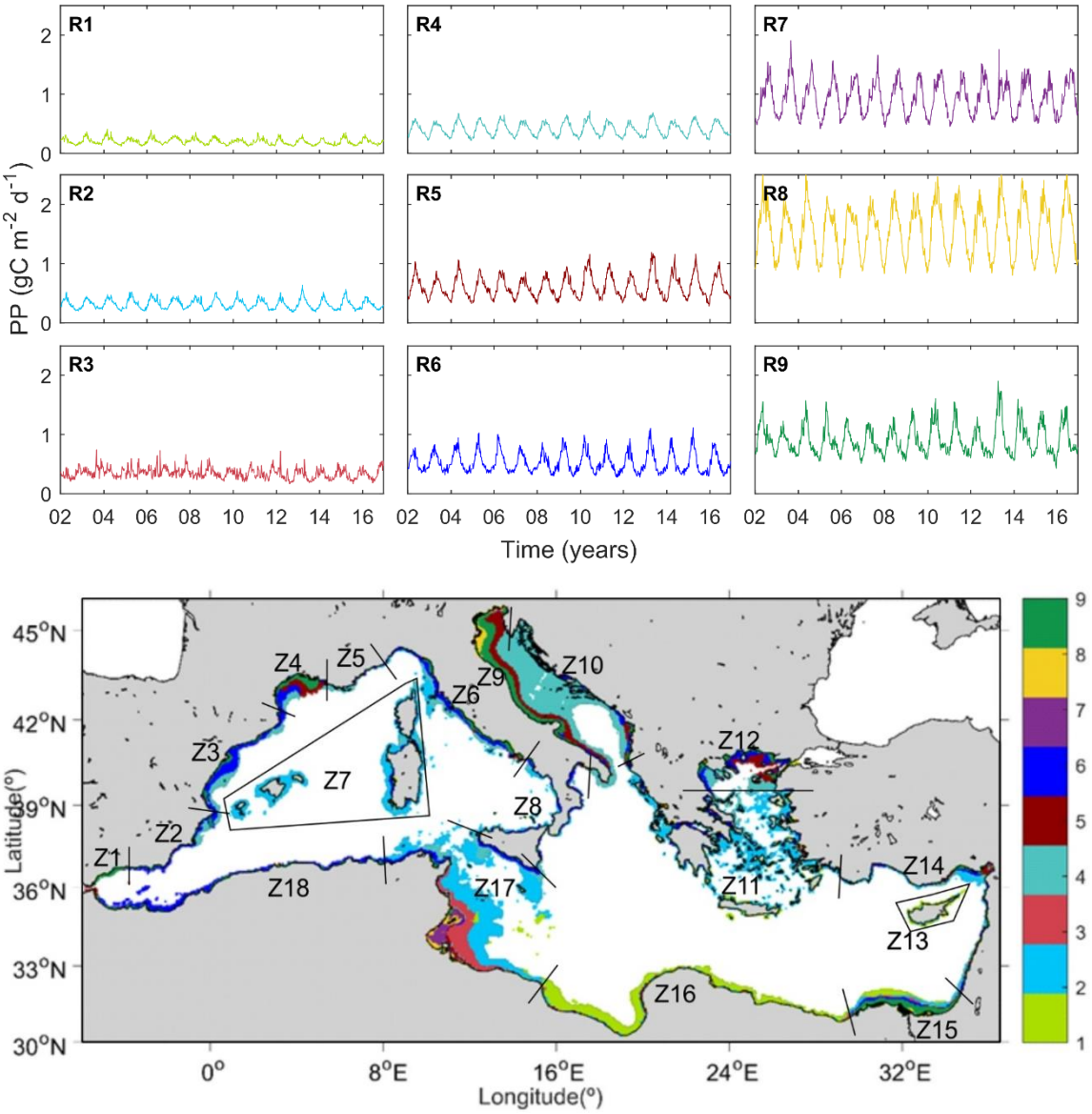

Fig. 8. a) Characteristic temporal patterns of PP obtained from [3 x 3] SOM classification (R1 to R9) and b) coastal regions defined from alongshore variations of the SOM – regions (Z1 to Z18).

Variations in mean PP among the SOM regions reveal that R2, the pattern with the highest occurrence (29% of the total surface area), comprises vast shelf regions around the main Mediterranean islands such as the Balearics, Corsica, Sardinia and Sicily but also the central Aegean coastal region. R4 pattern, the second extended surface was localized mainly in the deepest coastal areas of the Adriatic basin. Both R2 and R4 clusters were characterized by a ΣPP of approximately 0.016 Gt C m^{-2} yr^{-1}, contributing together to 44% of the total productivity of the coastal areas. In contrast, R7, R8 and R9 represented the highest productive areas (PP_{Amean} >340 gC m^{-2} d^{-1}; Table 2). R8 and R9 clusters are constrained to ROFIs (Simpson, 1997) next to the Nile, Po and Rhone deltas, but also represents the northern Alboran sea. Indeed, R8 is exclusively restricted to the mouth of the rivers and presents a range of variation of 0.76 to 2.62 gC m^{-2} d^{-1}

with PP_{Amean} 1.5 ± 0.42 gC m^{-2} d^{-1}. R7 pattern is exclusively located in the shallowest inner shelf of the Gulf of Gabes and it is bounded by R3, a transition region between the inner and outer shelf. Unlike the other regions, where PP peaks in late winter-spring, maximum PP in R7 occurs in fall. Finally, R5 and R6 are transition regions accounting for 23.6% of the total productivity and covering 17.7% of the total coastal region. While R5 is mainly located in deltas areas, R6 is located in the western Mediterranean shelf, including the north African coast (0.78 - 1.11 gC m^{-2} d^{-1}; Fig. 8).

Table 3. Coastal surface area and its coverage percentage, annual mean PP (PP_{Amean}) annual integrated PP (ΣPP) and its contribution in each SOM-defined region to the total coastal Mediterranean Sea PP.

	Area		PP_{Amean}	ΣPP	
	(km^2)	(%)	(gC m^{-2} yr^{-1})	(10^{-3} GtC yr^{-1})	(%)
R1	87,281	16.6	73 ± 39	5.30 ± 0.42	7.1
R2	152,572	28.9	115 ± 50	16.60 ± 0.69	22.3
R3	24,013	4.6	127 ± 67	2.84 ± 0.26	3.8
R4	116,484	22.1	151 ± 63	16.42 ± 0.67	22.0
R5	43,211	8.3	227 ± 116	8.85 ± 0.46	11.8
R6	49,053	9.4	195 ± 108	8.93 ± 0.40	11.8
R7	9,962	2	346 ± 180	2.70 ± 0.17	3.6
R8	13,944	2.7	575 ± 283	5.28 ± 0.30	7.1
R9	26,135	5	341 ± 179	7.77 ± 0.44	10.4

The SOM-based regionalization in Fig. 8 reveals two different groups of coastal waters; those with low cross-shore variability (including one or two SOM regions; i.e. Z1, Z13, Z16 and Z18); and those strong cross-shore gradients, including several SOM-regions from (i.e. Z4, Z9, Z12, Z15¸ Supp. Table 1). The first pattern is typically observed in narrow continental shelf areas with low influence river inputs whereas the second group is found in regions with wider continental shelf such as ROFIs (the Rhone delta, the north and western coastline of the Adriatic Sea and the Nile Delta) and the Gulf of Gabes. Table 4 shows the mean and ΣPP of the eighteen alongshore zones obtained. The western Adriatic (Z9) and the Gulf of Gabes (Z17) are the largest contributors to $ΣPP_{Coast}$ contributing together to 40% of total shelf production in the Mediterranean Sea but, in the case of Z17, it is mainly due to its large extension. Mean PP per surface area is high in the norther Alboran sea (Z1), Nile delta (Z15), the western Adriatic (Z9), and Gulf of Lions (Z4). With the exception of Z1, these zones receive important riverine fluxes (Q).

Table 4: Surface, river discharge flow (Q), annual mean PP (PP_{Amean}), annual integrated PP (ΣPP) and its contribution respect to the total coastal Mediterranean Sea PP for each of the 18 alongshore zones characterized in the Mediterranean Sea after the SOM regionalization.

	Area		Q*	PP_{Amean}	ΣPP	
	(km^2)	(%)	($km^3\ yr^{-1}$)	($gC\ m^{-2}\ yr^{-1}$)	($x10^{-3}\ GtC\ yr^{-1}$)	(%)
Z1	1,891	0.4	0.5	321 ± 189	0.51 ± 0.05	0.7
Z2	7,312	1.4	1.2	178 ± 99	1.17 ± 0.11	1.6
Z3	19,095	3.6	21.4	180 ± 101	3.18 ± 0.25	4.2
Z4	15,377	2.9	57.7	224 ± 125	3.14 ± 0.21	4.2
Z5	888	0.2	1.9	142 ± 84	0.10 ± 0.01	0.1
Z6	20,636	3.8	14.6	176 ± 121	3.24 ± 0.25	4.3
Z7	30,020	5.6	0.5	120 ± 68	3.24 ± 0.26	4.3
Z8	8,276	1.5	3.7	146 ± 89	1.00 ± 0.09	1.3
Z9	65,553	14.1	70.5	225 ± 169	13.44 ± 1.11	17.9
Z10	41,486	7.2	35.8	147 ± 71	5.37 ± 0.35	7.2
Z11	58,947	11.0	21.5	122 ± 89	5.94 ± 0.46	7.9
Z12	26,027	4.9	21.2	203 ± 153	4.48 ± 0.56	6.0
Z13	3,108	0.6	0	76 ± 42	0.19 ± 0.02	0.3
Z14	17,014	3.2	21.3	160 ± 108	2.32 ± 0.15	3.1
Z15	28,884	5.4	17	231 ± 196	5.91 ± 0.26	7.9
Z16	46,614	8.7	0	70 ± 46	3.07 ± 0.28	4.1
Z17	124,539	23.2	1.1	140 ± 106	16.54 ± 0.79	22.1
Z18	13,571	2.5	6.1	209 ± 111	2.54 ± 0.17	3.4

*(Ludwig et al., 2009; Milliman and Farnsworth, 2011; Skoulikidis et al., 2009; Tokner et al., 2009)

4. DISCUSSION

4.1. Coastal primary production

To our knowledge, this is the first study focused on the contribution of coastal waters to overall PP in the Mediterranean Sea. We quantify in 20% the contribution of coastal waters to basin scale carbon fixation in the Mediterranean Sea, and mean coastal values (158 ± 126 $gC\ m^{-2}\ yr^{-1}$) are similar to the mean global values over the continental shelf (160 ± 40 $gC\ m^{-2}\ yr^{-1}$; Smith and Hollibaugh, 1993). While this estimation is subject to the uncertainties inherent to the limitation of ocean color information to the upper ocean (<25 m) and to the poor performance of the ocean color models in some areas (i.e. Case-II waters), it provides an approximation to net rates of carbon fixation in coastal areas that is consistent with global estimations of the contribution of coastal areas to oceanic production (14 - 30%; Gattuso et al., 1998). Bias in coastal Chl estimations is mainly due to the presence of non-phytoplankton components such as CDOM or other terrestrial substances (Morel et al., 2006). These compounds are originated by coastal erosion, resuspension in shallow areas, river inputs or anthropogenic effluents. Likewise, Case-II affects the propagation of photosynthetic radiation through the water column (Morel, 1991). However, for surface Chl values ranging from ~0.04 to ~3 $mg\ m^{-2}$, Φ in equation (1) would vary only by ± 4% around its mean (Morel, 1991; Morel and André, 1991). In any case, Case-I waters are largely

predominated in the coastal Mediterranean regions whereas Case-II waters are reduced to less than 5% of the whole basin. In particular, they are confined to the north Adriatic Sea, Gulf of Gabes and around Nile delta (Antoine et al., 1995; Bosc et al., 2004; Morel and André, 1991) where our PP estimations may present larger uncertainties. However, our values for the Nile river delta, >100 gC m^{-2} yr^{-1}, are only slightly higher than those reported by Antoine et al. (1995), 80-100 gC m^{-2} yr^{-1}. Highest values, >300 gC m^{-2} yr^{-1}, are restricted to a narrow coastal area. In the case of the Adriatic Sea, Zoppini et al. (1995) estimated PP rates from 210 to 260 C m^{-2} yr^{-1} in the north coastal areas of the Adriatic Sea that are between 15 and 30% lower than our estimations. However, Umani (1996) reported large PP variability in the Adriatic coastal areas, varying from ~50 to 200 gC m^{-2} yr^{-1}.

Because of its extension, the eastern basin contributes more importantly than the western basin to overall coastal production (48% and 28%, respectively; Table 1). Carbon fixation in the Adriatic is somewhat lower (24% of global Mediterranean basin) but it cannot be omitted considering its reduced extension (19% of Mediterranean coastal waters). The relevance of the contribution of the Adriatic relies in two main characteristics; (1) coastal waters (<200 m) constitute a large part of the Adriatic Sea and (2) about one third of the river discharge in the Mediterranean is concentrated in the Adriatic Sea (Table 4; Ludwig et al. (2009). Indeed, patterns in the northern Adriatic Sea reflect a variation in the drivers of PP with respect to other regions. For example, while internal processes (i.e. vertical diffusion and mixing) and, less so, atmospheric deposition, drive PP in most coastal waters, production in the north Adriatic would be mainly driven by fluvial sources of carbon and regeneration through bacterial pathways (Umani et al., 2007). Moreover, distinctive dynamics in this sea is driven by the influence of river outflows on stratification and general circulation patterns (Djakovac et al., 2012; Giani et al., 2012).

Here, from *ef*-ratios, we estimated that on average only 23 ± 15 % of the coastal production (37 gC m^{-2} yr^{-1}) in the Mediterranean Sea is new and the rest is sustained via regenerated sources. This PP_{new} value is comparable mean organic carbon that sinks to the sea floor (28%, estimated following Muller-Karger et al., 2005; and Pace et al., 1987; Supp. Fig. S3) but higher than PP_{new} estimations provided by Vidussi et al. (2001) for oceanic waters in the eastern basin (15% of total production). However, it should be noted that our coastal average not only includes the more productive waters in the eastern basin, but also, the highly productive areas in the northern Adriatic. Indeed, higher *ef*-ratios (>0.3) are observed in the areas where nutrient inputs from the Atlantic and river effluents significantly enhance PP_{new} (Fig. 3a). Further, *ef*-ratios present significant seasonality, varying between 0.29 ± 0.04 in the most productive winter-spring season and 0.16 ± 0.02 in summer, when the water column is strongly stratified and food web shifts to a more recycling dominated system.

Morán et al. (2002) estimated in 16%, the fraction of total PP that is directly released by phytoplankton to the dissolved carbon pool sustaining bacterial production, but values as high as 35% have been reported by López-Sandoval et al. (2011) in the oceanic waters in the Mediterranean Sea. Because of the nutrient limitations and predominance of microbial pathways, exportation to the adjacent ocean or to sinking of organic matter is weak. Unlike, the oceanic waters in which POC sinks to the deep ocean, sinking organic matter in coastal waters is intercepted by the seabed, which explains the richness of some benthic communities. For

example, areas favouring accumulation, such as submarine canyons are site of enhanced benthic productivity (Palanques et al., 2005).

PP in the coastal ocean is in the root of the sustainment of high trophic level organisms. The fate PP in the ocean is determined by food web structure. Picoplankton and small autotrophs that are grazed by microheterotrophs typically characterize pelagic assemblages in the Mediterranean Sea for most of the seasonal cycle (Siokou-Frangou et al., 2010). This community is known to be highly responsive to local or episodic variations in nutrient availability presenting high variability in its composition along the coast (Caroppo et al., 2006). Major switches occur during the late winter-spring bloom and, occasionally on autumn, when this community switches to a diatom dominated assemblage (Psarra et al., 2000). The fate of this production can be tightly controlled by microheterotrophs (Drira et al., 2010).

Duarte and Cebrián, (1996) estimated that grazing by microheterotrophs (mainly protists) and mesozooplankton removes about 57% and 41% of oceanic and coastal marine PP, respectively. Accordingly, Schmoker et al. (2013) estimated a mean consumption of 57% of PP in regions such as the Mediterranean Sea with a PP consumption five times higher for micro- than for mesozooplankton. This value is subject to strong seasonal variations, with up to 100% of phytoplankton production removed daily by microbial grazers in summer and only 25% in winter, which is attributed to changes in the planktonic community composition (Calbet, 2008). This implies that about 0.03 GtC yr^{-1} would be grazed by microherbivores. Approximately 35% of this ingested carbon would be respired allowing about 0.02 GtC yr^{-1} to be available for higher trophic levels (Bougis, 1974; Kiørboe et al., 1985; Pagano et al., 1993; Schmoker et al., 2011). This value is consistent with estimations of the proportion of primary production that sustain fisheries (between 24.2% for tropical coastal shelves and up to 35.3% for temperate coastal shelves; Pauly and Christensen, 1995). Nevertheless, while strong linkage between PP and fisheries production has been reported (Chassot et al., 2010), it is uncertain to what extent these PP rates sustain the complex fishery, composed by a great number of fishes, crustaceans and mollusks with different biological requirements (Lleonart and Maynou, 2003). A more direct effect is the influence of PP rates on the location of fish spawning in this Sea, as reported by Sabatés et al. (2007).

4.2. Long-term variability and trends

Long-term trends obtained from available ocean color data present a high degree of uncertainty particularly if decadal variability is sufficiently large. Indeed, as reported by Henson et al. (2010), decadal variability can appear to reverse a climate change trend when short datasets are examined. Despite these limitations, satellite observations of ocean color over the last decades suggest relationship between warming and reduced productivity, yet most remarkable changes are observed in permanently stratified areas (Behrenfeld et al., 2006). Since clear tendencies of warming are observed in the Mediterranean Sea (Nykjaer, 2009; Pastor et al., 2017), intensification of stratification and consequent mixed layer depth reduction would limit nutrient supply to phytoplankton and, thus, limit PP (Behrenfeld et al., 2006; Stambler, 2014).

Barale et al. (2008) observed a general decrease in Chl biomass in the Mediterranean Sea over the period 1998–2003. However, some coastal areas in their study displayed an inverse tendency. Macias et al. (2015) anticipated no future global changes of integrated PP in the Mediterranean

Sea from modelling results. They predicted a tendency to oligotrophication in the western basin and increase in the productivity of the eastern basin. Our study reveals that, with the available satellite data, global trends in $\Sigma PP_{Coastal}$ in the Mediterranean Sea are not significant (Fig. 5a). However, slight tendencies were observed in the Eastern and in the Adriatic basin (-12.5 and +10.5 TC decade^{-1}; Fig. 5c-d). A detailed spatial analysis reveals that, even in the western basin, some regions present weak but spatially coherent and significant tendencies ($p< 0.05$; Fig. 6). In particular, the eastern coast of Spain and the northern coast of Africa present declining productivities. Conversely, trends in some areas of the Adriatic Sea were markedly positive (>0.1 gC m^{-2} decade^{-1}) mainly due to the PP increase after 2008. While the negative tendency of the eastern basin seems to fit with the assumed model of PP limitation associated with increasing temperatures, the origin of the positive trend in the Adriatic basin is more uncertain. A plausible explanation is the variation in the flux or/and loads of the northern Adriatic rivers. Indeed, Giani et al. (2012) observed an increase of the Po River flow increasing phosphate and dissolved nitrogen concentrations in the Po's delta and its surrounding shelf waters. Alternatively, changes occurring between 2004 and 2006 in the deep structure of the Mediterranean Sea could have affected mass and nutrient exchanges between the Adriatic and the north Ionian Sea (Font et al., 2007; Schroeder et al., 2008; Šolić et al., 2008; Viličić et al., 2012).

Long-term variations in the eastern and western basins are mostly coupled, suggesting that they share the same PP drivers at this basin scale (Fig. 5b-c). A major feature in the interannual pattern is a global decrease in productivity in 2012 that it extended to the following years in the eastern basin (up to 2014). Durrieu De Madron et al. (2013) reported peculiar atmospheric conditions in the Mediterranean Sea during 2012 that triggered a massive formation of dense water on the continental shelf and in the deep basin of the Gulf of Lions. A similar anomaly was described in the Adriatic shelf where unprecedented dense water generation was preconditioned by a dry and warm year resulting in a significant reduction of coastal freshwaters and basin-wide salinity increase (Mihanović et al., 2013; Raicich et al., 2013). Additionally, Pastor et al. (2017) observed an anomalously temperature increase in the Mediterranean Sea during summer 2012. From our analysis, we believe that this climate-related event had strong influence on the global coastal PP of the Mediterranean Sea.

It has been often assumed that open ocean was more sensitive to climate influences while coastal regions are more sensitive to land-based impacts. However, similarly to our results, several studies have reported influence of climate variations in the coast (Belgrano et al., 1999; Cloern et al., 2007). In agreement, we observed that climate driven forcings are also major drivers of coastal productivity as suggest the inverse correlations between ΣPP and SST and, more loosely, with NAO and MOI (Fig. 7). While these correlations emphasize the pre-eminent role of climate variability in the regulation of interannual to decadal scale coastal on coastal productivity, the pathways through which this control of the atmosphere over coastal productivity is exerted are complex and may regionally differ (e.g. Grbec et al. 2009).

Climate can influence phytoplankton growth by direct effect of temperature on algal metabolism, by changes in basin scale circulation (including exchanges with adjacent seas), by regulating nutrient supply through variations in the thermocline intensity, by changes in wind patterns affecting mixing and dust deposition pathways or through changes in precipitation that have direct influence on wet deposition and on river runoff. Nevertheless, these effects are modulated

by changes in the biota and in the interaction between organisms (e.g. Molinero et al., 2005). The relative importance of climate driven processes depends on regional characteristics and may be seasonally varying. For example, variations in dust deposition are expected to be more important in the eastern and southern Mediterranean coasts because to their proximity to the Saharan dust sources and to the low relevancy of riverine inflows. Indeed, dust is considered to sustain more than 50% of new production in the Levantine basin (Herut et al., 2002; Kress and Herut, 2001). Likewise, variations in cooling and vertical mixing are expected to be more effective during late winter when PP peaks and when diatoms dominate proliferate in the Mediterranean Sea (Lacroix and Nival, 1998; Marty, 2002; Marty and Chiavérini, 2010).

Further, our results reveal that in contrast to other shelf areas like the North Sea (Capuzzo et al., 2017) or the Arctic Ocean (Gregg et al., 2003) the coastal Mediterranean Sea did not globally display a marked decline in PP during the last decades. We believe that in coastal areas, unlike oceanic regions, a decrease in vertical nutrient supply though the thermocline may be compensated by other nutrient sources. Variations in atmospheric deposition, groundwater and river outflows together with the influence of human activities through changes in landscape use and nutrient management are important sources of nutrient in the ecossytem and thus, act as major drivers of PP in these waters (e.g. Paerl et al., 1999). As consequence of human activities both terrestrial and coastal ecosystems have experienced progressive nutrient enrichment (Conley et al., 2009; Deegan et al., 2012). However, while this effect is evident nearshore, its influence in the ocean is estimated to be minimal (Wang et al., 2018). In the Mediterranean Sea, high coast population growth rates and concomitant food demand have resulted in dramatic increase of water demand for irrigation farming and fertilizer use (Ryan, 2008). Indeed, while Mediterranean rivers have seen a significant reduction in freshwater discharge during recent decades (~20%) their total nitrogen inputs are estimated to have increased by a factor of >5 fuelling PP in river influenced areas (Ludwig et al., 2009). While the importance of groundwater in the Mediterranean Sea could be comparble to that of rivers (Rodellas et al., 2015) and generalized nitrification of Mediterranean coastal aquifers is acknowledged (EEA, 1995; Zalidis et al., 2002) general trends in groundwater discharges remain largely unknown.

4.3. Coastal primary production

Contrastingly, other drivers such as coastal upwelling, riverine inputs or inflows from adjacent seas regulate regions like the northern Alboran Sea, northwestern Adriatic or the northern Aegean. Depending on the magnitude of these processes a high degree of regional variation in PP is observed (>4-fold) between the most productive areas (Z1 = 321 ± 189 gC m^{-2} yr^{-1}) and the more oligotrophic areas (Z16 = 70 ± 46 gC m^{-2} yr^{-1}). In regions such as the northern Adriatic, PP may be controlled by the rate of oxidation of organic matter supplied by river inflows. This fact, together with the combined influence of the rivers discharging along the western Adriatic coast, may explain the wide extension of influence of the Po River in the PP of the Adriatic Sea.

Coastal regionalization reveals marked differences in the productivity of coastal waters in the Mediterranean Sea. Values range from 321 ± 189 gC m^{-2} yr^{-1} in Z1 (north Alboran) to 70 ± 46 gC m^{-2} yr^{-1} in Z16, extending along the coasts of Egypt and Libya. These values fit well with published data, yet, literature values in coastal waters are highly variable depending on methodology, depth

and/or sampling date. For example, Garcia-gorriz and Carr (2001) estimate values of 300 - 900 gC m^{-2} yr^{-1} for Z1 but Morán and Estrada (2001) narrow this range to mean values between 366 and 121 gC m^{-2} yr^{-1} depending on distance from the coast. Pugnetti et al. (2008) reported mean values of 150 gC m^{-2} yr^{-1} that are consistent with our values at Z8. In the lower range, Sournia (1973) estimated 30 - 60 gC m^{-2} yr^{-1} in Z16. In this sense, despite the limitations inherent to satellite data, the preset work provides estimations based on a homogeneous methodology.

The nine characteristic temporal patterns obtained from SOM analysis (Fig. 8) reveal small differences in PP among the different regions. Most variations are due to changes in the magnitude of carbon fixation but seasonality remains very similar. Exceptions are R7 and R3, in the Gulf of Gabes, where seasonal PP maximum occurs late in the year and R8, and in the mouth of major rivers, where seasonal peak is delayed between one and two months. Likewise, interannual variations among regions are highly coherent among regions, following the basin scale pattern shown in Fig. 5, including the exceptionally low productivity in 2012. Exceptions are R1 in the Gulf of Sirte and R7 in Gulf of Gabes where a different interannual variability suggests alternative sources of PP variability in this region. Indeed, the Gulf of Gabes is a peculiar region displaying consistently high Chl and PP in most studies (e.g. Barale et al., 2008; Bosc et al., 2004). Drira et al. (2008) reported high biomass and toxic dinoflagellate blooms in the inner shelf of the Gulf of Gabes where surface nitrate concentration often exceeded 1 µM. This enrichment is associated with degradation of the water quality attributed to industrial and urban activities (Hamza-Chaffai et al., 1997; Zairi and Rouis, 1999). However, even though these waters may suffer from eutrophication, satellite-borne data overestimates Chl with in these waters, as revealed by in situ data. Katlane et al. (2011) observed constant high turbidity and suspended matter of industrial origin affecting these waters but also, reflection from the bottom affecting MODIS data. This suggests that general Chl algorithms may be particularly inaccurate in this region.

The magnitude of coastal PP has been often related to both shelf width and magnitude of river discharge (Liu et al 2010). Our data does not display a general relationship between shelf width, Q and PP_{Amean} (Table 4 & Fig. 9). Indeed, wide shelves with important river discharge flux from the Po, and Rhone and Nile rivers display high productivity (Z4, Z9 and Z15> 224 gC m^{-2} yr^{-1}) whereas production is low in narrowest shelves like Z2, Z5 and Z16. However, PP in some regions with important river inflows, like Z10, are significantly lower (147 ± 71 gC m^{-2} yr^{-1}). In other regions, like R1 and R8 productivity is high despite the lack of important freshwater sources.

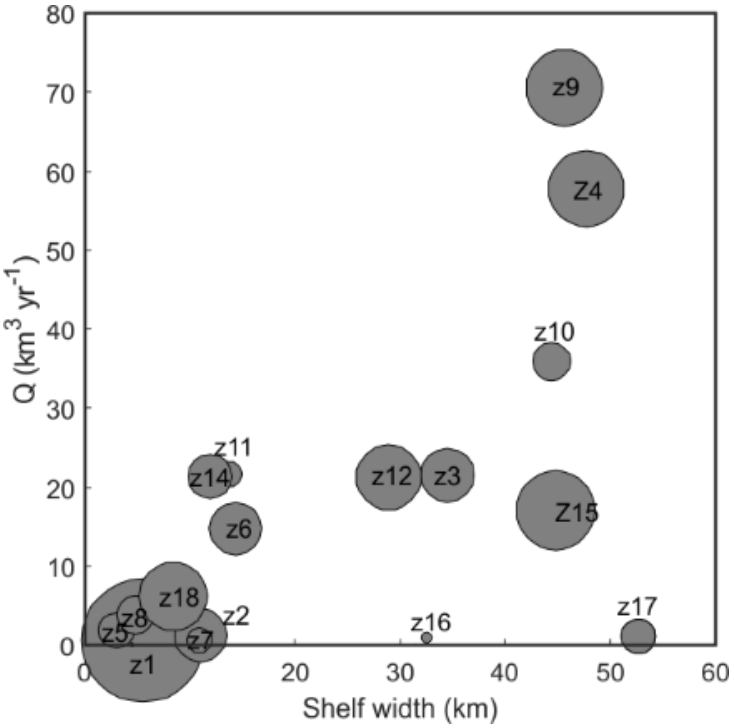

Fig. 9: Relation between shelf width and river discharge flow (Q). The size of the bubbles is proportional to the annual mean PP (PP_{Amean}) of each of the 18-defined zones (see Fig. 8 and Table 4).

The role played by river discharges depends both on Q and on nutrient loads. Most Mediterranean rivers have lost their natural flows and discharges to the sea are strongly regulated by dams and water abstractions. As a consequence, their outflow to the Mediterranean Sea is highly uncoupled from climatic variability. Indeed, some rivers flowing into the Adriatic and Ionian Seas, like the Acheloos, Nestos or Aliakmon nowadays present high to maximum discharge in July due to peak hydropower production (Skoulikidis et al., 2009).

Nutrient and organic matter loads have globally increased during the last century (Beusen et al., 2016). Concentrations exported to nearby seas depend on the combined effects of lithology and the effects of urban effluents, industry and agriculture in catchment basins that are often difficult to quantify. Rivers like the Rhone and Po with important influence on coastal productivity flow through extensive areas accumulating the impact from anthropogenic activities. Agricultural practices and urban effluents can strongly determine the concentration and molar ratios of the nutrients flowing into coastal waters. For example, despite the flux of the Nile river has been drastically reduced after the operation of the Aswan Dam (from 47 to 17 km^3 yr^{-1}, Ludwig et al. (2009), with a consequent diminishing of major nutrient contribution to this area (Azov, 1991), the coastal region is still highly productive. This is explained by the fact that since the dam was built in 1969–72 there has been a remarkable increase in inputs of nitrate from fertilizers and sewage (Nixon, 2004, 2003; Turley, 1999). Conversely, pollution pressures in the western Balkan basins are relatively low and the Neretva (Z10), running through a karstic region in Croatia display considerably lower nutrient levels than the formerly mentioned rivers (Ludwig et al., 2009; Skoulikidis et al., 2009).

Finally, other oceanographic processes determine the productivity of coastal regions. In particular, Z1 and Z18, in the Alboran Sea are comparatively more productive than other areas.

The influence of winds and circulation patterns favouring subsurface water upwelling higher productivity in the northern Alboran Sea where described by Garcia-gorriz and Carr, (2001). Also, localized patterns of relatively high primary production were found in persistent deep water density fronts resulting from the interaction of MAW and Mediterranean water by Lohrenz et al. (1988).

5. CONCLUSIONS

In summary, PP in shelves coastal regions of the Mediterranean Sea during the period 2002-2016 is estimated in this study for the first time using the longest high-resolution NASA ocean-color product available. This analysis demonstrates that although their reduced extension, interannual variability and regional differences, their influence to the global Mediterranean productivity may not be undervalued and ought to be included in future productivity studies.

In the present work, we estimated that 20% of PP of the Mediterranean Sea is attributable to coastal production and from that, about 77% of this carbon fixation is sustained by regenerated pathways. High PP variation was observed among the different regions that is mainly driven by major river effluents. Our analysis also reveals that, with the available satellite data, global Mediterranean climate trends in PP are non-significant but locally they mostly exhibit weakly negative tendencies. Since most of the variability at larger scales is dominated by interannual or sub-decadal variations, PP trends should be considered cautiously and longer records are necessary for robust assessment of climate scale trends. Finally, we identify 18 alongshelf zones based on temporal PP patterns. Two main PP groups were observed: zones with strong cross-shore gradients, typically found in wider estuarine regions and homogeneous zones with narrow continental shelf areas. This regionalization could help for a better comprehension and scientific-based management of the coastal Mediterranean Sea.

6. ACKNOWLEDGEMENTS

This article is a result of the Ministry of Economy and Competitiveness (MINECO) of Spain Project Fine-scale structure of cross-shore GRADIENTS along the Mediterranean coast (CTM2012-39476). P.M. Salgado-Hernanz, was supported by a Ph.D. Doctoral research fellowship FPI (Formación Personal Investigación) fellowship BES-2013-067305 from MINECO. We are grateful to National Aeronautics and Space Administration, NASA (https://oceancolour.gsfc.nasa.gov/) and EU Copernicus Marine Environment Monitoring Service, CMEMS (http://marine.copernicus.eu/) for the freely available ocean-colour remotely-sensed data.

7. SUPPLEMENTARY TABLES AND FIGURES

Supp. Table 1: Percentages of SOM regions presence at each alongshore zone characterized in Fig. 7 and Table 4 respect to the total number of pixels at each zone region.

	%R1	% R2	% R3	% R4	% R5	% R6	% R7	% R8	% R9
Z1	1	0	0	0	10	16	1	5	67
Z2	2	7	0	48	3	36	0	1	3
Z3	3	2	0	43	4	44	0	0	4
Z4	2	2	0	25	34	19	1	2	15
Z5	7	32	0	45	8	7	0	0	1
Z6	2	26	0	29	6	27	0	1	9
Z7	8	85	0	5	0	2	0	0	0
Z8	7	49	0	18	2	23	0	0	1
Z9	1	0	0	49	26	0	2	7	15
Z10	4	9	0	77	6	3	0	0	1
Z11	23	58	0	11	2	4	0	1	1
Z12	3	10	0	33	28	16	0	5	5
Z13	90	7	0	2	1	0	0	0	0
Z14	6	39	0	28	13	8	1	1	4
Z15	27	14	6	4	4	9	3	15	18
Z16	96	2	0	1	1	0	0	0	0
Z17	8	54	17	8	2	4	6	1	0
Z18	2	2	0	1	7	80	0	1	7

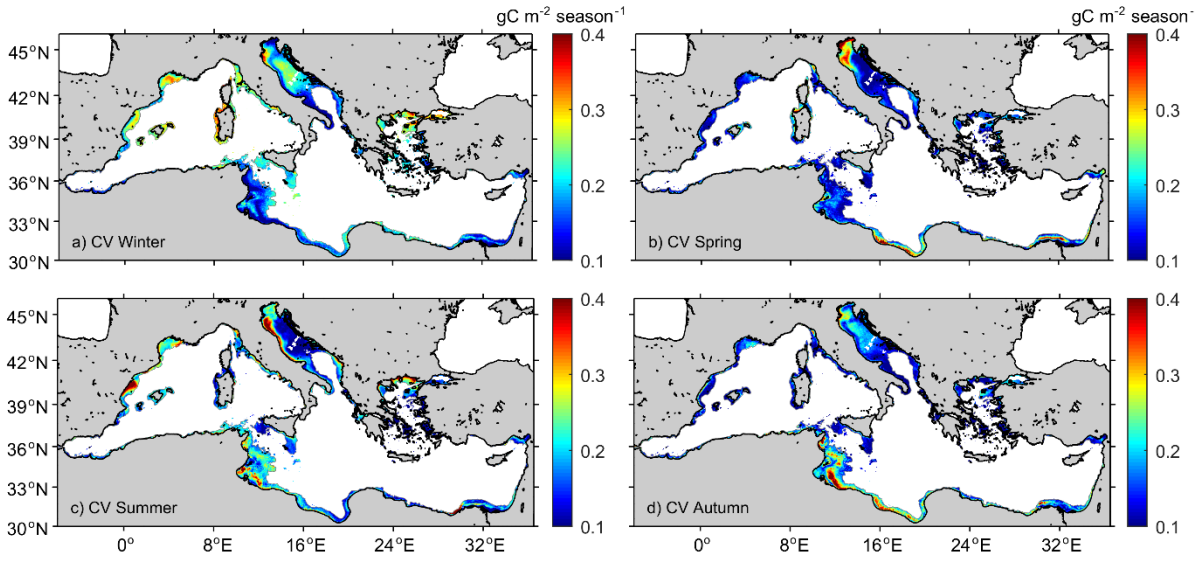

Supp. Fig. S1. Coefficient of variation for mean seasonal PP values over the 2002–2016 period for the coastal Mediterranean areas (< 200 m isobath). Quarterly composites: a & e) winter (Dec-Jan-Feb), b & f) spring (Mar-Apr-May), c & g) summer (Jun-Jul-Agu) and d & h) autumn (Sep-Oct-Nov).

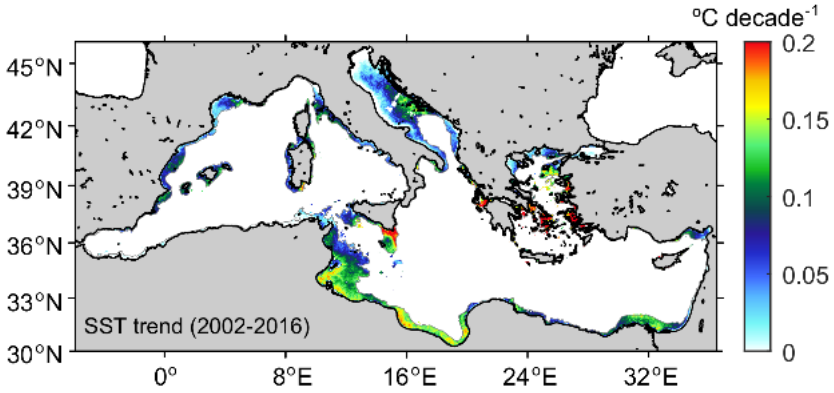

Supp. Fig. S2. Sea Surface Temperature (SST) significant concentration Theil-Sen trend (in gC m^{-2} $decade^{-1}$) over the Mediterranean coastal Sea for the 2002–2016 period.

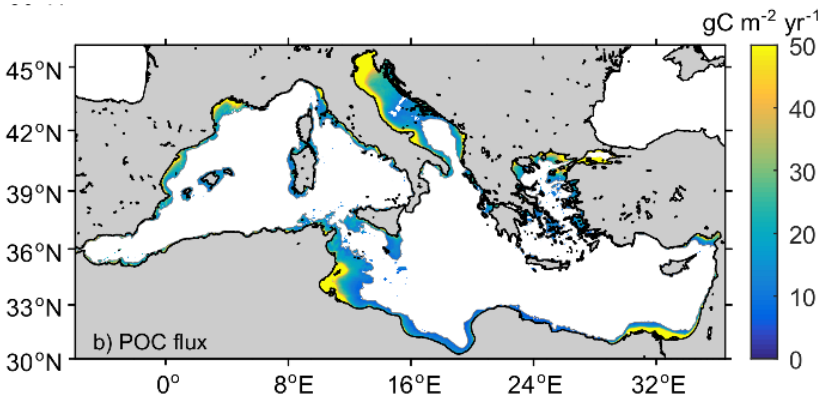

Supp. Fig. S3. Averaged annual ef ratio and annual Particulate Organic Carbon flux (POC flux, in gC m^{-2} yr^{-1}) deposited on the Mediterranean coastal bottom between 2002 and 2016.

IV. GENERAL DISCUSSION

This work provides insight on three main aspects of phytoplankton dynamics in the Mediterranean Sea. Section III - Chapter 1 addresses the characterization of the seasonal and non-seasonal components of phytoplankton variability, emphasizing differences in the response of oceanic and coastal regions. Much of phytoplankton variability in the open ocean is generated by the annual cycles of solar radiation and atmospheric heat input (Cushing, 1959; Sverdrup, 1953) and, indeed, seasonality is the strongest Chl signal for most the Mediterranean Sea. However, we show that in shelf areas and regions with particular dynamics (i.e. straits and sills), phytoplankton variability is affected by many additional processes acting at either shorter or larger timescales. We also show that seasonal patterns are time varying, as demonstrated by the observed trends in phytoplankton phenology. These long-term trend estimations, still present large uncertainties, but they provide an interesting perspective of decadal and climatic variation in the ocean.

Section III - Chapter 2 emphasizes the need to consider the regional differences in the Mediterranean Sea as far as the long-term phytoplankton dynamics is concerned. The Mediterranean is a region characterized by strong climatic contrasts that are indebted to the restrictions to ocean and atmospheric flows by coastal topography and land orography, which results in large differences in driving forces such as wind stress or river outflows (Trigo et al., 2006). This section investigates the importance of these regional differences in the response to climate driven variability.

Section III - Chapter 3 assesses the contribution of coastal waters to basin scale carbon fixation rates. Coastal waters (i.e. <200 m depth) represent up to 20% of the Mediterranean waters and therefore are proportionally more relevant than in the global ocean. Thus, their contribution to carbon cycles in the Mediterranean Sea cannot be neglected. Mediterranean shelf regions display great variability and are highly susceptible to environmental and anthropogenic changes (Pinardi et al., 2004). Consequently, in this section the coastal zone is divided into several regions that display marked regional differences in PP. Most of these variations are due to bathymetric characteristics of the shelf (i.e. width, shallowness) or to the presence of major river discharges.

The interannual variability at basin and regional scale and its relationship with climate indices is also considered in this chapter.

The present work addresses different aspects of phytoplankton dynamics in the Mediterranean Sea by focusing on Chl and PP variability. Regional and interannual variability has been considered as a fundamental part of each chapter as well as the differences between coastal and oceanic regions. The subsections below discuss more in detail the main relevant aspects reported in each of the three chapters presented in Section III.

Chapter 1. Trends in phytoplankton phenology

This chapter provides a vision on the seasonal, the irregular and the interannual variability of phytoplankton in the Mediterranean Sea. Since seasonality is a major driver of phytoplankton variability, characterizing phenology is crucial to understand the long term responses of marine ecosystems. In this chapter, phytoplankton phenology has been characterized by using a threshold-based methodology (Racault et al., 2017b). This approach has not been applied to the Mediterranean Sea until now but its adequateness has been tested in previous studies in other world areas (Kassi et al., 2018; Land et al., 2014; Platt and Sathyendranath, 2008; Racault et al., 2012; Siegel et al., 2002). This method, based on a pixel-by-pixel time series threshold approach, brings novelty compared to previous phenological studies in the Mediterranean region, such as the ones by D'Ortenzio and Ribera d'Alcalà (2009) or Lavigne et al. (2013), that are based on climatological patterns. Additionally, the threshold method allows to detect more than one phytoplankton growing period. Secondary blooms have been previously described in regional scale studies (e.g. Macias et al., 2018; Mayot et al., 2017); however, a comprehensive assessment of the occurrence of secondary blooms in the Mediterranean Sea had not been addressed before.

Several studies demonstrate that climate change influences the phenological responses of marine phytoplankton. Phenological changes affect the rates of carbon sequestration in the ocean. Also, changes in the phenological response of phytoplankton disturb the interactions with other components of the pelagic food webs and may cause mismatch in the trophic exchanges (Edwards and Richardson, 2004). These mismatches can be caused by either shifts in bloom timing, variations in seasonal biomass peaks or changes in species composition affecting prey-predator relationships (Hillebrand et al., 2018).

There is plenty scientific evidence indicating that climate warming induces shifts in phytoplankton biomass and in its phenology. Indeed, SST in the Mediterranean Sea have increased over the last 4 decades (Nykjaer, 2009; Shaltout and Omstedt, 2014) and models expect conditions to be warmer and drier with increase evaporation at least until 2100 (Mariotti et al., 2015; Sakalli, 2017). Poloczanska et al. (2013) reported a general trend in the onset of the phytoplankton spring bloom of -4.4 ± 0.7 days decade^{-1} attributed to global warming. However, the Mediterranean phenological trends herein reported show a delay in the onset of the main phytoplankton growing period (+9 ± 5 days decade^{-1}) and in the peak timing (+12 ± 8 days decade^{-1}). While this may seem contradictory with global trends, there are evidences demonstrating different responses in phytoplankton phenology depending on the particularities of each oceanic system. For example, Henson et al. (2018) reported that there is no clear global tendency since bloom timing generally shifts later at mid-latitudes and earlier at high and low latitudes by ~5 days per decade. Also,

Gittings et al. (2018) reported that for the period 1998 - 2015, the tropical northern Red Sea presented weaker winter phytoplankton blooms, initiating later and lasting shorter.

Large uncertainties remain in the estimation of long term trends in phytoplankton phenology derived from ocean color information (Mélin et al., 2017). Nevertheless, although some of the presently derived tendency may be highly influenced by decadal patterns of variation, large improvements are expected as longer satellite data time series become available.

Chapter 2. Patterns of chlorophyll interannual variability

In this chapter, SOM analysis of ocean color data is used to define different regions in the Mediterranean Sea based on their temporal Chl variations. With some exceptions (i.e. Solidoro et al. 2007), this is a clustering technique that had not been applied before to the study of phytoplankton dynamics in the Mediterranean Sea. SOM analysis can be used as an alternative to traditional *k*-means clustering with the advantage that is 'topology preserving': i.e., similar neighboring clusters are usually grouped together.

The results of the regionalization obtained in this chapter somewhat differ from previous studies (e.g. D'Ortenzio and Ribera d'Alcalà, 2009; Lavigne et al., 2013). One of the most relevant discrepancies is that while an extensive homogeneous region is obtained in the eastern basin using SOM analysis, other methodologies delimit different sub regions in this basin (Ayata et al., 2018). Another relevant characteristic depicted from SOM analysis is that a detailed definition of coastal gradient zones is obtained. This allows to discriminate coastal regions affected by different features such as rivers, shallow regions or slope areas where Chl varies at small spatial scales. This high pattern definition allows to adequately detect characteristics poorly defined in previous studies.

The PSC spatial distribution examined for the different SOM-defined regions demonstrated that the three defined phytoplankton sizes (pico-,nano-,micro-) coexist at every region. The predominance of one group over the others is strongly dependent on the physical and biological processes occurring at each region. Our regionalization reveals that in oceanic oligotrophic regions picoplankton Chl contribution can suppose >50%. By contrast, bigger phytoplankton sizes (nanoplankton and microplankton) shows relevant percentage values (~50% nano-,20 - 25% micro- against a lower value of about ~30% from pico-) in areas controlled by external nutrient inputs such as the north Adriatic, the Alboran Sea or the NWMS (i.e. river discharges or winter convection processes that inject nutrients to the surface layers). This is consistent with previous studies performed in the Mediterranean Sea (Di Cicco et al., 2017; Sammartino et al., 2015). Nevertheless, Di Cicco et al. (2017) reported that nanoplankton Chl contribution dominates in the western basin and coastal regions, ranging from 30 to 40% of total phytoplankton, whereas picoplankton is the principal Chl contribution size group in the eastern basin. Although this partly agrees with our results, our regionalization allows to identify some oceanic areas in the western basin where picoplankton Chl contribution is also dominant, such as the south Balearic and the Tyrrhenian Seas.

Uitz et al. (2012) quantified the contribution of each PSC to the PP of the Mediterranean Sea using the classification described in D'Ortenzio and Ribera d'Alcalà (2009). These authors concluded

that 48% of the PP at basin-scale was due to nanoplankton. They also reported that microplankton increases its contribution to PP during the spring bloom (~38% vs. 27% coming from nanoplankton). Despite that our study does not quantify the contribution to PP of the different size groups, we also observe an increase in the microplankton community to Chl contribution (up to >20%) during winter and spring, mainly in coastal regions.

A main result portrayed in Chapter 2 is the response of phytoplankton biomass at each biogeographical region to climate forcing. The different regions present dissimilar response to climate variability. For instance, the regions in the western basin are more influenced by NAO than the eastern ones. Negative phases of NAO are associated with an increase precipitation and lower SST in winter in the western basin with a subsequent increase in Chl. The enhanced mixing and river runoff could be the cause of that increase in Chl concentration. Contrastingly, ENSO is more influential in the central and eastern basins in its positive phase. We speculatively infer that this is mediated by the effect of enhanced dust deposition in this region. Our study reports that dust concentration practically doubles in regions located in the eastern basin (i.e from 30 - 40 μmg m^{-3} in the Gulf of Gabes and the extended eastern basin). Therefore, years with more nutrient-rich dust deposition may be associated with a positive phase of ENSO and a subsequent increase in Chl (DeFlorio et al., 2016).

The wavelets analysis reveals that a high correlation between NAO and Chl signal is observed at periods of 1.2 years (mainly in the western basin) and, to a lesser degree, at a 3.4 years in the most productive waters. Besides this 1.2 year Chl - NAO relationship pattern (i.e. phytoplankton dynamics to climate variability), a shift is observed around years 2004-2007 revealing non – stationary coherence of mainly winter Chl with NAO at the same time interval. NAO changed from positive to negative value in 2005, and the relevant period of correlation changed from the 1.2 to be the 3.4 period after. This shift may be caused by caused by global environmental factors affecting the Mediterranean Sea thought the NAO index. For instance Schroeder et al. (2016) reported an abrupt change in 2005 in the intermediate and deep layers of the western Mediterranean waters that brought significant dense water formation events with an increase in the Chl level of the basin.

This chapter sustains the idea that regional scale responses ought to be considered in future climatological studies in the Mediterranean Sea. Global scale analyses miss relevant information for the interpretation of phytoplankton dynamics and composition. Moreover, this study reveals that the influence of climate variations on marine phytoplankton are non-stationary and that other factors may override present relationships between Chl and climate.

Chapter 3. Primary production in coastal waters

This chapter is focused on coastal regions since they have been traditionally avoided in satellite-based studies due to their complex optical characteristics. Present understanding on the contribution and trends of PP shelves is very limited because PP estimations have been traditionally inferred from *in situ* observations at discrete locations during a specific time and using different methodologies. In this work, a homogeneous and spatially coherent satellite-based method is used to estimate PP in the coastal waters of the Mediterranean Sea. In particular,

a specific light-dependent and depth-integrated and time-resolved version of the model for carbon fixation is used to estimate PP (Morel 1991; Antoine and Morel 1996).

One of the most relevant contributions of the present study is the estimation of overall contribution of coastal waters to basin-scale PP in the Mediterranean Sea. It is estimated that coastal regions contribute to 20% of the total annual integrated PP in this sea. This is mainly due to the contribution of the eastern basin, and specifically to the carbon fixation rates occurring at the extensive Gabes-Sicily region. This area represents 22% of the total integrated annual PP which is on average 28 times higher than PP in other areas. The Adriatic region is the basin with the highest annual mean PP (~200 gC m^{-2} yr^{-1}). This region is highly influenced by the Po River which is the one the largest rivers discharging in the Mediterranean Sea (Struglia et al., 2004).

A second important aspect to consider in this chapter is that approximately 80% of total carbon fixation is of regenerated origin. Only about 20% comes from new nutrients. As main sources of these allochtonous nutrients are river discharges, new PP is mainly located in the Po, Rhone and Nile delta. This new PP presents marked seasonal variability, being higher in spring and winter and lower in autumn. Bethoux (1989) reported that new PP in the Mediterranean Sea varies between 12 and 35 gC m^{-2} yr^{-1}, and anticipated an increase of this value during the 21st century due to the increasing of anthropogenic P discharges. Using a different approach, our study reveals a higher value of mean new PP at basin scale of 40 gC m^{-2} yr^{-1}. No study has been found reporting global new and regenerated PP. However, their relative contribution can be inferred from global *ef*-ratio maps reported in Laws et al. (2011), i.e., the higher the ratio, the higher the new PP. At a global scale, *ef*-ratios varied from 0.1 to 0.9, being higher values placed at high latitudes (e.g Arctic Sea). Herein, it is reported an averaged *ef*-ratio of 0.23 for the Mediterranean Sea, which indicates that most PP in the Mediterranean Sea is sustained by nutrient regeneration.

Another relevant aspect to consider in this chapter is that, although PP rate in the entire basin does nor display a clear tendency in the last decades, there are some coastal Mediterranean regions displaying weak but significant PP trends. Consistently, Macias et al. (2015) did not observe a global trend at basin-scale during the period 1960 - 2012. However, they performed some simulations to foresee a future oligotrophication in the western basin due to an increase in stratification, and an increase in surface PP in the eastern basin because of increasing evaporation rate. The results in this chapter show negative trends in the eastern basin (-12.5 TC $decade^{-1}$) and positive trends in the Adriatic Sea (+10.5 TC $decade^{-1}$). Regionally, weakly declining productivity trends are observed in the western side, particularly in the Gulf of Gabes and along the Spanish coast. As mentioned in Section III - Chapter 1, there is evidence of warming in the Mediterranean Sea (e.g. Shaltout and Omstedt, 2014). Here we observe that PP is inversely correlated with SST and although more poorly, with the climatic indices such as NAO and MOI. This may be a consequence of an increase in stratification due to SST and subsequent decrease in productivity. Contrastingly, the Adriatic sea shows an inverse pattern that may be attributed to variations in the nutrient discharges by the Po River (Giani et al., 2012).

The final contribution of this chapter is that we illustrate the importance of regionalizing the Mediterranean coastal waters. The resultant classification is consistent with the one obtained in the previous chapter where regional differences are mainly due to the presence of different degree of cross-shore variability patterns in shelf regions, which tend to be more common in wider zones and regions affected by river inputs. PP magnitudes between the defined zones can

vary by a factor of 5. This difference may be mainly due to its extension and input of nutrients. Generically, regions that are more productive are the one with river presence.

Quantifying PP in coastal areas has special importance due to two main causes. Firstly, PP in the coast maintains richer food webs than in the open ocean. Therefore, understanding changes in PP in coastal areas is fundamental to the understanding the dynamics and productivity of coastal ecosystems. The PP decrease seen in certain coastal waters may provoke a reduction of energy and biomass transfer up (e.g. plankton to fish) in the food web (Macias et al., 2014). Secondly, PP is a key ecological climate regulator since is responsible of organic matter exported to the deep ocean. As a consequence, understanding PP variability is crucial to understand and predict the effects of global warming, ocean acidification and the productivity of coastal fisheries (Cheung et al., 2010; Doney et al., 2009; Keeling et al., 2010).

V. CONCLUSIONS

As results of what has been exposed in the present work, we can extract the following general conclusions:

1. Ocean color remote sensing data is a valuable tool to address phytoplankton dynamics and primary production variability at fine space–time resolution in the Mediterranean Sea in both oceanic and coastal regions.

2. The assessment of phytoplankton dynamics reveals that seasonal variations are dominant in oceanic Mediterranean areas whereas non-seasonal variability is important in specific regions dominated by particular forcings (i.e. runoff, local winds).

3. Phenological indices (i.e. in timings and biomass) present differences between oceanic and coastal areas, as well as at regional scale. It results relevant that at sub-basin scale, the main growing period last about 20 days more and doubles the peak magnitude in the western basin (~170 days and 0.9 mg m^{-3}) respect to the eastern one (~150 days and 0.35 mg m^{-3}).

4. The probability of occurrence of second growing periods is higher (~80 %) in coastal waters, the NWMS and in the Strait of Gibraltar. In these regions, the main phytoplankton growing period generally shortens with respect to the regions with only one growing period.

5. A significant positive trend in Chl of +0.015mg m^{-3} $decade^{-1}$ is observed in the western basin. Contrastingly, the eastern basin reflects a negative Chl trend of about -0.004 mg m^{-3} $decade^{-1}$ over the period 1998-2014. These changes are reflected in the trends of phenological indices where an increase in both amplitude and duration of the spring bloom is observed in the western basin (bloom peak rising about +0.3 mg m^{-3} and lasting +10 days $decade^{-1}$) whereas the opposite occurs in the eastern basin (bloom peak reducing about -0.03 mg m^{-3} and lasting -12 days $decade^{-1}$).

6. It is demonstrated that phytoplankton response to climate is regionally varying. Long-term Chl interannual variability is influence with NAO variability in the western biogeographical regions whereas a better coherence with the positive phase of ENSO in seen in the eastern and central zones.

7. A shift occurred in the coherence between NAO and Chl around year 2005 in western basin. This change in phytoplankton is consistent with previous studies reporting changes in intermediate and deep layers of the western Mediterranean basin during the same year.

8. Coastal regions contribute to 20% of the overall primary production in the Mediterranean Sea, with a mean primary production of about 200 gC m^{-2} yr^{-1} and a total value of 0.075 GtC yr^{-1}. Up to 50% of this carbon fixation occurs in the eastern basin, 28% in the western shelf and 24% in the Adriatic.

9. High spatial variability is observed in the primary production of coastal Mediterranean waters. Values range between 70 and 500 gC m^{-2} yr^{-1}.

10. About 80% of primary production in the coastal Mediterranean Sea is regenerated. New primary production is constraint to specific regions where sources of nutrients are frequent such as the north Adriatic Sea or the Alboran Sea.

11. An inverse correlation is found between the long-term primary production and sea surface temperature variations (r = -0.5) at basin scale. A similar correlation is seen with climatic indices NAO and MOI although with a slightly reduced value (r = -0.3 and 0.4 respectively)

12. No significant trend is detected at basin scale in primary production in the Mediterranean Sea during the period 2002-2015. However, sub-basin scale differences are observed. The Adriatic Sea has significantly increased its productivity by +10.5TC $decade^{-1}$. Conversely, the eastern basin is becoming less productive, showing a reduction of -12.5 TC $decade^{-1}$ during the period of study.

REFERENCES

Agirbas, E., Martinez-Vicente, V., Brewin, R.J.W., Racault, M.F., Airs, R.L., Llewellyn, C.A., 2015. Temporal changes in total and size-fractioned chlorophyll-a in surface waters of three provinces in the Atlantic Ocean (September to November) between 2003 and 2010. J. Mar. Syst. 150, 56–65. doi:10.1016/j.jmarsys.2015.05.008

Ainsworth, E.J., 1999. Visualization of ocean colour and temperature from multi-spectral imagery captured by the Japanese ADEOS satellite. J. Vis. 2, 195–204. doi:10.1007/BF03181523

Alheit, J., Bakun, A., 2010. Population synchronies within and between ocean basins: Apparent teleconnections and implications as to physical-biological linkage mechanisms. J. Mar. Syst. 79, 267–285. doi:10.1016/j.jmarsys.2008.11.029

Alvain, S., Moulin, C., Dandonneau, Y., Bréon, F.M., 2005. Remote sensing of phytoplankton groups in case 1 waters from global SeaWiFS imagery. Deep Sea Res. Part I Oceanogr. Res. Pap. 52, 1989–2004. doi:10.1016/j.dsr.2005.06.015

Alvain, S., Moulin, C., Dandonneau, Y., Loisel, H., 2008. Seasonal distribution and succession of dominant phytoplankton groups in the global ocean: A satellite view. Global Biogeochem. Cycles 22, n/a-n/a. doi:10.1029/2007GB003154

Amante, C., Eakins, B.W., 2009. ETOPO1 1 Arc-minute global relief model: Procedures, data sources and analysis. NOAA Tech. Memo. NESDIS NGDC-24. Natl. Geophys. Data Center, NOAA. doi:10.7289/V5C8276M

Antoine, D., André, J.-M., Morel, A., 1996. Oceanic primary production. 2. Estimation at global scale from satellite (Coastal Zone Color Scanner) chlorophyll. Global Biogeochem. Cycles 10, 57–69. doi:10.1029/95GB02832

Antoine, D., Morel, A., 1996. Oceanic primary production. 1. Adaptation of a spectral light-photosynthesis model in view of application to satellite chlorophyll observations. Glob. Biogeochem. Cycleschemical Cycles 10, 43–55. doi:10.1029/95GB02831

Antoine, D., Morel, A., André, J.-M., 1995. Algal pigment distribution and primary production in the eastern Mediterranean as derived from coastal zone color scanner observations. J. Geophys. Res. 100, 16193. doi:10.1029/95JC00466

Arin, L., Guillén, J., Segura-Noguera, M., Estrada, M., 2013. Open sea hydrographic forcing of nutrient and phytoplankton dynamics in a Mediterranean coastal ecosystem. Estuar. Coast. Shelf Sci. 133, 116–128. doi:10.1016/j.ecss.2013.08.018

Arístegui, J., Tett, P., Hernández-Guerra, A., Basterretxea, G., Montero, M.F., Wild, K., Sangrá, P., Hernández-León, S., Cantón, M., García-Braun, J.A., Pacheco, M., Barton, E.., 1997. The influence of island-generated eddies on chlorophyll distribution : a study of mesoscale variation around Gran Canaria. Deep Sea Res. Part I Oceanogr. Res. Pap. 44, 77–96.

Armstrong, R.A., 2006. Optimality-based modeling of nitrogen allocation and photoacclimation in photosynthesis. Deep. Res. Part II 53, 513–531. doi:10.1016/j.dsr2.2006.01.020

Asanuma, I., 2006. Depth and time resolved primary productivity model examined for optical properties of water. Elsevier Oceanogr. Ser. 73, 89–106. doi:10.1016/S0422-9894(06)73004-5

Asch, R.G., 2015. Climate change and decadal shifts in the phenology of larval fishes in the California current ecosystem. Proc. Natl. Acad. Sci. 112, E4065–E4074. doi:10.1073/pnas.1421946112

Astraldi, M., Balopoulos, S., Candela, J., Font, J., Gacic, M., Gasparini, G.P., Manca, B., Theocharis, A., Tintoré, J., 1999. The role of straits and channels in understanding the characteristics of Mediterranean circulation. Prog. Oceanogr. 44, 65–108. doi:10.1016/S0079-6611(99)00021-X

Ayata, S., Irisson, J., Aubert, A., Berline, L., Dutay, J., Mayot, N., Nieblas, A., Ortenzio, F.D., Palmiéri, J., Reygondeau, G., Rossi, V., Guieu, C., 2018. Regionalisation of the Mediterranean basin, a MERMEX synthesis. Prog. Oceanogr. 163, 7–20. doi:10.1016/j.pocean.2017.09.016

Azam, F., 1998. Microbial control of oceanic carbon flux: The plot thickens. Science (80-.). 280, 694–696. doi:10.1126/science.280.5364.694

Azam, F., Fenchel, T., Field, J., Gray, J., Meyer-Reil, L., Thingstad, F., 1983. The ecological role of water-column microbes in thesea. Mar. Ecol. Prog. Ser. 10, 257–263. doi:10.3354/meps010257

Azov, Y., 1991. Eastern Mediterranean-a marine desert? Mar. Pollut. Bull. 23, 225–232. doi:10.1016/0025-326X(91)90679-M

Azov, Y., 1986. Seasonal patterns of phytoplankton productivity and abundance in nearshore oligotrophic waters of the Levant Basin (Mediterranean). J. Plankton Res. 8, 41–53. doi:doi.org/10.1093/plankt/8.1.41

Bakker, W.H., Feringa, W., Gieske, A.S.M., Gorte, B.G.H., Grabmaier, K.A., Hecker, C.A., Horn, J.A., Huurneman, G.C., Janssen, L.L.F., Kerle, N., Meer, F.D. Van Der, Parodi, G.N., Pohl, C., Reeves, C. V, Ruitenbeek, F.J. Van, Schetselaar, E.M., Tempfli, K., Weir,

M.J.C., Westinga, E., Woldai, T., 2009. Principles of Remote Sensing. The International Institute for Geo-Information Science and Earth Observation (ITC), Enschede, The Netherlands.

Bakun, A., Agostini, V.N., 2001. Seasonal patterns of wind-induced upwelling/ downwelling in the Mediterranean Sea. Sci. Mar. 65, 243–257.

Balbín, R., López-Jurado, J.L., Flexas, M.M., Reglero, P., Vélez-Velchí, P., González-Pola, C., Rodríguez, J.M., García, A., Alemany, F., 2014. Interannual variability of the early summer circulation around the Balearic Islands: Driving factors and potential effects on the marine ecosystem. J. Mar. Syst. 138, 70–81. doi:10.1016/j.jmarsys.2013.07.004

Balkis, N., 2009. Seasonal variations of microphytoplankton assemblages and environmental variables in the coastal zone of bozcaada island in the aegean sea (NE mediterranean sea) : mmicrophytoplankton and environmental variables of bozcaada island. Aquat. Ecol. 43, 249–270. doi:10.1007/s10452-008-9175-x

Barale, V., Gade, M. (Eds.), 2008. Remote Sensing of the European Seas. Springer.

Barale, V., Jaquet, J.-M., Ndiaye, M., 2008. Algal blooming patterns and anomalies in the Mediterranean Sea as derived from the SeaWiFS data set (1998–2003). Remote Sens. Environ. 112, 3300–3313. doi:10.1016/j.rse.2007.10.014

Barale, V., Zin, I., 2000. Impact of continental margins in the Mediterranean Sea: Hints from the surface colour and temperature historical record. J. Coast. Conserv. 6, 5–14. doi:10.1007/BF02730462

Barbieux, M., Uitz, J., Bricaud, A., Organelli, E., Poteau, A., Schmechtig, C., Gentili, B., Obolensky, G., Leymarie, E., Penkerc'h, C., D'Ortenzio, F., Claustre, H., 2018. Assessing the variability in the relationship between the particulate backscattering coefficient and the chlorophyll a concentration from a global biogeochemical-Argo database. J. Geophys. Res. Ocean. 123, 1229–1250. doi:10.1002/2017JC013030

Barnston, A.G., Chelliah, M., Goldenberg, S.B., 1997. Documentation of a highly ENSO-related SST region in the equatorial Pacific. Atmos. - Ocean 35, 367–383.

Basterretxea, G., Font-Muñoz, J.S., Salgado-Hernanz, P.M., Arrieta, J., Hernández-Carrasco, I., 2018. Patterns of chlorophyll interannual variability in Mediterranean biogeographical regions. Remote Sens. Environ. 215, 7–17. doi:10.1016/j.rse.2018.05.027

Basterretxea, G., Tovar-Sanchez, A., Beck, A.J., Masqué, P., Bokuniewicz, H.J., Coffey, R., Duarte, C.M., Garcia-Orellana, J., Garcia-Solsona, E., Martinez-Ribes, L., Vaquer-Sunyer, R., 2010. Submarine groundwater discharge to the coastal environment of a Mediterranean island (Majorca, Spain): Ecosystem and biogeochemical significance. Ecosystems 13, 629–643. doi:10.1007/s10021-010-9334-5

Basu, S., Mackey, K.R.M., 2018. Phytoplankton as key mediators of the biological carbon pump: Their responses to a changing climate. Sustainability 10. doi:10.3390/su10030869

Bauer, J.E., Cai, W., Raymond, P.A., Bianchi, T.S., Hopkinson, C.S., Regnier, P.A.G., 2013.

The changing carbon cycle of the coastal ocean. Nature 504, 61–70. doi:10.1038/nature12857

Behrenfeld, M.J., Boss, E., Siegel, D.A., Shea, D.M., 2005. Carbon-based ocean productivity and phytoplankton physiology from space. Glob. Biochem. Cycles 19. doi:10.1029/2004GB002299

Behrenfeld, M.J., Falkowski, P.G., 1997. Photosynthetic rates derived from satellite-based chlorophyll concentration. Limnol. Oceanogr. 42, 1–20. doi:10.4319/lo.1997.42.1.0001

Behrenfeld, M.J., O'Malley, R.T., Siegel, D. a, McClain, C.R., Sarmiento, J.L., Feldman, G.C., Milligan, A.J., Falkowski, P.G., Letelier, R.M., Boss, E.S., 2006. Climate-driven trends in contemporary ocean productivity. Nature 444, 752–755. doi:10.1038/nature05317

Belgrano, A., Lindahl, O., Hernroth, B., 1999. North Atlantic Oscillation Primary Productivity and Toxic Phytoplankton in the Gullmar Fjord, Sweden (1986-1996). Proc. Biol. Sci. R. Soc. 266, 425–430. doi:10.1098/rspb.1999.0655

Belkin, I.M., 2009. Rapid warming of large marine ecosystems. Prog. Oceanogr. 81, 207–213. doi:10.1016/j.pocean.2009.04.011

Ben Mustapha, Z., Alvain, S., Jamet, C., Loisel, H., Dessailly, D., 2014. Automatic classification of water-leaving radiance anomalies from global SeaWiFS imagery: Application to the detection of phytoplankton groups in open ocean waters. Remote Sens. Environ. 146, 97–112. doi:10.1016/j.rse.2013.08.046

Bergamasco, A., Malanotte-Rizzoli, P., 2010. The circulation of the Mediterranean Sea: a historical review of experimental investigations. Adv. Oceanogr. Limnol. 1, 11–28. doi:10.1080/19475721.2010.491656

Berline, L.O., Rammou, A.M., Doglioli, A., Molcard, A., Petrenko, A., 2014. A connectivity-based Eco-regionalization method of the mediterranean sea. PLoS One 9, 3–11. doi:10.1371/journal.pone.0111978

Berthon, J.-F., Zibordi, G., 2004. Bio-optical relationships for the northern Adriatic Sea. Int. J. Remote Sens. 25, 1527–1532. doi:10.1080/01431160310001592544

Bethoux, J.P., 1989. Oxygen consumption, new production, vertical advection and environmental evolution in the Mediterranean Sea. Deep Sea Res. Part A, Oceanogr. Res. Pap. 36, 769–781. doi:10.1016/0198-0149(89)90150-7

Bethoux, J.P., Gentili, B., Raunet, J., Tailliez, D., 1990. Warming trend in the western Mediterranean deep water. Nature 347.

Béthoux, J.P., Morin, P., Chaumery, C., Connan, O., Gentili, B., Ruiz-Pino, D., 1998. Nutrients in the Mediterranean Sea, mass balance and statistical analysis of concentrations with respect to environmental change. Mar. Chem. 63, 155–169. doi:10.1016/S0304-4203(98)00059-0

Beusen, A.H.W., Bouwman, A.F., Beek, L.P.H. Van, Mogollón, J.M., Middelburg, J.J., 2016. Global riverine N and P transport to ocean increased during the 20th century despite

increased retention along the aquatic continuum. Biogeosciences 13, 2441–2451. doi:10.5194/bg-13-2441-2016

Blondeau-Patissier, D., Gower, J.F.R., Dekker, A.G., Phinn, S.R., Brando, V.E., 2014. A review of ocean color remote sensing methods and statistical techniques for the detection, mapping and analysis of phytoplankton blooms in coastal and open oceans. Prog. Oceanogr. 123, 123–144. doi:10.1016/j.pocean.2013.12.008

Boldrin, A., Miserocchi, S., Rabitti, S., Turchetto, M.M., Balboni, V., Socal, G., 2002. Particulate matter in the southern Adriatic and Ionian Sea: Characterisation and downward fluxes. J. Mar. Syst. 33–34, 389–410. doi:10.1016/S0924-7963(02)00068-4

Bosc, E., Bricaud, A., Antoine, D., 2004. Seasonal and interannual variability in algal biomass and primary production in the Mediterranean Sea, as derived from 4 years of SeaWiFS observations. Global Biogeochem. Cycles 18, n/a-n/a. doi:10.1029/2003GB002034

Bougis, P., 1974. Écologie du plancton marin. 1. Le phytoplancton. 2. Le zooplancton., Limnology and Oceanography. Paris. doi:10.1017/S0003598X00101735

Boyd, P.W., Sundby, S., Pörtner, H.-O., 2014. Cross-chapter box on net primary production in the ocean, in: Field, C.B., Barros, V.R., Dokken, D.J., Mach, K.J., Mastrandrea, M.D., Bilir, T.E., Chatterjee, M., Ebi, K.L., Estrada, Y.O., Genova, R.C., Girma, B., Kissel, E.S., Levy, A.N., MacCracken, S., Mastrandrea, P.R., White, L.L. (Eds.), Climate Change 2014: Impacts, Adaptation, and Vulnerability. Part A: Global and Sectoral Aspects. Contribution of Working Group II to the Fifth Assessment Report of the Intergovernmental Panel on Climate Change. Cambridge University Press, United Kingdom and New York, pp. 133–136.

Brandimarte, L., Di Baldassarre, G., Bruni, G., D'Odorico, P., Montanari, A., 2011. Relation between the North-Atlantic Oscillation and hydroclimatic conditions in Mediterranean areas. Water Resour. Manag. 25, 1269–1279. doi:10.1007/s11269-010-9742-5

Brewin, R.J.W., Hardman-Mountford, N.J., Lavender, S.J., Raitsos, D.E., Hirata, T., Uitz, J., Devred, E., Bricaud, A., Ciotti, A., Gentili, B., 2011. An intercomparison of bio-optical techniques for detecting dominant phytoplankton size class from satellite remote sensing. Remote Sens. Environ. 115, 325–339. doi:10.1016/j.rse.2010.09.004

Brewin, R.J.W., Sathyendranath, S., Hirata, T., Lavender, S.J., Barciela, R.M., Hardman-Mountford, N.J., 2010. A three-component model of phytoplankton size class for the Atlantic Ocean. Ecol. Modell. 221, 1472–1483. doi:10.1016/j.ecolmodel.2010.02.014

Brewin, R.J.W., Sathyendranath, S., Müller, D., Brockmann, C., Deschamps, P.-Y., Devred, E., Doerffer, R., Fomferra, N., Franz, B., Grant, M., Groom, S., Horseman, A., Hu, C., Krasemann, H., Lee, Z., Maritorena, S., Mélin, F., Peters, M., Platt, T., Regner, P., Smyth, T., Steinmetz, F., Swinton, J., Werdell, J., White III, G.N., 2015. The Ocean Colour Climate Change Initiative: III. A round-robin comparison on in-water bio-optical algorithms. Remote Sens. Environ. 162, 271–294.

doi:10.1016/j.rse.2013.09.016

Bricaud, A., Bosc, E., Antoine, D., 2002. Algal biomass and sea surface temperature in the Mediterranean Basin. Remote Sens. Environ. 81, 163–178. doi:10.1016/S0034-4257(01)00335-2

Bristow, L.A., Mohr, W., Ahmerkamp, S., Kuypers, M.M., 2017. Nutrients that limit growh in the ocean. Curr. Biol. 27, R474–R478. doi:10.1016/j.cub.2017.03.030

Brönnimann, S., 2007. Impact of El Niño-Southern Oscillation on European climate. Rev. Geophys. 45. doi:10.1029/2006RG000199.1

Brown, C.W., Yoder, J.A., 1994. Coccolithophorid blooms in the global ocean. J. Geophys. Res. 99, 7467–7482. doi:10.1029/93JC02156

Brümmer, F., 2003. Living inside a glass box - Silica in Diatoms, in: Müller, W.E.G. (Ed.), Silicon Biomineralization. p. 340.

Cabré, A., Shields, D., Marinov, I., Kostadinov, T.S., 2016. Phenology of size-partitioned phytoplankton carbon-biomass from ocean color remote sensing and CMIP5 models. Front. Mar. Sci. 3, 1–20. doi:10.3389/fmars.2016.00039

Cai, W., 2011. Estuarine and Coastal Ocean Carbon Paradox: CO 2 Sinks or Sites of Terrestrial Carbon Incineration? Ann. Rev. Mar. Sci. 3, 123–145. doi:10.1146/annurev-marine-120709-142723

Calbet, A., 2008. The trophic roles of microzooplankton in marine systems. ICES J. Mar. Sci. 65, 325–331. doi:10.1093/icesjms/fsn013

Calbet, A., Landry, M.R., 2004. Phytoplankton growth, microzooplankton grazing, and carbon cycling in marine systems. Limnol. Oceanogr. 49, 51–57. doi:10.4319/lo.2004.49.1.0051

Campbell, J., Antoine, D., Armstrong, R., Arrigo, K., Balch, W., Barber, R., Behrenfeld, M., Bidigare, R., Bishop, J., Carr, M., Esaias, W., Falkowski, P., Hoepffner, N., Iverson, R., Kiefer, D., Lohrenz, S., Marra, J., Morel, A., Ryan, J., Vedernikov, V., Waters, K., Yentsch, C., Yoder, J., 2002. Comparison of algorithms for estimating ocean primary production from surface chlorophyll, temperature, and irradiance. Glob. Biochem. Cycles 16. doi:10.1029/2001GB001444

Capone, D.G., Bronk, D.A., Muholland, M.R., Carpenter, E.J. (Eds.), 2008. Nitrogen in the marine environment. Academic Press. doi:10.1016/B978-0-12-372522-6.X0001-1

Capuzzo, E., Lynam, C.P., Barry, J., Stephens, D., Forster, R.M., Greenwood, N., McQuatters-Gollop, A., Silva, T., van Leeuwen, S.M., Engelhard, G.H., 2017. A decline in primary production in the North Sea over 25 years, associated with reductions in zooplankton abundance and fish stock recruitment. Glob. Chang. Biol. 24, e352–e364. doi:10.1111/gcb.13916

Carlson, C.A., Bates, N.R., Hansell, D.A., Steinberg, D.K., 2001a. Carbon cycle, in: Encyclopedia of Ocean Sciences, Volume 1. Elsevier Ltd, pp. 390–400. doi:10.1016/b978-012374473-9.00272-1

Carlson, C.A., Bates, N.R., Hansell, D.A., Steinberg, D.K., 2001b. Nutrient cycling: Carbon

Cycle, in: Steele, J., Thorpe, S., Turekian, K. (Eds.), Encyclopedia of Ocean Sciences. Academic Press, London, pp. 390–400. doi:10.1006/rwos.2001.0272

Caroppo, C., Turicchia, S., Margheri, M.C., 2006. Phytoplankton assemblages in coastal waters of the northern Ionian Sea (eastern Mediterranean), with special reference to cyanobacteria. J. Mar. Biol. Assoc. U.K. 86, 827–937. doi:10.1017/S0025315406013889

Carr, M.-E., 2002. Estimation of potential productivity in Eastern Boundary Currents using remote sensing. Deep. Res. Part II 49, 59–80. doi:10.1016/S0967-0645(01)00094-7

Carr, M.-E., Friedrichs, M. a. M., Schmeltz, M., Noguchi Aita, M., Antoine, D., Arrigo, K.R., Asanuma, I., Aumont, O., Barber, R., Behrenfeld, M., Bidigare, R., Buitenhuis, E.T., Campbell, J., Ciotti, A., Dierssen, H., Dowell, M., Dunne, J., Esaias, W., Gentili, B., Gregg, W., Groom, S., Hoepffner, N., Ishizaka, J., Kameda, T., Le Quéré, C., Lohrenz, S., Marra, J., Mélin, F., Moore, K., Morel, A., Reddy, T.E., Ryan, J., Scardi, M., Smyth, T., Turpie, K., Tilstone, G., Waters, K., Yamanaka, Y., 2006. A comparison of global estimates of marine primary production from ocean color. Deep Sea Res. Part II Top. Stud. Oceanogr. 53, 741–770. doi:10.1016/j.dsr2.2006.01.028

Cebrian, J., 2002. Variability and control of carbon consumption, export and accumulation in marine communities. Limnol. Oceanogr. 47, 11–22. doi:10.4319/lo.2002.47.1.0011

Chambers, R.C., Trippel, E.A., 1997. Early Life History and Recruitment in Fish Populations. Fish and Fisheries Series 21. Chapman and Hall, London.

Charantonis, A.A., Badran, F., Thiria, S., 2015. Retrieving the evolution of vertical profiles of Chlorophyll-a from satellite observations using Hidden Markov Models and Self-Organizing Topological Maps. Remote Sens. Environ. 163, 229–239. doi:10.1016/j.rse.2015.03.019

Chassot, E., Bonhommeau, S., Dulvy, N.K., Mélin, F., Watson, R., Gascuel, D., Le Pape, O., 2010. Global marine primary production constrains fisheries catches. Ecol. Lett. 13, 495–505. doi:10.1111/j.1461-0248.2010.01443.x

Chavez, F.P., Messié, M., Pennington, J.T., 2011. Marine primary production in relation to climate cariability and change. Ann. Rev. Mar. Sci. 3, 227–260. doi:10.1146/annurev.marine.010908.163917

Cheung, W.W., Lam, V.W.Y., Sarmiento, J.L., Kearney, K., Watson, R., Zeller, D., Pauly, D., 2010. Large-scale redistribution of maximum fisheries catch potential in the global ocean under climate change. Glob. Chang. Biol. 16, 24–35. doi:10.1111/j.1365-2486.2009.01995.x

Chisholm, S.W., 1992. Phytoplankton size, in: Falkowski, P.G., Woodhead, A.D. (Eds.), Primary Productivity and Biogeochemical Cycles in the Sea. Plenum Press, New York, pp. 213–238.

Christaki, U., Giannakourou, A., Van Wambeke, F., Grégori, G., 2001. Nanoflagellate predation on auto- and heterotrophic picoplankton in the oligotrophic Mediterranean Sea. J. Plankton Res. 23, 1297–1310. doi:10.1093/plankt/23.11.1297

Ciotti, A.M., Bricaud, A., 2006. Retrievals of a size parameter for phytoplankton and spectral light absorption by colored detrital matter from water-leaving radiances at SeaWiFS channels in a continental shelf region off Brazil. Limnol. Oceanogr. Methods 4, 237–253. doi:10.4319/lom.2006.4.237

Ciotti, Á.M., Lewis, M.R., Cullen, J.J., 2002. Assessment of the relationships between dominant cell size in natural phytoplankton communities and the spectral shape of the absorption coefficient. Limnol. Oceanogr. 47, 404–417.

Civitarese, G., Gačić, M., Lipizer, M., Eusebi Borzelli, G.L., 2010. On the impact of the Bimodal Oscillating System (BiOS) on the biogeochemistry and biology of the Adriatic and Ionian seas (eastern Mediterranean). Biogeosciences 7, 3987–3997. doi:10.5194/bg-7-3987-2010

Cloern, J.E., Foster, S.Q., Kleckner, A.E., 2014. Phytoplankton primary production in the world's estuarine-coastal ecosystems. Biogeosciences 11, 2477–2501. doi:10.5194/bg-11-2477-2014

Cloern, J.E., Jassby, A.D., 2008. Complex seasonal patterns of primary producers at the land-sea interface. Ecol. Lett. 11, 1294–1303. doi:10.1111/j.1461-0248.2008.01244.x

Cloern, J.E., Jassby, A.D., Thompson, J.K., Hieb, K.A., 2007. A cold phase of the East Pacific triggers new phytoplankton blooms in San Francisco Bay. Pnas 104, 18561–18565.

Cole, J.J., Prairie, Y.T., Caraco, N.F., McDowell, W.H., Tranvik, L.J., Striegl, R.G., Duarte, C.M., Kortelainen, P., Downing, J.A., Middelburg, J.J., Melack, J., 2007. Plumbing the global carbon cycle: Integrating inland waters into the terrestrial carbon budget. Ecosystems 10, 171–184. doi:10.1007/s10021-006-9013-8

Colella, S., D'Ortenzio, F., Marullo, S., Santoleri, R., Ragni, M., D'Alcala, M.R., 2003. Primary production variability in the Mediterranean Sea from SeaWiFS data, in: Primary Production Variability in the Mediterranean Sea from SeaWiFS Data. Proceedings of SPIE - The International Society for Optical Engineering, pp. 371–383. doi:10.1117/12.516791

Colella, S., Falcini, F., Rinaldi, E., Sammartino, M., Santoleri, R., 2016. Mediterranean ocean colour chlorophyll trends. PLoS One 11, 1–16. doi:10.1371/journal.pone.0155756

Coll, M., Piroddi, C., Steenbeek, J., Kaschner, K., Lasram, F.B.R., Aguzzi, J., Ballesteros, E., Bianchi, C.N., Corbera, J., Dailianis, T., Danovaro, R., Estrada, M., Froglia, C., Galil, B.S., Gasol, J.M., Gertwage, R., Gil, J., Guilhaumon, F., Kesner-Reyes, K., Kitsos, M.S., Koukouras, A., Lampadariou, N., Laxamana, E., de la Cuadra, C.M.L.F., Lotze, H.K., Martin, D., Mouillot, D., Oro, D., Raicevich, S., Rius-Barile, J., Saiz-Salinas, J.I., Vicente, C.S., Somot, S., Templado, J., Turon, X., Vafidis, D., Villanueva, R., Voultsiadou, E., 2010. The biodiversity of the Mediterranean Sea: Estimates, patterns, and threats. PLoS One 5. doi:10.1371/journal.pone.0011842

Conan, P., Pujo-Pay, M., Raimbault, P., Leveau, M., 1998. Variabilité hydrologique et biologique du golfe du Lion. II. Productivité sur le bord interne du courant. Oceanol. Acta 21, 767–782. doi:10.1016/S0399-1784(99)80004-8

Conley, D.J., Paerl, H.W., Howarth, R.W., Boesch, D.F., Seitzinger, S.P., Havens, K.E., Lancelot, C., Likens, G.E., 2009. Controlling eutrophication : Nitrogen and phosphorus. Science (80-.). 323. doi:10.1126/science.1167755

Conversi, A., Umani, S.F., Peluso, T., Molinero, J.C., Santojanni, A., Edwards, M., 2010. The mediterranean sea regime shift at the end of the 1980s, and intriguing parallelisms with other european basins. PLoS One 5. doi:10.1371/journal.pone.0010633

Coppini, G., Lyubarstev, V., Pinardi, N., Colella, S., Santoleri, R., Christiansen, T., 2013. The use of ocean-colour data to estimate Chl-a trends in European seas. Int. J. Geosci. 4, 927–949. doi:10.4236/ijg.2013.46087

Corredor-Acosta, A., Morales, C.E., Hormazabal, S., Andrade, I., Correa-Ramirez, M.A., 2015. Phytoplankton phenology in the coastal upwelling region off central-southern Chile (35ºS–38ºS): Time-space variability, coupling to environmental factors, and sources of uncertainty in the estimates. J. Geophys. Res. Ocean. 122, 2012–2028. doi:10.1002/2014JC010330.Received

Cramer, W., Guiot, J., Fader, M., Garrabou, J., Gattuso, J., Iglesias, A., Lange, M.A., Lionello, P., Llasat, M.C., Paz, S., Peñuelas, J., Snoussi, M., Toreri, A., Tsimplis, M.N., Xoplaki, E., 2018. Climate change and interconnected risks to sustainable development in the Mediterranean. Nat. Clim. Chang. doi:10.1038/s41558-018-0299-2

Criado-Aldeanueva, F., Soto-Navarro, F.J., 2013. The mediterranean oscillation teleconnection index: Station-based versus principal component paradigms. Adv. Meteorol. 2013. doi:10.1155/2013/738501

Crise, A., Allen, J.I., Baretta, J., Crispi, G., Mosetti, R., Solidoro, C., 1999. The Mediterranean pelagic ecosystem response to physical forcing. Prog. Oceanogr. 44, 219–243. doi:10.1016/S0079-6611(99)00027-0

Cullen, J.J., 2001. Primary production methods. Encycl. Ocean Sci. Vol. 4. doi:10.1016/B978-012374473-9.00203-4

Cullen, J.J., 1982. The deep chl maximum: comparing vertical profiles of chla.pdf. Fish Aquat. Sci. 39, 791–803. doi:10.1139/cjfas-2014-0209

Cushing, D.H., 1975. Marine Ecology and Fisheries, Prometheus. Cambridge University Press, England. doi:10.1080/08109020320000050000

Cushing, D.H., 1959. The seasonal variation in oceanic production as a problem in phytoplankton dynamics. J. Cons. Int. pour l' Explor. la mer 24, 455–464. doi:doi.org/10.1093/icesjms/24.3.455

Cushman-Roisin, B., Gačić, M., Poulain, P.-M., Artegiani, A., 2001. Physical Oceanography of the Adriatic Sea. Past, Present and Future. Kluwer Academic Publishers.

D'Alimonte, D., Mélin, F., Zibordi, G., Berthon, J.F., 2003. Use of the novelty detection technique to identify the range of applicability of empirical ocean color algorithms. IEEE Trans. Geosci. Remote Sens. 41, 2833–2843. doi:10.1109/TGRS.2003.818020

D'Alimonte, D., Zibordi, G., 2003. Phytoplankton determination in an optically complex

coastal region using a multilayer perceptron neural network. IEEE Trans. Geosci. Remote Sens. 41, 2861–2868. doi:10.1109/TGRS.2003.817682

D'Ortenzio, F., Iudicone, D., de Boyer Montegut, C., Testor, P., Antoine, D., Marullo, S., Santoleri, R., Madec, G., 2005. Seasonal variability of the mixed layer depth in the Mediterranean Sea as derived from in situ profiles. Geophys. Res. Lett. 32, 1–4. doi:10.1029/2005GL022463

D'Ortenzio, F., Lavigne, H., Besson, F., Claustre, H., Coppola, L., Garcia, N., Laës-Huon, A., Le Reste, S., Malardé, D., Migon, C., Morin, P., Mortier, L., Poteau, A., Prieur, L., Raimbault, P., Testor, P., 2014. Observing mixed layer depth, nitrate and chlorophyll concentrations in the northwestern Mediterranean: A combined satellite and NO3 profiling floats experiment. Geophys. Res. Lett. 6443–6451. doi:10.1002/2014GL061020.Received

D'Ortenzio, F., Marullo, S., Ragni, M., Ribera d' Alcalà, M., Santoleri, R., 2002. Validation of empirical SeaWiFS algorithms for chlorophyll-a retrieval in the Mediterranean Sea. A case study for oligotrophic seas. Remote Sens. Environ. 82, 79–94. doi:10.1016/S0034-4257(02)00026-3

D'Ortenzio, F., Ribera d'Alcalà, M., 2009. On the trophic regimes of the Mediterranean Sea: A satellite analysis. Biogeosciences 5, 2959–2983. doi:10.5194/bgd-5-2959-2008

Dandonneau, Y., Deschamps, P.Y., Nicolas, J.M., Loisel, H., Blanchot, J., Montel, Y., Thieuleux, F., Bécu, G., 2004. Seasonal and interannual variability of ocean color and composition of phytoplankton communities in the North Atlantic, equatorial Pacific and South Pacific. Deep. Res. II 51, 303–318. doi:doi:10.1016/j.dsr2.2003.07.018

Deegan, L.A., Johnson, D.S., Warren, R.S., Peterson, B.J., Fleeger, J.W., Fagherazzi, S., Wollheim, W.M., 2012. Coastal eutrophication as a driver of salt marsh loss. Nature 490, 388–392. doi:10.1038/nature11533

DeFlorio, M.J., Goodwin, I.D., Cayan, D.R., Miller, A.J., Ghan, S.J., Pierce, D.W., Russell, L.M., Singh, B., 2016. Interannual modulation of subtropical Atlantic boreal summer dust variability by ENSO. Clim. Dyn. 46, 585–599. doi:10.1007/s00382-015-2600-7

Di Cicco, A., Sammartino, M., Marullo, S., Santoleri, R., 2017. Regional empirical algorithms for an improved identification of phytoplankton functional types and size classes in the Mediterranean Sea using satellite data. Front. Mar. Sci. 4, 1–18. doi:10.3389/fmars.2017.00126

Dickey, T., Lewis, M., Chang, G., 2006. Optical oceanography: Recent advances and future directions using global remote sensing and in situ observations, in: Reviews of Geophysics. pp. 1–39. doi:10.1029/2003RG000148

Dierssen, H.M., 2010. Perspectives on empirical approaches for ocean color remote sensing of chlorophyll in a changing climate. PNAS 107, 17073–17078. doi:10.1073/pnas.0913800107

Directive 2008/56/EC, 2008. Directive 2008/56/EC of the European Parliament and of the Council. Off. J. Eur. Union L 164/19, 19–40.

Djakovac, T., Degobbis, D., Supic, N., Precali, R., 2012. Marked reduction of eutrophication pressure in the northeastern Adriatic in the period 2000 e 2009. Estuaries and Coasts 115, 25–32. doi:10.1016/j.ecss.2012.03.029

Dolan, J.R., 2000. Tintinnid ciliate diversity in the Mediterranean Sea: Longitudinal patterns related to water column structure in late spring - early summer. Aquat. Microb. Ecol. 22, 69–78.

Doney, S.C., Fabry, V.J., Feely, R.A., Kleypas, J.A., 2009. Ocean Acidification : The other CO2 problem. Ann. Rev. Mar. Sci. 1, 169–92. doi:10.1146/annurev.marine.010908.163834

Donner, S.D., Scavia, D., 2007. How climate controls the flux of nitrogen by the Mississippi River and the development of hypoxia in the Gulf of Mexico. Limnol. Oceanogr. 52, 856–861. doi:10.4319/lo.2007.52.2.0856

Drira, Z., Hamza, A., Bel Hassen, M., Ayadi, H., Bouain, A., Aleya, L., 2010. Coupling of phytoplankton community structure to nutrients, ciliates and copepods in the Gulf of Gabès (south Ionian Sea, Tunisia). J. Mar. Biol. Assoc. United Kingdom 90, 1203–1215. doi:10.1017/S0025315409990774

Drira, Z., Hamza, A., Belhassen, M., Ayadi, H., Bouaïn, A., Aleya, L., 2008. Dynamics of dinoflagellates and environmental factors during the summer in the Gulf of Gabes (Tunisia, eastern Mediterranean Sea). Sci. Mar. 72, 59–71. doi:10.3989/scimar.2008.72n159

Druon, J.N., Fiorentino, F., Murenu, M., Knittweis, L., Colloca, F., Osio, C., Mérigot, B.H., Garofalo, G., Mannini, A., Jadaud, A.H., Sbrana, M.H., Scarcella, G., Tserpes, G., Peristeraki, P.H., Carlucci, R., Heikkonen, J., 2015. Modelling of European hake nurseries in the Mediterranean Sea: an ecological niche approach. Prog. Oceanogr. 130, 188–204. doi:10.1016/j.pocean.2014.11.005

Duarte, C.M., Cebrián, J., 1996. The fate of marine autotrophic production. Limnol. Oceanogr. 41, 1758–1766. doi:10.4319/lo.1996.41.8.1758

Dubois, M., Rossi, V., Ser-Giacomi, E., Arnaud-Haond, S., López, C., Hernández-García, E., 2016. Linking basin-scale connectivity, oceanography and population dynamics for the conservation and management of marine ecosystems. Glob. Ecol. Biogeogr. 25, 503–515. doi:10.1111/geb.12431

Dugdale, R.C., Goering, J.J., 1967. Uptake of new and regenerated forms of nitrogen in primary productivity. Limnol Ocean. 23, 196–206. doi:10.4319/lo.1967.12.2.0196

Dugdale, R.C., Wilkerson, F.P., 1998. Silicate regulation of new production in the equatorial Pacific upwelling. Nature 391, 270–273. doi:10.1038/34630

Dunne, J.P., Sarmiento, J.L., Gnanadesikan, A., 2007. A synthesis of global particle export from the surface ocean and cycling through the ocean interior and on the seafloor. Glob. Biochem. Cycles 21. doi:10.1029/2006GB002907

Durrieu De Madron, X., Houpert, L., Puig, P., Sanchez-Vida, A., Testor, P., Bosse, A., Estournel, C., Somot, S., Bourrin, F., Bouin, M.N., Beauverger, M., Beguery, L., Calafat, A., Canals, M., Cassou, C., Coppola, L., Dausse, D., Ortenzio, F.D., Font, J.,

Heussner, S., Kunesch, S., Lefevre, D., Goff, H. Le, Martín, J., Mortier, L., Palanques, A., Raim, 2013. Interaction of dense shelf water cascading and open-sea convection in the northwestern Mediterranean during winter 2012. Geophys. Res. Lett. 40, 1–7. doi:10.1002/grl.50331

Durrieu De Madron, X., Ludwig, W., Civitarese, G., Gacic, M., Raimbault, P., Krasakopoulou, E., Goyet, C., 2010. The Mediterranean Sea : The shelf-slope systems, in: Liu, K.-K., Atkinson, L., Quinones, R., Talaure-McManus, L. (Eds.), Carbon and Nutrient Fluxes in Continental Margins. Springer-Verlag Berlin Heidelbergh. doi:10.1007/978-3-540-92735-8_1

Edwards, M., Richardson, A.J., 2004. Impact of climate change on marine pelagic phenology and trophic mismatch. Lett. to Nat. 430, 881–884. doi:10.1038/nature02808

EEA, 1995. Europe's Environment - The Dobris Assessment.

Efthymiadis, D., Goodess, C.M., Jones, P.D., 2011. Trends in Mediterranean gridded temperature extremes and large-scale circulation influences. Nat. Hazards Earth Syst. Sci. 11, 2199–2214. doi:10.5194/nhess-11-2199-2011

Eppley, R.W., Peterson, B.J., 1979. Particulate organic matter flux and planktonic new production in the deep ocean. Nature 282. doi:10.1038/282677a0

Eppley, R.W., Stewart, E., Abbott, M.R., Heyman, U., 1985. Estimating ocean primary production from satellite chlorophyll. Introduction to regional differences and statistics for the Southern California Bight. J. Plankton Res. 7, 57–70. doi:10.1093/plankt/7.1.57

Erasmi, S., Schucknecht, A., Barbosa, M.P., Matschullat, J., Gottingen, G., Commission, E., Environmental, I., Federal, U., Grande, D.C., 2014. Vegetation Greenness in Northeastern Brazil and Its Relation to 3041–3058. doi:10.3390/rs6043041

Estrada, M., 1996. Primary production in the northwestern Mediterranean. Sci. Mar. 60, 55–64.

Evans, R.H., Gordon, H.R., 1994. Coastal zone color scanner "system calibration'': a retrospective examination." J. Geophys. Res. 99, 7293–7307. doi:10.1029/93JC02151

Falkowski, P., Scholes, R.J., Boyle, E., Canadell, J., Canfield, D., Elser, J., Gruber, N., Hibbard, K., Högberg, P., Linder, S., Mackenzie, F.T., Moore III, B., Pedersen, T., Rosenthal, Y., Seitzinger, S., Smetacek, V., Steffen, W., 2000. The global carbon cycle: A test of our knowledge of Earth as a system. Science (80-.). 290, 291–296. doi:10.1126/science.290.5490.291

Falkowski, P.G., 1997. Evolution of the nitrogen cycle and its influence on the biological sequestration of CO2 in the ocean. Nature 387, 272–275. doi:10.1038/387272a0

Falkowski, P.G., 1981. Light-shade adaptation and assimilation numbers. J. Plankton Res. 3, 203–216. doi:10.1093/plankt/3.2.203

Falkowski, P.G., Barber, R.T., Smetacek, V., 1998. Biogeochemical controls and feedbacks

on ocean primary production. Sci. Spec. Sect. Chem. Biol. Ocean. 281, 200–206. doi:10.1126/science.281.5374.200

Falkowski, P.G., Raven, J.A., 2007. Aquatic Photosynthesis. Princenton University Press, Princenton, NJ.

Falkowski, P.G., Woodhead, A.D., 1992. Primary production and biogeochemical. Plenum Press, New York.

Farikou, O., Sawadogo, S., Niang, A., Diouf, D., Brajard, J., Mejia, C., Dandonneau, Y., Gasc, G., Crepon, M., Thiria, S., 2015. Inferring the seasonal evolution of phytoplankton groups in the Senegalo-Mauritanian upwelling region from satellite ocean-color spectral measurements. J. Geophys. Res. Ocean. 120, 6581–6601. doi:10.1002/2015JC010738

Fenchel, T., 2008. The microbial loop – 25 years later. J. Exp. Mar. Bio. Ecol. 366, 99–103. doi:10.1016/j.jembe.2008.07.013

Fendereski, F., Vogt, M., Payne, M.R., Lachkar, Z., Gruber, N., Salmanmahiny, A., Hosseini, S.A., 2014. Biogeographic classification of the Caspian Sea. Biogeosciences 11, 6451–6470. doi:10.5194/bg-11-6451-2014

Ferreira, A.S., Visser, A.W., MacKenzie, B.R., Payne, M.R., 2014. Accuracy and precision in the calculation of phenologymetrics. J. Geophys. Res. Ocean. 119, 2121–2128. doi:10.1002/jgrc.20224

Field, C.B., Behrenfeld, M.J., Randerson, J.T., Falkowski, P.G., 1998. Primary Production of the Biosphere : Integrating Terrestrial and Oceanic Components. Science (80-.). 281. doi:10.1126/science.281.5374.237

Font, J., Puig, P., Salat, J., Palanques, A., Emelianov, M., 2007. Sequence of hydrographic changes in NW Mediterranean deep water due to the exceptional winter of 2005. Sci. Mar. 71, 339–346. doi:10.3989/scimar.2007.71n2339

Forget, P., André, G., 2007. Can Satellite-derived Chlorophyll imagery be used to trace surface dynamics in coastal zone? A case study in the Northwestern Mediterranean Sea. Sensors 7, 884–904.

Forget, P., Ouillon, S., 1998. Surface suspended matter off the Rhone river mouth from visible satellite imagery. Oceanol. Acta 21, 739–749.

Foukal, N.P., Thomas, A.C., 2014. Biogeography and phenology of satellite-measured phytoplankton seasonality in the California current. Deep. Res. Part I Oceanogr. Res. Pap. 92, 11–25. doi:10.1016/j.dsr.2014.06.008

Frank, J., Maseey, J., 1951. The Kolmogorov-Smirnov test for goodness of fit. J. Am. Stat. Assoc. 46:253, 3-17–335. doi:10.1016/0378-3758(90)90051-U

Friedland, K.D., Leaf, R.T., Kane, J., Tommasi, D., Asch, R.G., Rebuck, N., Ji, R., Large, S.I., Stock, C., Saba, V.S., 2015. Spring bloom dynamics and zooplankton biomass response on the US Northeast Continental Shelf. Cont. Shelf Res. 102, 47–61. doi:10.1016/j.csr.2015.04.005

Friedland, K.D., Mouw, C.B., Asch, R.G., Ferreira, A.S.A., Henson, S., Hyde, K.J.W., Morse,

R.E., Thomas, A.C., Brady, D.C., 2018. Phenology and time series trends of the dominant seasonal phytoplankton bloom across global scales. Glob. Ecol. Biogeogr. 551–569. doi:10.1111/geb.12717

Friedrichs, M.A.M., Carr, M., Barber, R.T., Scardi, M., Antoine, D., Armstrong, R.A., Asanuma, I., Behrenfeld, M.J., Buitenhuis, E.T., Chai, F., Christian, J.R., Ciotti, A.M., Doney, S.C., Dowell, M., Dunne, J., Gentili, B., Gregg, W., Hoepffner, N., Ishizaka, J., Kameda, T., Lima, I., Marra, J., Mélin, F., Moore, J.K., Morel, A., Malley, R.T.O., Reilly, J.O., Saba, V.S., Schmeltz, M., Smyth, T.J., Tjiputra, J., Waters, K., Westberry, T.K., Winguth, A., 2009. Assessing the uncertainties of model estimates of primary productivity in the tropical Pacific Ocean. J. Mar. Syst. 76, 113–133. doi:10.1016/j.jmarsys.2008.05.010

Gačić, M., Civitarese, G., Miserocchi, S., Cardin, V., Crise, A., Mauri, E., 2002. The open-ocean convection in the Southern Adriatic: a controlling mechanism of the spring phytoplankton bloom. Cont. Shelf Res. 22, 1897–1908. doi:10.1016/S0278-4343(02)00050-X

Gallisai, R., 2016. Saharan dust deposition effects on production in the Mediterranean Sea. Universidad Politécnica de Catalunya.

Gallisai, R., Peters, F., Volpe, G., Basart, S., Baldasano, J.M., 2014. Saharan dust deposition may affect phytoplankton growth in the Mediterranean Sea at ecological time scales. PLoS One 9. doi:10.1371/journal.pone.0110762

García-Comas, C., Stemmann, L., Ibanez, F., Berline, L., Mazzocchi, M.G., Gasparini, S., Picheral, M., Gorsky, G., 2011. Zooplankton long-term changes in the NW Mediterranean Sea: decadal periodicity forced by winter hydrographic conditions related to large-scale atmospheric changes? J. Mar. Syst. 87, 216–226. doi:10.1016/j.jmarsys.2011.04.003

Garcia-Gorriz, E., Carr, M.-E., 2001. Physical control of phytoplankton distributions in the Alboran Sea: A numerical and satellite approach. J. Geophys. Res. 106, 795–805. doi:10.1029/1999JC000029

Gasol, J.M., Cardelús, C., Morán, X.A.G., Balagué, V., Forn, I., Marrasé, C., Massana, R., Pedrós-alió, C., Sala, M.M., Simó, R., Vaqué, D., Estrada, M., 2016. Seasonal patterns in phytoplankton photosynthetic parameters and primary production at a coastal NW Mediterranean site. Sci. Mar. 80S1, 63–77. doi:10.3989/scimar.04480.06E

Gattuso, J.-P., Frankignoulle, M., Wollast, R., 1998. Carbon and carbonate metabolism in coastal aquatic ecosystems. Annu. Rev. Ecol. Syst. 29, 405–434. doi:10.1146/annurev.ecolsys.29.1.405

Giani, M., Djakovac, T., Degobbis, D., Cozzi, S., Solidoro, C., Fonda, S., 2012. Recent changes in the marine ecosystems of the northern Adriatic Sea. Estuar. Coast. Shelf Sci. 115, 1–13. doi:10.1016/j.ecss.2012.08.023

Gilbert, R.O., 1987. Detecting and estimating trends. Pacific Northwest Laboratory, New. doi:10.2307/2531935

Gittings, J.A., Raitsos, D.E., Krokos, G., Hoteit, I., 2018. Impacts of warming on

phytoplankton abundance and phenology in a typical tropical marine ecosystem. Nat. Sci. Reports 8, 1–12. doi:10.1038/s41598-018-20560-5

Goffart, A., Hecq, J.H., Legendre, L., 2002. Changes in the development of the winter-spring phytoplankton bloom in the Bay of Calvi (NW Mediterranean) over the last two decades: A response to changing climate? Mar. Ecol. Prog. Ser. 236, 45–60. doi:10.3354/meps236045

Gomez, F.A., Spitz, Y.H., Batchelder, H.P., Correa-ramirez, M.A., 2017. Intraseasonal patterns in coastal plankton biomass off central Chile derived from satellite observations and a biochemical model. J. Mar. Syst. 174, 106–118. doi:10.1016/j.jmarsys.2017.05.003

Goolsby, D.A., Battaglin, W.A., 2001. Long-term changes in concentrations and flux of nitrogen in the Mississippi River Basin , USA. Hydrol. Process. 15, 1209–1226. doi:10.1002/hyp.210

Gregg, W.W., Conkright, M.E., 2002. Decadal changes in global ocean chlorophyll. Geophys. Res. Lett. 29, 1–4. doi:10.1029/2002GL014689

Gregg, W.W., Conkright, M.E., Casey, N.W., 2003. Ocean primary production and climate: Global decadal changes. Geophys. Res. Lett. 30, 10–13. doi:10.1029/2003GL016889

Gregg, W.W., Rousseaux, C.S., 2014. Decadal trends in global pelagic ocean chlorophyll: a new assessment integrating multiple satellites, in situ data, and models. J. Geophys. Res. Ocean. 5921–5933. doi:10.1002/2014JC010158.Received

Gregg, W.W., Rousseaux, C.S., Franz, B.A., 2017. Global trends in ocean phytoplankton: A new assessment using revised ocean colour data. Remote Sens. Lett. 8, 1102–1111. doi:10.1080/2150704X.2017.1354263

Grinsted, A., Moore, J.C., Jevrejeva, S., 2004. Nonlinear Processes in Geophysics Application of the cross wavelet transform and wavelet coherence to geophysical time series. Nonlinear Process. Geophys. 11, 561–566.

Guidi, L., Stemmann, L., Jackson, G.A., Ibanez, F., Claustre, H., Legendre, L., Picheral, M., Gorsky, G., 2009. Effects of phytoplankton community on production, size and export of large aggregates: A world-ocean analysis. Limnol. Oceanogr. 54, 1951–1963. doi:10.4319/lo.2009.54.6.1951

Gurley, K., Kareem, A., 1999. Applications of wavelet transforms in earthquake, wind and ocean engineering. Eng. Struct. 21, 149–167. doi:10.1.1.472.8163

Gurley, K., Kijewski, T., Kareem, A., 2003. First- and higher-order correlation detection using wavelet transforms. J. Eng. Mech. 129, 188–201. doi:10.1061/(ASCE)0733-9399(2003)129:2(188)

Hamad, N., Millot, C., Taupier-Letage, I., 2005. A new hypothesis about the surface circulation in the eastern basin of the mediterranean sea. Prog. Oceanogr. 66, 287–298. doi:10.1016/j.pocean.2005.04.002

Hamza-Chaffai, A., Armiad-Triquet, C., El Abed, A., 1997. Metallothionein-like protein: Is it an efficient biomarker of metal contamination? A case study based on fish from

the Tunisian coast. Arch. Environ. Contam. Toxicol. 33, 53–62. doi:10.1007/s002449900223

Hays, G.C., Richardson, A.J., Robinson, C., 2005. Climate change and marine plankton. Trends Ecol. Evol. 20. doi:10.1016/j.tree.2005.03.004

Henson, S.A., Cole, H.S., Hopkins, J., Martin, A.P., Yool, A., 2018. Detection of climate change-driven trends in phytoplankton phenology. Glob. Chang. Biol. 24, e101–e111. doi:10.1111/gcb.13886

Henson, S.A., Sanders, R., Madsen, E., 2012. Global patterns in efficiency of particulate organic carbon export and transfer to the deep ocean. Glob. Biochem. Cycles 26, 1–14. doi:10.1029/2011GB004099

Henson, S.A., Sarmiento, J.L., Dunne, J.P., Bopp, L., Lima, I., Doney, S.C., John, J., Beaulieu, C., 2010. Detection of anthropogenic climate change in satellite records of ocean chlorophyll and productivity. Biogeosciences 7, 621–640. doi:10.5194/bg-7-621-2010

Herut, B., Collier, R., Krom, M.D., 2002. The role of dust in supplying nitrogen and phosphorus to the Southeast Mediterranean. Limnol. Oceanogr. 47, 870–878. doi:10.4319/lo.2002.47.3.0870

Herut, B., Zohary, T., Krom, M.D., Mantoura, R.F.C., 2005. Response of East Mediterranean surface water to Saharan dust: On-board microcosm experiment and field observations. Deep Sea Res. Part II 52, 3024–3040. doi:10.1016/j.dsr2.2005.09.003

Hillebrand, H., Brey, T., Gutt, J., Hagen, W., Metfies, K., Meyer, B., Lewandowska, A., 2018. Climate change : warming impacts on marine biodiversity. Secion 3: Pollution from diffuse sources., in: Salomon, M., Markus, T. (Eds.), Marine Environment Protection Science, Impacts and Sustainable Management. Springer. doi:10.1007/978-3-319-60156-4

Hinchey, E.K., Nicholson, M.C., Zajac, R.N., Irlandi, E.A., 2008. Preface: Marine and coastal applications in landscape ecology. Landsc. Ecol. 23, 1–5. doi:10.1007/s10980-007-9141-3

Hooker, S.B., Esaias, W.E., Feldman, G.C., Gregg, W.W., McClain, C.R., 1992. An overview of SeaWiFS and ocean color. NASA technical memorandum.1048. Greenbelt; Maryland.

Hopkins, J., Lucas, M., Dufau, C., Sutton, M., Stum, J., Lauret, O., Channelliere, C., 2013. Detection and variability of the Congo River plume from satellite derived sea surface temperature, salinity, ocean colour and sea level. Remote Sens. Environ. 139, 365–385. doi:10.1016/j.rse.2013.08.015

Houpert, L., Testor, P., Madron, X.D. De, Somot, S., Ortenzio, F.D., Estournel, C., Lavigne, H., 2015. Seasonal cycle of the mixed layer , the seasonal thermocline and the upper-ocean heat storage rate in the Mediterranean Sea derived from observations. Prog. Oceanogr. 132, 333–352. doi:10.1016/j.pocean.2014.11.004

Howarth, R.W., 1988. Nutrient limitation of net primary production in marine

ecosystems. Annu. Rev. Ecol. Syst. 19, 89–110. doi:10.1146/annurev.es.19.110188.000513

Hu, C., Lee, Z., Franz, B., 2012. Chlorophyll a algorithms for oligotrophic oceans: A novel approach based on three-band reflectance difference. J. Geophys. Res. Ocean. 117, 1–25. doi:10.1029/2011JC007395

Hurrell, J., Van Loon, H., 1997. Decadal variations in climate associated with the North Atlantic Oscillation. Clim. Change 36, 301–326. doi:10.1023/a:1005314315270

Hurrell, J.W., 1995. Decadal trends in the North Atlantic Oscillation: Regional Temperatures and Precipitation. Science (80-.). 269, 7–10. doi:10.1126/science.269.5224.676#_blank

Hurrell, J.W., Kushnir, Y., Visbeck, M., 2001. The North Atlantic Oscillation. Science (80-.). 603–605. doi:10.1126/science.1058761

Ignatiades, L., Gotsis-Skretas, O., Pagou, K., Krasakopoulou, E., 2009. Diversification of phytoplankton community structure and related parameters along a large-scale longitudinal east-west transect of the Mediterranean Sea. J. Plankton Res. 31, 411–428. doi:10.1093/plankt/fbn124

Ignatiades, L., Psarra, S., Zervakis, V., Pagou, K., Souvermezoglou, E., Assimakopoulou, G., Gotsis-Skretas, O., 2002. Phytoplankton size-based dynamics in the Aegean Sea (eastern Mediterranean). J. Mar. Syst. 36, 11–28. doi:10.1016/S0924-7963(02)00132-X

IOCCG, 2014. Phytoplankton Functional Types from Space. Sathyendranath, S. (ed.), Reports of the International Ocean-Colour Coordinating Group, No. 15, IOCCG, Dartmouth, Canada.

IOCCG, 2009. Remote sensing in fisheries and aquaculture. and Aquaculture. Forget, M.-H., Stuart, V. and Platt, T. (eds.), Reports of the International Ocean-Colour Coordinating Group, No. 8, IOCCG, Dartmouth, Canada.

Jacobeit, J., Jönsson, P., Bärring, L., Beck, C., Ekström, M., 2001. Zonal indices for Europe 1780-1995 and running correlations with temperature. Clim. Chang. 48, 219–241. doi:10.1023/A:1005619023045

Jassby, A.D., Platt, T., 1976. Mathematical formulation of the relationship photosynthesis and light for phytoplankton. Limnol. Oceanogr. 21, 540–547. doi:10.4319/lo.1976.21.4.0540

Ji, R., Edwards, M., MacKas, D.L., Runge, J.A., Thomas, A.C., 2010. Marine plankton phenology and life history in a changing climate: current research and future directions. J. Plankton Res. 32, 1355–1368. doi:10.1093/plankt/fbq062

Jordi, A., Basterretxea, G., Anglès, S., 2009. Influence of ocean circulation on phytoplankton biomass distribution in the Balearic Sea: Study based on Sea-viewing Wide Field-of-view Sensor and altimetry satellite data. J. Geophys. Res. 114, C11005. doi:10.1029/2009JC005301

Jumars, P.A., 1993. Concepts in Biological Oceanography. Oxford University Press.

Kahru, M., Brotas, V., Manzano-Sarabia, M., Mitchell, G.G., 2011. Are phytoplankton blooms occurring earlier in the Arctic? Glob. Chang. Biol. 17, 1733–1739. doi:10.1111/j.1365-2486.2010.02312.x

Kahru, M., Mitchell, B.G., 2001. Seasonal and nonseasonal variability of satellite-derived chlorophyll and colored dissolved organic matter concentration Current. J. Geophys. Res. 106, 2517–2529. doi:10.1029/1999JC000094

Kassi, J.-B., Racault, M.-F., Mobio, B., Platt, T., Sathyendranath, S., Raitsos, D., Affian, K., 2018. Remotely Sensing the biophysical drivers of Sardinella aurita variability in Ivorian waters. Remote Sens. 10, 785. doi:10.3390/rs10050785

Katara, I., Illian, J., Pierce, G.J., Scott, B., Wang, J., 2008. Atmospheric forcing on chlorophyll concentration in the Mediterranean. Hydrobiologia 612, 33–48. doi:10.1007/s10750-008-9492-z

Katlane, R., Nechad, B., Ruddick, K., Zargouni, F., 2011. Optical remote sensing of turbidity and total suspended matter in the Gulf of Gabes. Arab. J. Geosci. 6, 1527–1535. doi:10.1007/s12517-011-0438-9

Kavanaugh, M.T., Oliver, M.J., Chavez, F.P., Letelier, R.M., Muller-Karger, F.E., Doney, S.C., 2016. Seascapes as a new vernacular for pelagic ocean monitoring, management and conservation. ICES J. Mar. Sci. 73, 1839–1850. doi:10.1093/icesjms/fsw086

Keeling, R.F., Arne, K., Gruber, N., 2010. Ocean deoxygenation in a warming world. Ann. Rev. Mar. Sci. 2, 199–229. doi:10.1146/annurev.marine.010908.163855

Keller, M.D., Bellows, W.K., Guillard, R.R.L., 1989. Dimethyl Sulfide Production in Marine Phytoplankton, in: Saltzman, E.S., Cooper, W.J. (Eds.), Biogenic Sulfur in the Environment. American Chemical Society, pp. 167–182. doi:10.1021/bk-1989-0393.ch011

Kiørboe, T., Møhlenberg, F., riisgård, H.U., 1985. In situ feeding rates of plantonic copepods: A comparison of four methods. J. Exp. Mar. Bio. Ecol. 88, 67–81. doi:10.1016/0022-0981(85)90202-3

Kirk, J.T.O., 2011. Light & photosynthesis in aquatic ecosystems, Third. ed. Cambridge University Press.

Koeller, P., Fuentes-Yaco, C., Platt, T., Sathyendranath, S., Richards, A., Ouellet, P., Orr, D., Skúladóttir, U., Wieland, K., Savard, L., Aschan, M., 2009. Basin-scale coherence in phenology of shrimps and phytoplankton in the North Atlantic Ocean. Science 324, 791–793. doi:10.1126/science.1170987

Kohonen, T., 2001. Self-Organizing Maps. Springer-Verlag Berlin Heidelbergh.

Kohonen, T., 1997. Self-Organizing Maps (2nd ed.). Springer, Heidelberg, Germany.

Kohonen, T., 1982. Self-organized formation of topologically correct feature maps. Biol. Cybern. 43, 59–69. doi:10.1007/BF00337288

Kostadinov, T.S., Cabré, A., Vedantham, H., Marinov, I., Bracher, A., Brewin, R.J.W., Bricaud, A., Hirata, T., Hirawake, T., Hardman-Mountford, N.J., Mouw, C., Roy, S., Uitz, J., 2017. Inter-comparison of phytoplankton functional type phenology metrics

derived from ocean color algorithms and Earth System Models. Remote Sens. Environ. 190, 162–177. doi:10.1016/j.rse.2016.11.014

Kreft, H., Jetz, W., 2010. A framework for delineating biogeographical regions based on species distributions. J. Biogeogr. 37, 2029–2053. doi:10.1111/j.1365-2699.2010.02375.x

Kress, N., Herut, B., 2001. Spatial and seasonal evolution of dissolved oxygen and nutrients in the Southern Levantine Basin (western Mediterranean Sea): Chemical characterization of the water masses and inferences on the N:P ratios. Deep Sea Res. Part I 48, 2347–2372. doi:10.1016/S0967-0637(01)00022-X

Krichak, S.O., Breitgand, J.S., Gualdi, S., Feldstein, S.B., 2014. Teleconnection – extreme precipitation relationships over the Mediterranean region. Theor. Appl. Climatol. 117, 679–692. doi:10.1007/s00704-013-1036-4

Krom, M.D., Emeis, K., Cappellen, P. Van, 2010. Why is the eastern Mediterranean phosphorus limited? Prog. Oceanogr. 85, 236–244. doi:10.1016/j.pocean.2010.03.003

Krom, M.D., Groom, S., Zohary, T., 2003. The Eastern Mediterranean, in: Black, K.D., Shimmield, G.B. (Eds.), Biogeochemistry of Marine Systems. Backwell publishing, Oxford, pp. 91–122.

Krom, M.D., Kress, N., Brenner, S., Gordon, L.I., 1991. Phosphorus limitation of primary productivity in the eastern Mediterranean Sea. Limnol. Oceanogr. 36, 424–432. doi:10.4319/lo.1991.36.3.0424

Kudela, R.M., Banas, N.S., Barth, J.A., Frame, E.R., Jay, D.A., Largier, J.L., Lessard, E.J., Peterson, T.D., Wander Woude, A.J., 2008. New insights into the controls and mechanisms of the northern California Current System plankton productivity in coastal upwelling waters. Oceanography 21, 46–59. doi:10.5670/oceanog.2008.04

Lachkar, Z., Gruber, N., 2012. A comparative study of biological production in eastern boundary upwelling systems using an artificial neural network 293–308. doi:10.5194/bg-9-293-2012

Lacombe, H., Gascard, J.C., Gonella, J., Darse, L., 1981. Response of the Mediterranean to the water and energy fluxes across its surface, on seasonal and interannual scales. Oceanol. Acta 4, 247–255. doi:00121/23209/

Lacroix, G., Nival, P., 1998. Influence of meteorological variability on primary production dynamics in the Ligurian Sea (NW Mediterranean Sea) with a 1D hydrodynamic/biological model. J. Mar. Res. 16, 23–50.

Land, P.E., Shutler, J.D., Platt, T., Racault, M.F., 2014. A novel method to retrieve oceanic phytoplankton phenology from satellite data in the presence of data gaps. Ecol. Indic. 37, 67–80. doi:10.1016/j.ecolind.2013.10.008

Laufkötter, C., Vogt, M., Gruber, N., Aumont, O., Bopp, L., Doney, S.C., Dunne, J.P., Hauck, J., John, J.G., Lima, I.D., Seferian, R., Völker, C., 2016. Projected decreases in future marine export production : the role of the carbon flux through the upper ocean ecosystem. Biogeosciences 13, 4023–4047. doi:10.5194/bg-13-4023-2016

Lavender, S.J., Moufaddal, W.M., Pradhan, Y.D., 2009. Assessment of temporal shifts of chlorophyll levels in the Egyptian Mediterranean shelf and satellite detection of the Nile bloom. Egypt. J. Aquat. Res. 35, 121–135.

Lavigne, H., Civitarese, G., Gacic, M., Ortenzio, F.D., 2017. Impact of decadal reversals of the North Ionian circulation on phytoplankton phenology. Biogeosciences Discuss. 1–25. doi:10.5194/bg-15-4431-2018

Lavigne, H., D'Ortenzio, F., Migon, C., Claustre, H., Testor, P., D'Alcalà, M.R., Lavezza, R., Houpert, L., Prieur, L., 2013. Enhancing the comprehension of mixed layer depth control on the Mediterranean phytoplankton phenology. J. Geophys. Res. Ocean. 118, 3416–3430. doi:10.1002/jgrc.20251

Lavigne, H., D'Ortenzio, F., Ribera d'Alcalà, M., Claustre, H., Sauzède, R., Gacic, M., 2015. On the vertical distribution of the chlorophyll a concentration in the Mediterranean Sea: A basin-scale and seasonal approach. Biogeosciences 12, 5021–5039. doi:10.5194/bg-12-5021-2015

Laws, E.A., D'Sa, E., Naik, P., 2011. Simple equations to estimate ratios of new or export production to total production from satellite-derived estimates of sea surface temperature and primary production. Limnol. Oceanogr. Methods 9, 593–601. doi:10.4319/lom.2011.9.593

Lazzari, P., Solidoro, C., Ibello, V., Salon, S., Teruzzi, A., Béranger, K., Colella, S., Crise, A., 2012. Seasonal and inter-annual variability of plankton chlorophyll and primary production in the Mediterranean Sea: A modelling approach. Biogeosciences 9, 217–233. doi:10.5194/bg-9-217-2012

Lazzari, P., Solidoro, C., Salon, S., Bolzon, G., 2016. Spatial variability of phosphate and nitrate in the Mediterranean Sea : A modeling approach. Deep. Res. Part I 108, 39–52. doi:10.1016/j.dsr.2015.12.006

Lee, Z., Marra, J., Jane, M., Kahru, M., 2015. Estimating oceanic primary productivity from ocean color remote sensing : A strategic assessment. J. Mar. Syst. 149, 50–59. doi:10.1016/j.jmarsys.2014.11.015

Legendre, L., 1990. The significance of microalgal blooms for fisheries and for the export of particulate organic carbon in oceans. J. Plankton Res. 12, 681–699. doi:10.1093/plankt/12.4.681

Leloup, J.A., Lachkar, Z., Boulanger, J.-P., Thiria, S., 2007. Detecting decadal changes in ENSO using neural networks. Clim. Dyn. 28, 147–162. doi:10.1007/s00382-006-0173-1

Li, W.K.W., 2002. Macroecological patterns of phytoplankton in the northwestern North Atlantic Ocean. Nature 419, 154–157. doi:10.1038/nature00983.1.

Lin, J., Cao, W., Wang, G., Hu, S., 2014. Satellite-observed variability of phytoplankton size classes associated with a cold eddy in the South China Sea. Mar. Pollut. Bull. 83, 190–197. doi:10.1016/j.marpolbul.2014.03.052

Lionello, P., Malanotte-Rizzoli, P., Boscolo, R., Alpert, P., Artale, V., Li, L., Luterbacher, J., May, W., Trigo, R., Tsimpli, M., Ulbrich, U., Xoplaki, E., 2006. The Mediterranean

Climate : An overview of the main characteristics and issues, in: Lionello, P., Malanotte-Rizzoli, P., Boscolo, R. (Eds.), Developements in Earth and Environmental Sciences. Elsevier, pp. 1–21. doi:10.1016/S1571-9197(06)80003-0

Lionello, P., Scarascia, L., 2018. The relation between climate change in the Mediterranean region and global warming. Reg. Environ. Chang. 18, 1481–1493.

Liu, K.-K., Chao, S.-Y., 2000. Continental margin carbon fluxes, in: Hanson, R.B., Ducklow, H.W., Field, J.G. (Eds.), The Changing Ocean Carbon Cycle: A Midterm Synthesis of the Joint Global Ocean Flux Study. International Geosphere-Biosphere Programme Book Series, Cambridge University Press, pp. 187–239.

Liu, Y., Weisberg, R.H., 2005. Patterns of ocean current variability on the West Florida Shelf using the self-organizing map. J. Geophys. Res. 110, 1–12. doi:10.1029/2004JC002786

Liu, Y., Weisberg, R.H., Mooers, C.N.K., 2006. Performance evaluation of the self-organizing map for feature extraction. J. Geophys. Res. Ocean. 111, 1–14. doi:10.1029/2005JC003117

Liu, Y., Weisberg, R.H., Vignudelli, S., Mitchum, G.T., 2016. Patterns of the loop current system and regions of sea surface height variability in the eastern Gulf of Mexico revealed by the self-organizing maps. J. Geophys. Res. Ocean. 121, 2347–2366. doi:10.1002/2015JC011493.Received

Lleonart, J., Maynou, F., 2003. Fish stock assessments in the Mediterranean: state of the art. Sci. Mar. 67, 37–49.

Lo-Yat, A., Simpson, S.D., Meekan, M., Lecchini, D., Martinez, E., Galzin, R., 2011. Extreme climatic events reduce ocean productivity and larval supply in a tropical reef ecosystem. Glob. Chang. Biol. 17, 1695–1702. doi:10.1111/j.1365-2486.2010.02355.x

Lobanova, P., Tilstone, G.H., Bashmachnikow, I., Brotas, V., 2018. Accuracy assessment of primary production models with and without photoinhibition using Ocean-Colour Climate Change Initiative data in the north east Atlantic Ocean. Remote Sens. 10, 1–24. doi:10.3390/rs10071116

Lohrenz, S.E., Wiesenburg, D.A., DePalma, I.P., Johnsont, K.S., Gustafson, D.E., 1988. Interrelationships among primary production, chlorophyll, and environmental conditions in frontal regions of the western Mediterranean Sea. Deep Sea Res. 35, 793–810. doi:10.1016/0198-0149(88)90031-3

López-Bustins, J.-A., Sánchez- Lorenzo, A., Azorin-Molina, C., Ordóñez-López, A., 2008. Tendencias de la precipitación invernal en la fachada oriental de la Península Ibérica. EGU/AGU Sess. Earth Radiat. budget, Radiat. forcing Clim. Chang.

Lopez-Jurado, J.L., Lafuente, J.G., Pinot, J.-M., Alvarez, A., 1996. Water exchanges in the Balearic channels. Bull. l'Institut Océanographique, Monaco.

López-Sandoval, D.C., Fernández, A., Marañón, E., 2011. Dissolved and particulate primary production along a longitudinal gradient in the Mediterranean Sea. Biogeosciences 8, 815–825. doi:10.5194/bg-8-815-2011

Ludwig, W., Dumont, E., Meybeck, M., Heussner, S., 2009. River discharges of water and nutrients to the Mediterranean and Black Sea: Major drivers for ecosystem changes during past and future decades? Prog. Oceanogr. 80, 199–217. doi:10.1016/j.pocean.2009.02.001

Macias, D., Garcia-Gorriz, E., Piroddi, C., Stips, A., 2014. Biogeochemical control of marine productivity in the Mediterranean Sea during the last 50 years. Global Biogeochem. Cycles 28, 897–907. doi:10.1002/2014GB004846

Macias, D., Garcia-Gorriz, E., Stips, A., 2018. Deep winter convection and phytoplankton dynamics in the NW Mediterranean Sea under present climate and future (horizon 2030) scenarios. Sci. Rep. 22, 1–15. doi:10.1038/s41598-018-24965-0

Macias, D., Garcia-Gorriz, E., Stips, A., 2017. Major fertilization sources and mechanisms for Mediterranean Sea coastal ecosystems. Limnol. Oceanogr. 63, 897–914. doi:10.1002/lno.10677

Macias, D., Navarro, G., Echevarría, F., García, C.M., Cueto, J.L., 2007. Phytoplankton pigment distribution in the northwestern Alboran Sea and meteorological forcing: A remote sensing study. J. Mar. Res. 65, 523–543. doi:10.1357/002224007782689085

Macias, D.M., Garcia-Gorriz, E., Stips, A., 2015. Productivity changes in the Mediterranean Sea for the twenty-first century in response to changes in the regional atmospheric forcing. Front. Mar. Sci. 2, 1–13. doi:10.3389/fmars.2015.00079

Madec, G., 2008. NEMO Ocean Engine. Note du Pole de Modélisation. Institut Pierre-Simon Laplace (IPSL), France.

Maderich, V., Ilyin, Y., Lemeshko, E., 2015. Seasonal and interannual variability of the water exchange in the TUrkish Straits System estimated by modelling. Mediterr. Mar. Sci. 16, 444–459. doi:10.12681/mms.1103

Mann, K.H., Lazier, J.R.N., 1991. Dynamics of marine ecosystems: biological physical interactions in the oceans. Blackwell Scientific Publications, Boston, MA.

Margalef, R., 1974. Ecologia. Barcelona.

Marini, M., Grilli, F., Guarnieri, A., Jones, B.H., Klajic, Z., Pinardi, N., 2010. Is the southeastern Adriatic Sea coastal strip an eutrophic area? Estuar. Coast. Shelf Sci. 88, 395–406. doi:10.1016/j.ecss.2010.04.020

Mariotti, A., Pan, Y., Zeng, N., Alessandri, A., 2015. Long - term climate change in the Mediterranean region in the midst of decadal variability. Clim. Dy. doi:10.1007/s00382-015-2487-3

Mariotti, A., Struglia, M.V., Zeng, N., Lau, K.M., 2002a. The hydrological cycle in the Mediterranean region and implications for the water budget of the Mediterranean sea. J. Clim. 15, 1674–1690. doi:10.1175/1520-0442

Mariotti, A., Zeng, N., Lau, K.M., 2002b. Euro-Mediterranean rainfall and ENSO-a seasonally varying relationship. Geophys. Res. Lett. 29. doi:10.1029/2001GL014248

Marra, J., Ho, C., Trees, C.C., 2003. An algorithm for the calculation of primary productivity from remote sensing data. LDEO Tech. Rep. #LDEO-2003-1.

Marshall, J., Kushnir, Y., Battisti, D., Chang, P., Czaja, A., Robert, D., Hurrel, J., McCartney, M., Saravanan, R., Visbeck, M., 2001. Review North Atlantic Climate Variability : Phenomena , Impacts and Mechanisms. Int. J. Climatol. 21, 1863–1898. doi:10.1002/joc.693

Martin, J.H., Fitzwater, S.E., 1988. Iron deficiency limits phytoplankton growth in the north-east Pacific subarctic. Nature 331, 341–343. doi:10.1038/331341a0

Martínez-Asensio, A., Marcos, M., Tsimplis, M.N., Gomis, D., Josey, S., Jordà, G., 2014. Impact of the atmospheric climate modes on Mediterranean sea level variability. Glob. Planet. Change 118, 1–15. doi:10.1016/j.gloplacha.2014.03.007

Martinez, E., Antoine, D., D'Ortenzio, F., Gentili, B., 2012. Climate-driven basin-scaleoceanic phytoplankton. Science (80-.). 326, 1253. doi:10.1126/science.1177012

Marty, J.C., 2002. The DYFAMED time-series program (French-JGOFS). Deep. Res. Part II Top. Stud. Oceanogr. 49, 1963–1964. doi:10.1016/S0967-0645(02)00021-8

Marty, J.C., Chiavérini, J., 2010. Hydrological changes in the Ligurian Sea (NW Mediterranean, DYFAMED site) during 1995-2007 and biogeochemical consequences. Biogeosciences 7, 2117–2128. doi:10.5194/bg-7-2117-2010

Marty, J.C., Chiavérini, J., Pizay, M.D., Avril, B., 2002. Seasonal and interannual dynamics of nutrients and phytoplankton pigments in the western Mediterranean Sea at the DYFAMED time-series station (1991-1999). Deep. Res. Part II Top. Stud. Oceanogr. 49, 1965–1985. doi:10.1016/S0967-0645(02)00022-X

Mauri, E., Poulain, P.-M., Zivko, J.-Z., 2007. MODIS chlorophyll variability in the northern Adriatic Sea and relationship with forcing parameters. J. Geophys. Res. 112, 1–14. doi:10.1029/2006JC003545

Mayot, N., D'Ortenzio, F., D'Alcalà, M.R., Lavigne, H., Claustre, H., 2016. Interannual variability of the Mediterranean trophic regimes from ocean color satellites. Biogeosciences 13, 1901–1917. doi:10.5194/bg-13-1901-2016

Mayot, N., D'Ortenzio, F., Taillandier, V., Prieur, L., de Fommervault, O.P., Claustre, H., Bosse, A., Testor, P., Conan, P., 2017a. Physical and biogeochemical controls of the phytoplankton blooms in north western Mediterranean sea: A multiplatform approach over a complete annual cycle (2012–2013 DEWEX experiment). J. Geophys. Res. Ocean. 122, 9999–10019. doi:10.1002/2016JC012052

Mayot, N., Ortenzio, F.D., Uitz, J., Gentili, B., Ras, J., 2017b. Influence of the phytoplankton community structure on the spring and annual primary production in the North-Western Mediterranean Sea. J. Geophys. Res.

Mcclain, C.R., Feldman, G.C., Hooker, S.B., 2004. An overview of the SeaWiFS project and strategies for producing a climate research quality global ocean bio-optical time series. Deep Sea Res. Part II 51, 5–42. doi:10.1016/j.dsr2.2003.11.001

McGinty, N., Guðmundsson, K., Ágústsdóttir, K., Marteinsdóttir, G., 2016. Environmental and climactic effects of chlorophyll-a variability around Iceland using reconstructed satellite data field. J. Mar. Syst. 163, 31–42. doi:10.1016/j.jmarsys.2016.06.005

Mélin, F., 2016. Impact of inter-mission differences and drifts on chlorophyll-a trend estimates. Int. J. Remote Sens. 37, 2233–2251. doi:10.1080/01431161.2016.1168949

Mélin, F., Sclep, G., 2015. Band shifting for ocean color multi-spectral reflectance data. Opt. Express 23, 2262. doi:10.1364/OE.23.002262

Mélin, F., Vantrepotte, V., Chuprin, A., Grant, M., Jackson, T., Sathyendranath, S., 2017. Assessing the fitness-for-purpose of satellite multi-mission ocean color climate data records: A protocol applied to OC-CCI chlorophyll-a data. Remote Sens. Environ. 203, 139–151. doi:10.1016/j.rse.2017.03.039

Mélin, F., Vantrepotte, V., Clerici, M., D'Alimonte, D., Zibordi, G., Berthon, J.F., Canuti, E., 2011. Multi-sensor satellite time series of optical properties and chlorophyll-a concentration in the Adriatic sea. Prog. Oceanogr. 91, 229–244. doi:10.1016/j.pocean.2010.12.001

Mercado, J.M., Ramírez, T., Cortés, D., Sebastián, M., Vargas-Yáñez, M., 2005. Seasonal and inter-annual variability of the phytoplankton communities in an upwelling area of the Alborán Sea (SW Mediterranean Sea). Sci. Mar. 69, 451–465. doi:10.3989/scimar.2005.69n4451

Mihanović, H., Vilibić, I., Carniel, S., Tudor, M., Russo, A., Bergamasco, A., Bubić, N., Ljubešić, Z., Viličić, D., Boldrin, A., Malačič, V., Celio, M., Comici, C., Raicich, F., 2013. Exceptional dense water formation on the adriatic shelf in the winter of 2012. Ocean Sci. 9, 561–572. doi:10.5194/os-9-561-2013

Milliman, J.D., Farnsworth, K., 2011. River Discharge to the Coastal Ocean – A Global Synthesis. doi:10.1017/CBO9780511781247

Millot, C., 1999. Circulation in the western Mediterranean Sea. J. Mar. Syst. 20, 423–442. doi:10.1016/S0924-7963(98)00078-5

Millot, C., Taupier-Letage, I., 2005. Circulation in the Mediterranean Sea. Environ. Chem. 5, 29–66. doi:10.1007/b107143

Mobley, C.D., Boss, E., Roesler, C., 2011. Ocean optics web book.

Molinero, J.C., Ibanez, F., Nival, P., Buecher, E., Souissi, S., 2005. North Atlantic climate and northwestern Mediterranean plankton variability. Limnol. Oceanogr. 50, 1213–1220. doi:10.4319/lo.2005.50.4.1213

Montanari, A., 2012. Hydrology of the Po River: Looking for changing patterns in river discharge. Hydrol. Earth Syst. Sci. 16, 3739–3747. doi:10.5194/hess-16-3739-2012

Moon, J., Lee, K., Tanhua, T., Kress, N., Kim, I., 2016. Temporal nutrient dynamics in the Mediterranean Sea in response to anthropogenic inputs. Geophys. Res. Lett. 5243–5251. doi:10.1002/2016GL068788

Morán, X.A.G., Estrada, M., 2001. Short-term variability of photosynthetic parameters and particulate and dissolved primary production in the Alboran Sea (SW Mediterranean). Mar. Ecol. Prog. Ser. 212, 53–67.

Morán, X.A.G., Estrada, M., Gasol, J.M., Pedrós-Alió, C., 2002. Dissolved Primary

Production and the Strength of Phytoplankton ± Bacterioplankton Coupling in Contrasting Marine Regions. Microb. Ecol. 44, 217–223. doi:10.1007/s00248-002-1026-z

Morán, X.A.G., Taupier-letage, I., Vázquez-Domínguez, E., Ruiz, S., Arin, L., Raimbault, P., Estrada, M., 2001. Physical-biological coupling in the Algerian Basin (SW Mediterranean): Influence of mesoscale instabilities on the biomass and production of phytoplankton and bacterioplankton. Deep Sea Res. Part I 48, 405–437.

Morel, A., 1997. Consequences of a Synechococcus bloom upon the optical properties of oceanic (case 1) waters. Limnol. Oceanogr. 42, 1746–1754. doi:10.4319/lo.1997.42.8.1746

Morel, A., 1991. Light and marine photosynthesis: a spectral model with geochemical and climatological implications. Prog. Oceanogr. 26, 263–306. doi:10.1016/0079-6611(91)90004-6

Morel, A., 1978. Available , usable , and stored radiant energy in relation to marine photosynthesis. Deep Sea Res. 25, 673–688.

Morel, A., André, J.-M., 1991. Pigment distribution and primary production in the Western Mediterranean as derived and modeled from Coastal Zone Color Scanner observations. J. Geophys. Res. 96, 685–698. doi:10.1029/95JC00466

Morel, A., Antoine, D., Babin, M., Dandonneau, Y., 1996. Measured and modeled primary production in the northeast Atlantic (EUMELI JGOFS program): The impact of natural variations in photosynthetic parameters on model predictive skill. Deep. Res. Part I. 43, 1273–1304. doi:10.1016/0967-0637(96)00059-3

Morel, A., Berthon, J.-F., 1989. Surface pigments, algal biomass profiles, and potential production of the euphotic layer: Relationships reinvestigated in view of remote-sensing applications. Limnol. Oceanogr. 34, 1545–1562. doi:10.4319/lo.1989.34.8.1545

Morel, A., Gentili, B., Chami, M., Ras, J., 2006. Bio-optical properties of high chlorophyll Case 1 waters and of yellow-substance-dominated Case 2 waters. Deep. Res. Part I Oceanogr. Res. Pap. 53, 1439–1459. doi:10.1016/j.dsr.2006.07.007

Morel, A., Huot, Y., Gentili, B., Werdell, P.J., Hooker, S.B., Franz, B.A., 2007. Examining the consistency of products derived from various ocean color sensors in open ocean (Case 1) waters in the perspective of a multi-sensor approach. Remote Sens. Environ. 111, 69–88. doi:10.1016/j.rse.2007.03.012

Morel, A., Maritorena, S., 2001. Bio-optical properties of oceanic waters: A reappraisal. J. Geophys. Res. 106, 7163–7180. doi:10.1029/2000JC000319

Morel, A., Prieur, L., 1977. Analysis of variations in ocean color. Limnol. Oceanogr. 22, 709–722. doi:10.4319/lo.1977.22.4.0709

Moutin, T., Raimbault, P., 2002. Primary production , carbon export and nutrients availability in western and eastern Mediterranean Sea in early summer 1996 (MINOS cruise). J. Mar. Syst. 34, 273–288. doi:10.1016/S0924-7963(02)00062-3

Mouw, C.B., Barnett, A., Mckinley, G.A., Gloege, L., Pilcher, D., 2016. Phytoplankton size impact on export flux in the global ocean. AGU Publ. Glob. Biochem. cycles 1542–1562. doi:10.1002/2015GB005355.Received

Mozetič, P., Solidoro, C., Cossarini, G., Socal, G., Precali, R., Francé, J., Bianchi, F., De Vittor, C., Smodlaka, N., Fonda Umani, S., 2009. Recent trends towards oligotrophication of the northern adriatic: Evidence from chlorophyll a time series. Estuaries and Coasts 33, 362–375. doi:10.1007/s12237-009-9191-7

Muller-Karger, F.E., Varela, R., Thunell, R., Luerssen, R., Hu, C., Walsh, J.J., 2005. The importance of continental margins in the global carbon cycle. Geophys. Res. Lett. 32, 1–4. doi:10.1029/2004GL021346

Nair, A., Sathyendranath, S., Platt, T., Morales, J., Stuart, V., Forget, M.-H., Devred, E., Bouman, H., 2008. Remote sensing of phytoplankton functional types. Remote Sens. Environ. 112, 3366–3375. doi:10.1016/j.rse.2008.01.021

NASA, 1986. Report of the EOS data panel, Earth Observating system. Data and Information System. Technical memorandum 87777.

Navarro, G., Alvain, S., Vantrepotte, V., Huertas, I.E., 2014. Identification of dominant phytoplankton functional types in the Mediterranean Sea based on a regionalized remote sensing approach. Remote Sens. Environ. 152, 557–575. doi:10.1016/j.rse.2014.06.029

Nittis, K., Lascaratos, 1999. Intermediate water formation in the Levantine Sea: The response to interannual variability of atmospheric forcing, in: Malanotte-rizzoli, P., Eremeevm, V.N. (Eds.), The Eastern Mediterranean as a Laboratory Basin for the Assessment of Contrasting Ecosystems. NATO Science Series (Series 2: Environmental Security), Vol 51. Springer, Dordrecht. doi:10.1007/978-94-011-4796-5

Nixon, S.W., 2004. The artificial Nile: The Aswan high dam blocked and diverted nutrients and destroyed a Mediterranean fishery, but human activities may have revived it. Am. Sci. 92, 158–165. doi:NATURE DOI: 10.1038/325803a0

Nixon, S.W., 2003. Replacing the Nile : Are anthropogenic nutrients providing the fertility once brought to the Mediterranean by a Great River? AMBIO A J. Hum. Environ. 32, 30–39. doi:10.1579/0044-7447-32.1.30

Nykjaer, L., 2009. Mediterranean Sea surface warming 1985 – 2006. Clim. Resea 39, 11–17. doi:10.3354/cr00794

O'Reilly, J., Sherman, K., 2016. Chapter 5.1. Primary productivity patterns and trends, Large Marine Ecosystems: Status and Trends. IOC-UNESCO and UNEP. United Nations Environment Programme, Nairobi.

O'Reilly, J.E., Maritorena, S., Mitchell, B.G., Siegel, D. a., Carder, K.L., Garver, S. a., Kahru, M., McClain, C., 1998a. Ocean color chlorophyll algorithms for SeaWiFS. J. Geophys. Res. 103, 24937. doi:10.1029/98JC02160

O'Reilly, J.E., Maritorena, S., Mitchell, B.G., Siegel, D.A., Carder, K.L., Garver, S.A., Kahru, M., McClain, C.R., 1998b. Ocean color chlorophyll algorighms for SeaWiFS. J.

Geophys. Res. 103, 24937–24953. doi:10.1029/98JC02160

O'Reilly, J.E., Maritorena, S., O'Brien, M., Siegel, D., Toole, D., Menzies, D., Smith, R., Mueller, J.L., Mitchell, G., Kahru, M., Chavez, F., Strutton, P., Cota, G., McClain, C., Carder, K., Muller-Karger, F., Harding, L., Magnuson, A., Phinney, D., Moore, G., Aiken, J., Arrigo, K., Letelier, R., Culver, M., 2000. SeaWiFS postlaunch technical report series. NASA Tech. Memo. 11, 1–49.

Oguz, T., Macias, D., Garcia-Lafuente, J., Pascual, A., Tintore, J., 2014. Fueling plankton production by a meandering frontal jet: A case study for the Alboran sea (Western Mediterranean). PLoS One 9. doi:10.1371/journal.pone.0111482

Ozer, T., Gertman, I., Kress, N., Silverman, J., Herut, B., 2017. Interannual thermohaline (1979–2014) and nutrient (2002–2014) dynamics in the Levantine surface and intermediate water masses, SE Mediterranean Sea. Glob. Planet. Change 151, 60–67. doi:10.1016/j.gloplacha.2016.04.001

Pace, M.L., Knauer, G.A., Karl, D.M., Martin, J.H., 1987. Primary production, new production and vertical flux in the eastern Pacific Ocean. Lett. to Nat. 325.

Paerl, H. w., Willey, J.D., Go, M., Peierls, B.L., Pinckney, J.L., Fogel, M.L., 1999. Rainfall stimulation of primary production in western Atlantic Ocean waters : roles of different nitrogen sources and CO-limiting nutrients. Mar. Ecol. Prog. Ser. 176, 205–214.

Pagano, M., Gaudy, R., Thibault, D., Lochet, F., 1993. Vertical migrations and feeding rhythms of mesozooplanktonic organisms in the Rhône River Plume Area (North-west Mediterranean Sea). Estuar. Coast. Shelf Sci. doi:10.1006/ecss.1993.1055

Palanques, A., García-Ladona, E., Gomis, D., Martín, J., Marcos, M., Pascual, A., Puig, P., Gili, J.M., Emelianov, M., Monserrat, S., Guillén, J., Tintoré, J., Segura, M., Jordi, A., Ruiz, S., Basterretxea, G., Font, J., Blasco, D., Pagès, F., 2005. General patterns of circulation, sediment fluxes and ecology of the Palamós (La Fonera) submarine canyon, northwestern Mediterranean. Prog. Oceanogr. 66, 89–119. doi:10.1016/j.pocean.2004.07.016

Palutikof, J.P., 2003. Analysis of Mediterranean Climate Data: Measured and Modelled, in: Bolle, H.J. (Ed.), Mediterranean Climate: Variability and Trends. Springer-Verlag Berlin Heidelbergh. doi:10.1007/978-3-642-55657-9_6

Park, M.G., Yih, W., Coats, D.W., 2004. Parasites and phytoplankton, with special emphasis on dinoflagellate infections. J. Eukaryot. Microbiol. 51, 145–155. doi:10.1111/j.1550-7408.2004.tb00539.x

Pasqueron De Fommervault, O., D'Ortenzio, F., Magnin, A., Serra, R., Migon, C., Claustre, H., Lavigne, H., Ribera d' Alcala, M., Prieur, L., Taillandier, V., Schmechtig, C., Poteau, A., Leymarie, E., Dufour, A., Besson, F., Obolensky, G., 2015. Seasonal variability of nutrient concentrations in the Mediterranean Sea: Contribution of Bio-Argo floats. J. Geophys. Res. Ocean. 120, 8528–8550. doi:10.1002/2015JC011103.Received

Pastor, F., Valiente, J.A., Luis Palau, J., 2017. Sea surface temperature in the Mediterranean: Trends and apatial patterns (1982 – 2016). Pure Appl. Geophys.

doi:10.1007/s00024-017-1739-z

Pauly, D., Christensen, V., 1995. Primary production required to sustain global fisheries. Nature 374, 255–257. doi:10.1038/374255a0

Pauly, D., Christensen, V., Guénette, S., Pitcher, T.J., Sumaila, U.R., Walters, C.J., Watson, R., Zeller, D., 2002. Towards sustainability in sorld fisheries. Nature 418, 689–695. doi:10.1038/nature01017

Pinardi, N., Zavatarelli, M., Arneri, E., Crise, A., Ravaioli, M., 2004. Chapter 32.The physical, sedimentary and ecological structure and variability of shelf areas in the Mediterranean Sea (27,S), in: Robinson, A.R., Brink, K.H. (Eds.), The Sea. The Global Coastal Ocean. Vol. 14 Part B. pp. 1243–1272.

Pinot, J., Ganachaud, A., 1999. The role of winter intermediate waters in the spring-summer circulation of the Balearic Sea 1. Hydrography andinverse box modeling. J. Geophys. Res. 104. doi:10.1029/1999JC900202

Pinot, J., Tintoré, J., Lopez-jurado, J.L., Fernandez de Puelles, M.L., Jansa, J., 1995. Three-dimensional circulation of a mesoscale eddy / front system and its biological implications. Oceanol. Acta 18, 389–400.

Pitarch, J., Colella, S., Brando, V.E., Volpe, G., 2016. Quality Information Docuent For Ocean Colour Mediterranean and Black Sea Observation Product (CMEMS-OC-QUID-009-038to045-071-073-078-079-095-096, dated on 04/04/2016).

Platt, T., 1986. Primary production of the ocean water column as a function of surface light intensity: Algorithms for remote sensing. Deep Sea Res. 33, 149–163. doi:10.1016/0198-0149(86)90115-9

Platt, T., Caverhill, C., Sathyendranath, S., 1991. Basin-scale estimates of oceanic primary production by remote sensing: The north Atlantic. J. Geophys. Res. 96. doi:10.1029/91JC01118

Platt, T., Fuentes-Yaco, C., Frank, K.T., 2003. Spring algal bloom and larval fish survival. Nature 423, 398–399. doi:10.1038/423398a

Platt, T., Gallegos, C.L., Harrison, W.G., 1980. Photoinhibition of photosynthesis in natural assemblages of marine phytoplankton. J. Mar. Res. 38.

Platt, T., Jassby, A.D., 1976. The relationship between photosynthesis and light for natural assemblages of coastal marine phytoplankton. J. Phycol. 12, 421–430. doi:10.1111/j.1529-8817.1976.tb02866.x

Platt, T., Sathyendranath, S., 2008. Ecological indicators for the pelagic zone of the ocean from remote sensing. Remote Sens. Environ. 112, 3426–3436. doi:10.1016/j.rse.2007.10.016

Platt, T., Sathyendranath, S., 1993. Estimators of primary production for interpretation of remotely sensed data on ocean color. J. Geophys. Res. 98, 14,561-14,576. doi:10.1029/93JC01001

Platt, T., Sathyendranath, S., 1988. Oceanic primary production: Estimation by remote sensing at local and regional scales. Science (80-.). 241, 1613–1620.

doi:10.1126/science.241.4873.1613

Platt, T., White III, G.N., Zhai, L., Sathyendranath, S., Roy, S., 2009. The phenology of phytoplankton blooms: Ecosystem indicators from remote sensing. Ecol. Modell. 220, 3057–3069. doi:10.1016/j.ecolmodel.2008.11.022

Poloczanska, E.S., Brown, C.J., Sydeman, W.J., Kiessling, W., Schoeman, D.S., Moore, P.J., Brander, K., Bruno, J.F., Buckley, L.B., Burrows, M.T., Duarte, C.M., Halpern, B.S., Holding, J., Kappel, C. V., O'Connor, M.I., Pandolfi, J.M., Parmesan, C., Schwing, F., Thompson, S.A., Richardson, A.J., 2013. Global imprint of climate change on marine life. Nat. Clim. Chang. 3, 919–925. doi:10.1038/nclimate1958

Polovina, J.J., Mitchum, G.T., Evans, G.T., 1995. Decadal and basin-scale variation in mixed layer depth and the impact on biological production in the Central and North Pacific, 1960-88. Deep. Res. Part I 42, 1701–1716. doi:10.1016/0967-0637(95)00075-H

Pomeroy, L.R., 1974. The ocean's food web, a changing paradigm. Bioscience 24, 499–504. doi:10.2307/1296885

Pozo-Vazquez, D., Esteban-Parra, M.J., Rodrigo, F.S., Castro-Díez, Y., 2001. The Association between ENSO and winter atmospheric circulation and temperature in the north Atlantic region. J. Clim. 14, 3408–3420.

Psarra, S., Tselepides, A., Ignatiades, L., 2000. Primary productivity in the oligotrophic Cretan Sea (NE Mediterranean): Seasonal and interannual variability. Prog. Oceanogr. 46, 187–204. doi:10.1016/S0079-6611(00)00018-5

Pugnetti, A., Bazzoni, A.M., Beran, A., Aubry, F.B., Camatti, E., Celussi, M., Coppola, J., Crevatin, E., Negro, P. Del, Paoli, A., 2008. Changes in biomass structure and trophic status of the plankton communities in a highly dynamic ecosystem (Gulf of Venice , Northern Adriatic Sea). Mar. Ecol. 29, 367–374. doi:10.1111/j.1439-0485.2008.00237.x

Pujo-Pay, M., Conan, P., Joux, F., Oriol, L., Naudin, J.J., Cauwet, G., 2006. Impact of phytoplankton and bacterial production on nutrient and DOM uptake in the Rhône River plume (NW Mediterranean). Mar. Ecol. Prog. Ser. 315, 43–54. doi:10.3354/meps315043

Pujol, M.I., Larnicol, G., 2005. Mediterranean sea eddy kinetic energy variability from 11 years of altimetric data. J. Mar. Syst. 58, 121–142. doi:10.1016/j.jmarsys.2005.07.005

Racault, M.F., Le Quéré, C., Buitenhuis, E., Sathyendranath, S., Platt, T., 2012. Phytoplankton phenology in the global ocean. Ecol. Indic. 14, 152–163. doi:10.1016/j.ecolind.2011.07.010

Racault, M.F., Platt, T., Sathyendranath, S., Ağirbaş, E., Martinez Vicente, V., Brewin, R., 2014a. Plankton indicators and ocean observing systems: Support to the marine ecosystem state assessment. J. Plankton Res. 36, 621–629. doi:10.1093/plankt/fbu016

Racault, M.F., Raitsos, D.E., Berumen, M.L., Brewin, R.J.W., Platt, T., Sathyendranath, S., Hoteit, I., 2015. Phytoplankton phenology indices in coral reef ecosystems:

Application to ocean-color observations in the Red Sea. Remote Sens. Environ. 160, 222–234. doi:10.1016/j.rse.2015.01.019

Racault, M.F., Sathyendranath, S., Brewin, R.J.W., Raitsos, D.E., Jackson, T., Platt, T., 2017a. Impact of El Niño variability on oceanic phytoplankton. Front. Mar. Sci. 4. doi:10.3389/fmars.2017.00133

Racault, M.F., Sathyendranath, S., Menon, N., Platt, T., 2017b. Phenological responses to ENSO in the global oceans. Surv. Geophys. 38, 277–293. doi:10.1007/s10712-016-9391-1

Racault, M.F., Sathyendranath, S., Platt, T., 2014b. Impact of missing data on the estimation of ecological indicators from satellite ocean-colour time-series. Remote Sens. Environ. 152, 15–28. doi:10.1016/j.rse.2014.05.016

Rahav, E., Herut, B., Levi, A., Mulholland, M.R., Berman-Frank, I., 2013. Springtime contribution of dinitrogen fixation to primary production across the Mediterranean Sea. Ocean Sci. 9, 489–498. doi:10.5194/os-9-489-2013

Raicich, F., Malacic, V., Celio, M., Giaiotti, D., Cantoni, C., Colucci, R.R., Cermelj, B., Pucillo, A., 2013. Extreme air-sea interactions in the Gulf of Trieste (North Adriatic) during the strong Bora event in winter 2012. J. Geophys. Res. Ocean. 118, 5238–5250. doi:10.1002/jgrc.20398

Redfield, A.C., 1934. On the proportions of organic derivatives in sea water and their relation to the composition of plankton. James Johnstone Meml. Vol. James John, 176–192.

Reygondeau, G., Guieu, C., Benedetti, F., Irisson, J., Ayata, S., Gasparini, S., Koubbi, P., 2017. Biogeochemical regions of the Mediterranean Sea : an objective multidimensional and multivariate environmental approach now at : Nippon Foundation-Nereus Program and Changing Ocean Research Unit , Institute. Prog. Oceanogr. 151, 138–148. doi:10.1016/j.pocean.2016.11.001

Richardson, A.J., Risi En, C., Shillington, F.A., 2003. Using self-organizing maps to identify patterns in satellite imagery. Prog. Oceanogr. 59, 223–239. doi:10.1016/j.pocean.2003.07.006

Rixen, M., Beckers, J.M., Levitus, S., Antonov, J., Boyer, T., Maillard, C., Fichaut, M., Balopoulos, E., Iona, S., Dooley, H., Garcia, M.J., Manca, B., Giorgetti, A., Manzella, G., Mikhailov, N., Pinardi, N., Zavatarelli, M., 2005. The western Mediterranean deep water: A proxy for climate change. Geophys. Res. Lett. 32, 1–4. doi:10.1029/2005GL022702

Robinson, A.R., Golnaraghi, M., 1993. The physical and dynamical oceanography of the Mediterranean Sea, Ocean processes in climate dynamics: Global and Mediterranean examples. Kluwer Academic Publishers, Proceedings of the 4th National Symposium on Oceanography and Fisheries, Rhodes Isl, (Greece), 26-29 April 1993, pp. 9-13.

Robinson, A.R., Leslie, W.G., Theocharis, A., Lascaratos, A., 2001. Mediterranean Sea circulation, in: Indira (Ed.), Encyclopedia of Ocean Sciences: Second Edition. pp. 710–

725. doi:10.1016/B978-012374473-9.00376-3

Rodellas, V., Garcia-orellana, J., Masqué, P., Feldman, M., Weinstein, Y., 2015. Submarine groundwater discharge as a major source of nutrients to the Mediterranean Sea. Pnas 112, 3926–3930. doi:10.1073/pnas.1419049112

Rodó, X., Baert, E., Comin, F.A., 1997. Variations in seasonal rainfall in Southern Europe during the present century: Relationships with the North Atlantic Oscillation and the El Niño-Southern Oscillation. Clim. Dyn. 13, 275–284. doi:10.1007/s003820050165

Ropelewski, C.F., Halpert, M.S., 1997. Global and regional precipitation patterns associated with the El Niño / Southern Oscillation. Mon. Weaterh Rev. Am. Meteorol. Soc. 115, 1606–1626. doi:10.1175/1520-0493

Rossi, V., Ser-giacomi, E., López, C., Hernández-garcía, E., 2014. Hydrodynamic provinces and oceanic connectivity from a transport network help designing marine reserves. Geophys. Res. Lett. 2883–2891. doi:10.1002/2014GL059540.Received

Rost, B., Riebesell, U., 2004. Coccolithophores and the biological pump: responses to environmental changes, in: Thierstein, H.R., Yound, J.R. (Eds.), Coccolithophores: From Molecular Processes to Global Impacts. Springer, Berlin, pp. 99–125. doi:10.1007/978-3-662-06278-4_5

Rousseaux, C.S., Gregg, W.W., 2014. Interannual Variation in phytoplankton primary production at a global scale. Remote Sens. 6, 1–19. doi:10.3390/rs6010001

Ryan, J., 2008. Crop nutrients for sustainable agricultural production in the drought-stressed mediterranean region. J. Agric. Sci. Technol. 10, 295–306. doi:10.1.1.885.2917

Saba, V.. S., Friedrichs, M.A.M., Antoine, D., Armstrong, R.A., Asanuma, I., Behrenfeld, M.J., Ciotti, A.M., Dowell, M., Hoepffner, N., Hyde, K.J.W., Ishizaka, J., Kameda, T., Marra, J., Félin, F., Morel, A., O'Reilly, J., Scardi, M., Smith Jr., W.O., Smyth, T.J., Tang, S., Uitz, J., Waters, K., Westberry, T.K., 2011. An evaluation of ocean color model estimates of marine primary productivity in coastal and pelagic regions across the globe. Biogeosciences 8, 489–503. doi:10.5194/bg-8-489-2011

Sabatés, A., Olivar, M.P., Salat, J., Palomera, I., Alemany, F., 2007. Physical and biological processes controlling the distribution of fish larvae in the NW Mediterranean. Prog. Oceanogr. 74, 355–376. doi:10.1016/j.pocean.2007.04.017

Sakalli, A., 2017. Sea surface temperature change in the mediterranean sea under climate change: A linear model for simulation of the sea surface temperature up to 20100. Appl. Ecol. Environ. Res. doi:10.15666/aeer/1501

Salmi, T., Määttä, A., Anttila, P., Ruoho-Airola, T., Amnell, T., 2002. Detecting trends of annual values of atmospheric pollutants by the Mann-Kendall test and Sen's Solpe estimates the excel template application MAKESENS. Finnish Meteorol. Institute, Air Qual. Res. 31.

Sammari, C., Koutitonsky, V.G., Moussa, M., 2006. Sea level variability and tidal resonance in the Gulf of Gabes, Tunisia. Cont. Shelf Res. 26, 338–350. doi:10.1016/j.csr.2005.11.006

Sammartino, M., Di Cicco, A., Marullo, S., Santoleri, R., 2015. Spatio-temporal variability of micro-, nano- and pico-phytoplankton in the Mediterranean Sea from satellite ocean colour data of SeaWiFS. Ocean Sci. 11, 759–778. doi:10.5194/os-11-759-2015

Sanchez-Lorenzo, A., Enriquez-Alonso, A., Calbó, J., González, J.A., Wild, M., Folini, D., Norris, J.R., Vicente-Serrano, S.M., 2017. Fewer clouds in the Mediterranean: Consistency of observations and climate simulations. Sci. Rep. 7, 1–10. doi:10.1038/srep41475

Sannino, G., Herrmann, M., Carillo, A., Rupolo, V., Ruggiero, V., Artale, V., Heimbach, P., 2009. An eddy-permitting model of the Mediterranean Sea with a two-way grid refinement at the Strait of Gibraltar. Ocean Model. 30, 56–72. doi:10.1016/j.ocemod.2009.06.002

Santoreli, R., Volpe, G., Salvatore, M., Buongiorno Nardelli, B., 2008. Open Waters Optical Remote Sensing of the Mediterranean Sea, in: Barale, V., Gade, M. (Eds.), Remote Sensing of the European Seas. Springer, p. 513. doi:10.1007/978-1-4020-6772-3

Sarmiento, J.L., Thiele, G., Key, R.M., Moore, W.S., 1990. Oxygen and nitrate new production and remineralization in the north Atlantic subtropical gyre. J. Geophys. Res. 95, 18,303-18,315.

Sarthou, G., Timmermans, K.R., Blain, S., Tréguer, P., 2005. Growth physiology and fate of diatoms in the ocean: A review. J. Sea Res. 53, 25–42. doi:10.1016/j.seares.2004.01.007

Sathyendranath, S., Brewin, R.J.W., Jackson, T., Mélin, F., Platt, T., 2017. Ocean-colour products for climate-change studies: What are their ideal characteristics? Remote Sens. Environ. doi:doi.org/10.1016/j.rse.2017.04.017

Sathyendranath, S., Krasemann, H., 2014. Ocean Colour Climate Change Initiative (OC - CCI) - Phase One, Climate Assessment Report (CAR). Available online at: http://www.esa-oceancolour-cci.org/?q=documents.

Sathyendranath, S., Platt, T., 2007. Spectral effects in bio-optical control on the ocean system. Oceanologia 49: 5-39. Oceanologia 49, 5–39.

Sathyendranath, S., Platt, T., 2001. Primary production distribution. Encycl. Ocean Sci. Vol. 4. doi:10.1016/B978-012374473-9.00204-6

Sathyendranath, S., Watts, L., Devred, E., Platt, T., Caverhill, C., Maass, H., 2004. Discrimination of diatoms from other phytoplankton using ocean-colour data. Mar. Ecol. Prog. Se 272, 59–68. doi:10.3354/meps272059

Schmoker, C., Hernández-León, S., Calbet, A., 2013. Microzooplankton grazing in the oceans: Impacts, data variability, knowledge gaps and future directions. J. Plankton Res. 35, 691–706. doi:10.1093/plankt/fbt023

Schmoker, C., Thor, P., Hernández-León, S., Hansen, B., 2011. Feeding, growth and metabolism of the marine heterotrophic dinoflagellate Gyrodinium dominans. Aquat. Microb. Ecol. 65, 65–73. doi:10.3354/ame01533

Schowengerdt, R.A., 2007. Remote Sensing. Models and methods for image processing,

Thirid. ed. Academic Press.

Schroeder, K., Chiggiato, J., Bryden, H.L., Borghini, M., Ben Ismail, S., 2016. Abrupt climate shift in the Western Mediterranean Sea. Sci. Rep. 6, 1–7. doi:10.1038/srep23009

Schroeder, K., Chiggiato, J., Josey, S.A., Borghini, M., Aracri, S., Sparnocchia, S., 2017. Rapid response to climate change in a marginal sea. Sci. Rep. 7, 1–7. doi:10.1038/s41598-017-04455-5

Schroeder, K., Josey, S.A., Herrmann, M., Grignon, L., Gasparini, G.P., Bryden, H.L., 2010. Abrupt warming and salting of the Western Mediterranean Deep Water after 2005 : Atmospheric forcings and lateral advection. J. Geophys. Res. 115, 1–18. doi:10.1029/2009JC005749

Schroeder, K., Ribotti, A., Borghini, M., Sorgente, R., Perilli, A., Gasparini, G.P., 2008. An extensive western Mediterranean deep water renewal between 2004 and 2006. Geophys. Res. Lett. 35, 1–7. doi:10.1029/2008GL035146

Sempéré, R., Charrière, B., Van Wambecke, F., Cauwet, G., 2000. Carbon inputs of the Rhône River to th Mediterranean Sea: Biogeochemical implications. Global Biogeochem. Cycles 14, 669–681.

Sen, P.K., 1968. Estimates of the regression coefficient based on Kendall ' s Tau Pranab Kumar Sen. J. Am. Stat. Assoc. 63, 1379–1389.

Severin, T., Conan, P., Madron, X.D. De, Houpert, L., Oliver, M.J., Oriol, L., Caparros, J., Ghiglione, J.F., Pujo-pay, M., 2014. Deep-Sea Research I Impact of open-ocean convection on nutrients , phytoplankton biomass and activity. Deep. Res. Part I 94, 62–71. doi:10.1016/j.dsr.2014.07.015

Shaltout, M., Omstedt, A., 2014. Recent sea surface temperature trends and future scenarios for the Mediterranean Sea. Oceanologia 56, 411–443. doi:10.5697/oc.56-3.411

Shaman, J., Tziperman, E., 2007. Summertime ENSO – North African – Asian Jet teleconnection and implications for the Indian monsoons. Geophys. Res. Lett. 34, 1–7. doi:10.1029/2006GL029143

Shevyrnogov, A., Vysotskaya, G., 2006. Spatial distribution of chlorophyll concentration seasonal dynamics types in the ocean based on the autocorrelation analysis of SeaWiFS data. Adv. Sp. Res. 38, 2176–2181. doi:10.1016/j.asr.2006.03.034

Shi, W., Wang, M., 2007. Observations of a Hurricane Katrina-induced phytoplankton bloom in the Gulf of Mexico. Geophys. Res. Lett. 34, 1–5. doi:10.1029/2007GL029724

Shiskin, J., 1978. Seasonal adjustment of sensitive indicators, in: Zeller, A. (Ed.), Seasonal Analysis of Economic Time Series. US Department of Commerce, Bureau of the Census, pp. 97–103.

Sieburth, J.M., Smetacek, V., Lenz, J., 1978. Pelagic ecosystem structure: Heterotrophic compartments of the plankton and their relationship to plankton size fractions. Limnol. Ocean. 23, 1256–1263.

Siegel, D.A., Buesseler, K.O., Behrenfeld, M.J., Benitez-nelson, C.R., Boss, E., Brzezinski, M.A., Burd, A., Carlson, C.A., Asaro, E.A.D., Doney, S.C., Perry, M.J., Stanley, R.H.R., Steinberg, D.K., 2016. Prediction of the export and fate of global ocean net primary production : The EXPORTS science plan. Front. Mar. Sci. 3, 1–10. doi:10.3389/fmars.2016.00022

Siegel, D.A., Doney, S.C., Yoder, J.A., 2002. The North Atlantic spring phytoplankton bloom and Sverdrup's critical depth hypothesis, Science. doi:10.1126/science.1069174

Simpson, J.H., 1997. Physical processes in the ROFI regime. J. Mar. Syst. 12, 3–15. doi:10.1016/S0924-7963(96)00085-1

Simpson, J.H., Bos, W.G., Schirmer, F., Souza, A.J., Rippeth, T.P., Jones, S.E., Hydes, D., 1993. Periodic stratification in the Rhine ROFI in the North Sea. Oceanol. Acta 16, 23–32.

Siokou-Frangou, I., Christaki, U., Mazzocchi, M.G., Montresor, M., Ribera d'Alcalà, M., Vaqué, D., Zingone, A., 2010. Plankton in the open Mediterranean Sea : a review. Biogeosciences 1, 1543–1586. doi:10.5194/bg-7-1543-2010

Skliris, N., Sofianos, S., Gkanasos, A., Mantziafou, A., Vervatis, V., Axaopoulos, P., Lascaratos, A., 2012. Decadal scale variability of sea surface temperature in the Mediterranean Sea in relation to atmospheric variability. Ocean Dyn. 62, 13–30. doi:10.1007/s10236-011-0493-5

Skoulikidis, N.T., Economou, A.N., Gritzalis, K.C., Zogaris, S., 2009. Rivers of the Balkans, in: Rivers of Europe. Elsevier, pp. 421–466. doi:10.1016/B978-0-12-369449-2.00011-4

Smetacek, V., Cloern, J.E., 2008. Oceans - On phytoplankton trends. doi:10.1126/science.1151330

Smith, R.C., Baker, K.S., 1978. The bio-optical state of ocean waters and remote sensing. Limnol. Oceanogr. 23, 247–259. doi:10.4319/lo.1978.23.2.0247

Smith, R.C., Eppley, R.W., Baker, K.S., 1982. Correlation of primary production as measured aboard ship in southern California coastal waters and as estimated from satellite shlorophyll images. Mar. Biol. 88.

Smith, S.V., Hollibaugh, J.T., 1993. Coastal Metabolism and the Oceanic Organic Carbon Balance. Rev. Geophys. 31, 75–89.

Smyth, T.J., Tilstone, G.H., Groom, S.B., 2005. Integration of radiative transfer into satellite models of ocean primary production. J. Geophys. Res. Ocean. 110, 1–11. doi:10.1029/2004JC002784

Sokolov, S., Rintoul, S.R., 2007. On the relationship between fronts of the Antarctic Circumpolar Current and surface chlorophyll concentrations in the Southern Ocean. J. Geophys. Res. 112, 1–17. doi:10.1029/2006JC004072

Solé, J., Ballabrera-Poy, J., Macías, D., Catalán, I.A., 2016. The role of ocean velocity in chlorophyll variability. A modelling study in the Alboran Sea. Sci. Mar. 80, 249–256. doi:10.3989/scimar.04290.04A

Šolić, M., Krstulović, N., Vilibić, I., Kušpilić, G., Šestanović, S., Šantić, D., Ordulj, M., 2008. The role of water mass dynamics in controlling bacterial abundance and production in the middle Adriatic Sea. Mar. Environ. Res. 65, 388–404. doi:10.1016/j.marenvres.2008.01.004

Solidoro, C., Bandelj, V., Barbieri, P., Cossarini, G., Umani, S.F., 2007. Understanding dynamic of biogeochemical properties in the northern Adriatic Sea by using self-organizing maps and k-means clustering. J. Geophys. Res. 112, 1–13. doi:10.1029/2006JC003553

Somot, S., Houpert, L., Sevault, F., Testor, P., Bosse, A., Taupier, I., Marie, L., Bouin, N., Waldman, R., Cassou, C., Sanchez, E., Xavier, G., Madron, D. De, Adloff, F., Nabat, P., Herrmann, M., 2018. Characterizing , modelling and understanding the climate variability of the deep water formation in the North - Western Mediterranean Sea. Clim. Dyn. 51, 1179–1210. doi:10.1007/s00382-016-3295-0

Sournia, A., 1973. La production primaire planctonique en Méditerranée: Essai de mise à jour. Bulletin Etude en Commun de la Méditerranée, 5, 128pp.

Sournia, A., Chétiennot-Dinet, Ricard, M., 1991. Marine phytoplankton : how many species in the world ocean? J. Plankton Res. 13, 1093–1099.

Spalding, M.D., Fox, H.E., Allen, G.R., Davidson, N., Ferdaña, Z.A., Finlayson, M.A.X., Halpern, B.S., Jorge, M.A., Lombana, A.L., Lourie, S.A., Martin, K.D., Manus, M.C., Molnar, J., Recchia, C.A., Robertson, J., 2007. Marine ecoregions of the world: A bioregionalization of coastal and shelf areas. Bioscience 57, 573–583.

Stambler, N., 2014. The Mediterranean Sea – Primary Productivity, in: S. Goffredo and Z. Dubinsky (Ed.), The Mediterranean Sea: Its History and Present Challenges. Springer, pp. 113–121. doi:10.1007/978-94-007-6704-1

Steele, J.H. (Ed.), 1978. Spatial pattern in plankton communities. NATO Conference series. Series IV: Marine Sciences. Springer Science + Business Media, LLC.

Steinberg, D.K., Landry, M.R., 2017. Zooplankton and the Ocean Carbon Cycle. Ann. Rev. Mar. Sci. doi:10.1146/annurev-marine-010814-015924

Stenseth, N.C., Ottersen, G., Hurrell, J.W., Mysterud, A., Lima, M., Chan, K., Yoccoz, N.G., Bjørn, A., 2003. Studying climate effects on ecology through the use of climate indices : the North Atlantic Oscillation , El Niño Southern Oscillation and beyond. Proc. R. Soc. London 270, 2087–2096. doi:10.1098/rspb.2003.2415

Strub, P.T.E.D., James, C., Thomas, A.C., Abbott, R., 1990. Seasonal and nonseasonal variability of satellite-derived surface pigment concentration in the California current. J. Geophys. Res. 95, 501–530.

Struglia, M.V., Mariotti, A., Filograsso, A., 2004. River discharge into the Mediterranean Sea: Climatology and aspects of the observed variability. J. Clim. 17, 4740–4751. doi:10.1175/JCLI-3225.1

Subramaniam, A., Carpenter, E.J., Falkowski, P.G., 1999. Bio-optical properties of the marine diazotrophic cyanobacteria Trichodesmium spp. II. A reflectance model for remote sensing. Limnol. Oceanogr. 44, 618–627.

Suthers, I.M., Rissik, D., 2009. Plankton. A guide to their ecology and monitoring for water quality. CSIRO.

Sverdrup, H.U., 1953. On conditions for the vernal blooming of phytoplankton. J. du Cons. doi:10.4319/lom.2007.5.269

Tanhua, T., Hainbucher, D., Schroeder, K., Cardin, V., Álvarez, M., Civitarese, G., 2013. The Mediterranean Sea system : a review and an introduction to the special issue. Ocean Sci. 9, 789–803. doi:10.5194/os-9-789-2013

Teruzzi, A., Cossarini, G., Lazzari, P., Salon, S., Bolzon, G., Crise, A., Solidoro, C., 2016. Mediterranean Sea biogeochemical reanalysis (CMEMS MED REA-Biogeochemistry 1999-2015 dataset). Copernicus Monit. Environ. Mar. doi:https://doi.org/10.25423/MEDSEA_REANALYSIS_BIO_006_008

Thackeray, S.J., Henrys, P.A., Hemming, D., Bell, J.R., Botham, M.S., Burthe, S., Helaouet, P., Johns, D.G., Jones, I.D., Leech, D.I., Mackay, E.B., Massimino, D., Atkinson, S., Bacon, P.J., Brereton, T.M., Carvalho, L., Clutton-brock, T.H., Duck, C., Edwards, M., Elliott, J.M., Hall, S.J.G., Harrington, R., James, W., Thompson, P.M., White, I., Winfield, I.J., Wanless, S., Pemberton, J.M., Sparks, T.H., 2016. Phenological sensitivity to climate across taxa and trophic levels. Nature 535, 241–245. doi:10.1038/nature18608

The MerMex Group., 2011. Marine ecosystems' responses to climatic and anthropogenic forcings in the Mediterranean. Prog. Oceanogr. doi:10.1016/j.pocean.2011.02.003

Thomas, A.C., Ted Strub, P., Weatherbee, R.A., James, C., 2012. Satellite views of Pacific chlorophyll variability: Comparisons to physical variability, local versus nonlocal influences and links to climate indices. Deep. Res. Part II Top. Stud. Oceanogr. 77–80, 99–116. doi:10.1016/j.dsr2.2012.04.008

Tokner, K., Uehlinger, U., Robinson, C.T., 2009. Rivers of Europe. Academic Press, London.

Törnros, T., 2013. On the relationship between the Mediterranean Oscillation and winter precipitation in the Southern Levant. Atmos. Sci. Lett. 14, 287–293. doi:10.1002/asl2.450

Torrence, C., Compo, G.P., 1998. A practical guide to Wavelet analysis. Bull. Am. Metereology Soc. 79, 61–78.

Torrence, C., Webster, P.J., 1999. Interdecadal Changes in the ENSO – Monsoon System. J. Clim. Am. Meteorol. Soc. 12, 2679–2690.

Tovar-Sanchez, A., Basterretxea, G., Ben Omar, M., Jordi, A., S??nchez-Quiles, D., Makhani, M., Mouna, D., Muya, C., Angl??s, S., 2016. Nutrients, trace metals and B-vitamin composition of the Moulouya River: A major North African river discharging into the Mediterranean Sea. Estuar. Coast. Shelf Sci. 176, 47–57. doi:10.1016/j.ecss.2016.04.006

Tovar-Sánchez, A., Basterretxea, G., Rodellas, V., Sánchez-Quiles, D., García-Orellana, J., Masqué, P., Jordi, A., López, J.M., Garcia-Solsona, E., 2014. Contribution of groundwater discharge to the coastal dissolved nutrients and trace metal concentrations in Majorca Island: Karstic vs Detrital Systems. Environ. Sci. Technol.

48, 11819–1827. doi:10.1021/es502958t

Trigo, R., Xoplaki, E., Zorita, E., Luterbacher, J., Krichak, S.O., Alpert, P., Jucundus, J., Sáens, J., Fernández, J., González-Rouco, F., Garcia-Herrera, R., Rodo, X., Brunetti, M., Nanni, T., Maugeri, M., Türkes, M., Gimeno, L., Ribera, P., Brunet, M., Trigo, I.F., Crepon, M., Mariotti, A., 2006. Relations between variability in the Mediterranean region and mid-latitude variability, in: Lionello, P., Malanotte-Rizzoli, P., Boscolo, R. (Eds.), Developements in Earth and Environmental Sciences: Mediterranean. Elsevier, pp. 179–226.

Trigo, R.M., Pozo-Vázquez, D., Osborn, T.J., Castro-Díez, Y., Gamiz-Fortis, S., Esteban-Parra, M.J., 2004. North Atlantic Oscillation influence on precipitation, river flow and water resources in the Iberian Peninsula. Int. J. Climatol. 24, 925–944. doi:10.1002/joc.1048

Tsagaraki, T.M., Herut, B., Rahav, E., Frank, I.R.B., Tsiola, A., Tsapakis, M., Giannakourou, A., Gogou, A., Panagiotopoulos, C., Violaki, K., Psarra, S., Lagaria, A., Christou, E.D., Papageorgiou, N., Zervoudaki, S., 2017. Atmospheric deposition effects on plankton communities in the eastern Mediterranean : A mesocosm experimental approach. Front. Mar. Sci. 4, 1–17. doi:10.3389/fmars.2017.00210

Turley, C.M., 1999. The changing Mediterranean Sea — a sensitive ecosystem? Prog. Oceanogr. 44, 387–400. doi:10.1016/S0079-6611(99)00033-6

Tyrrell, T., 1999. The relative influences of nitrogen and phosphorus on oceanic primary production. Nature 400, 525–531.

Uitz, J., Claustre, H., Gentili, B., Stramski, D., 2010. Phytoplankton class-specific primary production in the world's oceans: Seasonal and interannual variability from satellite observations. Global Biogeochem. Cycles 24, 1–19. doi:10.1029/2009GB003680

Uitz, J., Claustre, H., Morel, A., Hooker, S.B., 2006. Vertical distribution of phytoplankton communities in open ocean: An assessment based on surface chlorophyll. J. Geophys. Res. 111, C08005. doi:10.1029/2005JC003207

Uitz, J., Stramski, D., Gentili, B., D'Ortenzio, F., Claustre, H., 2012. Estimates of phytoplankton class-specific and total primary production in the Mediterranean Sea from satellite ocean color observations. Global Biogeochem. Cycles 26, 1–10. doi:10.1029/2011GB004055

Umani, S.F., 1996. Pelagic production and biomass in the Adriatic Sea. Sci. Mar. 60, 65–77.

Umani, S.F., Del Negro, P., Larato, C., De Vittor, C., Cabrini, M., Celio, M., Falconi, C., Tamberlich, F., Azam, F., 2007. Major inter-annual variations in microbial dynamics in the Gulf of Trieste (northern Adriatic Sea) and their ecosystem implications. Aquat. Microb. Ecol. 46, 163–175. doi:10.3354/ame046163

Uvo, C.B., 2003. Analysis and regionalization of northern european winter precipitation based on its relationship with the North Atlantic Oscillation. Int. J. Climatol. 23, 1185–1194. doi:10.1002/joc.930

Vantrepotte, V., Mélin, F., 2011. Inter-annual variations in the SeaWiFS global chlorophyll

a concentration (1997-2007). Deep. Res. Part I Oceanogr. Res. Pap. 58, 429–441. doi:10.1016/j.dsr.2011.02.003

Vantrepotte, V., Mélin, F., 2009. Temporal variability of 10-year global SeaWiFS time-series of phytoplankton chlorophyll a concentration. Int. Counc. Explor. Sea. Publ. by Oxford Journals. 2007. doi:10.1093/icesjms/fsp107

Verbesselt, J., Hyndman, R., Zeileis, A., Culvenor, D., 2010. Phenological change detection while accounting for abrupt and gradual trends in satellite image time series. Remote Sens. Environ. 114, 2970–2980. doi:10.1016/j.rse.2010.08.003

Vesanto, J., Alhoniemi, E., Member, S., 2000a. Clustering of the Self-Organizing Map. IEEE Trans. neural networks 11, 586–600. doi:10.1109/72.846731

Vesanto, J., Himberg, J., Alhoniemi, E., Parhankangas, J., 2000b. SOM Toolbox for Matlab 5, (Report A57). Hensinki University of Technological,Espoo, Finland.

Vidussi, F., Claustre, H., Manca, B.B., Luchetta, A., Marty, J.-C., 2001. Phytoplankton pigment distribution in relation to upper thermocline circulation in the eastern Mediterranean Sea during winter. J. Geophys. Res. 106, 939–956. doi:10.1.1.592.7009

Viličić, D., Matijević, J., Sepić, J., Kuspilić, G., 2012. Changes in the Adriatic oceanographic properties induced by the Eastern Mediterranean Transient. Biogeosciences 9, 2085–2097. doi:10.5194/bg-9-2085-2012

Vitousek, P.M., Howarth, R.W., 1991. Nitrogen limitation on land and in the sea: How can it occur? Biogeochemistry 13, 87–115. doi:10.1007/BF00002772

Volpe, G., Banzon, V.F., Evans, R.H., Santoleri, R., Mariano, A.J., Sciarra, R., 2009. Satellite observations of the impact of dust in a low-nutrient , low- chlorophyll region: Fertilization or artifact? Global Biogeochem. Cycles 23, 1–14. doi:10.1029/2008GB003216

Volpe, G., Nardelli, B.B., Cipollini, P., Santoleri, R., Robinson, I.S., 2012. Seasonal to interannual phytoplankton response to physical processes in the Mediterranean Sea from satellite observations. Remote Sens. Environ. 117, 223–235. doi:10.1016/j.rse.2011.09.020

Volpe, G., Santoleri, R., Vellucci, V., Ribera d'Alcalà, M., Marullo, S., D'Ortenzio, F., 2007. The colour of the Mediterranean Sea: Global versus regional bio-optical algorithms evaluation and implication for satellite chlorophyll estimates. Remote Sens. Environ. 107, 625–638. doi:10.1016/j.rse.2006.10.017

Walker, N.D., Rabalais, N.N., 2006. Relationships among satellite chlorophyll a, river inputs and hypoxia on the Louisiana continental shelf, Gulf of Mexico. Estuaries and Coasts 29, 1081–1093.

Wang, X.T., Cohen, A.L., Luu, V., Ren, H., Su, Z., Haug, G.H., Sigman, D.M., 2018. Natural forcing of the North Atlantic nitrogen cycle in the Anthropocene. Proc. Natl. Acad. Sci. 201801049. doi:10.1073/pnas.1801049115

Ward, B.A., Dutkiewicz, S., Moore, C.M., Follows, M.J., 2013. Iron, phosphorus, and

nitrogen supply ratios define the biogeography of nitrogen fixation. Limnol. Oceanogr. 58, 2059–2075. doi:10.4319/lo.2013.58.6.2059

Werdell, P.J., Bailey, S.W., 2005. An improved in-situ bio-optical data set for ocean color algorithm development and satellite data product validation 98, 122–140. doi:10.1016/j.rse.2005.07.001

Westberry, T., Behrenfeld, M.J., Siegel, D.A., Boss, E., 2008. Carbon-based primary productivity modeling with vertically resolved photoacclimation. Global Biogeochem. Cycles 22, 1–18. doi:10.1029/2007GB003078

Woodson, C.B., Litvin, S.Y., 2015. Ocean fronts drive marine fishery production and biogeochemical cycling. Proc. Natl. Acad. Sci. 112, 1710–1715. doi:10.1073/pnas.1417143112

Yacoub, M., Badran, F., Thiria, S., 2001. A topological hierarchical clustering: Application to ocean color classification. Lect. Notes Comput. Sci. doi:10.1007/3-540-44668-0_69

Yentsch, C.S., 1960. The influence of phytoplankton pigments on the colour of sea water. Deep Sea Res. 7, 1–9. doi:10.1016/0146-6313(60)90002-2

Yoder, J.A., Kennelly, M.A., 2003. Seasonal and ENSO variability in global ocean phytoplankton chlorophyll derived from 4 years of SeaWiFS measurements. Global Biogeochem. Cycles 17, 1112. doi:10.1029/2002GB001942

Yoder, J.A., Mcclain, C.R., Feldman, G.C., Esaias, W.E., 1993. Annual cycles of phytoplankton chlorophyll concentrations in the global ocean: a satellite view. Glob. Biochem. Cycles 7, 181–193. doi:10.1029/93GB02358

Yool, A., Martin, A.P., Fernández, C., Clark, D.R., 2007. The significance of nitrification for oceanic new production. Nature 447, 999–1002. doi:10.1038/nature05885

Zairi, M., Rouis, M.J., 1999. Impacts environnementaux du stockage du phosphogypse à Sfax (Tunisie). Bull. des Lab. des ponts chaussées 219, 29–40.

Zalidis, G., Stamatiadis, S., Takavakoglou, V., Eskridge, K., Misopolinos, N., 2002. Impacts of agricultural practices on soil and water quality in the Mediterranean region and proposed assessment methodology. Agric. Ecosyst. Environ. 88, 137–146. doi:10.1016/S0167-8809(01)00249-3

Zanchettin, D., Franks, S.W., Traverso, P., Tomasino, M., 2008. On ENSO impacts on European wintertime rainfalls and their modulation by the NAO and the Pacific multi-decadal variability described through the PDO index. Int. J. Climatol. 28, 995–1006. doi:10.1002/joc.1601

Zecchetto, S., De Biasio, F., 2007. Sea surface winds over the Mediterranean basin from satellite data (2000-04): Meso- and local-scale features on annual and seasonal time scales. J. Appl. Meteorol. Climatol. 46, 814–827. doi:10.1175/JAM2498.1

Zervakis, V., Georgopoulos, D., Karageorgis, A.P., Theocharis, A., 2004. On the response of the Aegean Sea to climatic varibility: A review. Int. J. Climatol. 24, 1845–1858. doi:10.1002/joc.1108

Zhai, L., Platt, T., Tang, C., Sathyendranath, S., Hernández Walls, R., 2011. Phytoplankton phenology on the Scotian shelf. ICES J. Mar. Sci. 68, 781–791. doi:10.1093/icesjms/fsq175

Zingone, A., Casotti, R., D'alcalà, M.R., Scardi, M., Marino, D., 1995. "St Martin's summer": The case of an autumn phytoplankton bloom in the Gulf of Naples (Mediterranean Sea). J. Plankton Res. 17, 575–593. doi:10.1093/plankt/17.3.575

Zoppini, A., Pettine, M., Totti, C., Puddu, A., Artegiani, A., Pagnotta, R., 1995. Nutrients, standing crop and primary production in western coastal waters of the Adriatic Sea. Estuarine, Coast. 41, 493–513.